R-07-19

Implementation of uncertainties in borehole geometries and geological orientation data in Sicada

Raymond Munier, Martin Stigsson
Svensk Kärnbränslehantering AB

December 2007

Svensk Kärnbränslehantering AB
Swedish Nuclear Fuel
and Waste Management Co
Box 250, SE-101 24 Stockholm
Tel +46 8 459 84 00

SKB

ISSN 1402-3091
SKB Rapport R-07-19

Implementation of uncertainties in borehole geometries and geological orientation data in Sicada

Raymond Munier, Martin Stigsson
Svensk Kärnbränslehantering AB

December 2007

A pdf version of this document can be downloaded from www.skb.se.

Contents

1 Introduction

Ever since investigation prior to the construction of the Äspö HRL, SKB has conducted advanced measurements and loggings aiming at determining the orientation of mapped structures in boreholes. Both instruments and methodologies have been continuously fine-tuned and updated as quality demands have increased. The site investigations at Forsmark and Simpevarp/Laxemar have produced a wealth of geological information. The fracture properties, including their orientation, have naturally attracted our focus. An unprecedented fracture analysis and modelling effort, from an SKB perspective, has revealed errors, flaws and deficiencies in structure orientation data and, as a consequence thereof, accentuated the need for a more rigorous treatment of orientation uncertainties.

Motivated by a quest for clarity, the authors of this report were appointed by SKB to, within the framework of a task force, evaluate and quantify the uncertainty in orientation data as a consequence of data errors identified in Sicada[1]. The Sicada database has been updated with regards to borehole geometries and orientation data in accordance to procedures developed within the task force.

In this report, we address the issue of uncertainty propagation and interaction. Additionally, we provide an explanation for the errors that have been detected in Sicada and countermeasures that has been taken. We here also argue for the need to quantify the uncertainty in orientation data and propose a method to compute this uncertainty.

To assess the impact of the changes made to Sicada, we here summarise the results of a comparison between data as present in Sicada in December 2006[2] and data present in Sicada in April 2008[3]. We accentuate that it is beyond the scope of this report to publish the full range of changes made to the tables in Sicada, or to provide elaborate quantifications of these changes. The sole purpose of this report is to document the checks made on the implementation in Sicada of various algorithms and to quantify the changes made to a selected set of orientation data since the work with quality improvement of orientation data began in late December 2006.

The main outcomes of the analyses presented here are the following:

- An analysis of the implemented orientation uncertainties in Sicada. This consisted of several independent steps:
    1. Checks that the algorithms for computation of borehole geometries (and their uncertainties) were correctly implemented in Sicada.
    2. Checks that the algorithms for the computation of strike and dip from alpha, beta (see below for explanations) and borehole geometries were correctly implemented in Sicada.
    3. Checks that the alpha and beta uncertainties were correctly implemented in Sicada.
- Quantification of orientation uncertainties. This enables us to address the issue of whether we have reached the goal of a maximum uncertainty of 10° dihedral angle (see below for explanation), according to the prerequisites of our assignment[4].

[1] Internal SKB reference: Bug ID 1830 (2006-05-03) and Bug ID 1968 (2006-09-05).

[2] Internal SKB reference: Data delivery defined in Documentum ID 1088725.

[3] Internal SKB reference: Data delivery SICADA-08-072.

[4] Internal SKB document. Documentum ID 1062926.

- A comparison of current orientation data (April 2008) with data prior to Sicada modifications (December 2006). This enables us to address to what extent previous models are valid in view of the changes made to the databases.
- A database containing fracture orientations, the uncertainty, and the angular changes in orientation since December 2006. The database is provided in two formats: A Statistica workbook containing all graphs and tables herein, and an Access database containing all computations.

2 Limitations of the analyses

The amount of boreholes and borehole mapping data in Sicada is overwhelming. Therefore, the task force, in collaboration with the site modelling groups, decided to restrict the update of data to boreholes stemming from the site investigations at Laxemar and Forsmark, hence excluding all data acquired prior to these investigations as well as all Äspö data. Additionally, a prioritisation was made, among the site investigation data, to set focus on boreholes judged relevant for the Site Descriptive Models.

For the prioritised boreholes, the following information was added to borehole orientation data:

- bearing uncertainty,
- inclination uncertainty, and, as a derivative thereof,
- uncertainty radius.

For the mapping data in the prioritised boreholes, the following information was added:

- alpha uncertainty,
- beta uncertainty,
- feature ID[5].

Accordingly, boreholes, or sections thereof, that do not fulfil these requirements were excluded from analysis. In total, 22 boreholes at Forsmark and 44 at Laxemar, were amenable for analysis given the requirements above. These are listed in Table 2-1.

Table 2-1. Boreholes amenable to analysis.

	Boreholes amenable to analysis		
	1 Forsmark	2 Laxemar	3 Laxemar *cont.*
1	KFM01A	KLX01	KLX11D
2	KFM01B	KLX02	KLX11E
3	KFM01C	KLX03	KLX11F
4	KFM01D	KLX04	KLX12A
5	KFM02A	KLX05	KLX13A
6	KFM03A	KLX06	KLX14A
7	KFM03B	KLX07A	KLX17A
8	KFM04A	KLX07B	KLX18A
9	KFM05A	KLX08	KLX19A
10	KFM06A	KLX09	KLX20A
11	KFM06B	KLX09B	KLX21A
12	KFM06C	KLX09C	KLX21B
13	KFM07A	KLX09D	KLX22A
14	KFM07B	KLX09E	KLX22B
15	KFM07C	KLX09F	KLX23A
16	KFM08A	KLX09G	KLX23B
17	KFM08B	KLX10	KLX24A
18	KFM08C	KLX10B	KLX25A
19	KFM09A	KLX10C	KLX26A
20	KFM09B	KLX11A	KLX26B
21	KFM10A	KLX11B	KLX28A
22	KFM11A	KLX11C	KLX29A

[5] The feature IDs for December -06 data were only computed for prioritised boreholes, to enable comparison of unique datum with April -08 data. However, since the analyses presented here were completed, all site investigation data (fractures, contacts, etc) and a considerable amount of Äspö data have obtained Feature IDs in Sicada. We plan to assign feature IDs to all Boremap/Petrocore mappings at the Äspö HRL.

Though the task assigned to the task force encompassed all orientation data in Sicada, we focus the analyses published here to borehole *fractures,* as their locations are spread over the entire boreholes and should they thus constitute an adequate proxy for other orientation data such as those for rock contacts, structures, radar measurements, stress measurements, etc. We here nevertheless analyse rock contacts and structure orientations, but to a lesser extent. Other orientation data such as radar reflectors and rock stress are left unattended in this report.

In Figure 2-1 we display the various contributions to orientation uncertainty that have been addressed in this report.

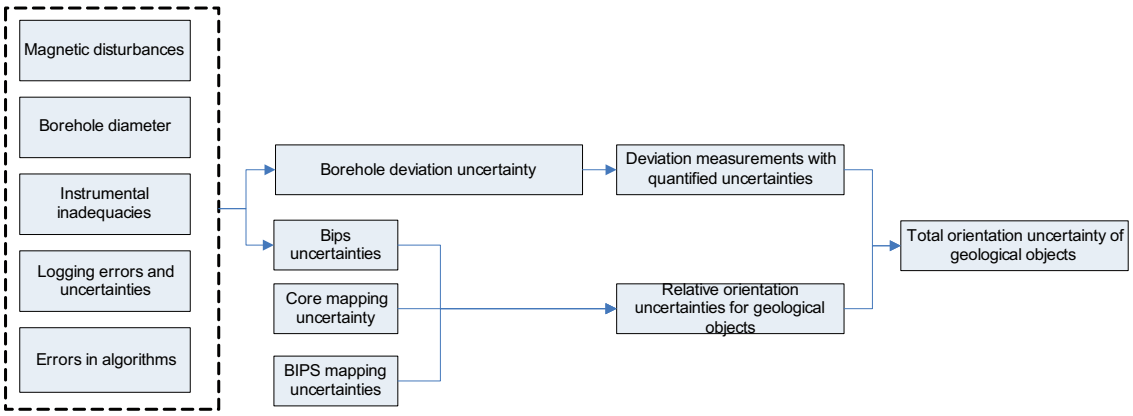

Figure 2-1. *Illustration of the various contributions to uncertainty that have been addressed in this report.*

3 Sources of errors and uncertainty

The sources of structure orientation uncertainty were thoroughly evaluated in a PM[6], the outcome of which is repeated here. In short, the authors of the PM identified the following main sources of uncertainties and errors:

- effects of variation of the borehole diameter,
- the core mapping uncertainty,
- the uncertainty of the orientation of the borehole,
- the uncertainty of orientation obtained from the BIPS picture, and
- errors due to the use of different calculation procedures in Boremap and Sicada.

The uncertainty of the orientation of the borehole consists of the following components; The uncertainty due to handling of the equipment, inadequacy of the equipment itself and, to a lesser degree, geomagnetic disturbance due to either solar magnetic activity (Appendix 1) or the presence of magnetic minerals in the rock.

3.1 Measurement of borehole geometries

3.1.1 Borehole deviation measurements

The instruments used for measuring borehole geometries during site investigations (see /Nilsson and Nissen 2007/ for details) are the Flexit Smart Tool (mag/acc), Reflex EZ-AQ/EMS (mag/acc) and the Reflex Maxibor (optical) instruments. Additionally, we made use of borehole radar, Televiewer and Mosnier tool (HF/HTPF) which have built-in mag/acc devices providing relatively reliable geometry data, though not as reliable as those obtained from the magnetometer/accelerometer-based tools. This, we judge, is due to the construction of these multifunction instruments which, due to space limitations, are prone to be affected by the electric currents in the cables, yielding oscillating deviation data (Figure 3-1).

Though it is possible reduce most of these artefacts, or anomalies, using various filters and moving averages, thereby obtaining a smoother, more realistic borehole trajectory, the local orientation and position of the borehole remains essentially unknown.

Such small-scale oscillations might be perceived as fairly insignificant. However, as illustrated in Figure 3-2, a small angular deviation can yield a considerable change in borehole azimuth, particularly in steep boreholes. Naturally, as fracture orientations are computed relative to the borehole orientations (azimuth) then their calculated strikes might be severely affected.

Several companies have been provided the opportunity to demonstrate alternative measuring methods to SKB but none have shown better results than those implemented in the site investigations. We can therefore not, as yet, point out any better instrument for the deviation measurements. We applied a principle, in the quality revision, to, with few exceptions, only use “official” deviation measurements from the Magnetometer/accelerometer-based tools and Maxibor instruments for the computation of borehole geometries, according to activity “EG154”, even if measurements from other instruments were in fact available.

[6] Internal SKB document. Documentum ID 1063373.

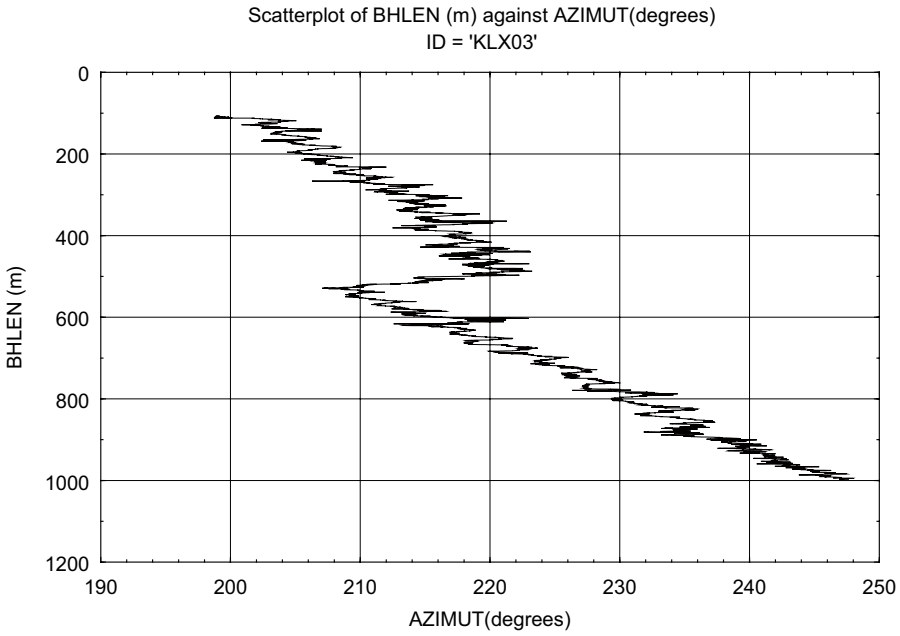

Figure 3-1. *The graph shows a deviation measurement in KLX03 using televiewer. The oscillating pattern is judged to be due to interference from cables close to the measuring device.*

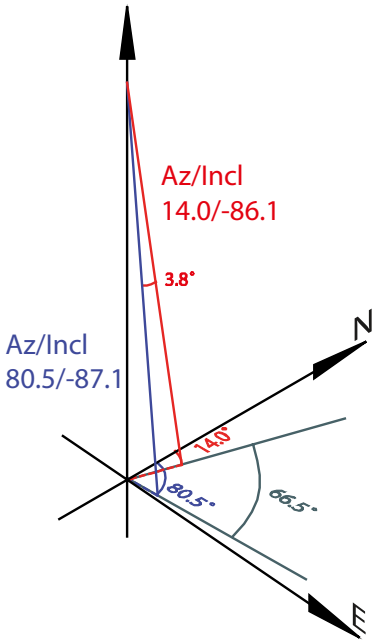

Figure 3-2. *In a steep borehole, the difference in azimuth can be considerable despite a small dihedral angle. In this example, the dihedral angle between the two tentative borehole measurements is 3.8° whereas the difference in azimuth is 66.5° The difference in inclination is only 1°.*

During site investigations, several failed attempts were made to locate boreholes suitable for calibration of the instruments, that is, boreholes for which the location of both ends are known. However, the value of such "calibrations" can be questioned due to the relatively poor repeatability of the deviation measurements (Figure 3-3), which has been our major concern. In either case, the issue of poor repeatability needs to be fully addressed prior such an evaluation. Thus, this point of view regarding calibration holes might be altered with more robust and repeatable measurements.

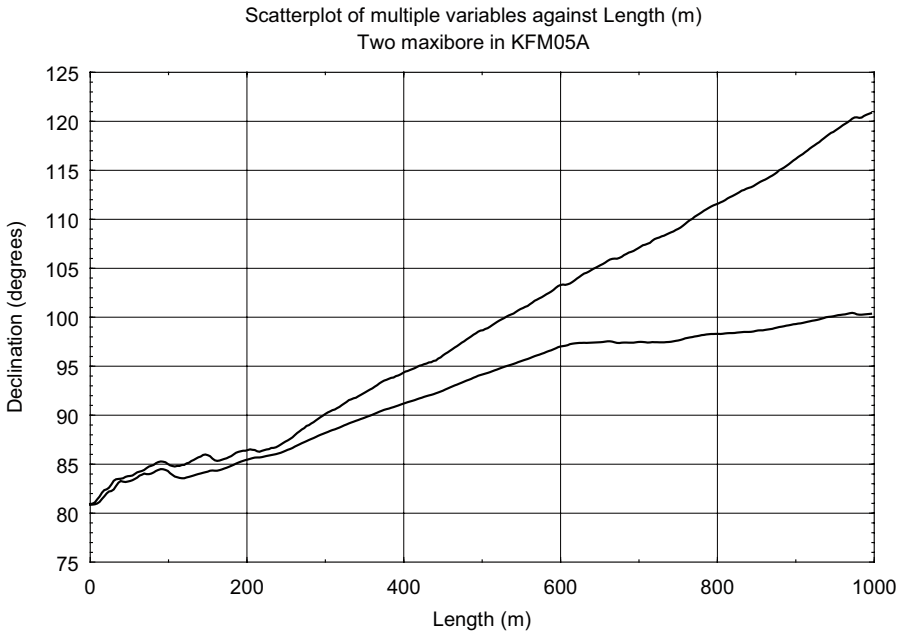

Figure 3-3. *The graph illustrates our clearest example of the lack of repeatability in the deviation measurements (Maxibor in KFM05A). These have now been error marked in Sicada.*

3.1.2 Error due to an inadequately implemented algorithm in Boremap

The "in-use" tagged deviation file in Sicada contains primary data from the deviation measurement (azimuth, recomputed to the reference system RT90, and inclination) and computed coordinates (Northing, Easting, Elevation). The standard procedure has been to import the in-use tagged file containing the coordinates into Boremap with which the azimuth and inclination were calculated from the coordinates. These orientations were then stored in Sicada in the table "bm_direction". Rather than computing orientations from the coordinates, Boremap should have used orientation from the azimuth and inclination provided directly by the measurements. Ideally, this recalculation should not have caused any problem as the angles would essentially be identical. However, due to intricate numerical circumstances and effects of minute rounding errors, a small angular difference can occur between the computed and measured orientations. In Figure 3-4 we display an example (KFM07C) in which the angular difference is up to 2–3°. The thus introduced angular error can yield an error in azimuth of almost 180° in steep (near 90°) boreholes which are particularly sensitive, as shown in Figure 3-2.

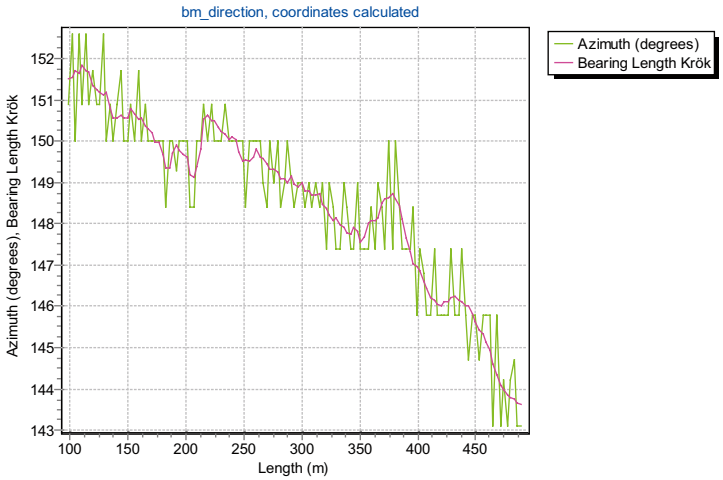

Figure 3-4. *Azimuths computed in Boremap (green oscillating curve) compared to the ones measured in KFM07C (red curve).*

3.1.3 Variations in borehole diameter

During fracture mapping, two angles are measured: The angle between the fracture plane and the core, α, and the angle between the fracture plane and a reference line along the core, β. If the fracture is visible in BIPS, both angles are derived from the image, from which the angle of relevance here, α, is obtained from the amplitude of the sinusoid, i.e. the intersection of the plane (the fracture) with a cylinder (the borehole). Figure 3-5 shows the relation between the angle α and the core. Obviously, variations in the borehole diameter will affect the measured amplitude and, accordingly, the angle α.

The real angle α is computed from:

$$\alpha = 90 - \arctan\left(amplitude \,/\, d_{real}\right) \qquad 3\text{-}1$$

Accordingly, the mapped angle α' is computed from:

$$\alpha' = 90 - \arctan\left(amplitude \,/\, d_{theoretical}\right) \qquad 3\text{-}2$$

Figure 3-6 shows the difference between real (α) and mapped (α') angles at various enlargements of a 76 mm diameter borehole. The largest errors occur at α-values near 45°.

In Figure 3-7 we display a cumulative density function (CDF) of the deviations from 76 mm diameter, for all KLX and KFM boreholes, measured with caliper. Sections with anomalously large diameters, typically at deformation zone intersections, were omitted from this analysis. The graph shows that roughly 96% of the caliper-data deviate less than 2 mm.

The distribution (CDF) of α-angles is displayed in Figure 3-8 from which we can deduce that roughly 30% of the data lie within 30°–50°, here defined as the critical range with respect to borehole diameter variations.

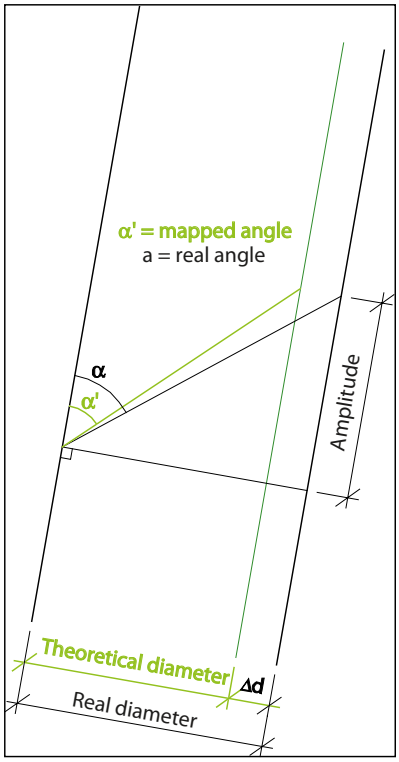

Figure 3-5. *Schematic illustration showing the mapped angle α' in relation to the real angle α.*

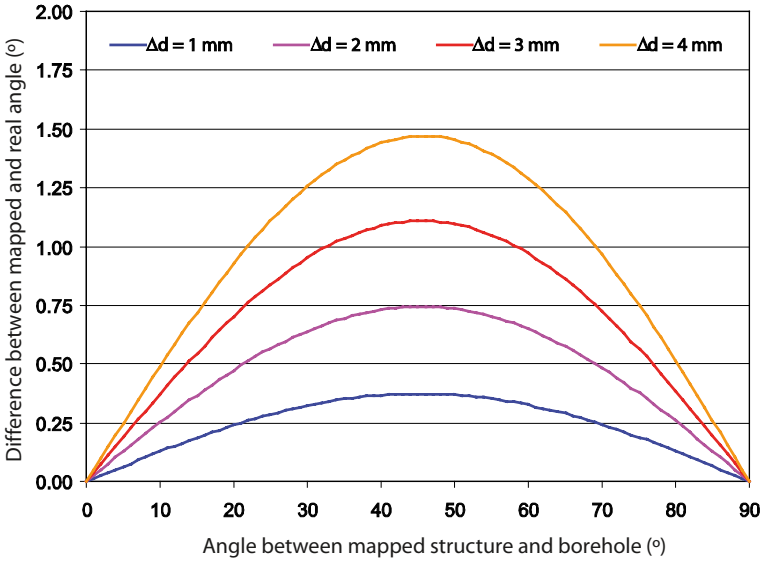

Figure 3-6. *The graph shows the error in mapping the angle α in relation to various permutations of the diameter of an originally 76 mm borehole. Δd = 4 mm corresponds to an expansion to 80 mm from 76 mm.*

Combining the findings of Figure 3-7 and Figure 3-8, and using the relation shown in Figure 3-6, we estimate that almost all data (99.8%) have an error, due to borehole diameter variations, less than 1°. Though, ideally, the α-angle should be computed on the basis of the local diameter from caliper measurements, rather than a single hypothesised diameter for the entire borehole, we perceive the error sufficiently small, *on average*, to be safely overlooked. However, as indicated above and shown in Figure 3-9, the local diameter can vary considerably and therefore, considerably affect a minor amount of orientations. Still, most such sections are affected by deformation zones, core loss etc, and contain little or no fracture data of importance to, say, DFN modelling. We therefore conclude that the borehole diameter is a subordinate issue provided, of course, that the present drilling procedures and QA are maintained throughout future drilling campaigns in any of the sites.

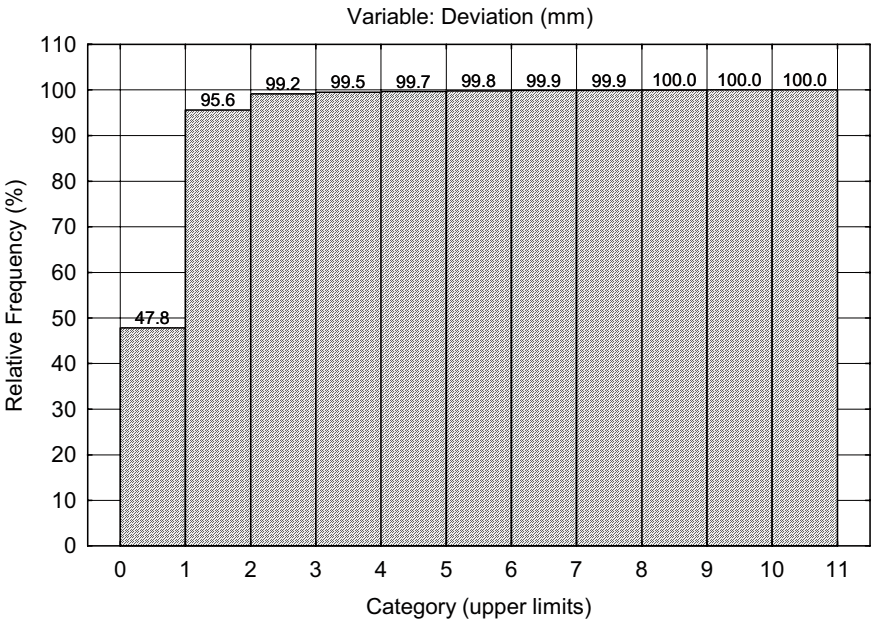

Figure 3-7. *This CDF shows the deviation in mm from the diameter 76 mm for all KLX and KFM boreholes. Deviations larger than 11 mm were filtered out.*

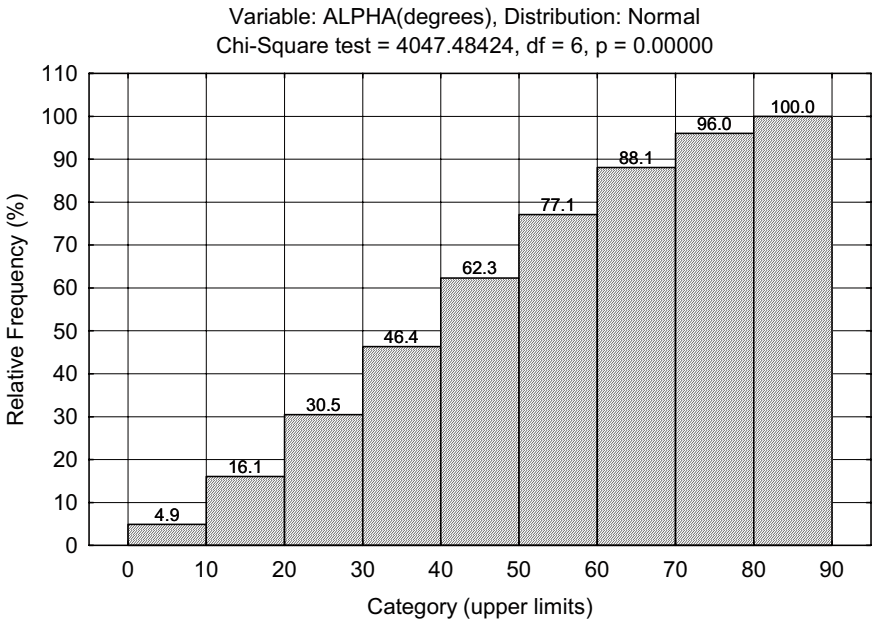

Figure 3-8. *This CDF shows the measured alpha angle in all KLX and KFM boreholes. Roughly 30 % of the data lie in the interval 30–50 degrees.*

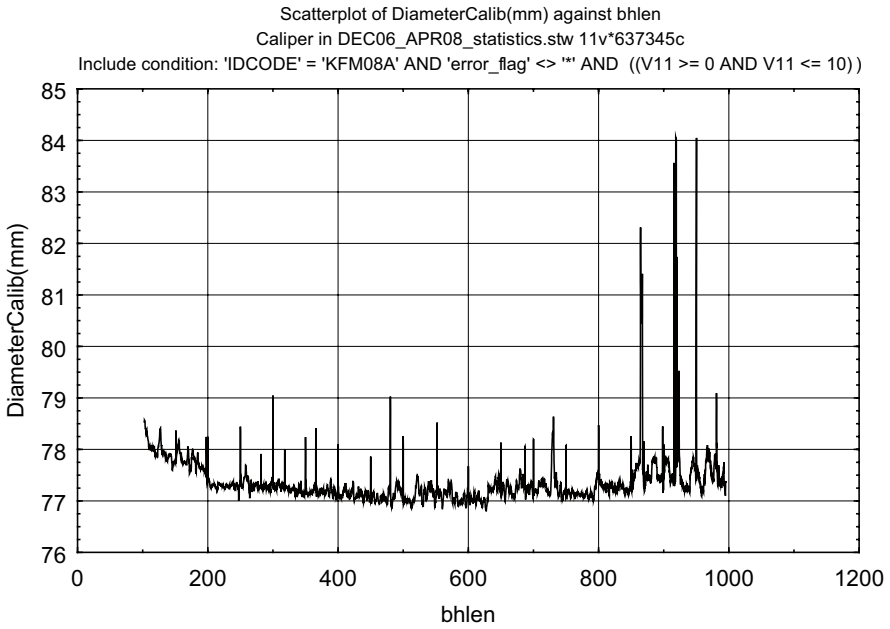

Figure 3-9. *Example of a diameter variation (caliper log) in a borehole (KFM08A).*

3.1.4 Magnetic field variations

Measurements with magnetometer/accelerometer are effected not only by magnetic anomalies in the rock surrounding the borehole, but also by external sources. The geomagnetic field is normally considered as constant over time but, actually, contains disturbances that, within the current framework, can be considerable. For instance, a nearby powercable or powerplant can alter the field with several degrees. The most common disturbance, however, is fluctuations caused by storms of charged particles from the sun. These storms cause large current loops in the earth ionosphere, and as a consequence thereof, magnetic field variations on the earth surface. These disturbances, in turn, can cause variations of the magnetic declination of several degrees, and need to be taken into account when measuring the borehole bearing with magnetometer based methods.

Such a solar eruption occurred in October 29, 2003 and, as shown in Figure 3-10a, induced fluctuations in the geomagnetic field of up to 4 degrees under short periods. We have checked that the borehole deviation measurements performed during site investigations were not performed during solar eruptions and, fortunately, found no critical measurements (diagrams for relevant periods are included in Appendix 1). However, future logging campaigns need to ensure that no solar eruption occurred during measurement. Following the recommendations of /Nilsson and Nissen 2007/ we propose the following:

- Accept a magnetometer/accelerometer logging if the fluctuations in the declination of the geomagnetic data do not exceed 0.5°.
- If the fluctuations exceed 0.5° the deviation logging should be ERROR-marked, and a new logging has to be conducted.

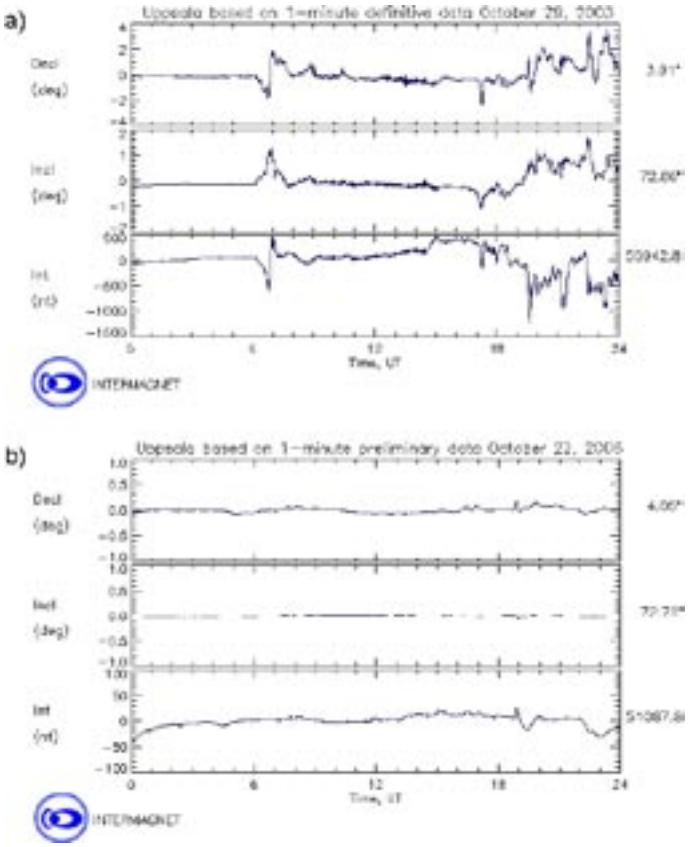

Figure 3-10. *Example of the temporal fluctuations of the geomagnetic field observed at the geomagnetic observatory in Uppsala. Figure "a" displays data from the beginning of the magnetic storm October 29–31 2003 where the variations are up to 4 degrees during short time frames. For comparison we display in figure "b" data from a magnetically calm day with small variations. Diagrams are obtained from /INTERMAGNET 2007/.*

3.2 The BIPS imaging system

The Boremap mapping system requires that the orientation of the BIPS probe is known in order to determine the orientation of mapped features. The orientation of the BIPS image can either be determined by the use of the internal compass (magnetic method) or by using a clinometer (gravimetric method).

The BIPS probe was originally equipped with a steel ball clinometer. We discovered, after some time of usage, that the construction was severely affected by inertia which locally rendered unacceptably large errors in the measurements. As a consequence thereof, the instrument was rebuilt and the steel ball clinometer was replaced by one using an air bubble which yielded more accurate measurements. This reconstruction of the instrument took place in November 2003 and the action was documented in a deviation report.

The current configuration of the imaging system is prone to human errors as the image is manually rotated with respect to the clinometer, as the probe is slowly moved down the borehole. This essentially requires the BIPS operator to be fully concentrated on the task during the entire duration of the logging, which often lasts several hours. Naturally, eye fatigue and the monotonous nature of this procedure may cause varying accuracy along the measured section. An example of an erroneously oriented image is displayed in Figure 3-11b.

3.2.1 Gravimetric method

The method description[7] prescribes that the orientation of the BIPS image shall be determined using the gravimetric method when the borehole is inclined between zero and 85° from the horizon. In this case the orientation of the BIPS image to the borehole axis is recorded using an air bubble, or, as used early in the investigations programme, a steel ball. During the measurement, a semi automatic correction of the orientation is performed. The operator checks that the air bubble always persists being at the top of the image. Using the described method the accuracy in the orientation of the image, due to the rotation of the probe around its axis is (at 85° inclination), assumed to be in the order of ± 6–7°.

The early measurements using steel ball was largely affected by inertia, causing the steel ball to move in steps rather than smoothly. As a consequence thereof, portions of borehole have large orientation errors, up to 45°. The earliest measurements using bubble level was affected by an oversized air bubble causing an estimated uncertainty in the orientation in the order of ± 6–7°.

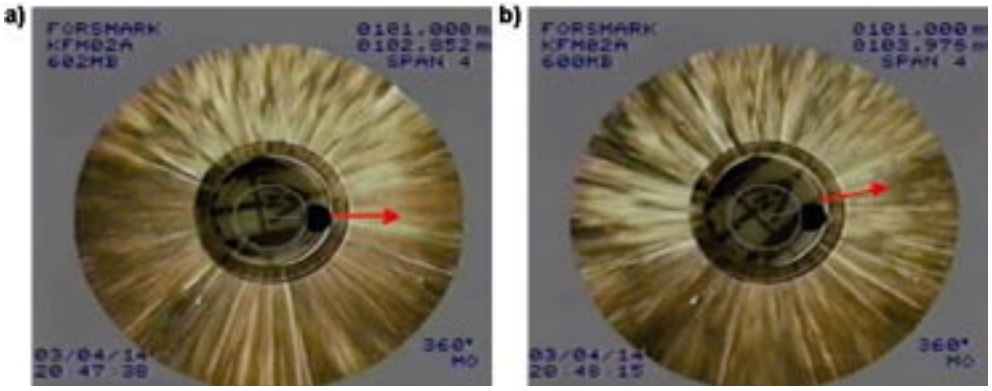

Figure 3-11. *In figure a, the probe is correctly oriented. The white pointer is directed towards the centre of the black steel clinometer. In figure b, the pointer is oblique, with an angular deviation of roughly 25°. Please note that a red pointer, parallel to the white pointer, has been manually drawn upon the original BIPS image for clarity.*

[7] Internal SKB document, MD 222-006.

3.2.2 Magnetic method

Subvertical boreholes (Inclination ≥ 85°) have been assumed perfectly vertical and the orientation of the BIPS probe has been measured using compass. There is a two-component magnetometer to aid the operator in orienting the image when the probe is rotating around its axis. However, using the magnetic method, the error is assumed to increase beyond ± 6–7° when the probe passes rock with high magnetic susceptibility.

The magnetic method was only used in a limited number of boreholes during the site investigations. In Laxemar magnetic methods were used in KLX09B and KLX11B and in Forsmark in HFM02 and HFM03. The reason is that most boreholes tend to be less steep the longer they are drilled. More importantly, there were problems with the magnetic instrument. The compass needle, mounted in an oil filled house, was too affected by inertia and reacted overly slow to rapid rotations of the BIPS probe, rendering erroneous data in sections of the boreholes.

3.2.3 Estimation of uncertainties

Thus, both the magnetic and gravimetric instruments are, to various degrees and under various conditions, affected by measurement inaccuracy and/or error. Naturally, it is only possible to quantify these uncertainties/errors if the boreholes are relogged using a better instrument. Under normal circumstances, such relogging cannot be performed as the boreholes are equipped with monitoring instruments. Fortunately, however, poor image quality of the BIPS obligated new imaging in 12 boreholes which could be used to assess the uncertainty. We compared the different loggings, during October 5–6 2006, focusing on the sharpest fractures that can be interpreted despite low visibility on the images. In total 69 fractures suitable for analysis could be identified.

Figure 3-12 shows an example of interpretation of the same fracture in KFM03 from two different loggings using the BIPS probe. The difference in interpreted strike is 30°.

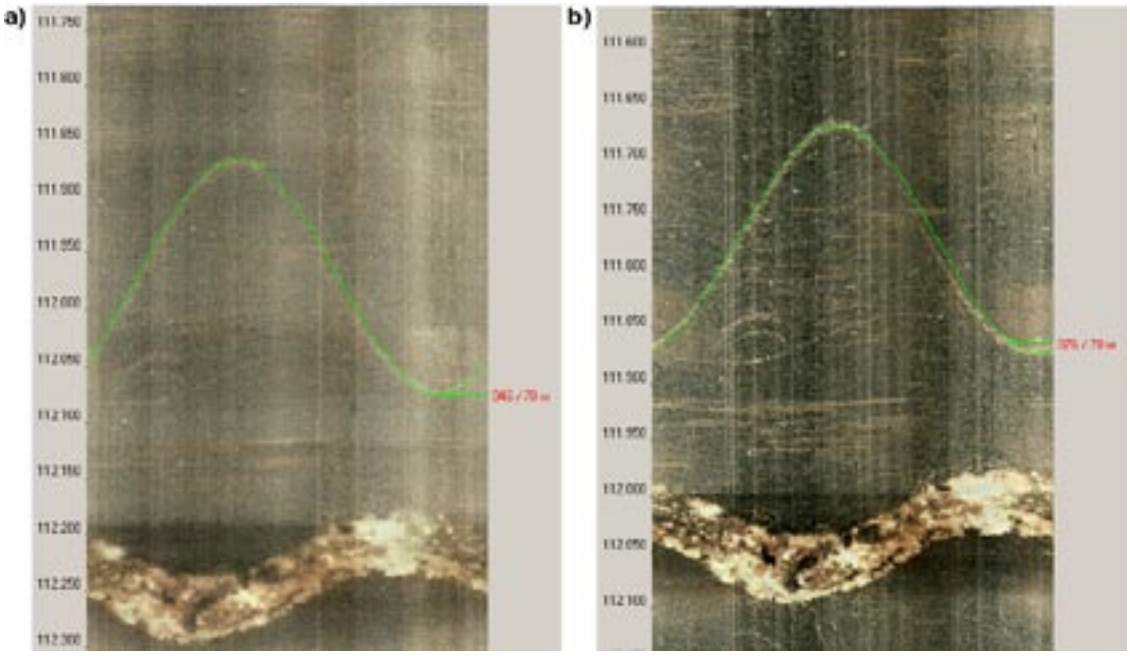

Figure 3-12. *Example of interpretation of the same fracture in KFM03A from two different measurements (a = BIPS-logging 2003-08-03, b = BIPS logging 2003-08-31) using the BIPS probe with steel ball clinometer. The difference in strike, in the example, is 30°. The uncertainty in the interpretation of the image is assumed to be in the order of ± 1°. Observe that the length scale to the left in the images is the recorded length[8] and thereby there are differences in the values.*

[8] The depth provided by the probe (recorded length) is adjusted to marks cut onto the borehole walls (adjusted length).

The difference in fracture orientation obtained from the two differently interpreted BIPS images are listed in Table 3-1, while the maximum values and method of orientation for each borehole is listed in Table 3-2. Please note that the table lists the largest *observed* uncertainty and, hence, there is a possibility that other sections or other boreholes have *even* larger differences. Only 69 fractures out of about 140,000 fractures were compared, i.e. less than 0.5‰.

Table 3-1. Difference in interpretation of fracture orientation between different BIPS loggings from 69 randomly chosen fractures in 12 boreholes in Forsmark and Laxemar. The column "Borehole length" refers to the approximate recorded borehole length where the fracture is identified in the two images. The column "alpha" is the angle of the fracture to the borehole axis. The column "Difference in beta" lists the differences due to the orientation of the probe.

	Borehole length (m)	alpha (°)	Difference in beta (°)
KFM01B	23.7	14	15
Incl=–79.0°	82.6	25	10
	187.7	24	22
	259.0	16	14
	413.4	28	8
	474.9	41	5
KFM02A	372.2	30	14
Incl=–85.4°	392.0	25	18
	462.7	24	18
	522.5	34	14
	564.8	20	22
	595.8	25	24
KFM03A	111.9	20	31
Incl=–85.7°	141.6	14	18
	214.8	10	3
	276.0	22	6
	322.3	17	9
	371.8	15	19
	415.8	14	18
	867.5	45	6
	932.9	14	8
	969.9	8	14
KFM04A	115.3	35	1
Incl = –60.1°	144.8	41	1
	187.1	34	2
	218.7	17	1
	297.9	10	2
	394.1	38	6
	450.3	12	0
	508.7	7	0
	559.7	10	0
KFM06B	8.6	6	12
Incl=–83.5°	47.6	26	14
	54.1	12	9
KFM07C	100.7	40	0
Incl=–85.4°	101.9	16	2
	151.6	10	12
	189.6	14	9
	244.4	14	1
	314.9	16	1
	371.9	12	3

	Borehole length (m)	alpha (°)	Difference in beta (°)
KLX08	111.0	7	9
Incl = –60.3°	167.1	16	4
	238.8	33	2
	344.6	11	2
	408.5	32	5
	534.0	32	2
	580.0	11	2
	627.1	7	1
	712.6	33	4
	812.0	16	2
	896.1	20	2
	944.7	18	5
KLX10	329.7	27	23
Incl=–85.2°	418.9	27	14
KLX11B	11.2	10	26
Incl=–89.9°	48.7	25	30
	50.8	13	64
	63.9	41	1
HFM17	9.6	5	12
Incl=–84.2°	18.2	2	16
	115.8	5	8
HFM26	25.5	2	17
Incl=–53.7°	49.6	2	2
	115.1	2	8
	181.5	3	5
HFM28	15.7	40	8
Incl=–84.8°	34.3	21	6
	51.5	32	0

Table 3-2. Largest observed difference, dihedral angle, in orientation of fractures from Table 3-1 together with the measuring method of the BIPS image and maximum inclination in the borehole.

Borehole ID	Meassuring method	Maximum borehole inclination (°)	alpha (°)	Largest difference in orientation (°)
KFM01B	Bubble level	–79.0	24	20
KFM02A	Bubble level	–85.4	25	22
KFM03A	Steel ball	–85.7	20	29
KFM04A	Bubble level	–60.1	38	5
KFM06B	Bubble level	–83.5	26	13
KFM07C	Bubble level	–85.4	10	12
KLX08	Bubble level	–60.3	7	9
KLX10	Bubble level	–85.2	27	20
KLX11B	##Compass? See text	*–89.9*	*13*	*62*
HFM17	Bubble level	–84.2	2	16
HFM26	Bubble level	*–53.7*	*2*	*17*
HFM28	Bubble level	–84.8	21	6

Table 3-2 indicates that the uncertainty can be substantial. For example, the uncertainty in KLX11B is at least 62° between the fracture planes interpreted in May 10 2006 and those interpreted in June 15 2006. This borehole, with a maximum inclination of 89.9°, is one of four boreholes in Forsmark and Laxemar where the magnetic method is used for orientation of the BIPS probe. In the remaining subvertical boreholes, the probe was gravimetrically oriented with, as shown in Table 3-1 an error of up to 20–30°. Note also that moderately inclined boreholes might have large differences too (Figure 3-13). For instance, HFM26 with an inclination of 53.7° displays a difference between the two different interpretations of roughly 17° (dihedral angle). A possible explanation could be that it is harder to properly centre the probe in percussion boreholes because these have a larger diameter compared to cored boreholes.

Figure 3-13 shows that there is not a clear correlation between the borehole inclination and the dihedral angle between the two interpretations, though it does indicate that steep boreholes can, but must not, have larger uncertainties than inclined boreholes.

3.2.4 Conclusions regarding the BIPS imaging system

BIPS images from boreholes with an inclination of 70° or less can be attributed an uncertainty in orientation of 10° at the 90th percentile or 2° as median (assuming Gaussian distribution). Though the computed value of the 90th percentile is 7.94° (Figure 3-13), we conservatively round this value to 10° as the sample is small and the representativity of the 69 analysed fractures is questionable. A similar reasoning has been applied for other inclination classes. Images from boreholes with inclinations between 70° and 85° were assigned an uncertainty of 20° at the 90th percentile with 10° as median value. In steeper boreholes (≥ 85°) we assume that 90% of the data have an uncertainty less than 30° (15° median), which is roughly half the largest measured difference between fractures mapped from the two BIPS images. We accentuate that Table 3-1 and Table 3-2 only document essentially random samples of the differences between BIPS loggings, there might be short sections in which there are larger differences. Additionally, even if the difference at a certain borehole section appears small, there might still be a large actual difference because the two independently logged BIPS images might have been rotated by roughly the same amount.

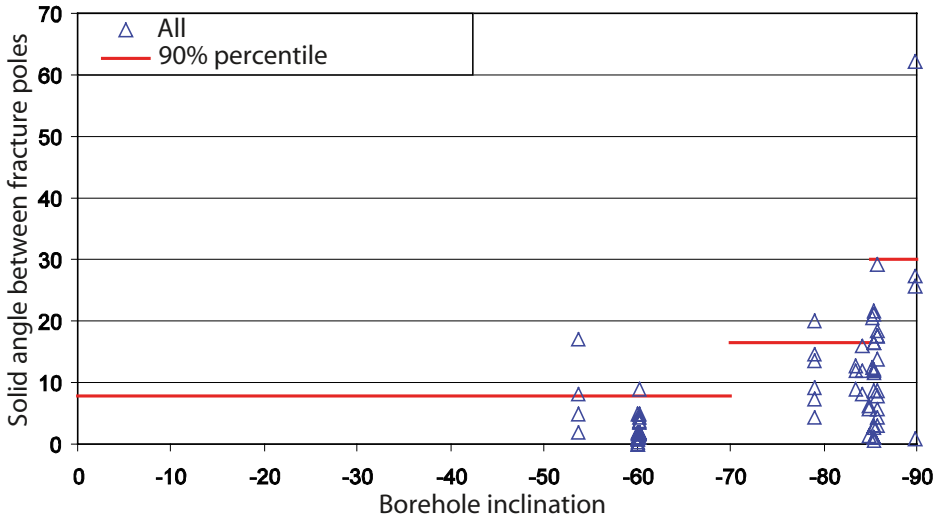

Figure 3-13. *The difference between interpreted orientations in two different BIPS images, expressed as dihedral angles, as a function of borehole inclination.*

To minimise errors and uncertainties induced by the BIPS imaging system itself (see also /Döse et al. 2008/ for details), we recommend the following:

- Future boreholes should not be drilled steeper than 80°.
- The current semiautomatic configuration of the BIPS system should be replaced with a fully automatic one, to minimise human errors. It is not reasonable to expect a BIPS operator to remain fully alert for several hours while waiting for an eventual, minor distortion of the orientation that requires a manual adjustment. The issue has been brought forward to SKBs section for handling instrument, "PLU-teknik".
- Dirt in the water or on the borehole walls, affects the image quality, sometimes severely. There is an optimal timeframe within which logging should be performed. It occurs after sedimentation of drilling debris, but prior to alteration or bacterial growth on the borehole walls. Ideally, logging should be performed a week or so after the drilling has been completed.

Once one of the major causes of BIPS uncertainty was identified, actions were taken to correct those sections of the BIPS images in which the orientation was erroneous. This tedious, manual, work lasted roughly a year and in total, BIPS images corresponding to roughly 43 km of borehole were reviewed in sections ranging from a few mm up to 5 m, and checked for rapid rotation, erroneous adjustment with respect to the bubble level, etc. The angular deviation was measured, recorded (Figure 3-14) and the borehole orientations in Sicada were all subsequently adjusted for these known errors.

Figure 3-14. *Measurement of the deviation between the pointer and the bubble level (c.f. Figure 3-11).*

3.3 The core mapping uncertainty

The uncertainty in orientation caused by mapping inaccuracy can be estimated by letting two independent teams map the same borehole or parts thereof. /Glamheden and Curtis 2006/ presented results from such a study, using two cores KFM06C, and KLX07B. However the result in /Glamheden and Curtis 2006/ only present differences between the total of the two populations and, hence, no comparison between individual fractures is carried out, effectively hindering analysis of orientation uncertainty. To overcome this obstacle, Nissen and Stigsson[9] proposed and applied an algorithm that automatically couples fractures mapped by one team to the same fracture mapped by the other team using fracture properties such as position, mineralogy, aperture, etc.

In the interval 176.5 to 332.1 m (recorded length) in KFM06C one team mapped 581 fractures while the other team mapped 593 fractures. The corresponding numbers in section 9.6 to 132.0 m (recorded length) in KLX07B was 699 respectively 721. Using the algorithm in Nissen and Stigsson, 904 fractures were identified as being the same. However, the algorithm identifies the fractures of being identical if there are no other fractures in the vicinity (defined as ± 2 cm), even if few parameters are equal. Therefore Nissen and Stigsson excluded approximately 15% of fractures with the lowest probability (based on similarity of mapped parameters) and based their analysis on the remaining 769 fractures. The difference in fracture orientation, expressed in terms of a dihedral angle, between using all coupled fractures and the most probable coupled fractures is shown in Figure 3-15.

Using the 85% of the data with highest probability to be correctly coupled, the uncertainty is calculated for the mapped α and β angles.

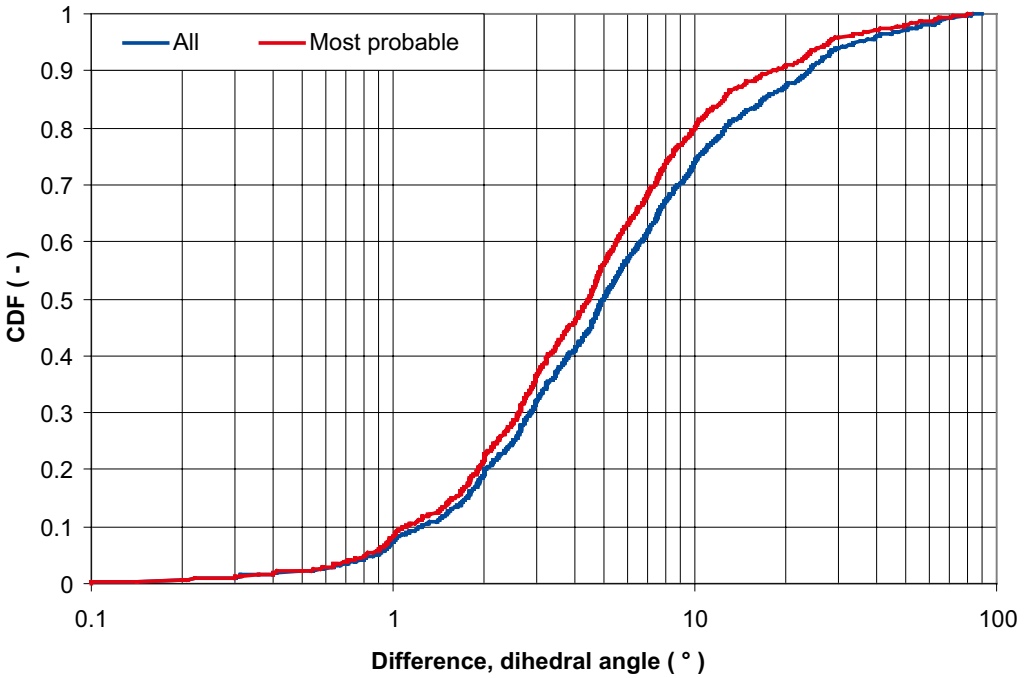

Figure 3-15. *The Cumulative Density Function of the dihedral angle between the fracture plane normal, caused by different mapping geologists. The blue line shows the CDF for all coupled fractures whilst the red shows the CDF when 15% of the fractures with lowest probability are excluded.*

[9] Internal SKB document. Documentum ID 1063373.

The relationship between the α angle and the α and β uncertainties is ambiguous; see Figure 3-16 to Figure 3-19, due to the small population of data. The uncertainties were calculated in three 30° bins for the fractures visible in BIPS and in one 90° bin for the non-visible fractures. An alternative would have been to fit a continuous function. However, we judge the population too small for such analysis. Table 3-3 shows the values of the uncertainty used for calculating the total uncertainty of a feature. Observe that the uncertainty is assumed to be half of the difference between the two mapping teams[10], thereby assuming that the correct orientation is the average of the two teams.

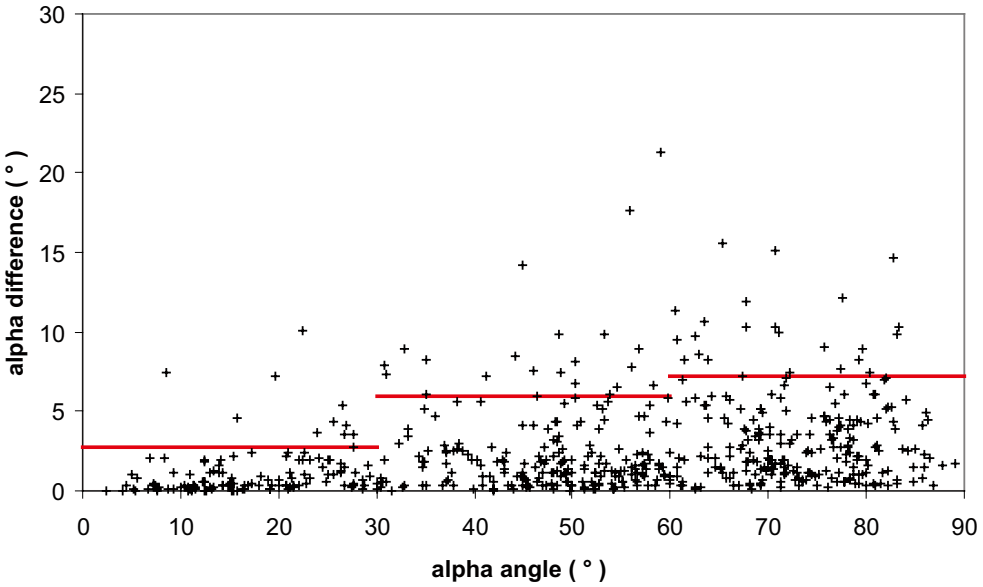

Figure 3-16. *The difference in alpha angle, for fractures visible in BIPS, as a function of the mapped alpha angle (black crosses) together with the three 90th percentile levels calculated (red line).*

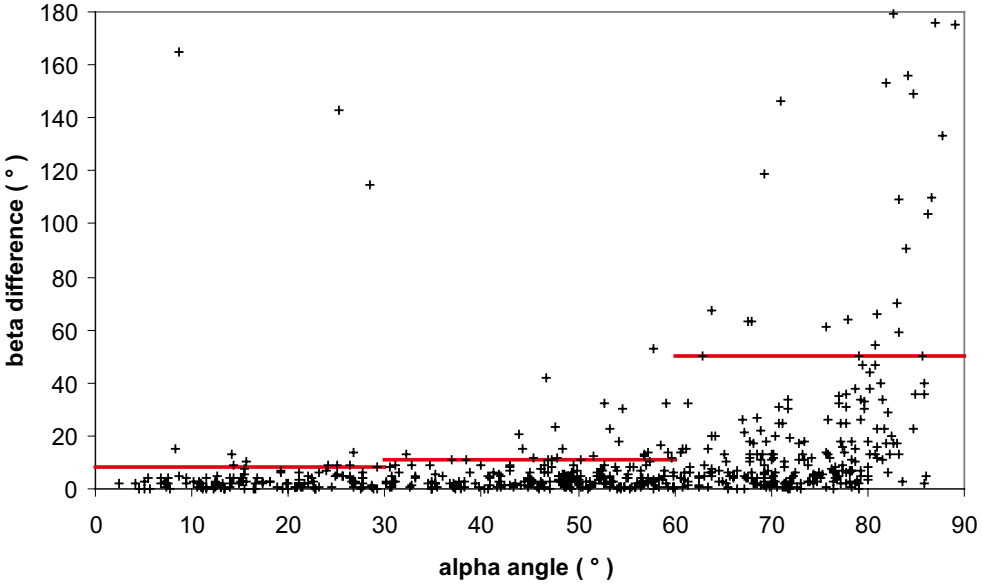

Figure 3-17. *The difference in beta angle, for fractures visible in BIPS, as a function of the mapped alpha angle (black crosses) together with the three 90th percentile levels calculated (red line).*

[10] Note that since the true value is unknown, the only means to address the uncertainty is to define such a value, here as the average of the two mapped orientations. This assumption relies upon a judgement that both teams are equally skilled and yet another assumption, that there are no systematic measuring errors in any of the mappings.

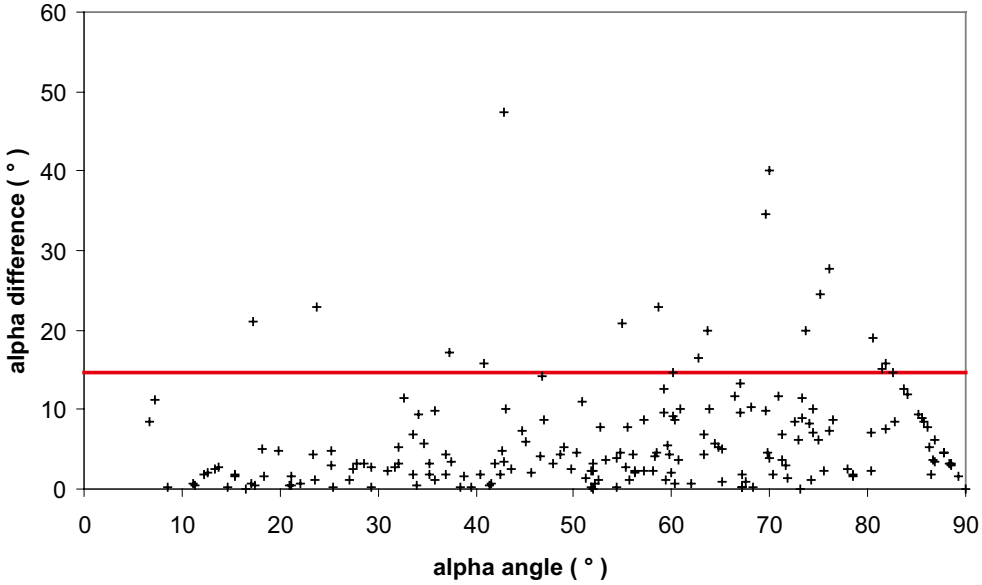

Figure 3-18. *The difference in alpha angle, for fractures not visible in BIPS, as a function of the mapped alpha angle (black crosses) together with the 90th percentile level calculated (red line).*

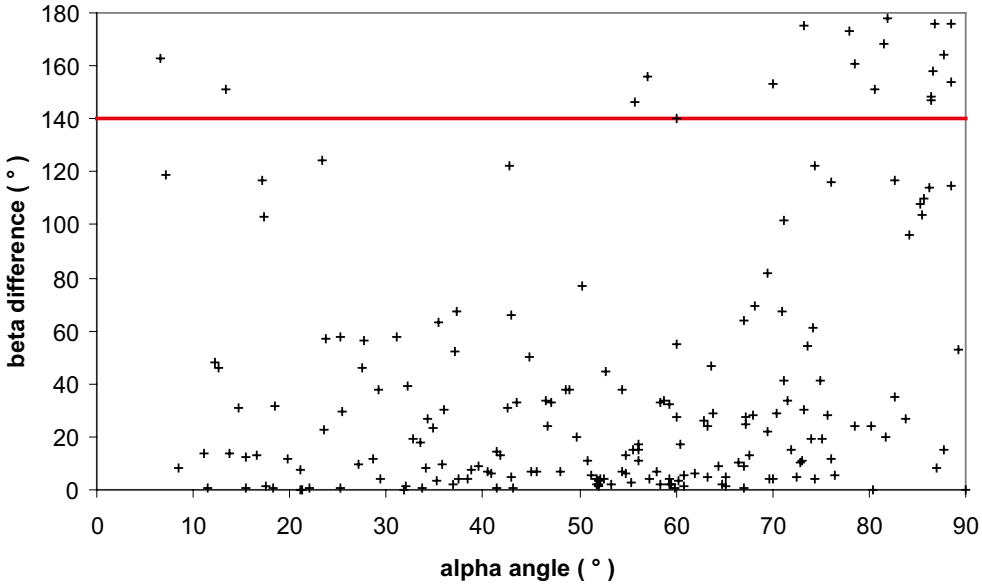

Figure 3-19. *The difference in beta angle, for fractures not visible in BIPS, as a function of the mapped alpha angle (black crosses) together with the 90th percentile level calculated (red line).*

Table 3-3. The calculated uncertainties originated during mapping.

Visibility in BIPS alpha angle	Visible 0°–30°	30°–60°	60°–90°	Not visible 0°–90°
alpha uncertainty	1.4°	3.0°	3.6°	7.4°
beta uncertainty	4.0°	5.6°	25°	70°

4 Implementation of algorithms in Sicada and Boremap to compute geometric uncertainties

An extensive effort has been invested in developing new algorithms in Sicada and Boremap to compensate for the lack of quantified geometric uncertainties for boreholes and rock mass structures. Several different computations have been implemented. Some were introduced to address the geometric uncertainty of the borehole while others to address the geometric uncertainty of the structures mapped along the boreholes.

The following computations, made in Sicada using "CalcCoord", were made to address aspects of the borehole geometries:

1. computation of bearing and inclination using multiple measurements,
2. computation of the 90th percentile of differences between the measured and the computed bearings and inclinations along the borehole,
3. the spatial position of the borehole and,
4. computation of an uncertainty radius, as a measure of positional uncertainty of the borehole (and implicitly, structures measured therein).

For the objects in the boreholes the computations are:

1. computation of strike and dip using alpha/beta from geological mapping and bearing/inclination from computed borehole geometries (#1 above),
2. computation of uncertainties for alpha angles and,
3. computation of uncertainties for beta angles.

Note that calculations of strike/dip and uncertainties are currently made in Boremap, but the calculations will be moved to Sicada shortly.

Additionally, we have independently computed the same parameters as listed above to check that the algorithms have been correctly implemented in Sicada and Boremap. However, we did not obtain sufficient information to be able to address all aspects of the beta uncertainties.

4.1 Brief overview of algorithms

The calculations we describe in section 4.1.1–4.1.4 are made in Sicada (CalcCoord) whereas the calculations described in section 4.1.5–4.1.7 are presently made in Boremap but will be moved to Sicada shortly (BoremapAngleCalc).

4.1.1 Bearing and inclination from multiple measurements

All deviation measurements judged by the Activity leaders to be adequate for the construction of the borehole orientations are used as input for calculating the bearing and inclination along the borehole. The measurements stem either from parts of the borehole or the entire borehole. The activity EG154 in Sicada documents which of the measurements that have been used for computing the orientation of the hole and the rationale for the choice, in terms of a decision protocol.

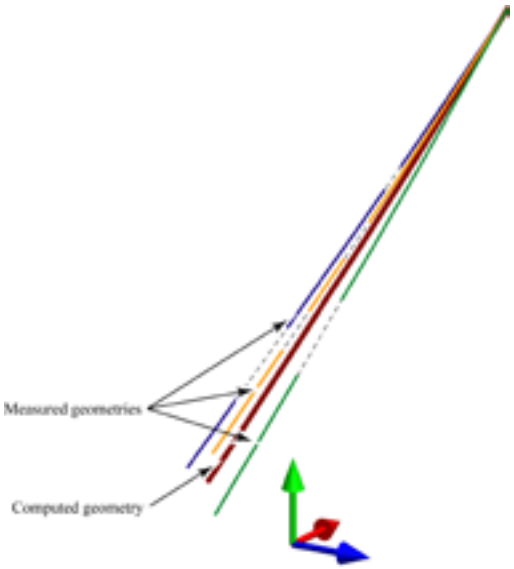

Figure 4-1. *Schematic illustration of the concept of computing borehole orientations from several, possibly incomplete, deviation measurements.*

The bearing and inclination are calculated at all 3 m intervals down the borehole, using the median from the group of all representative measurements at the actual 3 m interval, together with the values at one interval up and one interval down, as shown in example 1. If there are less than 2 different measurements in this group, no median is calculated and the blank field is later filled with a linear interpolation of the values above and below.

The borehole orientation is, accordingly, not a single measurement, as visualised in Figure 4-1, but the most likely estimate. This implies that it is also possible to calculate a probability of the orientation of the borehole and further on the probability in which volume the borehole will reside.

Example 1

In this example, three intervals of measurements, listed in Table 4-1, are subjectively chosen by the Activity leaders to be adequate for the construction of the borehole geometry. The bearing data from the three measurements are listed in Table 4-2. The coloured fields highlight the data that are chosen to be appropriate for geometry calculations. The calculated bearings are listed in Table 4-3 together with the data that underlay the calculations. For example, to calculate the bearing at 12 m borehole length, the median of the three coloured fields within the red frame in Table 4-2 is used. Please note that the uncoloured fields do not take part of the calculations since they are not chosen to be included according to Table 4-1. The data from the tables are visualized in Figure 4-2.

Table 4-1. The table lists which sections in different activities that are chosen to be adequate for calculating the borehole geometry, i.e. EG154 protocol.

Act_Id	Secup	Seclow
136527	15	459
287361	18	459
398393	12	459

Table 4-2. Measured bearing at different lengths in the boreholes, i.e. activities of type EG154, EG157 and EG159.

BH_len	136527	287361	398393
…	…	…	…
9	85.23	85.39	85.38
12	85.26	85.40	85.43
15	85.30	85.46	85.46
18	85.33	85.49	85.48
21	85.36	85.48	85.54
24	85.42	85.49	85.50
…	…	…	…

Table 4-3. Calculated bearing using the data in the two tables above.

BH_len	Bearing	Comment
9	–	only 1 measurement, i.e. not enough for calculations
12	85.430	median of [85.30 85.43 85.46]
15	85.445	median of [85.30 85.33 85.43 85.46 85.48 85.49]
18	85.470	median of [85.30 85.33 85.36 85.46 85.48 85.48 85.49 85.54]
21	85.480	median of [85.33 85.36 85.42 85.48 85.48 85.49 85.49 85.50 85.54]

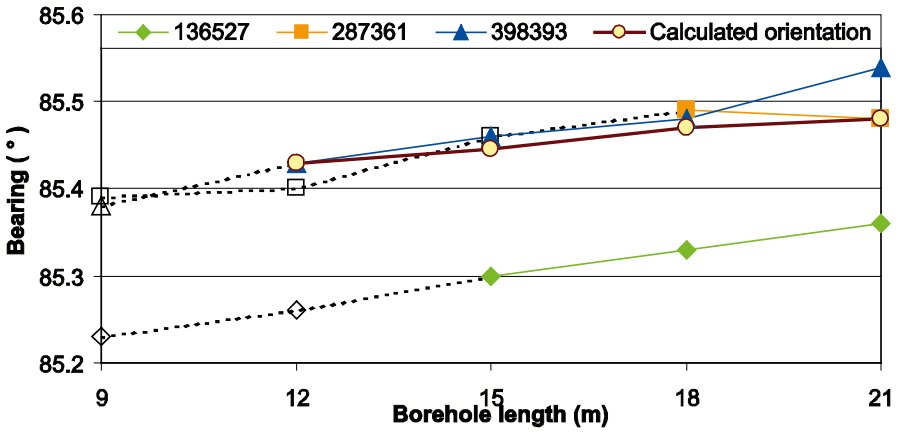

Figure 4-2. Calculated bearing for a fictive borehole together with the three chosen measurements.

4.1.2 90th percentile of differences between the measured and the calculated bearings and inclinations

Once the borehole orientation is calculated, the uncertainty can be computed using all measurements that are not marked as erroneous in Sicada. For all 3 m intervals where multiple measurements are made, i.e. more than one measure, the differences between the calculated and the measured orientations are computed.

All the computed differences along the borehole are stored in one set and the 90th percentile is calculated, see example 2. This value is then interpreted as the uncertainty of the orientation of the borehole. In the case where a borehole only has one measurement the uncertainties are set to the fixed values 4.9° for bearing and 1.8° for inclination. These values are based on the worst measured case among the prioritized boreholes at Forsmark and Laxemar.

Example 2

In the fictive borehole in example 1, above, one more deviation measurement was carried out that neither was judged to be erroneous nor chosen to be used for orientation calculations. All orientation data between 9 and 21 m are shown in Table 4-4 together with the calculated orientation from example 1. The absolute value of the differences between the measurements and the calculated orientation are computed as shown in Table 4-5. All the differences are put into one data set and the 90th percentile is calculated, in this example 0.1505°, see Figure 4-3. Observe that in this example only the five 3 m intervals shown in the tables are used for the calculation of the 90th percentile. In a real borehole, all 3 m intervals with more than one measurement are used.

Table 4-4. The Calculated bearings together with all measurements that are judged to be not erroneous.

BH_len	Calc Orient	136527	287361	398393	476219
…	…	…	…	…	…
9	85.385	85.23	85.39	85.38	85.42
12	85.430	85.26	85.40	85.43	85.37
15	85.445	85.30	85.46	85.46	85.33
18	85.470	85.33	85.49	85.48	85.32
21	85.480	85.36	85.48	85.54	85.33
…	…	…	…	…	…

Table 4-5. Absolute values of the differences between the measured and the calculated bearings.

BH_len	136527	287361	398393	476219
…	…	…	…	…
9	0.155	0.005	0.005	0.035
12	0.170	0.030	0.000	0.060
15	0.145	0.015	0.015	0.115
18	0.140	0.020	0.01.0	0.150
21	0.120	0.000	0.06.0	0.150
…	…	…	…	…

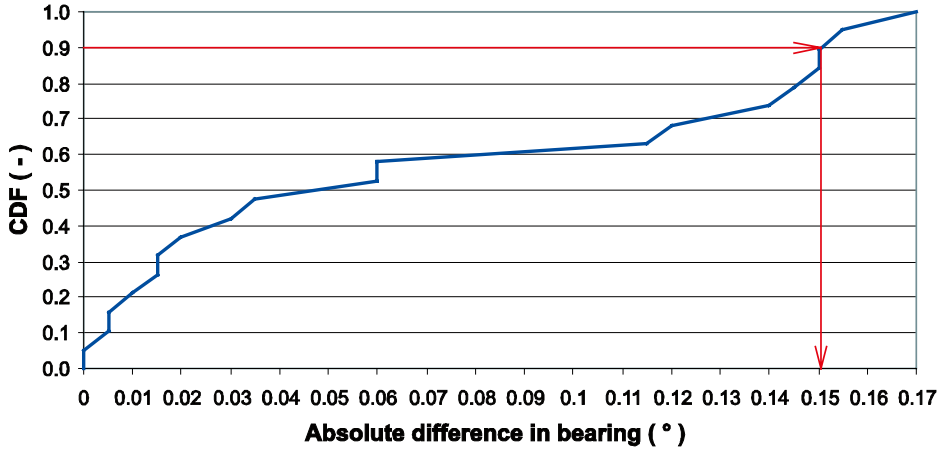

Figure 4-3. *The cumulative density function of the absolute differences between the calculated bearing and the measured. The 90th percentile in the example is 0.1505°.*

4.1.3 Spatial position of the borehole

The coordinates at all 3 m intervals are computed along the borehole using the bearing and inclination from the calculated orientations at the actual interval together with the coordinate and the bearing and inclination at the point above, see [1] and example 3.

$$\begin{bmatrix} x_i \\ y_i \\ z_i \end{bmatrix} = \begin{bmatrix} \cos(90-(B_i+B_{i-1})/2)\cdot\cos((I_i+I_{i-1})/2)\cdot l + x_{i-1} \\ \sin(90-(B_i+B_{i-1})/2)\cdot\cos((I_i+I_{i-1})/2)\cdot l + y_{i-1} \\ \sin((I_i+I_{i-1})/2)\cdot l + z_{i-1} \end{bmatrix} \quad [1]$$

where

x_i = the x-coordinate at current 3 m interval
x_{i-1} = the x-coordinate at the interval above the current
y_i = the y-coordinate at current 3 m interval
y_{i-1} = the y-coordinate at the interval above the current
z_i = the z-coordinate at current 3 m interval
z_{i-1} = the z-coordinate at the interval above the current
B_i = the bearing at current 3 m interval
B_{i-1} = the bearing at the interval above the current
I_i = the inclination at current 3 m interval
I_{i-1} = the inclination at the interval above the current
l = the length of the interval, i.e. 3 m

Example 3

The calculated bearings and inclinations from the fictive borehole are listed in Table 4-6 together with the coordinates of the top of casing of the borehole. Using these values the coordinate (x_i, y_i and z_i) for the borehole length 3 m can be calculated using equation [1] and the values from Table 4-6. When these coordinates are calculated the coordinates for the next 3 m interval can be computed using the newly calculated coordinates together with the orientations at actual interval and at the interval above. In Table 4-7 the coordinates for the first 21 m are calculated.

Table 4-6. Orientation data together with the coordinates at top of casing of the borehole.

BH_len	Incl	Bear	x	y	z
0	–82.310	85.360	157.163	624.398	12.350
3	–82.315	85.380	x_i	y_i	z_i
6	–82.320	85.395			
9	–82.325	85.385			
12	–82.335	85.430			
15	–82.350	85.445			
18	–82.360	85.470			
21	–82.355	85.480			
…	…	…			

$x_i = \cos(90–(B_i+B_{i–1})/2)\cdot\cos((I_i+I_{i–1})/2)\cdot(l_i–l_{i–1})+x_{i–1}$

$y_i = \sin(90–(B_i+B_{i–1})/2)\cdot\cos((I_i+I_{i–1})/2)\cdot(l_i–l_{i–1})+y_{i–1}$

$z_i = \sin((I_i+I_{i–1})/2)\cdot(l_i–l_{i–1})+z_{i–1}$

$x_i = \cos(90–(85.380+85.360)/2)\cdot\cos((–82.315+(–82.310))/2)\cdot(3–0)+ 157.163 = 157.563$

$y_i = \sin(90–(85.380+85.360)/2)\cdot\cos((–82.315+(–82.310))/2)\cdot(3–0)+ 624.398 = 624.430$

$z_i = \sin((–82.315+(–82.310))/2)\cdot(3–0)+ 12.350 = 9.377$

Table 4-7. Orientations and coordinates for the first 21 m of the borehole.

BH_len	Incl	Bear	x	y	z
0	–82.310	85.360	157.163	624.398	12.350
3	–82.315	85.380	157.563	624.430	9.377
6	–82.320	85.395	157.963	624.463	6.404
9	–82.325	85.385	158.362	624.495	3.431
12	–82.335	85.430	158.761	624.527	0.458
15	–82.350	85.445	159.160	624.559	–2.516
18	–82.360	85.470	159.558	624.590	–5.489
21	–82.355	85.480	159.955	624.622	–8.462
…	…	…	…	…	…

4.1.4 Uncertainty radius

The geometrical uncertainty can be computed using the calculated geometry together with the uncertainty in orientation. We have chosen to express the uncertainty as a single measure, the uncertainty radius. Well aware that it is possible to use the data to define other measures, we still think that it is a good approximation and an intuitive entity.

The uncertainty radius, R_U, is defined as the perpendicular distance to the borehole direction based on the 90th percentile in bearing and inclination. The uncertainty radius is calculated according to:

$$R_{U,n} = \sum_{i=1}^{n} (l_i - l_{i-1}) \cdot MAX\{\sin(I_U); \sin(B_U) \cdot \cos(I_i)\} \qquad [2]$$

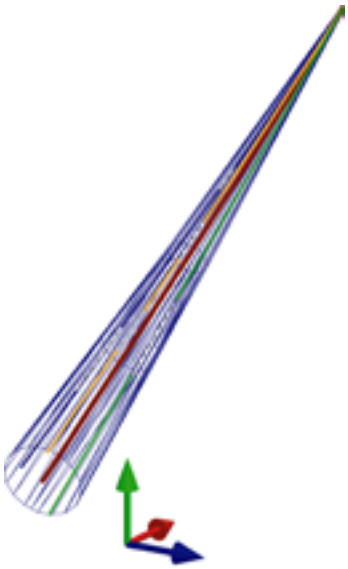

Figure 4-4. *Schematic illustration of borehole positional uncertainties, based on several deviation measurements according to [2].*

where

$R_{U,n}$ = The uncertainty radius at 3 m interval n

l_i = The borehole length at 3 m interval i

l_{i-1} = The borehole length at 3 m interval i–1

I_U = The inclination uncertainty, see section 4.1.2

B_U = The bearing uncertainty, see section 4.1.2

I_i = The inclination of the borehole at 3 m interval i

Example 4

The uncertainty radius can be calculated using the borehole orientations from example 3, listed in Table 4-8 together with the uncertainties in Table 4-9 (which are more realistic uncertainties than the one in example 2 that was based on 21 meters only). Using equation [2] the uncertainty radius can be calculated down the borehole. In the example the uncertainty radius is based on the Bearing uncertainty for the first 12 m and the inclination uncertainty between 15 and 21 m. Table 4-10 lists the radius uncertainty along the borehole.

Table 4-8. Orientations for the first 21 m of a borehole.

BH_len	Incl	Bear
0	–82.310	85.360
3	–82.315	85.380
6	–82.320	85.395
9	–82.325	85.385
12	–82.335	85.430
15	–82.350	85.445
18	–82.360	85.470
21	–82.355	85.480
…	…	…

Table 4-9. Orientation uncertainties.

Inclination uncertainty, I_U	Bearing Uncertainty, B_U
0.204°	1.532°

$R_{U,3m}$ = 0+ (3–0)·MAX[sin(0.204);**sin(1.532)·cos(–82.315)**]=0.010726

$R_{U,6m}$ = 0.010726+ (6–3)·MAX[sin(0.204);**sin(1.532)·cos(–82.320)**]=0.021444

$R_{U,9m}$ = 0.021444+ (9–6)·MAX[sin(0.204);**sin(1.532)·cos(–82.325)**]=0.032156

$R_{U,12m}$ = 0.032156+ (12–9)·MAX[sin(0.204);**sin(1.532)·cos(–82.335)**]=0.042854

$R_{U,15m}$ = 0.042854+ (15–12)·MAX[**sin(0.204)**;sin(1.532)·cos(–82.350)]=0.053535

Table 4-10. Orientations and the values 21 m of the borehole.

BH_len	Incl	Bear	sin(I_U)	Sin(B_U)·cos(I_I)	R_U
0	–82.310	85.360	0	0	0
3	–82.315	85.380	0.003560	**0.003575**	0.011
6	–82.320	85.395	0.003560	**0.003573**	0.021
9	–82.325	85.385	0.003560	**0.003571**	0.032
12	–82.335	85.430	0.003560	**0.003566**	0.043
15	–82.350	85.445	**0.003560**	0.003559	0.054
18	–82.360	85.470	**0.003560**	0.003554	0.064
21	–82.355	85.480	**0.003560**	0.003557	0.075
…	…	…	…	…	…

4.1.5 Strike and dip

The strike and dip of fractures and other rock structures are calculated using the alpha and beta angles mapped on the BIPS image, or the core if not visible in BIPS, together with the bearing and inclination of the borehole at the depth of the mapped structure.

The normal (pole) to the fracture plane can be expressed in terms of direction cosines as:

$$\begin{bmatrix}\lambda_1\\ \lambda_2\\ \lambda_3\end{bmatrix} = \begin{bmatrix} c(90-B)\cdot s(-I)\cdot c(-\beta)\cdot c(\alpha)-s(90-B)\cdot s(-\beta)\cdot c(\alpha)-c(90-B)\cdot c(-I)\cdot s(\alpha)\\ s(90-B)\cdot s(-I)\cdot c(-\beta)\cdot c(\alpha)+c(90-B)\cdot s(-\beta)\cdot c(\alpha)-s(90-B)\cdot c(-I)\cdot s(\alpha)\\ c(-I)\cdot c(-\beta)\cdot c(\alpha)+s(-I)\cdot s(\alpha)\end{bmatrix} \quad [3]$$

In which:

λ_1 = the x-cosine
λ_2 = the y-cosine
λ_3 = the z-cosine
I = inclination
B = bearing
α = the alpha angle
β = the beta angle
c = cosine
s = sine

The cosines are transferred to pole trend and plunge according to the equations:

$$\text{If } \lambda_3 > 0 \text{ then } \begin{bmatrix} \lambda_1 \\ \lambda_2 \\ \lambda_3 \end{bmatrix} = (-1) \cdot \begin{bmatrix} \lambda_1 \\ \lambda_2 \\ \lambda_3 \end{bmatrix} \quad [4]$$

$$Trend = \begin{cases} 450 - \arctan 2(\lambda_1, \lambda_2) & if \quad \arctan 2(\lambda_1, \lambda_2) > 90 \\ 90 - \arctan 2(\lambda_1, \lambda_2) & if \quad \arctan 2(\lambda_1, \lambda_2) \leq 90 \end{cases} \quad [5]$$

$$Plunge = \arcsin(-\lambda_3) \quad [6]$$

The pole trend and plunge are then transferred to strike and dip using:

$$Strike = \begin{cases} Trend + 90 & if \quad Trend < 270 \\ Trend - 270 & if \quad Trend \geq 270 \end{cases} \quad [7]$$

$$Dip = 90 - Plunge \quad [8]$$

4.1.6 Uncertainty of alpha

The alpha uncertainty is based on the two cores KFM06C and KLX07 that were mapped by two different teams of geologists. The results of the comparison are listed in Table 4-11. Currently, the alpha uncertainties are stored as rules in Boremap, but these will be transferred to Sicada shortly.

4.1.7 Uncertainty of beta

The beta uncertainty is calculated using the sum of the uncertainty of the beta roll of the BIPS image in each borehole and the uncertainty stemming from the mapping of the core. The uncertainty from the mapping is listed in Table 4-12. To obtain the total beta uncertainty, the mapping uncertainty in Table 4-12 must be added to the BIPS uncertainty in the Sicada table "bm_bips_beta_uncert", computed according to procedures in /Döse et al. 2008/. This is done in Sicada and all structures (e.g. fractures in p_fract_core) have a total orientation uncertainty assigned in terms of total alpha and total beta uncertainty (Table 4-13).

Table 4-11. The alpha uncertainty.

	α < 30°	30° ≤ α < 60°	60° ≤ α < 90°
Visible in BIPS	1.4	3.0	3.6
Not visible in BIPS	7.4	7.4	7.4

Table 4-12. The beta uncertainty (from core mapping only).

	α < 30°	30° ≤ α < 60°	60° ≤ α < 90°
Visible in BIPS	4	5.6	25
Not visible in BIPS	70	70	70

Table 4-13. Excerpt from the Sicada table p_fract_core showing orientation data.

STRIKE (degrees)	DIP (degrees)	ALPHA (degrees)	UNCERT_ALPHA (degrees)	BETA (degrees)	UNCERT_BETA (degrees)
108.5	48.3	57.2	3	84	11.6
39.5	82.7	10.7	1.4	246	10
77.1	42.6	40.2	3	60	11.6
121.1	81.2	41.4	3	133	11.6
126.6	81.9	43.3	3	140	11.6
103	50.7	52.3	3	84	11.6
17.4	36.4	18.1	1.4	25	10
…	…	…	…	…	…

4.2 Check of algorithms

Prior to in-use tagging of data in Sicada, we made an independent check that the algorithms implemented in Sicada performed as expected. The checks are briefly explained below. The codes used for these checks are listed in Appendix 2.

4.2.1 Bearing and inclination from multiple measurements

All data provided for bearing and inclination of boreholes are delivered with 2 decimals, i.e. one hundred of a degree and hence the largest difference between the stored data in Sicada and the test calculations should be 0.005.

This is fulfilled for the inclination in all prioritized boreholes at Forsmark and in 11 of 16 boreholes regarding bearing. The remaining boreholes, KFM01D, KFM02A, KFM06A, KFM08A and KFM08C, have a maximum difference that is 0.01 in bearing.

In KLX12A in Laxemar the maximum difference in bearing is 0.007 and exceeding the explicable but still small. Regarding the percussion boreholes the limit is exceeded in HLX13, HLX15 and HLX27, but still less than 0.01.

The difference is still small and hence judged to be of insignificant importance for uncertainty calculations. The source of these small differences will be tracked down when the algorithms are fully implemented in Sicada.

4.2.2 90th percentile of differences between measured and calculated borehole geometries

The maximum difference that can be explained by the number of digits is 0.005 for the 90th percentile uncertainty in bearing and inclination.

This is fulfilled for all 16 prioritized boreholes at Forsmark for both bearing and inclination, except for bearing in KFM06C, where the difference is 0.006.

None of the 47, prioritized, Laxemar boreholes, including cored and percussion drilled, have larger differences than 0.005 regarding the 90th percentile uncertainty in bearing or inclination.

The difference is judged to be negligible and hence further work to eliminate the difference is postponed to the time for implementing the algorithms in Sicada.

4.2.3 Spatial position of the borehole

The maximum observed difference between the location, i.e. x-, y- and z-coordinate, in Sicada and calculated from the excerptions from Sicada is less than 1 cm for all boreholes, except for KFM08A and 08C where it is 1.5 and 1.7 cm respectively. The differences are small and the algorithm is judged to be correctly implemented.

4.2.4 Uncertainty radius

No difference exceeds 7 mm regarding the uncertainty radius for the 16 prioritized boreholes in Forsmark and 47 prioritized in Laxemar.

4.2.5 The strike and dip

The calculation of strike and dip is carried out for the tables p_fract_core, p_rock and p_rock_feat and only for fractures that have a mapped angle (alpha/beta) together with Activity type GE041 (BOREMAP/BIPS/Core).

The 16 prioritized boreholes at Forsmark contain 56,514 data objects in total of which 55,478 fulfil the GE041 and angle criterion, i.e. 98%. The maximum dihedral angle difference between the stored values and the calculated is 0.5° with an arithmetic mean of 0.05°.

At Laxemar the prioritized boreholes contain 74,761 objects, and 73,141 of these fulfil the GE041 and angle criterion, i.e. 98%. The maximum difference in dihedral angle between the data stored in Sicada and the calculated using Sicada tables is 1.6°. The arithmetic mean is 0.07°. Four of the boreholes, KLX09, KLX09F, KLX10 and KLX29A, contribute to this slightly higher difference and hence focus should be set to these boreholes when sample testing the implementation of the algorithms in Sicada.

Despite these differences, we judge that the strike and dip are correctly implemented.

4.2.6 Uncertainty of alpha

Both for Forsmark and Laxemar data the differences between stored and the calculated uncertainties equal zero for all objects that have an orientation and are mapped using Activity type GE041. The implementation of the uncertainty of alpha is judged to be perfectly correct.

5 Quantification of changes to orientation data

5.1 Definitions

Here, we denote borehole geometries from December 2006 as "old geometries", and boreholes that have been subject to corrections of their geometries (April 2008) as "new geometries".

The changes are quantified by the following (see Figure 5-1 for details):

The absolute distance between any old SECUP and new SECUP is quantified by two measures. One measure regards the distance in 3D space between equivalent positions in old and new geometries respectively. This measure is denoted "absolute distance" (Figure 5-1a) and is computed as:

$$|d| = \sqrt{(x_{old} - x_{new})^2 + (y_{old} - y_{new})^2 + (z_{old} - z_{new})^2} \quad [9]$$

1. The vertical component of this vector, denoted ΔZ (Figure 5-1a), may be used by subsequent modellers to address differences in e.g. hydraulic pressures and densities. This is computed as:

   ΔZ = New "ELEVATION (m)" – Old "ELEVATION (m)"

   in which "ELEVATION (m)" is obtained from Sicada.

   As the computed Sicada parameter "ELEVATION (m)" is given as negative values with depth, a negative value of ΔZ means that the new position (e.g. adjusted_secup) is deeper than the old position.

2. One algorithm for computing borehole positional uncertainty is discussed in section 4.1.4. An outcome of that algorithm is a quantification of the positional uncertainty in terms of an uncertainty radius, R (Figure 5-1b), values of which are made public in the Sicada table as the parameter "RADIUS_UNCERT" in the table "OBJECT_LOCATION". The borehole geometry, and the uncertainty radius, are also published as RVS parameters, thereby enabling modellers to address the effect of borehole positional uncertainties.

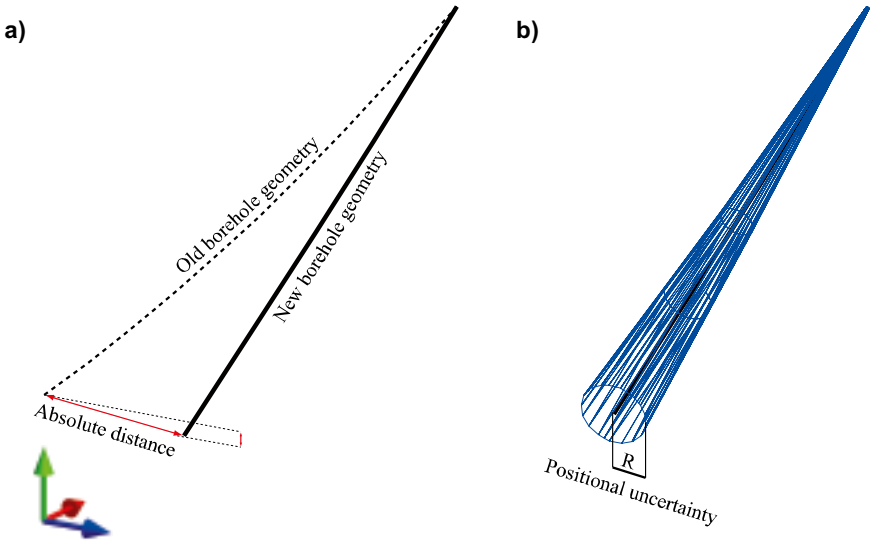

Figure 5-1. *Definitions used in this report.*

5.2 Analyses of borehole geometries

Changes to borehole geometries are summarised in Table 5-1. Please note that the boreholes KLX03, KLX06 and KLX11A did not have any "in-use" tagged deviation measurements in the database during December 22, i.e. treated as if they were perfectly straight.

A graphical representation of Table 5-1 is presented in Figure 5-2. For clarity, the legend has been excluded. However, graphs of each borehole, plotted separately, are provided in Appendix 3. The uncertainty in the Z coordinate can be obtained using procedures described in /Nilsson and Nissen 2007/.

Uncertainties in borehole geometries, "R(m)" in Table 5-1, display large variations. The representation of boreholes with positional uncertainties in RVS, can be visualised as shown in Figure 5-3.

Table 5-1. Summary statistics of borehole geometries at the bottom of the boreholes.

IDCODE	Length (m)	Absolute distance (m)	dZ (m)	Uncertainty radius (m)
KFM01A	1,001.49	0.33	0.04	31.46
KFM01B	500.52	0.19	0.05	15.72
KFM01D	800.24	4.97	–2.9	6.72
KFM02A	1,002.44	5.1	–0.16	9.23
KFM03A	1,001.19	0.11	0.01	31.45
KFM03B	101.54	0.02	0	3.19
KFM04A	1,001.42	3.48	–2.17	8.7
KFM05A	1,002.71	0.47	0.05	16.6
KFM06A	1,000.64	3.93	1.06	10.38
KFM06B	100.33	0.02	–0.01	3.15
KFM06C	1,000.91	11.03	–5.01	12.6
KFM07A	1,002.1	15.58	–4.21	5.92
KFM07B	298.93	8.3	–4.94	9
KFM07C	500.34	3.02	0.21	3.01
KFM08A	1,001.19	11.37	–6.8	14.12
KFM08B	200.54	2.58	0.24	3.27
KFM08C	951.08	1.13	0.19	7.42
KFM09A	799.67	10.22	0.18	15.2
KFM09B	616.45	10.47	–6.7	14.09
KFM10A	500.16	2.2	–1.54	4.28
KFM11A	851.21	0.56	–0.12	15.53
KLX01	1,077.99	2.47	0	56.42
KLX02	1,700.5	5.63	0	89
KLX03	1,000.42	9.85	–0.1	31.42
KLX04	993.49	0.16	0.01	31.21
KLX05	1,000.16	18.41	–2.94	26.86
KLX06	994.94	214.06	96.16	17.79
KLX07A	844.73	4.75	–2.96	14.82
KLX07B	200.13	0.38	–0.03	0.51
KLX08	1,000.41	5.7	–1.35	15.03
KLX09	880.38	11.59	1.33	15.21
KLX09B	100.22	0.13	0	0.34
KLX09C	120.05	0.5	0.05	0.91

IDCODE	Length (m)	Absolute distance (m)	dZ (m)	Uncertainty radius (m)
KLX09D	121.02	0.26	0	1.5
KLX09E	120	0.07	–0.03	0.83
KLX09F	152.3	0.02	–0.01	0.91
KLX09G	100.1	0.06	–0.01	1.03
KLX10	1,001.2	12.62	1.43	15.95
KLX10B	50.25	0.19	–0.01	0.73
KLX11A	992.29	6.54	–2.11	14.29
KLX11B	100.2	0.06	0	0.24
KLX11C	120.15	0.05	0	0.65
KLX11D	120.35	0.19	0.01	1.01
KLX11E	121.3	0.16	–0.05	0.65
KLX11F	120.05	0.05	–0.01	0.65
KLX12A	602.29	12.3	–3.3	4.04
KLX13A	595.85	7.75	–1.01	10.33
KLX17A	701.08	41.69	15	30.92
KLX18A	611.28	3.18	–0.55	4.43
KLX19A	800.07	9.24	–5.15	13.89
KLX20A	457.92	3.7	–2.51	5.75
KLX21A	75	1.25	–0.2	1.18
KLX21B	858.78	32.4	11.27	18.24
KLX22A	100.45	0.14	–0.07	0.6
KLX22B	100.25	0.18	0	1.2
KLX23A	100.15	0.04	0.01	0.42
KLX23B	50.27	0.02	0	0.24
KLX24A	100.17	0.08	0.03	0.77
KLX25A	50.24	0.01	0	0.25
KLX26B	50.37	0.01	0	0.27
KLX28A	80.23	0.22	–0.01	1.09
KLX28A	80.23	0.48	0.04	1.09
KLX29A	60.25	0.07	0	0.45
KLX29A	60.25	1.4	0.09	0.45

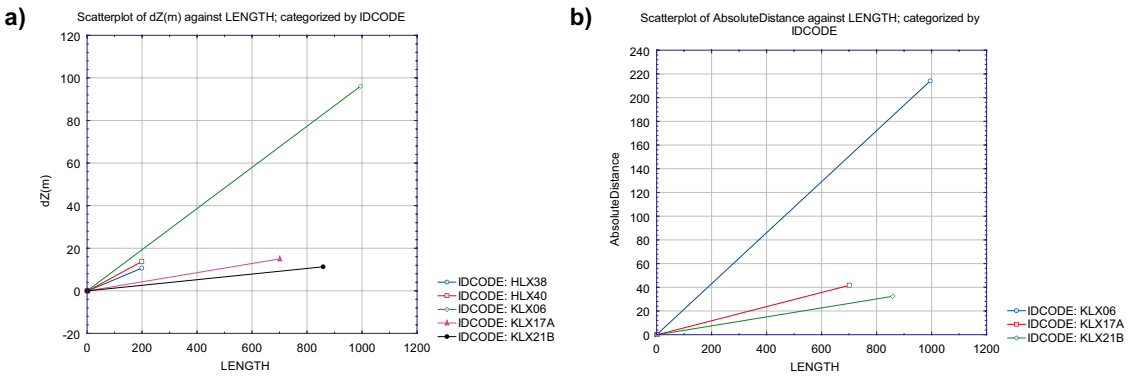

Figure 5-2. *Changes to borehole geometries expressed as (a) vertical deviation (ΔZ) and (b) absolute distance along borehole length. For clarity, only boreholes with ΔZ exceeding 10 m were included in "a", and in "b", only boreholes with maximum distance exceeding 25 m were included.*

a)

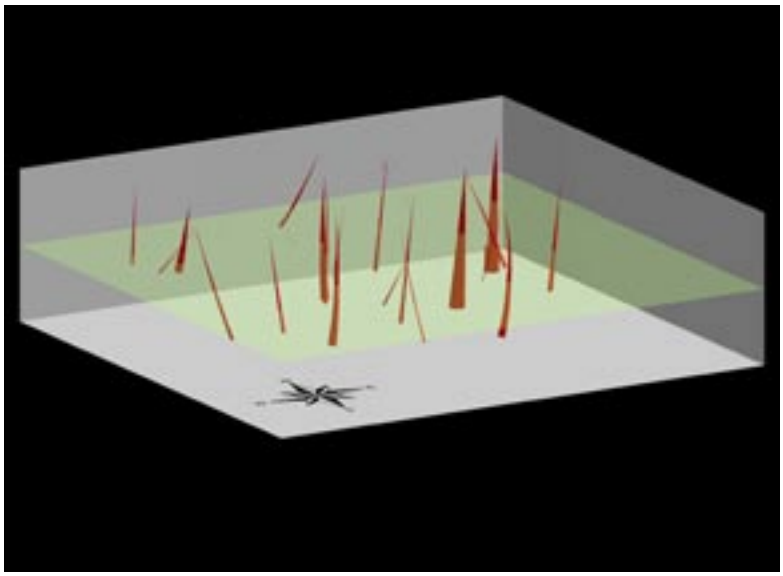

b)

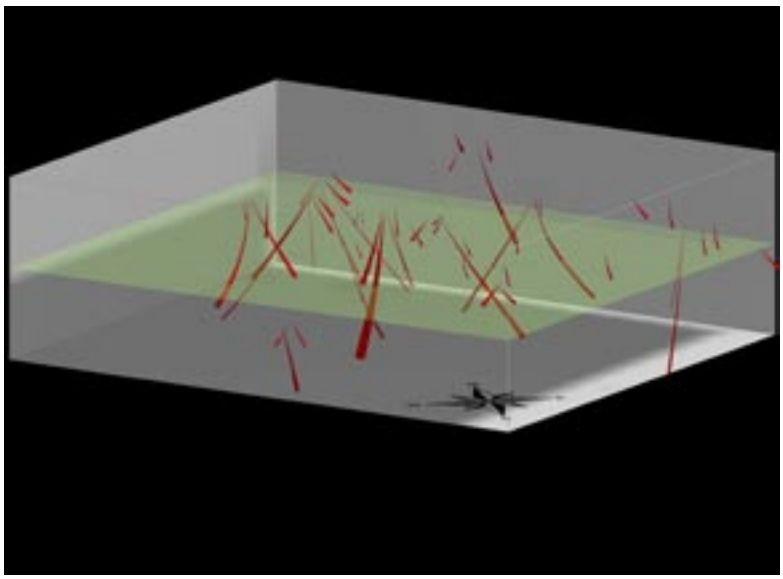

Figure 5-3. *RVS visualisation of uncertainty in borehole positions. a) Laxemar, local model volume. b) Forsmark, local model volume. The green horizon represents a possible repository depth (–500 m).*

5.3 Analyses of orientation data

Though the task assigned to the task force encompassed all orientation data in Sicada, we focus the analyses published here to borehole *fractures* as their locations are spread over the entire boreholes and should thus constitute an adequate proxy for other orientation data such as rock contacts, structures, radar measurements, stress measurements, etc. We here nevertheless analyse rock contact and structure orientations, but to a lesser extent.

Additionally, we performed a special study on PFL-f features[11], upon the explicit request of the SDM modelling groups.

[11] PFL is an abbreviation for Posiva Flow Log. PFL-f features, in this context, refer to the fracture that is judged to cause the anomaly.

5.3.1 Definitions

Orientations are measured as so called alpha and beta angles. That is, structure orientations are *mapped* as azimuth and inclination relative to the borehole axis and the strike and dip values, as provided in Sicada, are *computed* from these angles and the borehole geometry.

The procedure for estimating/computing the uncertainty in the measurement of alpha and beta angles were originally addressed in Nissen and Stigsson[12]. We recall that the beta uncertainty regards a rotational symmetry around the borehole axis, whereas the alpha uncertainty regards a symmetry perpendicular to the borehole in a plane containing its axis (Figure 5-4a). Figure 5-4b illustrates an example of bracketed uncertainties within specified alpha and beta uncertainty ranges.

In addition to uncertainties connected to the mapping of fractures, there is an uncertainty regarding borehole geometries. As strike and dip are computed from both alpha, beta and the borehole geometry, the borehole geometry uncertainty needs to be propagated into the strike/dip, and expressed in terms of a structure orientation uncertainty as visualised in Figure 5-5a.

The goal stated for this project[13] was to strive towards a total fracture orientation uncertainty less than or equal to 10°, expressed as a dihedral angle from the estimated orientation of the fracture normal. We have therefore found it practical, for comparative purposes, to express the orientation uncertainty in terms of a single value, Ω, that encompasses the combination of maximum alpha and maximum beta uncertainties, according to Figure 5-5b. It should be noted that the measure "Ω" should be avoided for simulation purposes as the possible range of uncertainties for a particular fracture is less than the range outlined by "Ω" and use thereof would yield overly conservative uncertainty estimates.

However, the vast majority of the uncertainty spaces (the shaded area in Figure 5-4b) are small and equidimensional. This means that the difference between the shape and area depicted by Ω and the ones depicted by the uncertainty spaces is small and the use of Ω might still be justified. That is, provided that the aspect ratio of alpha and beta uncertainty ranges is not too large, Ω can be computed according to the algorithm provided in terms of VB code in Appendix 2, enabling modellers to implement this measure in their analyses, if so desired.

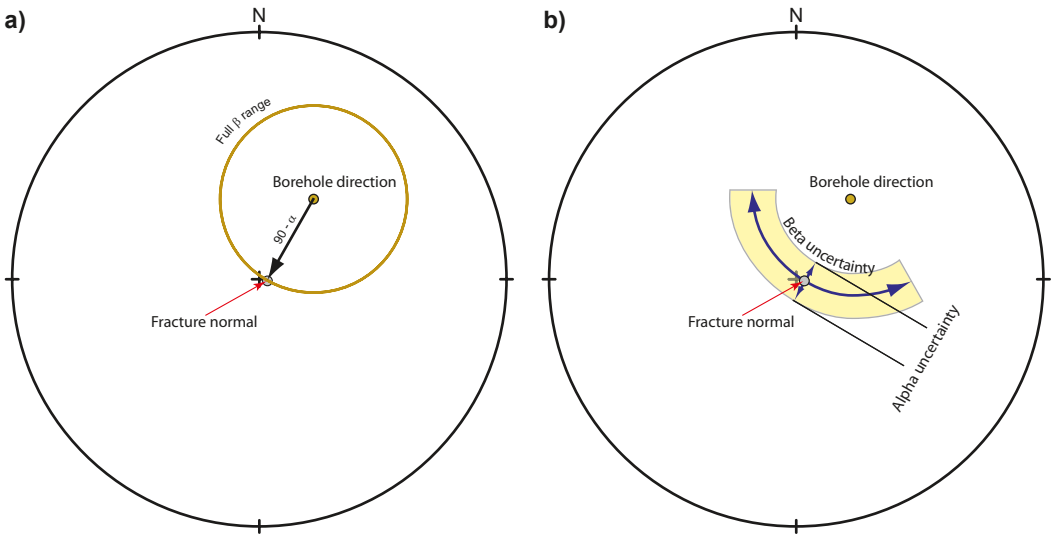

Figure 5-4. *Definition of the alpha (a) and beta (b) uncertainty.*

[12] Internal SKB document. Documentum ID 1063373.

[13] Internal SKB document. Documentum ID 1062926.

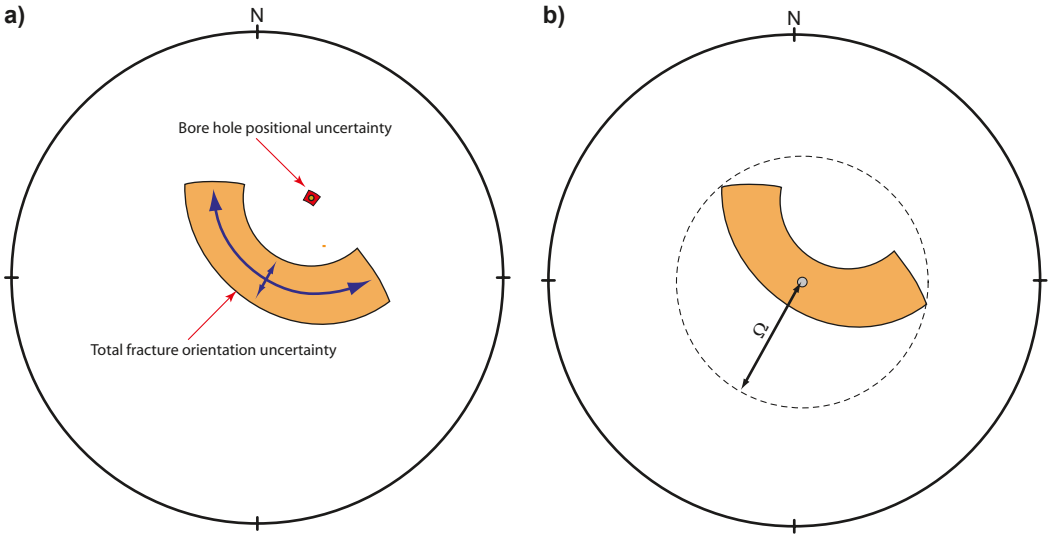

Figure 5-5. *Definition of the fracture orientation uncertainty.*

To quantify the difference between old and new data tables in Sicada, we have found it practical to make use of the dihedral angle, θ, between the normals of the fractures (Figure 5-6). The dihedral angle quantifies in a single value the differences in trend and in plunge of the two compared normals. The advantage is that small 3D changes in orientation of subhorisontal fractures will be reflected as small θ values, thereby avoiding the misleading importance of strike for such fractures.

As long as uncertainties are disregarded, comparison between old and new orientations is simple, and θ provides an adequate and unique measure. However, comparison is more complicated when uncertainties are taken under consideration (note that uncertainties are only defined for new data). For this, we define two other measures, θ_{min} and θ_{max} (see Figure 5-7 for explanation).

As shown on Figure 5-7a, the shape of the uncertainty space for a fracture orientation is rather complex, and can, to our knowledge, not with ease be solved analytically. The computation of θ_{min} and θ_{max}, as implemented here, therefore includes a search for minimum and maximum dihedral angle, according to procedures given in Appendix 2. Figure 5-7a shows a tentative example of a situation when the old orientation lies beyond the uncertainty space of the new orientation.

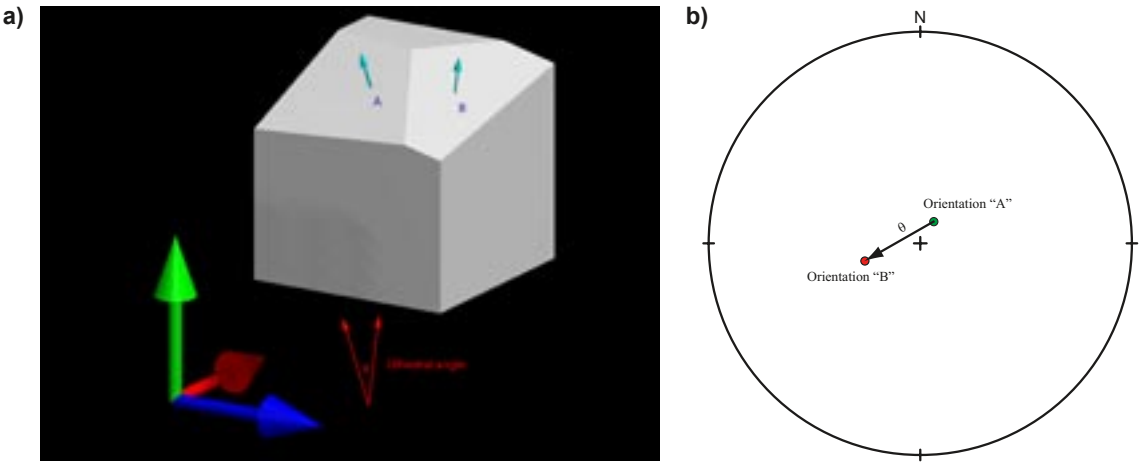

Figure 5-6. *Definition of the dihedral angle between two fracture normals, θ. Two subhorisontal surfaces are shown in (a). In (b), the normals to the planes are shown on a stereonet with the dihedral angle θ.*

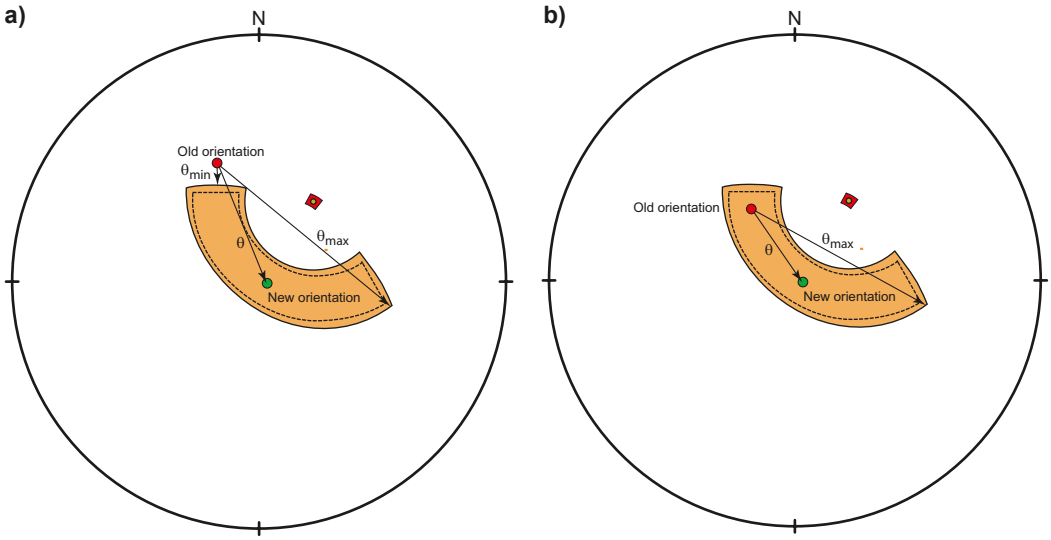

Figure 5-7. *Definition of θ_{min} and θ_{max}. See text for further explanation.*

The angular distances θ_{min} and θ_{max} are simply the shortest and longest distances respectively from the old position to the new positions uncertainty space as projected onto the hemisphere. If, however, the old position lies within the uncertainty space of the new position (Figure 5-7b), then θ_{min} reduces to zero. For most situations θ_{max} can be significantly larger than using θ alone. Hence, if it is regarded critical by the modellers to fully address the difference between old and new orientation data, the measures θ_{min} and θ_{max} should also be taken under consideration.

5.3.2 Quantification of difference between old an new orientations

Fractures

To be able to perform the comparison between old and new data, each fracture instance must have a unique "Feature ID", an orientation and an orientation uncertainty. In practice, this excludes all Activity Types but GE041 for fracture analysis using p_fract_core.

Forsmark

The differences between old and new fracture orientation data are summarised in Table 5-2 and Figure 5-8 (Graphs of each borehole are provided in Appendix 3). The mean dihedral angle, θ, varies between roughly 0.4° and 13.3° with an average of roughly 2.5°. With the exception of KFM02A, KFM03A, KFM03B and KFM07C, the average differences are small.

Table 5-2. Summary statistics of difference between old and new fracture orientations.

Breakdown Table of Descriptive Statistics (Comparison of FRACTURE orientations in DEC06_APR08_statistics.stw) N=56690 (No missing data in dep. var. list) Include condition: (SITE = 'FORSMARK')				
IDCODE	Theta Means	Theta N	Percentile 90.00000	Percentile 95.00000
KFM01A	5.89740	1472	12.43000	14.99000
KFM01B	3.08768	1641	6.82000	7.56000
KFM01C	1.35948	5419	3.23000	4.02000
KFM01D	0.99712	1631	2.06000	3.98000
KFM02A	9.32795	1816	21.41000	33.44000
KFM03A	13.30503	1755	24.82000	33.15000
KFM03B	13.17797	192	20.81000	21.14000
KFM04A	0.81141	4289	1.58000	2.05000
KFM05A	1.16392	2823	2.51000	3.41000
KFM06A	1.57902	3658	3.45000	5.06000
KFM06B	0.50833	552	0.93000	1.18000
KFM06C	1.02970	4424	2.03000	2.60000
KFM07A	1.58946	3172	2.69000	3.16000
KFM07B	1.43119	1677	1.96000	2.10000
KFM07C	8.62922	1764	14.99000	18.55000
KFM08A	1.77757	4265	4.03000	5.12000
KFM08B	1.04954	743	1.75000	1.90000
KFM08C	4.36992	4196	7.61000	8.97000
KFM09A	0.39591	5017	0.65000	0.76000
KFM09B	0.91524	3491	1.41000	1.56000
KFM10A	1.81683	2693	3.26000	3.46000
All Grps	2.51145	56690	6.11000	9.80000

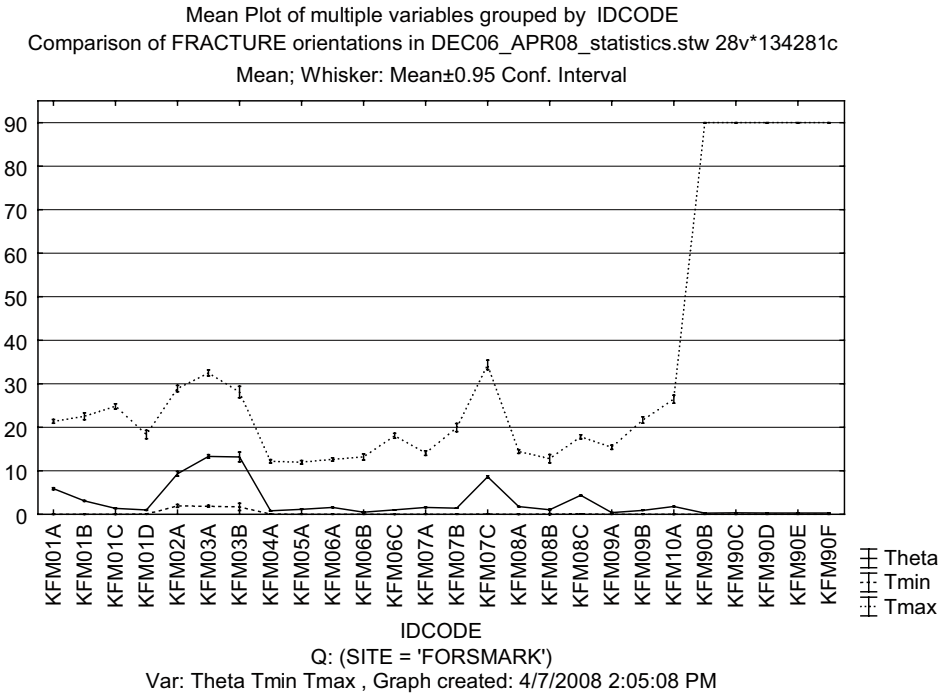

Figure 5-8. *Mean dihedral angle, θ, between old and new fracture orientations. The dashed lines outline mean θ_{min} and mean θ_{max}.*

Laxemar

The differences between old and new fracture orientation data are summarised in Table 5-3 and Figure 5-9 (Graphs of each borehole are provided in Appendix 3). In general, the differences in mean dihedral angle are very small.

Table 5-3. Summary statistics of difference between old and new fracture orientations.

Breakdown Table of Descriptive Statistics (Comparison of FRACTURE orientations in DEC06_APR08_statistics.stw)
Smallest N for any variable: 70759
Include condition: (SITE = 'LAXEMAR')

IDCODE	Theta Means	Theta N	Percentile 90.00000	Percentile 95.00000
KLX03	4.221653	4248	9.810000	11.42000
KLX04	2.611152	5183	6.210000	8.07000
KLX05	2.228691	3477	4.530000	4.85000
KLX07A	0.761083	6272	1.300000	1.50000
KLX08	1.234564	5296	2.720000	3.34000
KLX09	0.907048	4597	1.390000	1.56000
KLX09B	3.375497	584	7.380000	11.50000
KLX09C	0.629703	740	1.360000	1.59500
KLX09D	1.483333	855	2.550000	2.82000
KLX09E	1.770212	989	3.820000	4.73000
KLX09F	0.424530	1022	0.720000	0.92000
KLX09G	4.258804	828	6.490000	7.31000
KLX10	1.011109	5519	1.640000	2.00000
KLX10B	0.939007	604	1.760000	2.07000
KLX10C	1.439889	1533	3.440000	4.36000
KLX11A	1.837358	5341	4.170000	4.80000
KLX11B	3.627562	443	9.130000	12.27000
KLX11C	2.502623	446	6.000000	7.15000
KLX11D	2.026097	679	3.860000	4.50000
KLX11E	2.707298	655	6.690000	7.68000
KLX11F	2.191446	408	5.480000	6.42000
KLX12A	2.483127	2945	6.140000	8.12000
KLX13A	2.060936	3654	4.090000	5.65000
KLX14A	0.683988	1447	1.510000	2.33000
KLX18A	1.281207	3058	3.350000	4.71000
KLX19A	1.405385	2626	3.170000	4.15000
KLX20A	0.844175	2261	1.840000	3.07000
KLX22A	0.401010	693	0.670000	0.78000
KLX22B	2.498443	668	7.020000	8.60000
KLX23A	0.401667	204	0.670000	0.75000
KLX23B	0.743186	113	2.310000	3.33000
KLX24A	0.409126	881	0.690000	0.84000
KLX25A	0.365814	344	0.560000	0.63000
KLX26A	0.816067	801	1.940000	2.63000
KLX26B	3.753121	346	6.470000	6.69000
KLX28A	2.538639	551	5.060000	6.02000
KLX29A	0.995692	448	3.240000	3.78000
All Grps	1.707135	70759	4.180000	5.63000

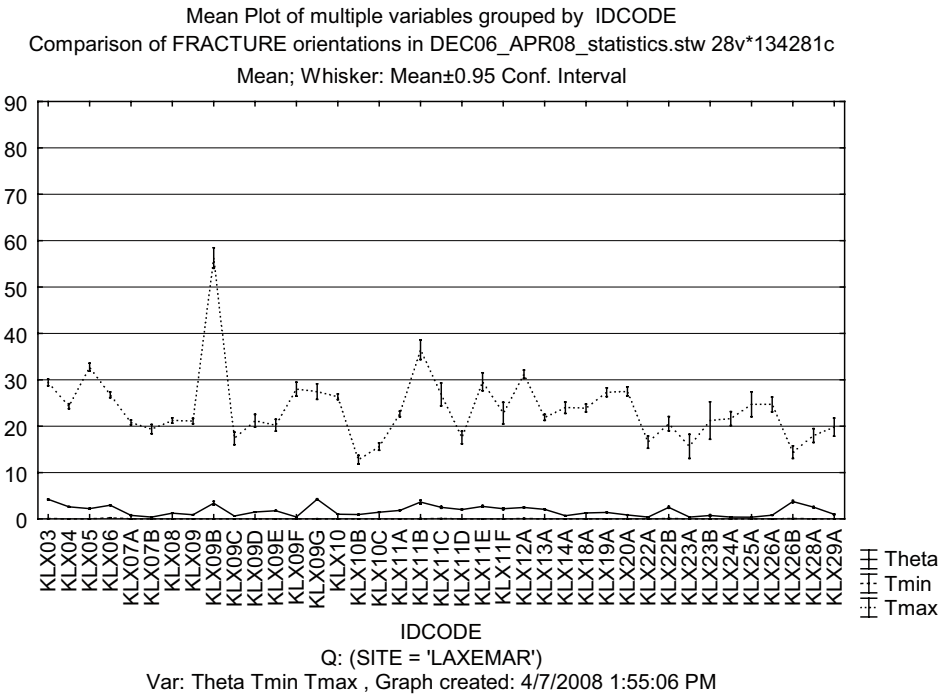

Figure 5-9. *Mean dihedral angle, θ, between old and new fracture orientations. The dashed lines outline mean θ_{min} and mean θ_{max}.*

Rock mass structures

There are different kinds of structures recorded in Sicada (Table 5-4). To restrict the extent of analyses, we here focus on the two largest subsets: “Foliated” and “Ductile Shear Zone”.

Structures of type “Foliated” represent the penetrative fabric in the rock. In the SDM, these are usually treated in terms of averages over the domains of interest. The “Ductile Shear Zone” and “Brittle-Ductile Shear zone”, on the other hand, represent intersections with structures that, mostly, are modelled deterministically. The implications of the analyses presented here are thus different for these to subclasses of structures.

The results of the analyses for each site are displayed below. In Forsmark we analysed “Foliated” and “Ductile Shear zone”, which together constitute over 90% of the structure data, Table 5-4 to Table 5-6 together with Figure 5-10 and Figure 5-11, whereas for Laxemar, we analysed “Foliated”, “Ductile Shear zone” and “Brittle-Ductile Shear zone” constituting roughly 70% of the data, Table 5-7 to Table 5-10 and Figure 5-12 to Figure 5-14.

Forsmark

Table 5-4. Types of structures recorded in Sicada

Category	Frequency table: TYPE: TYPE (Comparison of STRUCTURE orientations in DEC06_APR08_statistics.stw) Include condition: (SITE = 'FORSMARK') Count	Cumulative Count	Percent	Cumulative Percent
Foliated	1443	1443	74.88324	74.8832
Ductile Shear Zone	339	1782	17.59211	92.4754
Brittle-Ductile Shear Zone	111	1893	5.76025	98.2356
Brecciated	12	1905	0.62273	98.8583
Cataclastic	7	1912	0.36326	99.2216
Banded	10	1922	0.51894	99.7405
Mylonitic	5	1927	0.25947	100.0000
Missing	0	1927	0.00000	100.0000

Table 5-5. Summary statistics of difference between old and new structure orientations of type "Foliated".

Breakdown Table of Descriptive Statistics (Comparison of STRUCTURE orientations in DEC06_APR08_statistics.stw)
N=1424 (No missing data in dep. var. list)
Include condition: (SITE = 'FORSMARK') AND (TYPE = 'Foliated')

IDCODE	Theta Means	Theta N	Percentile 90.00000	Percentile 95.00000
KFM01A	7.45150	113	15.68000	16.90000
KFM01B	3.05684	38	6.40000	7.34000
KFM01C	2.68257	35	6.05000	6.93000
KFM01D	1.11333	75	2.96000	3.83000
KFM02A	15.27500	14	50.48000	53.65000
KFM03A	8.33686	35	15.00000	22.57000
KFM03B	11.29500	6	15.50000	15.50000
KFM04A	0.87126	119	1.70000	2.30000
KFM05A	0.99515	68	2.43000	2.89000
KFM06A	1.33700	80	2.61500	3.57500
KFM06B	0.52714	7	1.16000	1.16000
KFM06C	1.11046	65	2.01000	2.42000
KFM07A	1.82525	101	2.61000	3.06000
KFM07B	1.25143	70	1.77000	1.90000
KFM07C	13.93750	32	17.93000	20.19000
KFM08A	1.72780	141	3.58000	4.74000
KFM08B	1.39943	35	1.96000	2.49000
KFM08C	3.92838	117	7.15000	7.92000
KFM09A	0.50917	120	0.84500	0.89000
KFM09B	0.75785	65	1.13000	1.20000
KFM10A	1.31261	88	2.65000	2.76000
All Grps	2.63989	1424	6.55000	11.15000

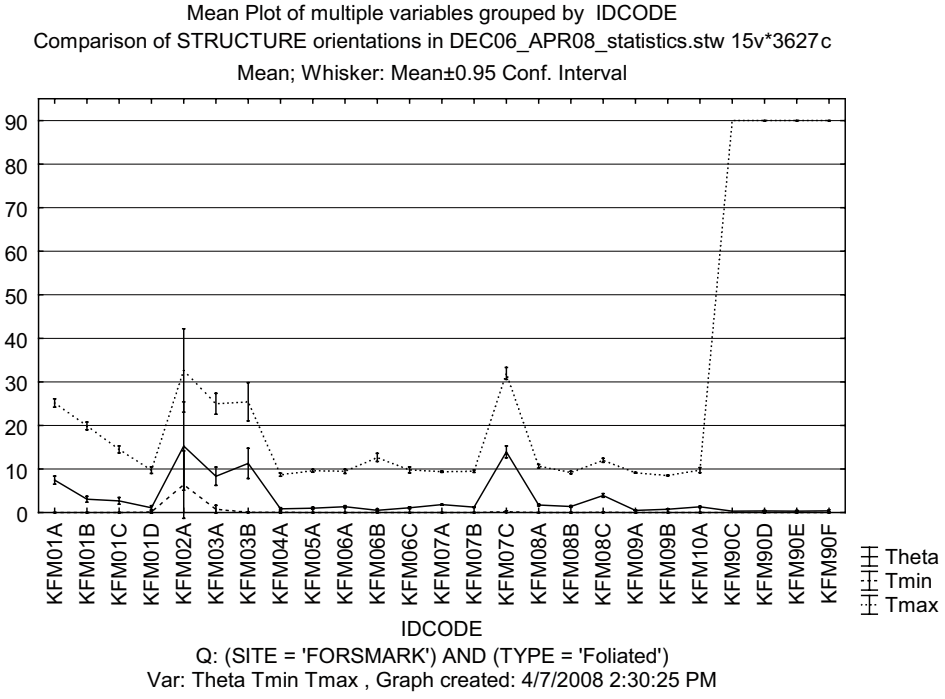

Figure 5-10. *Dihedral angle, θ, between old and new structure orientations. The dashed lines outline* θ_{min} *and* θ_{max}.

Table 5-6. Summary statistics of difference between old and new structure orientations of type "Ductile Shear Zone".

Breakdown Table of Descriptive Statistics (Comparison of STRUCTURE orientations in DEC06_APR08_statistics.stw)
N=339 (No missing data in dep. var. list)
Include condition: (SITE = 'FORSMARK') AND (TYPE = 'Ductile Shear Zone')

IDCODE	Theta Means	Theta N	Percentile 90.00000	Percentile 95.00000
KFM01A		0		
KFM01B	1.41167	6	3.08000	3.08000
KFM01C	0.46000	2	0.63000	0.63000
KFM01D	0.52500	6	0.92000	0.92000
KFM02A	1.55500	4	3.09000	3.09000
KFM03A	14.65000	6	28.21000	28.21000
KFM03B	9.90000	1	9.90000	9.90000
KFM04A	1.04921	63	1.91000	2.66000
KFM05A	0.63308	13	1.03000	2.60000
KFM06A	0.94800	20	1.68500	1.82000
KFM06B	1.53000	1	1.53000	1.53000
KFM06C	0.96455	11	1.51000	3.10000
KFM07A	1.86353	51	2.81000	3.49000
KFM07B		0		
KFM07C	17.94333	3	18.06000	18.06000
KFM08A	1.80638	47	4.54000	5.50000
KFM08B	1.43500	8	2.91000	2.91000
KFM08C	3.20214	14	4.65000	11.39000
KFM09A	0.46987	76	0.80000	0.91000
KFM09B	0.61250	4	0.76000	0.76000
KFM10A	1.70333	3	1.77000	1.77000
All Grps	1.63817	339	2.91000	4.65000

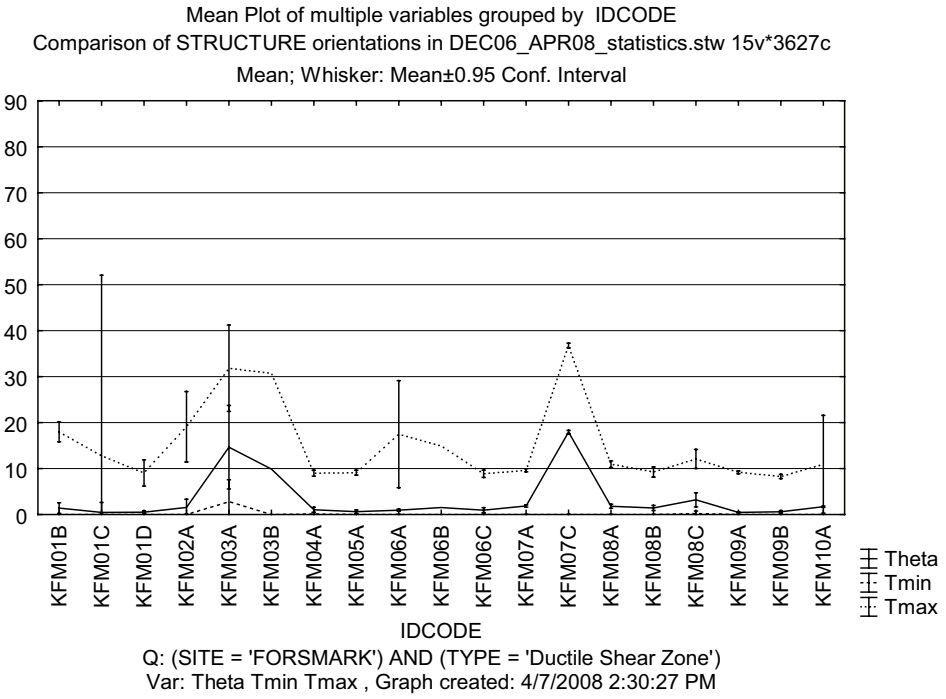

Figure 5-11. *Dihedral angle between old and new structure orientations of type "Ductile Shear Zone". The dashed lines outline θ_{min} and θ_{max}.*

Laxemar

Table 5-7. Types of structures recorded in Sicada.

Category	Frequency table: TYPE: TYPE (Comparison of STRUCTURE orientations in DEC06_APR08_statistics.stw) Include condition: (SITE = 'LAXEMAR') Count	Cumulative Count	Percent	Cumulative Percent
Foliated	477	477	40.76923	40.7692
Ductile Shear Zone	124	601	10.59829	51.3675
Brittle-Ductile Shear Zone	253	854	21.62393	72.9915
Brecciated	92	946	7.86325	80.8547
Cataclastic	68	1014	5.81197	86.6667
Banded	92	1106	7.86325	94.5299
Mylonitic	59	1165	5.04274	99.5726
Veined	2	1167	0.17094	99.7436
Bedded	2	1169	0.17094	99.9145
Schistose	1	1170	0.08547	100.0000
Missing	0	1170	0.00000	100.0000

Table 5-8. Summary statistics of difference between old and new structure orientations of type “Foliated”.

Breakdown Table of Descriptive Statistics (Comparison of STRUCTURE orientations in DEC06_APR08_statistics.stw)
N=461 (No missing data in dep. var. list)
Include condition: (SITE = 'LAXEMAR') AND (TYPE = 'Foliated')

IDCODE	Theta Means	Theta N	Percentile 90.00000	Percentile 95.00000
KLX03	3.469091	11	6.340000	6.85000
KLX04	2.487000	30	7.930000	10.23000
KLX05	2.682222	27	4.380000	5.02000
KLX07A	0.435000	8	0.990000	0.99000
KLX08	0.998750	8	1.960000	1.96000
KLX09	0.896765	34	1.410000	1.44000
KLX09B		0		
KLX09C		0		
KLX09D	0.910000	3	1.300000	1.30000
KLX09E	0.440000	1	0.440000	0.44000
KLX09F	0.340000	3	0.410000	0.41000
KLX09G		0		
KLX10	1.000000	6	1.980000	1.98000
KLX10B	1.950000	1	1.950000	1.95000
KLX10C	3.270000	1	3.270000	3.27000
KLX11A	1.419231	39	4.020000	4.62000
KLX11B	4.265000	10	6.435000	6.61000
KLX11C	2.609167	12	5.220000	6.27000
KLX11D	3.488000	5	4.850000	4.85000
KLX11E	1.882222	27	3.660000	3.93000
KLX11F	1.407857	14	4.400000	4.56000
KLX12A	1.494444	27	3.610000	5.52000
KLX13A	1.786852	54	4.560000	6.01000
KLX14A	0.476667	6	1.080000	1.08000
KLX18A	0.842222	9	3.610000	3.61000
KLX19A	1.041613	31	2.300000	3.33000
KLX20A	1.016897	29	3.390000	3.40000
KLX22A	0.448125	16	0.580000	1.03000
KLX22B	3.892667	15	5.930000	6.44000
KLX23A	0.332500	8	0.630000	0.63000
KLX23B	0.790000	1	0.790000	0.79000
KLX24A	0.366154	13	0.540000	0.60000
KLX25A	0.120000	2	0.140000	0.14000
KLX26A	0.616667	6	1.210000	1.21000
KLX26B		0		
KLX28A	2.807500	4	3.270000	3.27000
KLX29A		0		
All Grps	1.643905	461	4.260000	5.30000

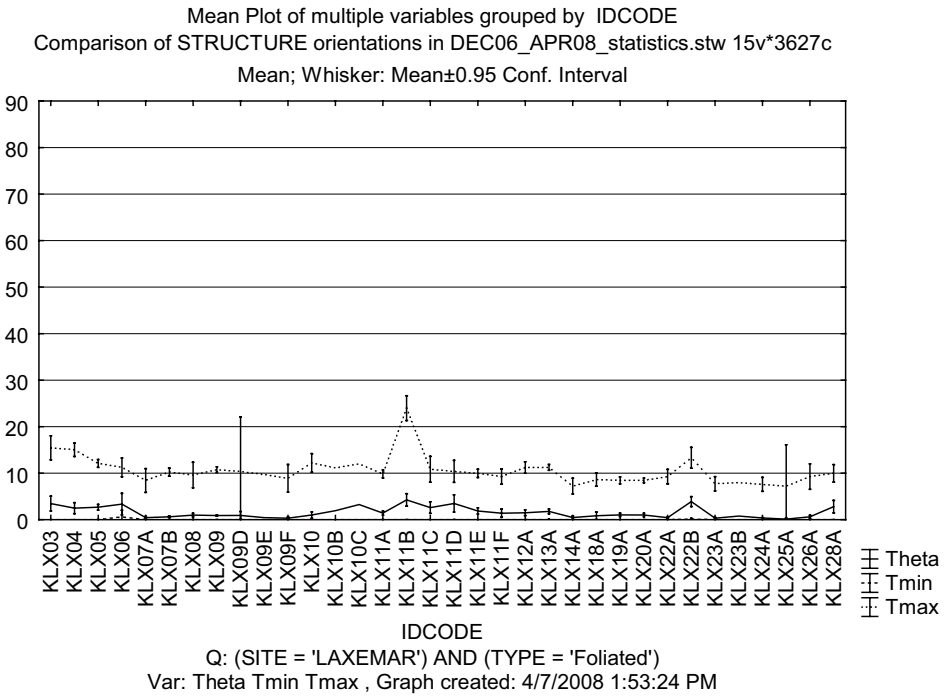

Figure 5-12. *Dihedral angle, θ, between old and new structure orientations. The dashed lines outline θ_{min} and θ_{max}.*

Table 5-9. Summary statistics of difference between old and new structure orientations of type "Ductile Shear Zone".

Breakdown Table of Descriptive Statistics (Comparison of STRUCTURE orientations in DEC06_APR08_statistics.stw)
N=118 (No missing data in dep. var. list)
Include condition: (SITE = 'LAXEMAR') AND (TYPE = 'Ductile Shear Zone')

IDCODE	Theta Means	Theta N	Percentile 90.00000	Percentile 95.00000
KLX03		0		
KLX04		0		
KLX05	0.540000	2	0.700000	0.700000
KLX07A	0.733333	3	1.140000	1.140000
KLX08	0.670000	1	0.670000	0.670000
KLX09	1.070000	2	1.140000	1.140000
KLX09B		0		
KLX09C		0		
KLX09D	1.825000	2	1.940000	1.940000
KLX09E	1.476667	3	2.440000	2.440000
KLX09F		0		
KLX09G		0		
KLX10		0		
KLX10B		0		
KLX10C		0		
KLX11A	2.142500	4	6.380000	6.380000
KLX11B	3.407500	4	7.770000	7.770000
KLX11C	0.895000	4	2.590000	2.590000
KLX11D		0		
KLX11E	1.275000	14	3.830000	4.340000
KLX11F	2.780000	5	6.840000	6.840000
KLX12A	1.972857	7	4.000000	4.000000
KLX13A	1.255000	12	3.020000	4.170000
KLX14A	0.481250	8	1.090000	1.090000
KLX18A	0.655000	12	1.230000	1.350000
KLX19A		0		
KLX20A	0.600000	4	0.800000	0.800000
KLX22A	0.371429	7	0.630000	0.630000
KLX22B		0		
KLX23A		0		
KLX23B		0		
KLX24A	0.451250	8	0.840000	0.840000
KLX25A		0		
KLX26A	0.350000	10	0.695000	0.770000
KLX26B	6.190000	1	6.190000	6.190000
KLX28A	1.886667	3	3.650000	3.650000
KLX29A	2.750000	2	2.970000	2.970000
All Grps	1.201186	118	3.050000	4.170000

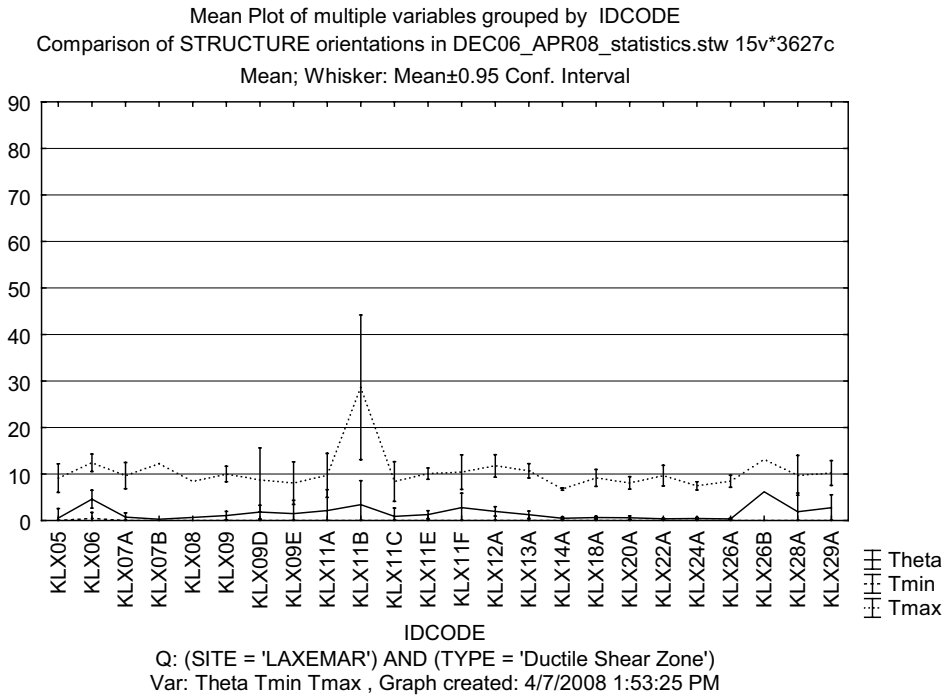

Figure 5-13. *Dihedral angle between old and new structure orientations of type "Ductile Shear Zone". The dashed lines outline θ_{min} and θ_{max}.*

Table 5-10. Summary statistics of difference between old and new structure orientations of type "Brittle-Ductile Shear Zone".

Breakdown Table of Descriptive Statistics (Comparison of STRUCTURE orientations in DEC06_APR08_statistics.stw)
N=251 (No missing data in dep. var. list)
Include condition: (SITE = 'LAXEMAR') AND (TYPE = 'Brittle-Ductile Shear Zone')

IDCODE	Theta Means	Theta N	Percentile 90.00000	Percentile 95.00000
KLX03		0		
KLX04	2.010000	1	2.010000	2.010000
KLX05	1.655000	2	1.870000	1.870000
KLX07A	0.980000	1	0.980000	0.980000
KLX08		0		
KLX09	1.023333	3	1.260000	1.260000
KLX09B		0		
KLX09C		0		
KLX09D		0		
KLX09E		0		
KLX09F	0.255000	2	0.410000	0.410000
KLX09G	5.082000	5	5.770000	5.770000
KLX10		0		
KLX10B	0.930000	2	1.430000	1.430000
KLX10C	2.452857	7	4.180000	4.180000
KLX11A	1.915610	41	4.110000	4.380000
KLX11B	0.200000	1	0.200000	0.200000
KLX11C	2.852500	4	6.790000	6.790000
KLX11D		0		
KLX11E	0.300000	2	0.410000	0.410000
KLX11F	1.556667	3	3.240000	3.240000
KLX12A	0.520000	1	0.520000	0.520000
KLX13A	2.150000	11	3.280000	4.830000
KLX14A	0.552432	37	1.190000	1.400000
KLX18A	0.838571	35	1.530000	2.130000
KLX19A	1.942857	14	4.520000	6.520000
KLX20A	0.550000	6	1.030000	1.030000
KLX22A	0.440000	3	0.620000	0.620000
KLX22B		0		
KLX23A		0		
KLX23B		0		
KLX24A	0.280000	3	0.340000	0.340000
KLX25A	0.195000	2	0.280000	0.280000
KLX26A	0.767500	40	2.205000	2.540000
KLX26B	4.327778	9	7.030000	7.030000
KLX28A	1.645000	10	2.920000	3.970000
KLX29A	0.681667	6	1.920000	1.920000
All Grps	1.382231	251	3.820000	4.610000

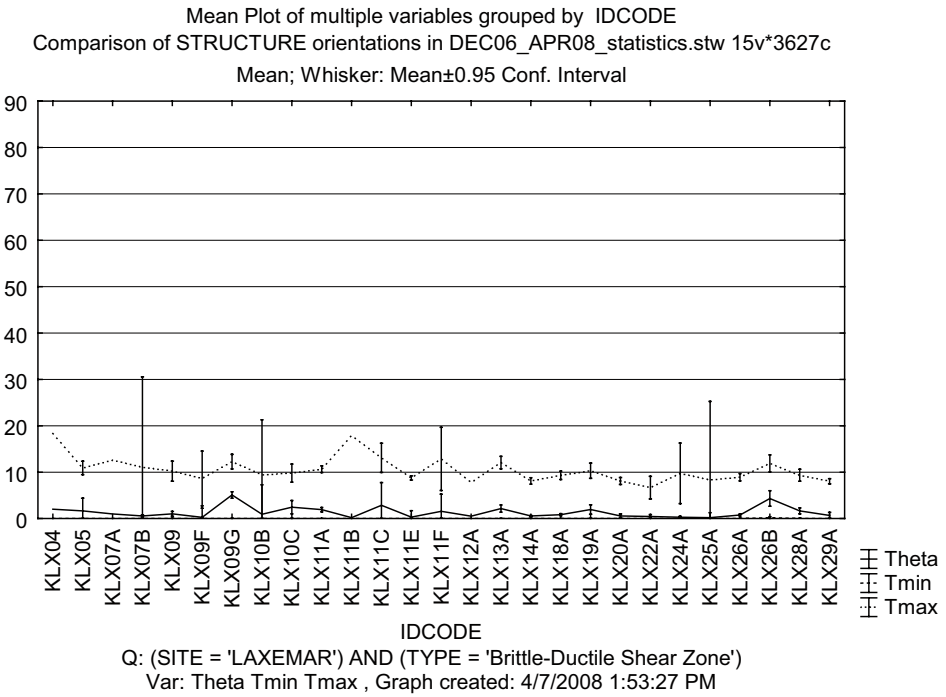

Figure 5-14. *Dihedral angle between old and new structure orientations of type "Brittle-Ductile Shear Zone". The dashed lines outline θ_{min} and θ_{max}.*

Rock contacts

The Sicada parameter "Rock contact" describes the contact between two different lithologies. In the modelling scales performed so far, little attention has been paid to the local orientation of the contact. The modelled shape of the lithological units has mostly been based upon extrapolation between boreholes and, when applicable, between boreholes and ground surface mapping. We nevertheless here display the results of our analyses of the differences between new and old data for completeness see Table 5-11 and Table 5-12 together with Figure 5-15and Figure 5-16.

Forsmark

Table 5-11. Summary statistics of difference between old and new rock contact orientations.

Breakdown Table of Descriptive Statistics (Comparison of CONTACT orientations in DEC06_APR08_statistics.stw) N=2291 (No missing data in dep. var. list) Include condition: (SITE = 'FORSMARK')				
IDCODE	Theta Means	Theta N	Percentile 90.00000	Percentile 95.00000
KFM01A	7.60187	107	15.35000	16.45000
KFM01B	2.84724	58	6.07000	6.94000
KFM01C	2.21818	77	5.13000	6.22000
KFM01D	1.06549	142	2.77000	3.76000
KFM02A	7.69362	138	21.94000	32.83000
KFM03A	11.08876	178	20.71000	25.69000
KFM03B	11.75600	20	18.30500	18.95500
KFM04A	0.81639	155	1.56000	1.78000
KFM05A	0.88314	121	2.22000	2.83000
KFM06A	1.16546	218	2.33000	2.87000
KFM06B	0.55800	20	1.30500	1.38500
KFM06C	0.89291	134	2.13000	2.87000
KFM07A	1.66953	150	2.80500	3.29000
KFM07B	1.21000	52	1.74000	1.84000
KFM07C	11.15587	63	17.83000	18.05000
KFM08A	1.41834	169	2.79000	3.17000
KFM08B	0.99257	35	1.51000	1.56000
KFM08C	4.19316	136	7.62000	8.56000
KFM09A	0.26735	155	0.51000	0.63000
KFM09B	1.28260	96	1.13000	1.30000
KFM10A	1.97075	67	2.50000	3.11000
All Grps	3.20692	2291	9.16000	14.31000

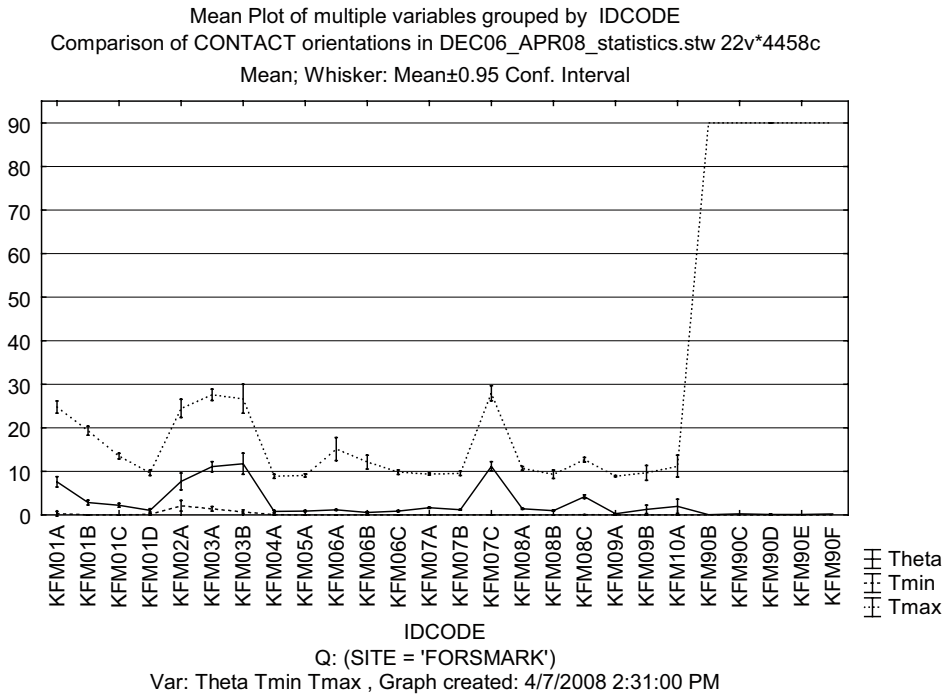

Figure 5-15. *Dihedral angle between old and new rock contact orientations. The dashed lines outline* θ_{min} *and* θ_{max}.

Laxemar

Table 5-12. Summary statistics of difference between old and new rock contact orientations.

Breakdown Table of Descriptive Statistics (Comparison of CONTACT orientations in DEC06_APR08_statistics.stw)
N=1240 (No missing data in dep. var. list)
Include condition: (SITE = 'LAXEMAR')

IDCODE	Theta Means	Theta N	Percentile 90.00000	Percentile 95.00000
KLX03	2.559079	76	6.67000	7.44000
KLX04	1.891782	101	5.53000	7.03000
KLX05	1.364537	108	2.90000	3.50000
KLX07A	0.757391	46	1.01000	1.07000
KLX08	0.654535	86	1.45000	1.70000
KLX09	0.752719	114	1.03000	1.11000
KLX09B	1.962143	14	4.99000	13.59000
KLX09C	0.197333	15	0.32000	0.42000
KLX09D	1.023889	18	1.99000	2.26000
KLX09E	0.968182	11	3.29000	3.69000
KLX09F	0.156316	19	0.40000	0.47000
KLX09G	3.615385	13	7.49000	7.78000
KLX10	0.868922	102	1.29000	1.63000
KLX10B	2.394286	7	9.70000	9.70000
KLX10C	0.532857	14	1.04000	3.83000
KLX11A	1.313538	65	4.71000	5.47000
KLX11B	0.477222	18	0.52000	6.84000
KLX11C	0.390000	19	2.06000	2.52000
KLX11D	0.603750	8	1.56000	1.56000
KLX11E	0.149615	26	0.22000	0.34000
KLX11F	0.122609	23	0.24000	0.24000
KLX12A	1.614068	59	4.56000	8.00000
KLX13A	1.729355	62	4.68000	5.10000
KLX14A	0.159000	10	0.30500	0.33000
KLX18A	1.329024	41	4.03000	5.65000
KLX19A	1.049184	49	1.41000	3.53000
KLX20A	0.662800	25	1.64000	1.80000
KLX22A	0.198000	15	0.33000	0.36000
KLX22B	1.134000	10	4.46000	6.97000
KLX23A	0.124706	17	0.29000	0.39000
KLX23B	0.345000	4	1.08000	1.08000
KLX24A	0.142500	8	0.26000	0.26000
KLX25A	0.100000	7	0.38000	0.38000
KLX26A	0.427273	11	0.65000	1.76000
KLX26B	3.103333	3	5.10000	5.10000
KLX28A	2.115000	10	5.87500	6.14000
KLX29A	6.993333	6	38.80000	38.80000
All Grps	1.184194	1240	2.82500	4.86000

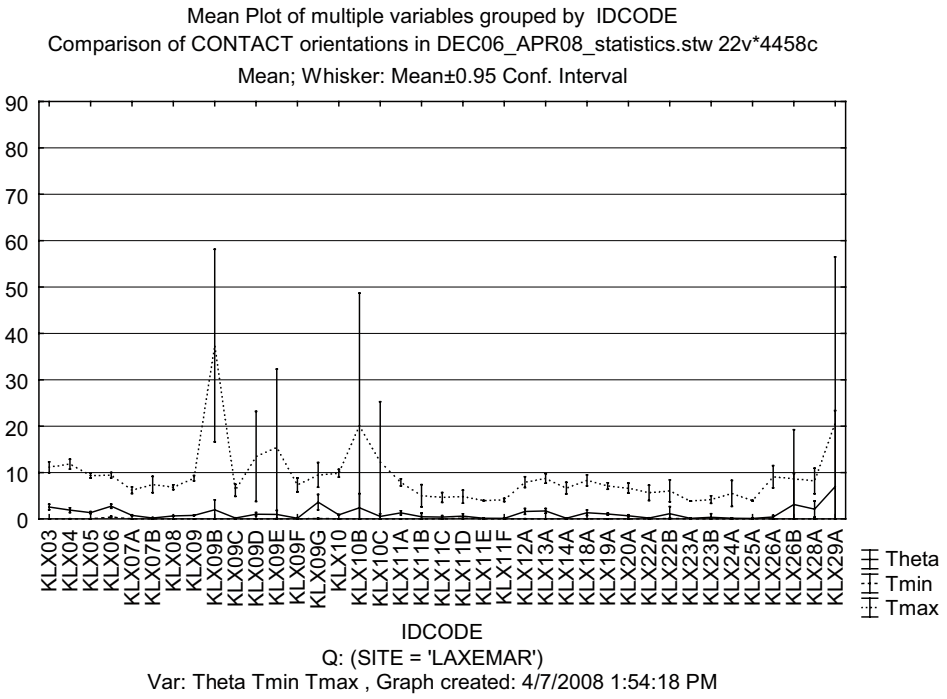

Figure 5-16. *Dihedral angle between old and new rock contact orientations. The dashed lines outline* θ_{min} *and* θ_{max}.

5.4 Acceptance criterion

The goal that was set for this project was to achieve an overall measurement uncertainty in orientation data of maximum 10°, expressed in terms of a dihedral angle around the mean structure normal, for the majority of rock structure data; the later was quantified as the 90th percentile.

It should be understood that the goal regarded the results of the actions taken to improve mapping routines, increase the quality of BIPS logging and its handling, decrease the uncertainty associated to borehole deviation measurements and, naturally, to propagate the collage of these factors into the structure orientations in Sicada. As indicated on Figure 5-17 the goal is met for less than 36% of the analysed fracture orientations.

The project was, however, not given any criterion for which uncertainties are regarded acceptable from a modelling point of view, nor were we required to provide such a criterion within the framework of this project. Nevertheless, as a result of our analyses (see 5.4.1), we have come to the conclusion that such a criterion is needed and of great help to the modellers.

As the modelling has many quite disparate purposes, we would need a set of criteria for each intended model type. We believe that the ultimate decision of whether to include a dataset or not, due to its data quality, should be made by the experts who intend to model the data. For some model types, such as DFN models, orientation data are averaged over fairly large volumes of rock and locally large orientation uncertainties have a small impact on the overall, propagated orientation uncertainty. Additionally, the DFN methodology has an inherent capability of quantifying and propagating such uncertainties. For other model types, such as for PFL-f features or rock domains, large local orientation uncertainties *might* have a *major* impact on the model but not necessarily so.

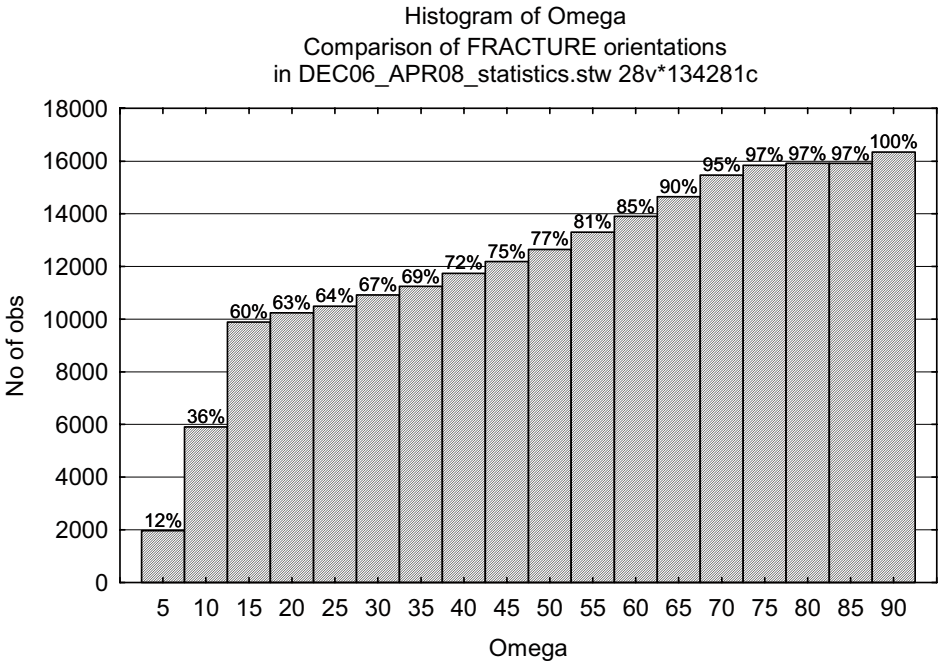

Figure 5-17. *CDF of fracture uncertainties for all analysed boreholes in both Forsmark and Laxemar. Omega is computed according to Figure 5-5b.*

An additional complication is the determination of whether the criterion should encompass the borehole as an entity, sections of the borehole or individual orientation measurements. Again, the usage of the data, i.e. the type of intended model, must steer this choice.

Any choice of discriminating criterion must contain some amount of subjective judgement in addition to statistical reasoning. However, once argued for, the criterion must remain fixed and the use thereof must be consistent to all orientation data.

We here propose the use of the *average* orientation uncertainty as a measure to determine if fracture orientation uncertainties in an entire borehole, or sections thereof, can be accepted for fracture orientation analyses in DFN modelling.

We suggest subdividing the orientation data into three classes:

- Boreholes that we judge acceptable for fracture orientation analyses.
- Boreholes in which we judge particular sections are acceptable for fracture orientation analyses.
- Boreholes that we do not recommend for orientation analyses.

In Figure 5-18 we illustrate how various uncertainties, Ω, would display on a stereonet using a simulated horizontal fracture set, using a spread around the mean pole of $\kappa = 30$[14]. An uncertainty of 10° (Figure 5-18b) is very hard to distinguish by visual inspection from the original data and the obtained κ-value is, from all practical purposes indistinguishable from the one of the original data set. However, larger uncertainties result in clear differences on the stereonets and significant changes to κ.

[14] We made use of the univariate Fisher distribution, which makes use of a single koncentration parameter, κ /Fisher et al. 1987/.

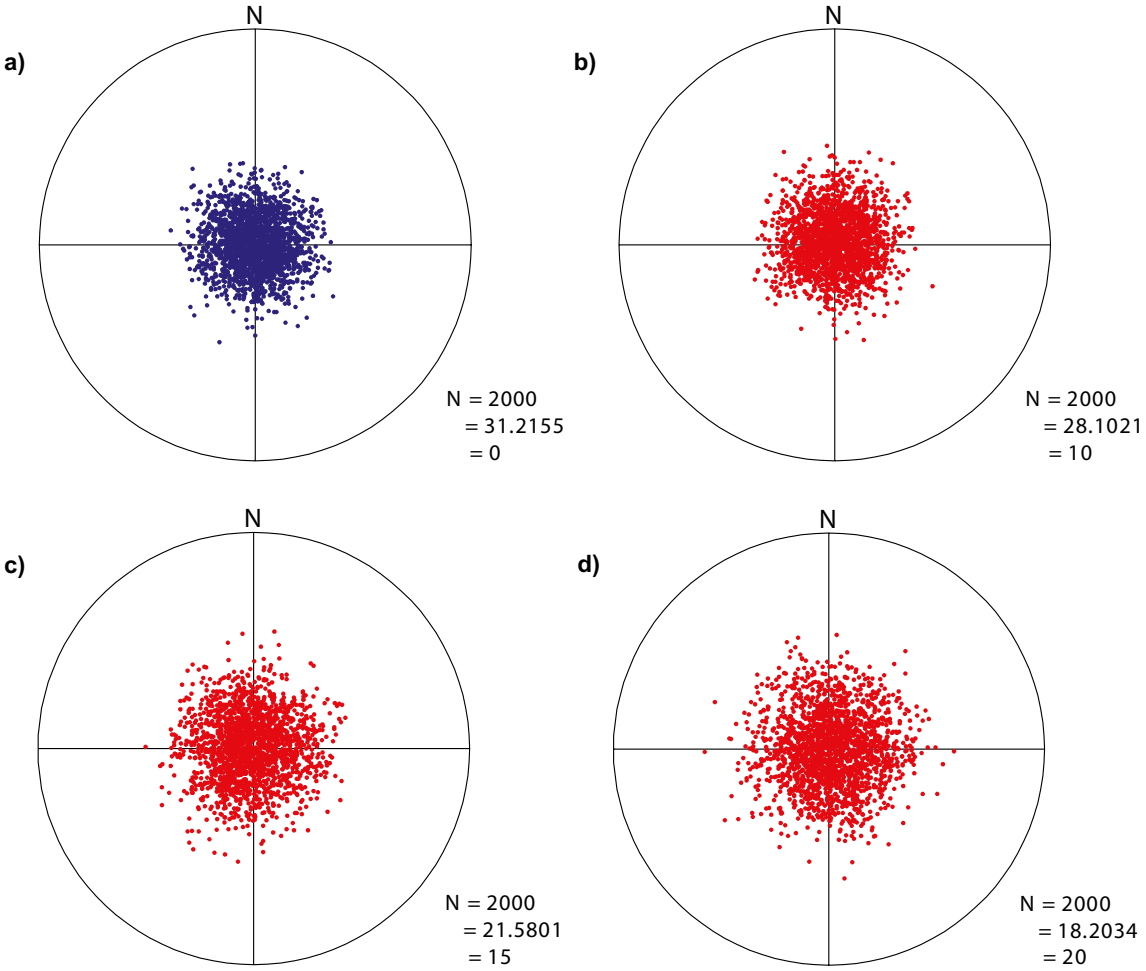

Figure 5-18. *Stereonets of a fracture set with various assigned uncertainties. a) The original fracture set. In b–d we permute each datum according to the uncertainties,* Ω*, in respective legend.*

Though we acknowledge that the choice is, due to the lack of solid arguments, entirely subjective we still find it realistic and convenient to introduce the following criteria using the mean uncertainty ($\overline{\Omega}$):

- $0° \leq \overline{\Omega} \leq 10°$, to accept a borehole entirely,
- $10° < \overline{\Omega} \leq 15°$, to eventually accept sections of a borehole,
- $15° < \overline{\Omega}$ to discriminate a borehole.

Using KFM01B, we provide in Figure 5-19 an example of how sections of boreholes with too high uncertainties could be identified using moving averages of Ω. Certainly, the choice of window size for the moving average will have an impact upon the section lengths. We wish to accentuate, however, that should this technique be applied by the modellers, the window size must be consistent for all used boreholes. We wish to stress that discussions of which borehole, or sections thereof, to be excluded from orientation analyses, should be held within the SDM groups to which we provide the analyses presented here as prerequisites for decisions.

Finally, we wish to remind the reader that the orientation uncertainties discussed in this report regard instrumental, computational and mapping uncertainties only. Other orientation uncertainties, such as those induced by undulating fracture surfaces, must be treated elsewhere.

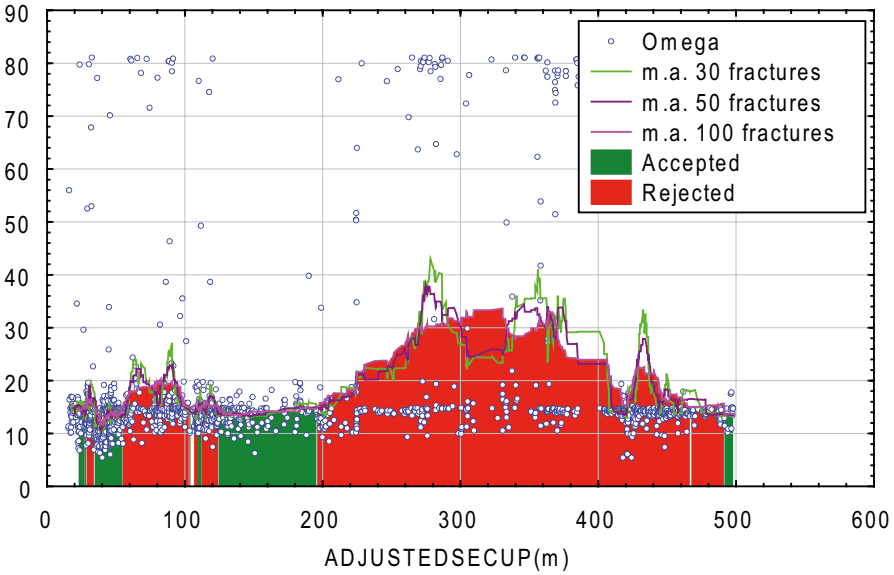

Figure 5-19. *Moving average of fracture orientation uncertainty in borehole KFM01B. In this example, the criterion for "acceptable" was set to 15°, using a moving average of ± 50 fractures.*

5.4.1 Quantification of orientation uncertainties

Fractures

Forsmark

The mean orientation uncertainties are listed in Table 5-13 and plotted on Figure 5-20. None of the boreholes fulfil the criterion of 10°. Table 5-14 lists the fraction of the fractures in each borehole that have uncertainties below 5, 10, 15 and 20 degrees respectively.

The main contributor to these large uncertainties are fractures tagged "VISIBLE_IN_BIPS = 0", i.e. fractures that could not be seen in the BIPS during logging. Table 5-15 and Figure 5-21 highlight the striking difference between fractures that are visible in BIPS and those that are not.

Table 5-13. Summary statistics of orientation uncertainty, Ω.

Breakdown Table of Descriptive Statistics (Comparison of FRACTURE orientations in DEC06_APR08_statistics.stw)
N=56690 (No missing data in dep. var. list)
Include condition: (SITE = 'FORSMARK')

IDCODE	Omega Means	Omega N	Percentile 90.00000	Percentile 95.00000
KFM01A	13.38567	1472	15.35526	15.74446
KFM01B	17.86613	1641	18.81511	71.63629
KFM01C	23.55451	5419	63.55533	70.75270
KFM01D	17.41430	1631	57.45877	65.17542
KFM02A	17.19291	1816	18.92263	39.35002
KFM03A	17.38934	1755	19.27116	41.68810
KFM03B	13.01750	192	16.14666	18.44123
KFM04A	11.29277	4289	14.07981	47.79440
KFM05A	10.70013	2823	12.81465	16.06609
KFM06A	10.83264	3658	13.63784	21.72386
KFM06B	10.95828	552	14.90561	16.16916
KFM06C	16.99996	4424	55.42395	65.93835
KFM07A	12.50194	3172	16.58059	57.74114
KFM07B	19.64836	1677	59.77381	66.57404
KFM07C	24.46047	1764	72.24765	80.20353
KFM08A	12.63275	4265	15.86341	56.40970
KFM08B	11.64689	743	15.06284	53.37824
KFM08C	13.42286	4196	15.92431	61.75504
KFM09A	15.11748	5017	51.25631	62.15992
KFM09B	21.30938	3491	61.51524	67.47803
KFM10A	24.71615	2693	67.45674	71.27543
All Grps	16.23277	56690	50.99581	64.26217

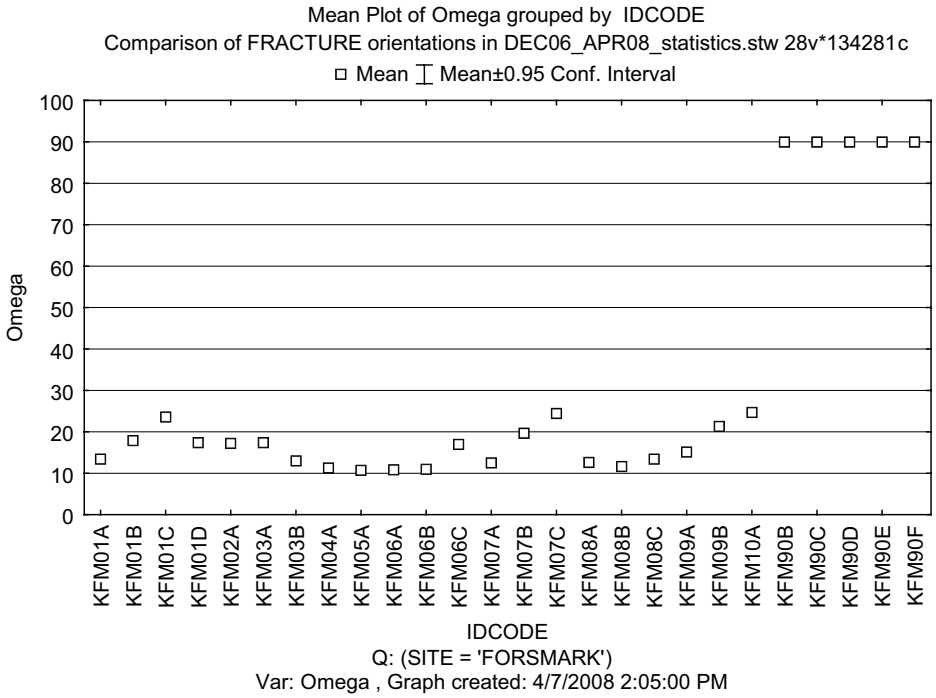

Figure 5-20. *Box-whisker plot of orientations uncertainty, Ω.*

Table 5-14. The proportion of fractures (%) that have uncertainties below those shown in the headers.

Breakdown Table of Descriptive Statistics (Comparison of FRACTURE orientations in DEC06_APR08_statistics.stw) N=57125 (No missing data in dep. var. list) Include condition: 'Site' = 'FORSMARK'				
IDCODE	5°	10°	15°	20°
KFM01A	0.00%	18.27%	71.20%	99.59%
KFM01B	0.00%	6.40%	81.05%	91.59%
KFM01C	0.07%	16.53%	71.38%	74.37%
KFM01D	0.12%	69.53%	77.38%	79.95%
KFM02A	0.33%	5.84%	41.91%	92.68%
KFM03A	0.00%	5.01%	39.43%	92.65%
KFM03B	0.00%	12.50%	88.02%	99.48%
KFM04A	0.12%	84.36%	91.56%	92.96%
KFM05A	0.04%	87.57%	93.09%	95.29%
KFM06A	0.19%	84.80%	93.30%	94.97%
KFM06B	0.00%	62.32%	90.40%	97.10%
KFM06C	0.00%	71.90%	79.43%	81.78%
KFM07A	0.19%	81.59%	88.87%	90.26%
KFM07B	0.00%	64.04%	72.93%	77.58%
KFM07C	2.44%	15.36%	36.22%	76.76%
KFM08A	0.12%	83.05%	88.68%	90.46%
KFM08B	0.00%	76.99%	89.64%	92.60%
KFM08C	0.00%	85.46%	88.80%	90.30%
KFM09A	0.02%	79.55%	83.83%	86.01%
KFM09B	0.00%	71.76%	73.13%	73.90%
KFM10A	0.26%	57.15%	63.87%	65.35%
KFM90B	0.00%	0.00%	0.00%	0.00%
KFM90C	0.00%	0.00%	0.00%	0.00%
KFM90D	0.00%	0.00%	0.00%	0.00%
KFM90E	0.00%	0.00%	0.00%	0.00%
KFM90F	0.00%	0.00%	0.00%	0.00%
All Grps	0.15%	61.28%	77.80%	85.10%

Table 5-15. Summary statistics of orientation uncertainty, Ω, classified by "VISIBLE_IN_BIPS".

Breakdown Table of Descriptive Statistics (Comparison of FRACTURE orientations in DEC06_APR08_statistics.stw) N=57125 (No missing data in dep. var. list) Include condition: (SITE = 'FORSMARK')				
VISIBLE_IN_BIPS	Omega Means	Omega N	Percentile 90.00000	Percentile 95.00000
0	55.89118	8520	73.57989	77.56032
1	9.94122	48605	14.80112	15.81504
All Grps	16.79450	57125	53.23055	66.10200

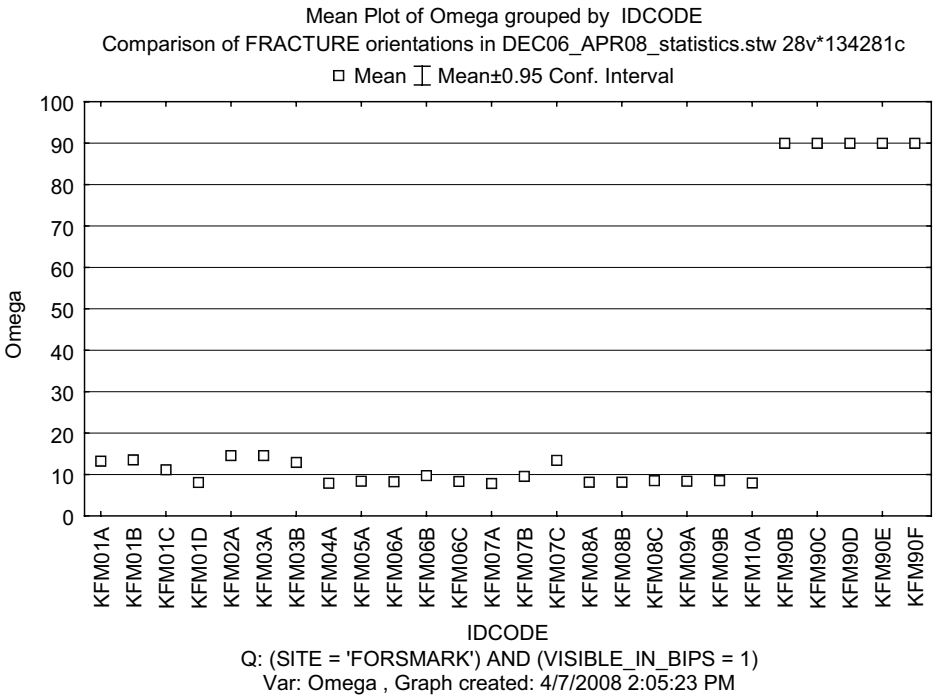

Figure 5-21. *Box-whisker plot of orientations uncertainty, Ω., only "VISIBLE_IN_BIPS = 1" included.*

In Table 5-16 we omitted fractures not visible in BIPS from analyses. We note that, formally, seven boreholes fail to fulfil the criterion. However, all boreholes have mean uncertainties below 15° which, considering the vast efforts invested in correcting the data, ought to be perceived as quite satisfactory.

Table 5-16. Summary statistics of fracture orientation uncertainty, Ω. Green ≤ 10°, 10° < yellow < 15°, red ≥ 15°.

Breakdown Table of Descriptive Statistics (Comparison of FRACTURE orientations in DEC06_APR08_statistics.stw)
N=48294 (No missing data in dep. var. list)
Include condition: (SITE = 'FORSMARK') AND (VISIBLE_IN_BIPS = 1)

IDCODE	Omega Means	Omega N	Percentile 90.00000	Percentile 95.00000
KFM01A	13.20359	1461	15.34898	15.46678
KFM01B	13.55138	1492	15.57697	16.98039
KFM01C	11.13963	4020	12.45539	13.29111
KFM01D	8.09849	1292	11.88534	14.10426
KFM02A	14.56492	1677	16.96423	18.39402
KFM03A	14.58574	1634	16.55991	18.74705
KFM03B	12.89883	189	16.14666	18.29387
KFM04A	7.88470	3959	8.71637	12.90635
KFM05A	8.40131	2678	9.10538	13.20155
KFM06A	8.29622	3468	10.57898	13.72147
KFM06B	9.72433	533	14.13320	15.43103
KFM06C	8.30674	3604	11.06461	14.02842
KFM07A	7.83757	2840	9.23155	12.99551
KFM07B	9.53894	1289	13.54512	15.10173
KFM07C	13.40361	1284	16.27081	16.36390
KFM08A	8.15717	3828	8.90162	12.24244
KFM08B	8.12352	682	13.05132	14.34942
KFM08C	8.50246	3776	9.31112	10.26964
KFM09A	8.37720	4298	9.15897	12.88844
KFM09B	8.48834	2565	9.26539	9.39127
KFM10A	7.96136	1725	10.65826	13.25150
All Grps	9.42566	48294	14.69236	15.68159

Laxemar

The analyses for Laxemar holes are displayed below. As for Forsmark, the influence upon the uncertainty is governed by fractures tagged “VISIBLE_IN_BIPS = 0” to such an extent that none of the boreholes pass the criterion (Table 5-17). When excluding fractures “VISIBLE_IN_BIPS = 0” from analyses, all but two boreholes pass the criterion (Table 5-20). The remaining boreholes, KLX04 and KLX11B, have mean uncertainties of 11° and 12° respectively which from most practical viewpoints ought to be considered satiosfactory.

Table 5-17. Summary statistics of orientation uncertainty, Ω.

Breakdown Table of Descriptive Statistics (Comparison of FRACTURE orientations in DEC06_APR08_statistics.stw)
Smallest N for any variable: 70759
Include condition: (SITE = 'LAXEMAR')

IDCODE	Omega Means	Omega N	Percentile 90.00000	Percentile 95.00000
KLX03	23.53865	4248	65.63802	72.69791
KLX04	20.12753	5183	55.22279	69.29656
KLX05	29.54791	3477	69.80680	72.92500
KLX07A	20.54284	6272	59.60377	66.52326
KLX08	19.87286	5296	59.56672	67.80374
KLX09	19.96501	4597	59.19436	70.17195
KLX09B	16.81053	584	42.47512	61.96344
KLX09C	16.88292	740	52.11988	63.03502
KLX09D	19.89530	855	58.62302	67.53474
KLX09E	18.52945	989	57.94830	65.07086
KLX09F	27.71192	1022	67.77951	72.10408
KLX09G	23.24887	828	65.69371	69.58866
KLX10	22.55057	5519	65.40792	72.19068
KLX10B	11.88682	604	15.41152	35.13646
KLX10C	14.29939	1533	41.15705	59.44626
KLX11A	20.73187	5341	63.38852	70.62416
KLX11B	24.09401	443	68.62667	73.50400
KLX11C	24.33675	446	70.72686	72.62394
KLX11D	15.56339	679	50.77840	62.31390
KLX11E	26.89435	655	67.85684	71.41470
KLX11F	20.62922	408	67.55809	70.76788
KLX12A	28.45497	2945	69.96716	72.93706
KLX13A	18.95415	3654	57.49614	67.54698
KLX14A	23.46951	1447	65.60097	69.17601
KLX18A	22.55742	3058	65.75315	71.20275
KLX19A	26.41162	2627	68.94073	72.70848
KLX20A	26.93082	2261	64.62297	69.26081
KLX22A	16.21403	693	48.68676	61.81949
KLX22B	17.98838	668	57.47985	66.76064
KLX23A	15.29174	204	53.04195	66.48069
KLX23B	20.50819	113	62.35760	63.57226
KLX24A	21.30824	881	64.49415	70.12470
KLX25A	24.39891	344	67.93282	70.93715
KLX26A	23.87645	801	61.94649	68.14657
KLX26B	10.74264	346	14.12011	46.38782
KLX28A	15.40409	551	53.38667	62.85321
KLX29A	18.87357	448	59.95160	68.38545
All Grps	21.79858	70760	63.40517	70.31598

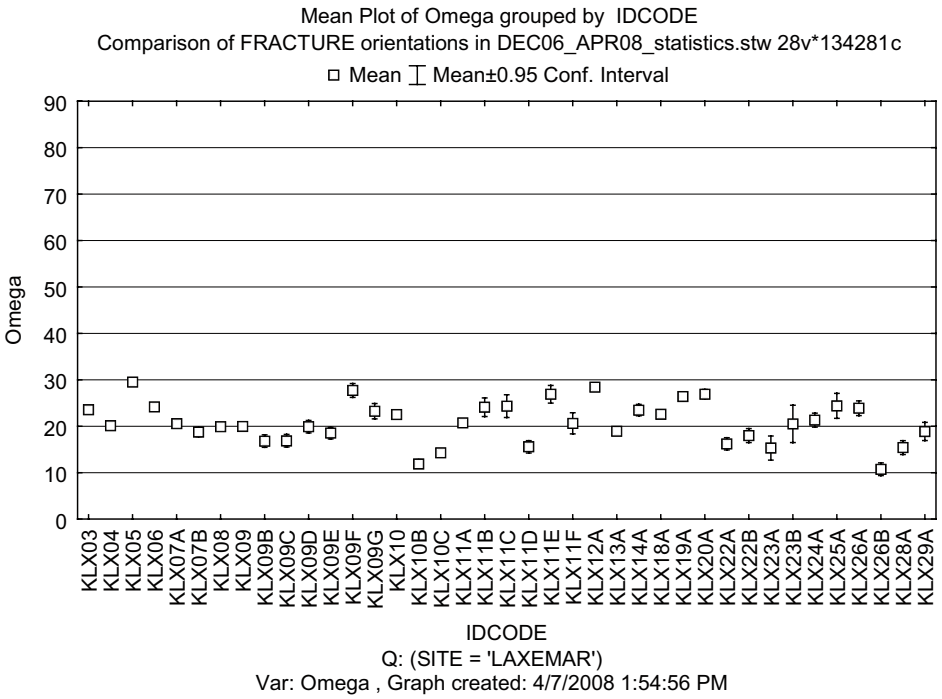

Figure 5-22. *Box-whisker plot of orientations uncertainty, Ω.*

Table 5-18. The proportion of fractures (%) that have uncertainties below those shown in the headers.

Breakdown Table of Descriptive Statistics (Comparison of FRACTURE orientations in DEC06_APR08_statistics.stw)
N=77156 (No missing data in dep. var. list)
Include condition: 'Site' = 'LAXEMAR'

IDCODE	5°	10°	15°	20°
KLX03	0.00%	50.33%	62.50%	67.98%
KLX04	0.00%	43.20%	67.47%	76.29%
KLX05	0.00%	52.57%	56.08%	57.81%
KLX06	0.10%	54.63%	61.85%	64.47%
KLX07A	0.19%	59.31%	69.58%	73.18%
KLX07B	1.22%	31.68%	72.89%	79.59%
KLX08	0.26%	59.72%	71.32%	73.68%
KLX09	1.26%	54.93%	69.78%	75.24%
KLX09B	2.23%	47.26%	75.00%	79.79%
KLX09C	0.27%	66.89%	77.70%	79.59%
KLX09D	0.23%	50.99%	70.76%	74.62%
KLX09E	0.40%	62.49%	73.51%	74.92%
KLX09F	0.20%	50.49%	57.93%	60.47%
KLX09G	0.00%	62.08%	68.60%	69.08%
KLX10	0.91%	52.40%	65.46%	70.54%
KLX10B	0.66%	69.70%	86.42%	93.05%
KLX10C	1.76%	65.10%	84.80%	86.76%
KLX11A	1.44%	55.87%	70.64%	73.23%
KLX11B	0.68%	22.35%	53.50%	67.04%
KLX11C	0.00%	63.90%	68.61%	69.06%
KLX11D	0.44%	67.01%	81.74%	83.95%
KLX11E	0.31%	55.27%	60.15%	61.68%
KLX11F	0.25%	66.18%	73.28%	74.26%
KLX12A	0.51%	41.63%	51.14%	53.99%
KLX13A	0.57%	58.02%	73.48%	76.87%
KLX14A	0.69%	59.64%	65.17%	66.28%
KLX18A	1.41%	58.44%	68.28%	69.98%
KLX19A	0.30%	50.93%	60.83%	63.49%
KLX20A	0.35%	50.24%	56.61%	58.78%
KLX22A	0.00%	69.12%	78.79%	80.95%
KLX22B	0.15%	65.42%	76.05%	78.59%
KLX23A	0.49%	69.12%	81.86%	82.35%
KLX23B	0.00%	61.95%	69.91%	74.34%
KLX24A	0.23%	61.75%	69.47%	70.72%
KLX25A	0.00%	57.56%	67.73%	68.02%
KLX26A	0.25%	56.43%	63.30%	65.54%
KLX26B	0.87%	82.66%	91.91%	92.20%
KLX28A	0.00%	76.77%	83.48%	85.12%
KLX29A	0.22%	66.96%	76.12%	79.02%
All Grps	0.53%	54.73%	67.30%	70.87%

Table 5-19. Summary statistics of orientation uncertainty, Ω, classified by "VISIBLE_IN_ BIPS".

Breakdown Table of Descriptive Statistics (Comparison of FRACTURE orientations in DEC06_APR08_statistics.stw) Smallest N for any variable: 77155 Include condition: (SITE = 'LAXEMAR')				
VISIBLE_IN_BIPS	Omega Means	Omega N	Percentile 90.00000	Percentile 95.00000
0	50.39459	24229	72.33572	73.73781
1	8.85786	52927	13.26755	14.66354
All Grps	21.90148	77156	63.17034	70.12419

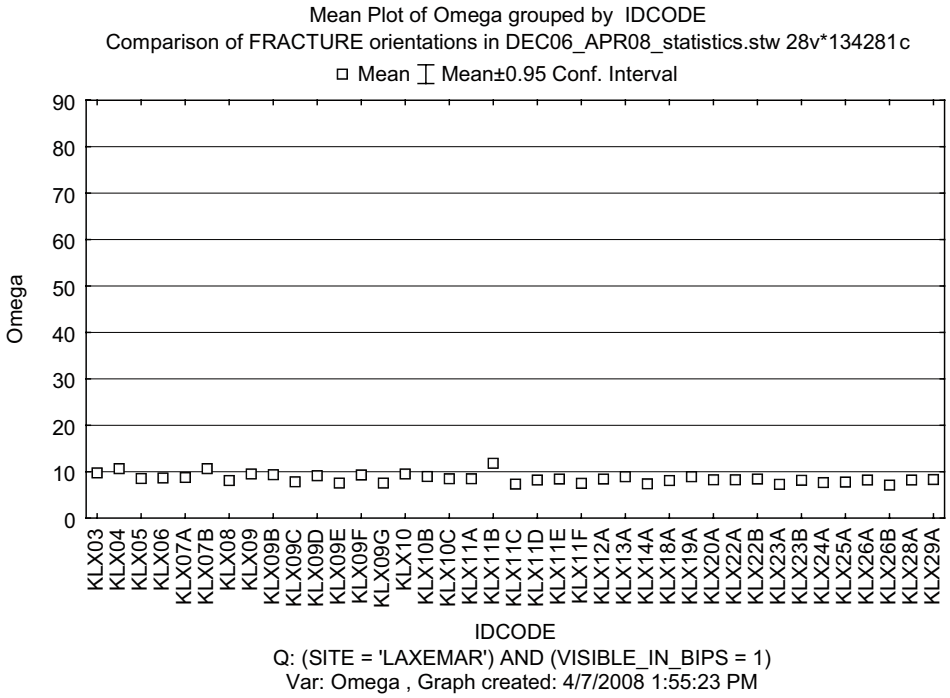

Figure 5-23. *Box-whisker plot of orientations uncertainty, Ω., only "VISIBLE_IN_BIPS = 1" included.*

Table 5-20. Summary statistics of fracture orientation uncertainty, Ω. Green ≤ 10°, 10° < yellow < 15°, red ≥ 15°.

Breakdown Table of Descriptive Statistics (Comparison of FRACTURE orientations in DEC06_APR08_statistics.stw) N=48695 (No missing data in dep. var. list) Include condition: (SITE = 'LAXEMAR') AND (VISIBLE_IN_BIPS = 1)				
IDCODE	Omega Means	Omega N	Percentile 90.00000	Percentile 95.00000
KLX03	9.74826	2817	13.92182	15.51390
KLX04	10.67504	3814	15.01058	16.13461
KLX05	8.52548	1993	9.25062	13.38607
KLX07A	8.77444	4487	12.82512	14.50651
KLX08	8.10729	3793	13.12062	14.35261
KLX09	9.50992	3225	13.57795	15.15616
KLX09B	9.35271	423	13.77951	14.29729
KLX09C	7.82353	583	13.01161	14.02649
KLX09D	9.13345	624	14.05599	14.91896
KLX09E	7.55491	719	11.83387	13.42941
KLX09F	9.31080	610	10.28432	14.04034
KLX09G	7.55646	566	9.64286	13.66064
KLX10	9.50691	3649	13.76320	15.24931
KLX10B	8.99818	559	14.37186	15.16370
KLX10C	8.51294	1316	13.05423	14.31032
KLX11A	8.46998	3760	13.36823	14.55271
KLX11B	11.82672	293	16.34131	18.92883
KLX11C	7.34576	305	8.03160	12.60447
KLX11D	8.18811	562	12.40262	13.93076
KLX11E	8.41091	389	9.41312	11.75391
KLX11F	7.48409	296	9.89709	12.19574
KLX12A	8.43676	1462	12.62274	14.01764
KLX13A	8.91128	2701	13.16652	14.50266
KLX14A	7.38097	942	9.60877	13.00003
KLX18A	8.13383	2082	12.10770	13.83335
KLX19A	8.92619	1639	11.96324	14.28842
KLX20A	8.28633	1268	11.73595	13.93500
KLX22A	8.25113	557	12.47671	14.15280
KLX22B	8.41876	522	13.25959	14.73500
KLX23A	7.31064	163	11.92493	13.15176
KLX23B	8.16357	81	13.43265	13.78659
KLX24A	7.69051	614	11.13830	13.66831
KLX25A	7.75054	233	11.99665	14.09718
KLX26A	8.19510	513	12.07053	14.38154
KLX26B	7.15219	317	9.70028	12.80361
KLX28A	8.22363	467	9.93523	13.35468
KLX29A	8.32746	351	12.90448	14.54663
All Grps	8.83382	48695	13.29464	14.66113

Rock mass structures

Forsmark

The uncertainties essentially mimic those of fracture orientations. The results of the analyses are displayed in Table 5-21. We note that, formally, roughly half of the boreholes fail to fulfil the criterion. However, all boreholes, with the possible exception of KFM07C, lie close or very close to the criterion.

Table 5-21. Summary statistics of structure orientation uncertainty, Ω. Green ≤ 10°, 10° < yellow < 15°, red ≥ 15°.

Breakdown Table of Descriptive Statistics (Comparison of STRUCTURE orientations in DEC06_APR08_statistics.stw
N=1908 (No missing data in dep. var. list)
Include condition: (SITE = 'FORSMARK')

IDCODE	Omega Means	Omega N	Percentile 90.00000	Percentile 95.00000
KFM01A	14.56520	113	15.23081	15.36596
KFM01B	13.85481	44	14.72114	14.80865
KFM01C	11.46473	57	12.52934	15.31825
KFM01D	8.57045	83	13.86206	14.81981
KFM02A	14.58229	18	19.06447	19.89871
KFM03A	14.76062	41	19.89457	20.10098
KFM03B	12.55742	7	18.97849	18.97849
KFM04A	7.68836	194	8.31910	8.44196
KFM05A	8.12341	82	8.83706	9.08328
KFM06A	9.46066	106	8.97533	13.71472
KFM06B	9.32377	11	10.23075	10.46936
KFM06C	8.52231	83	13.67417	14.85976
KFM07A	7.44097	163	8.33118	8.37675
KFM07B	8.86500	70	9.74612	9.76696
KFM07C	15.31717	35	15.90971	15.94787
KFM08A	8.80516	201	12.54019	13.80599
KFM08B	7.17427	44	8.21399	8.24645
KFM08C	8.27495	136	9.12432	9.35919
KFM09A	8.31348	249	9.08453	9.14219
KFM09B	8.14813	70	8.38506	8.43490
KFM10A	8.44021	101	13.95294	14.28213
All Grps	9.23459	1908	14.45579	15.07360

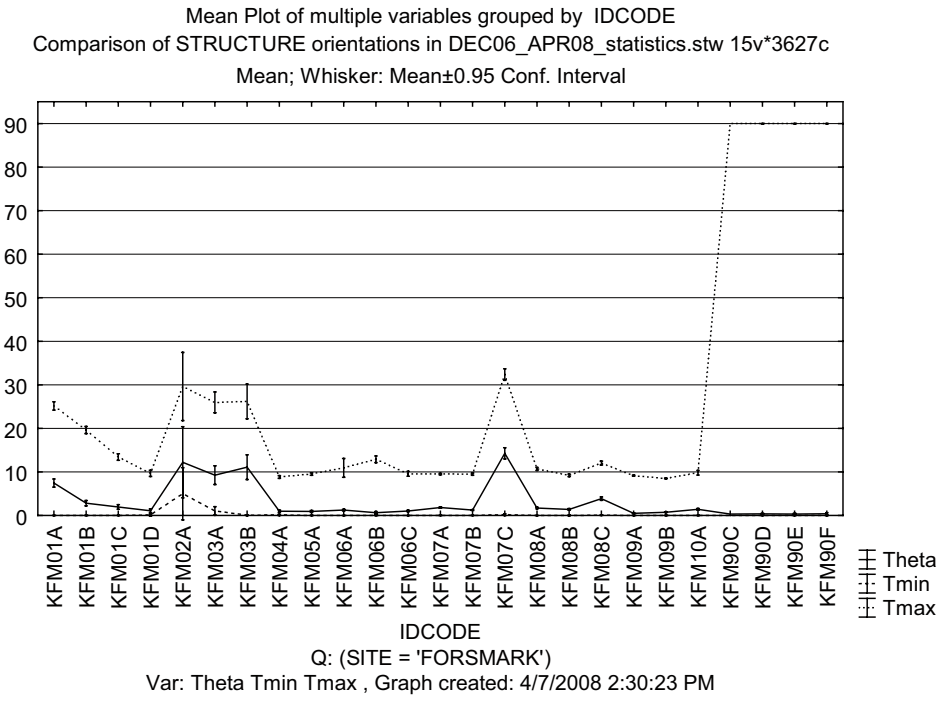

Figure 5-24. *Box-whisker plot of structure orientation uncertainty, Ω.*

Laxemar

Table 5-22. Summary statistics of structure orientation uncertainty, Ω. Green ≤ 10°, 10° < yellow < 15°, red ≥ 15°.

Breakdown Table of Descriptive Statistics (Comparison of STRUCTURE orientations in DEC06_APR08_statistics.stw)
N=1170 (No missing data in dep. var. list)
Include condition: (SITE = 'LAXEMAR')

IDCODE	Omega Means	Omega N	Percentile 90.00000	Percentile 95.00000
KLX03	9.52062	15	15.65395	16.20068
KLX04	10.84948	54	15.48754	16.00592
KLX05	8.58882	38	9.21124	14.67089
KLX06	7.76975	17	9.00101	9.09127
KLX07A	8.56735	16	12.27199	15.08539
KLX07B	9.88524	11	11.26441	11.55521
KLX08	8.49699	9	14.96302	14.96302
KLX09	9.54895	84	13.53367	15.37252
KLX09B	11.42665	7	14.67714	14.67714
KLX09C	11.21716	5	12.86261	12.86261
KLX09D	8.63043	6	15.55306	15.55306
KLX09E	6.87709	13	7.69482	9.78060
KLX09F	9.33777	17	15.04212	15.30229
KLX09G	6.92256	12	7.87341	8.28967
KLX10	9.69491	15	12.34077	14.59754
KLX10B	8.20662	7	8.86705	8.86705
KLX10C	8.91545	29	13.96075	14.10644
KLX11A	8.70447	115	13.49174	14.02445
KLX11B	12.51654	18	19.33748	20.63607
KLX11C	8.55383	21	14.20239	14.60980
KLX11D	6.89003	5	8.17918	8.17918
KLX11E	8.39270	47	9.05495	9.28465
KLX11F	8.43850	22	13.87557	13.92434
KLX12A	9.21630	40	13.71424	15.04651
KLX13A	8.48570	87	11.52484	14.11771
KLX14A	7.55023	74	10.02031	13.32862
KLX18A	9.01937	87	14.45423	14.65970
KLX19A	8.18320	51	9.88608	9.95444
KLX20A	7.83414	51	8.65378	9.21188
KLX22A	8.64786	28	14.19424	14.51617
KLX22B	9.71277	16	14.54801	15.26142
KLX23A	7.50171	11	9.80599	11.44203
KLX23B	7.69609	6	8.16572	8.16572
KLX24A	7.67479	27	11.81405	12.35508
KLX25A	7.51346	5	9.61673	9.61673
KLX26A	8.10691	61	10.27368	14.37620
KLX26B	7.40624	12	7.51394	14.12147
KLX28A	7.64840	18	8.48974	8.81540
KLX29A	7.48615	13	8.09300	10.72790
All Grps	8.69157	1170	13.11129	14.57353

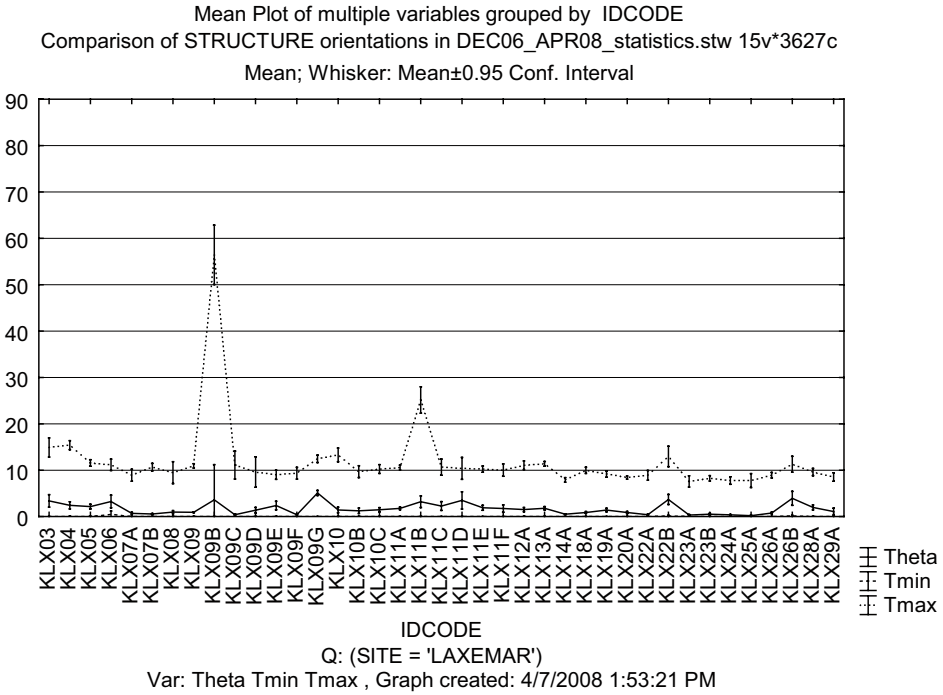

Figure 5-25. *Box-whisker plot of structure orientation uncertainty, Ω.*

Rock contacts

Forsmark

The results of the analyses are displayed in Table 5-23. In essence, the uncertainties are similar to those of "rock structures". We note that, formally, 8 of the 21 analysed boreholes fail to fulfil the criterion.

Table 5-23. Summary statistics of rock contact orientation uncertainty, Ω. Green ≤ 10°, 10° < yellow < 15°, red ≥ 15°.

Breakdown Table of Descriptive Statistics (Comparison of CONTACT orientations in DEC06_APR08_statistics.stw)
N=2291 (No missing data in dep. var. list)
Include condition: (SITE = 'FORSMARK')

IDCODE	Omega Means	Omega N	Percentile 90.00000	Percentile 95.00000
KFM01A	14.16698	107	15.30170	15.39140
KFM01B	13.82676	58	14.84323	16.25520
KFM01C	11.25988	77	12.45714	12.51490
KFM01D	8.54520	142	13.29894	14.56102
KFM02A	14.01612	138	16.78752	19.24215
KFM03A	14.56010	178	18.69442	19.47965
KFM03B	12.68342	20	17.02757	17.42732
KFM04A	7.94677	155	8.72093	13.79803
KFM05A	7.94954	121	9.00147	9.19435
KFM06A	13.85777	218	15.18116	90.00000
KFM06B	9.25613	20	10.83077	13.42828
KFM06C	8.80822	134	14.19559	14.97028
KFM07A	7.56159	150	8.42949	9.19227
KFM07B	8.96643	52	9.82836	14.17978
KFM07C	14.41849	63	16.18335	16.34455
KFM08A	9.15505	169	14.38955	15.25438
KFM08B	7.99521	35	12.92808	13.81106
KFM08C	8.49897	136	9.39746	12.82426
KFM09A	8.19012	155	8.93785	9.13692
KFM09B	9.30216	96	9.18530	13.17756
KFM10A	10.07318	67	14.94182	15.30504
All Grps	10.51376	2291	15.24959	16.00090

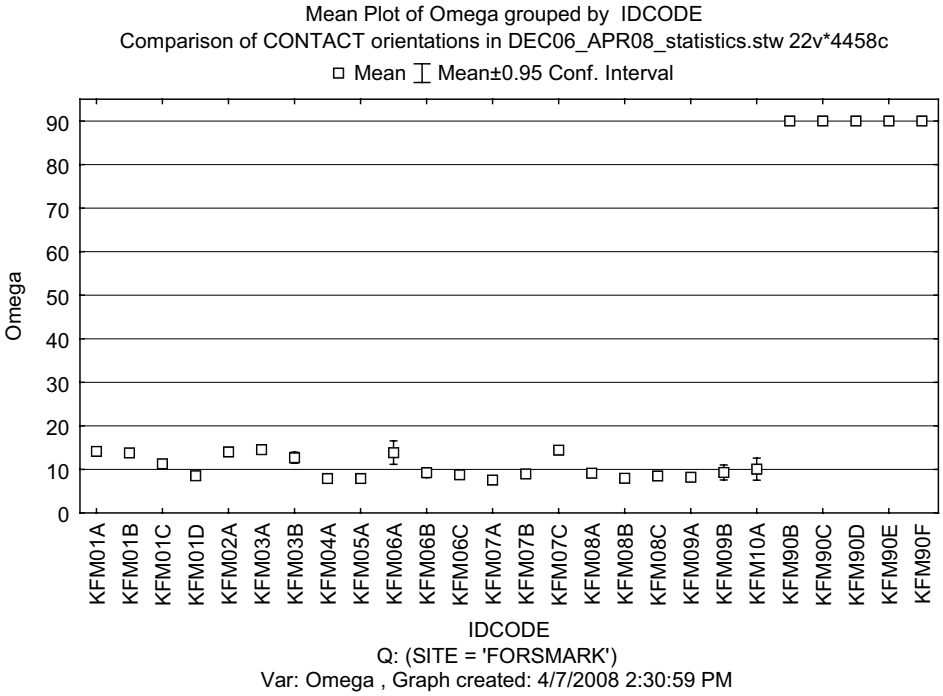

Figure 5-26. *Box-whisker plot of rock contact orientation uncertainty, Ω.*

Laxemar

Table 5-24. Summary statistics of contact orientation uncertainty, Ω. Green ≤ 10°, 10° < yellow < 15°, red ≥ 15°.

Breakdown Table of Descriptive Statistics (Comparison of CONTACT orientations in DEC06_APR08_statistics.stw) N=1240 (No missing data in dep. var. list) Include condition: (SITE = 'LAXEMAR')				
IDCODE	Omega Means	Omega N	Percentile 90.00000	Percentile 95.00000
KLX03	7.63889	76	10.23634	13.41267
KLX04	8.66774	101	12.22782	14.48585
KLX05	7.48251	108	9.22086	11.60758
KLX07A	5.48230	46	8.02806	11.03181
KLX08	6.09688	86	7.81159	11.41263
KLX09	7.82780	114	11.30049	14.45887
KLX09B	13.12768	14	13.58981	90.00000
KLX09C	6.14416	15	7.79910	13.39720
KLX09D	12.75929	18	15.17323	90.00000
KLX09E	14.71707	11	14.77428	90.00000
KLX09F	7.34871	19	9.93657	15.30663
KLX09G	5.93339	13	7.21166	9.15254
KLX10	7.45566	102	11.89321	12.87624
KLX10B	18.86905	7	90.00000	90.00000
KLX10C	11.86846	14	8.11241	90.00000
KLX11A	6.51216	65	9.35853	11.41197
KLX11B	4.09725	18	4.02207	9.86517
KLX11C	4.38831	19	7.83094	9.14989
KLX11D	4.51329	8	7.46571	7.46571
KLX11E	3.91304	26	3.91631	3.91631
KLX11F	4.14635	23	3.91394	6.30798
KLX12A	6.18604	59	8.53500	10.17337
KLX13A	6.50190	62	8.79126	12.16109
KLX14A	6.54191	10	8.46654	8.79705
KLX18A	6.94315	41	11.42595	12.19266
KLX19A	6.29418	49	9.87317	9.91194
KLX20A	6.02651	25	8.62470	8.71807
KLX22A	5.45515	15	8.78802	13.86996
KLX22B	5.22181	10	7.51225	7.58241
KLX23A	3.83829	17	3.85028	3.85087
KLX23B	3.87361	4	3.87956	3.87956
KLX24A	5.53839	8	13.47022	13.47022
KLX25A	3.88141	7	3.88419	3.88419
KLX26A	8.53541	11	13.74441	15.03465
KLX26B	5.68262	3	6.60763	6.60763
KLX28A	6.39760	10	8.16138	8.18399
KLX29A	20.31782	6	90.00000	90.00000
All Grps	7.13706	1240	10.10928	12.91299

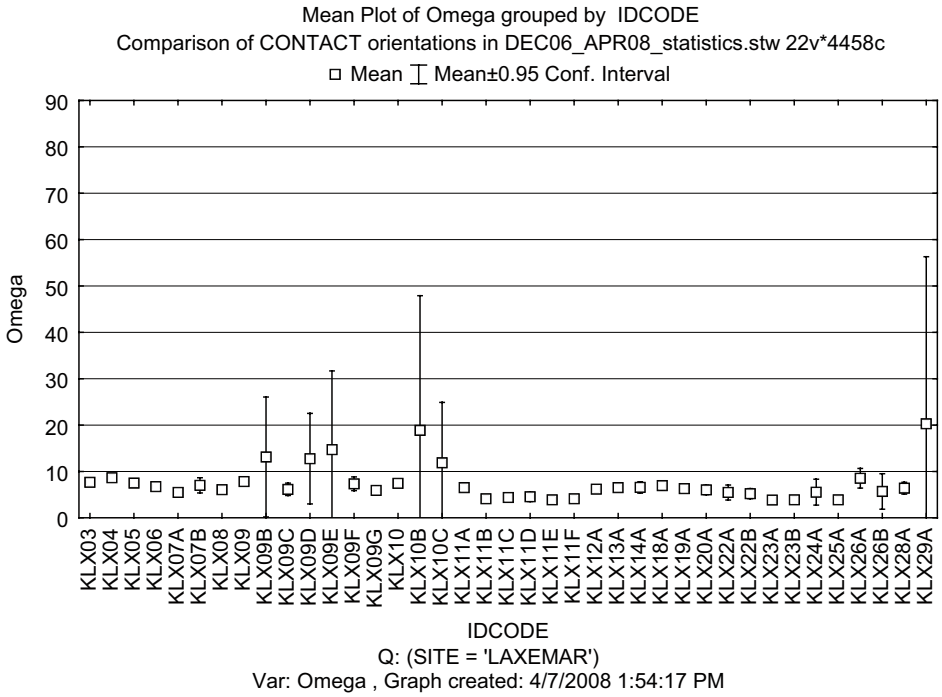

Figure 5-27. *Box-whisker plot of contact orientation uncertainty, Ω.*

5.4.2 PFL-f features

Forsmark

The results of the analyses are displayed in Table 5-25. Additional details are provided in Appendix 4. In Figure 5-28 we display the mean uncertainty with 95% confidence intervals.

PFL modelling is more deterministic than stochastic in character. Thus any assessment of uncertainty should be made based on individual fracture basis, rather than using means over larger domains, as is standard in DFN modelling. This is supported by Figure 5-29, in which it is obvious that only a handful of PFL at most, contribute to large uncertainties in each borehole.

Table 5-25. Summary statistics of PFL-f features. Green ≤ 10°, 10° < yellow < 15°, red ≥ 15°.

Breakdown Table of Descriptive Statistics (Comparison of FRACTURE orientations in DEC06_APR08_statistics.stw) N=543 (No missing data in dep. var. list) Include condition: (SITE = 'FORSMARK') AND (VISIBLE_IN_BIPS = 1) AND (PFLID <> "")				
IDCODE	dZ(m) Means	AbsoluteDistance(m) Means	Theta Means	Omega Means
KFM01A	0.002727	0.163909	2.59273	12.83551
KFM01B				
KFM01C				
KFM01D	-0.334242	0.672606	0.37455	8.33274
KFM02A	-0.052903	1.524333	13.47742	14.32498
KFM03A	0.106800	0.141100	10.41920	14.09837
KFM03B				
KFM04A	0.167101	1.042855	0.70623	8.30363
KFM05A	0.000769	0.022154	0.68462	10.35485
KFM06A	-0.699468	1.512734	0.86457	9.06550
KFM06B				
KFM06C				
KFM07A	-0.680000	2.343700	1.02250	7.83658
KFM07B				
KFM07C	0.098000	0.986800	5.17933	10.13485
KFM08A	-0.359750	1.922075	1.24950	8.44551
KFM08B				
KFM08C	0.090526	1.174579	4.42158	8.44155
KFM09A				
KFM09B				
KFM10A	-0.237843	0.754706	1.49804	7.91164
All Grps	-0.187201	1.087512	4.28842	10.38763

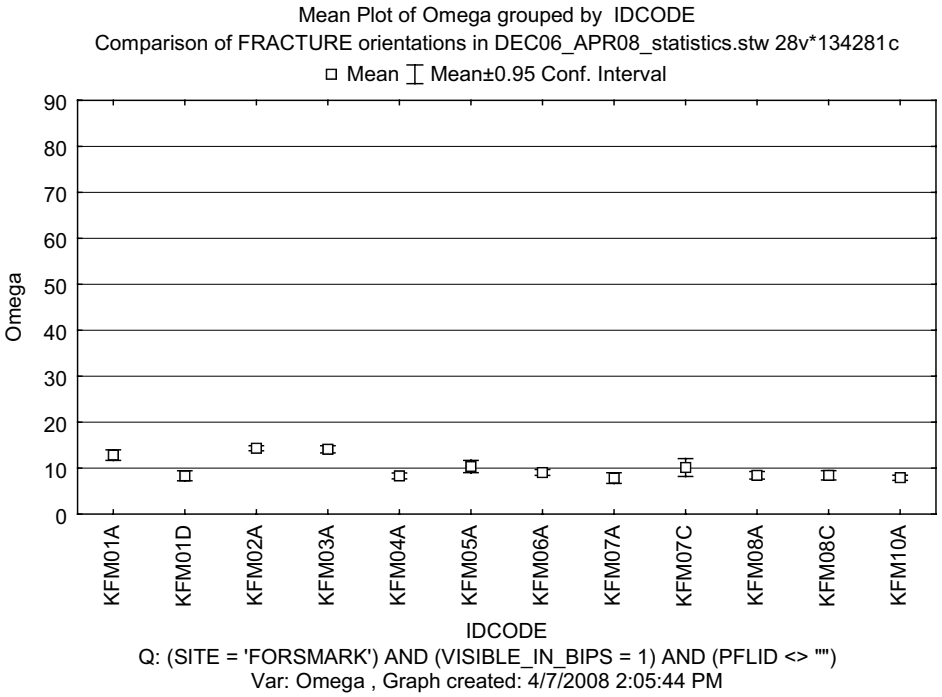

Figure 5-28. *Box-whisker plot of PFL orientation uncertainty, Ω.*

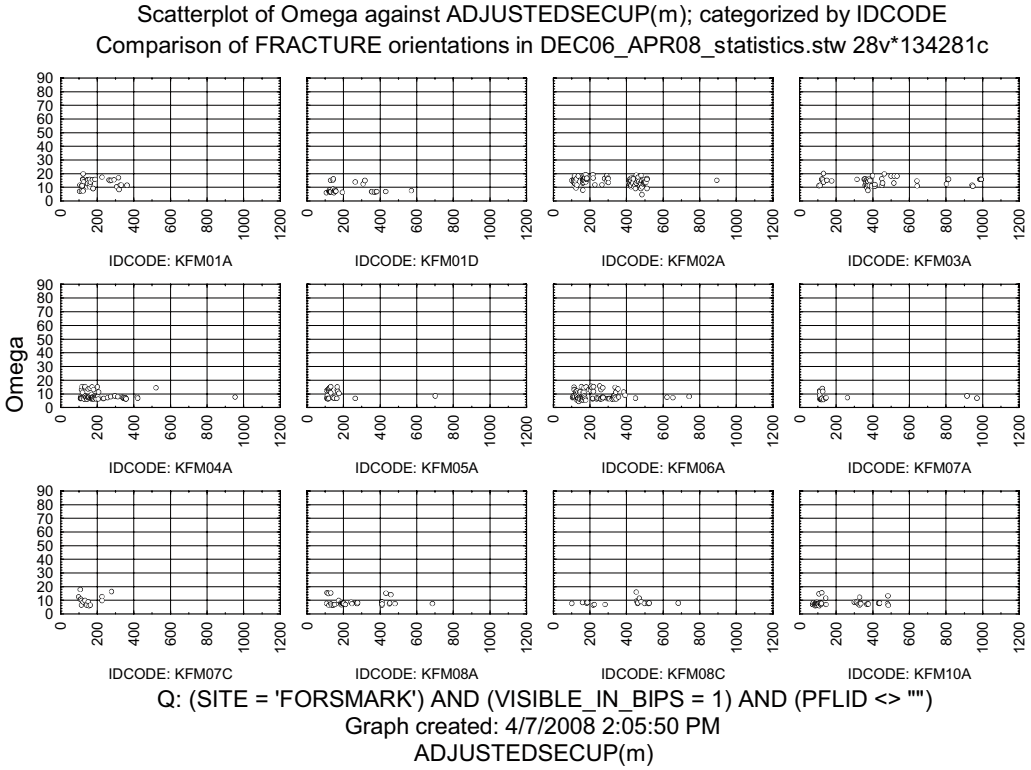

Figure 5-29. *Scatterplot of PFL orientation uncertainty, Ω, versus adjusted secup separated per borehole.*

Laxemar

Table 5-26. Summary statistics of PFL-f features. Green ≤ 10°, 10° < yellow < 15°, red ≥ 15°.

Breakdown Table of Descriptive Statistics (Comparison of FRACTURE orientations in DEC06_APR08_statistics.stw)
N=1956 (No missing data in dep. var. list)
Include condition: (SITE = 'LAXEMAR') AND (VISIBLE_IN_BIPS = 1) AND (PFLID <> "")

IDCODE	dZ(m) Means	Theta Means	Omega Means
KLX03	-0.18843	3.189804	10.45051
KLX04	0.02229	3.289063	10.11812
KLX05	-0.11867	0.779667	8.96425
KLX07A	0.55171	0.758389	8.71783
KLX08	0.23549	1.454344	8.01667
KLX09	0.39200	0.980333	9.43403
KLX09B	0.00000	3.624286	8.97630
KLX09C	0.01833	0.671944	7.71337
KLX09D	-0.00400	1.629429	9.05807
KLX09E	-0.01500	1.766875	6.94667
KLX09F	-0.00150	0.405000	8.73972
KLX09G	-0.00026	4.718421	7.59898
KLX10	0.40377	0.999877	9.43566
KLX10B	0.00000	0.619583	9.24326
KLX10C	-0.00250	1.586250	7.71951
KLX11A	0.22173	1.013077	8.77629
KLX11B	0.00000	3.485862	11.23922
KLX11C	-0.00029	2.675294	8.19696
KLX11D	0.00565	1.813913	8.88694
KLX11E	-0.01939	2.363939	8.31775
KLX11F	-0.00050	1.634000	8.14704
KLX12A	0.52603	1.422381	9.33158
KLX13A	-0.47496	2.463821	8.90640
KLX14A	0.03836	0.411642	7.10857
KLX18A	-0.21672	1.452836	7.47697
KLX19A	-1.11135	0.993462	8.70238
KLX20A	-0.85857	0.536429	8.98957
KLX22A	-0.05595	0.435238	8.56372
KLX22B	0.00364	2.433636	9.20974
KLX23A	0.01400	0.280667	7.13282
KLX23B	-0.00333	2.463333	6.56509
KLX24A	0.01475	0.384000	8.63110
KLX25A	0.00143	0.411429	9.33922
KLX26A	0.00773	1.008182	8.06271
KLX26B	0.00250	4.394375	6.71940
KLX28A	-0.12147	2.362941	8.54486
KLX29A	-0.04000	0.975926	8.57530
All Grps	0.04011	1.559657	8.69079

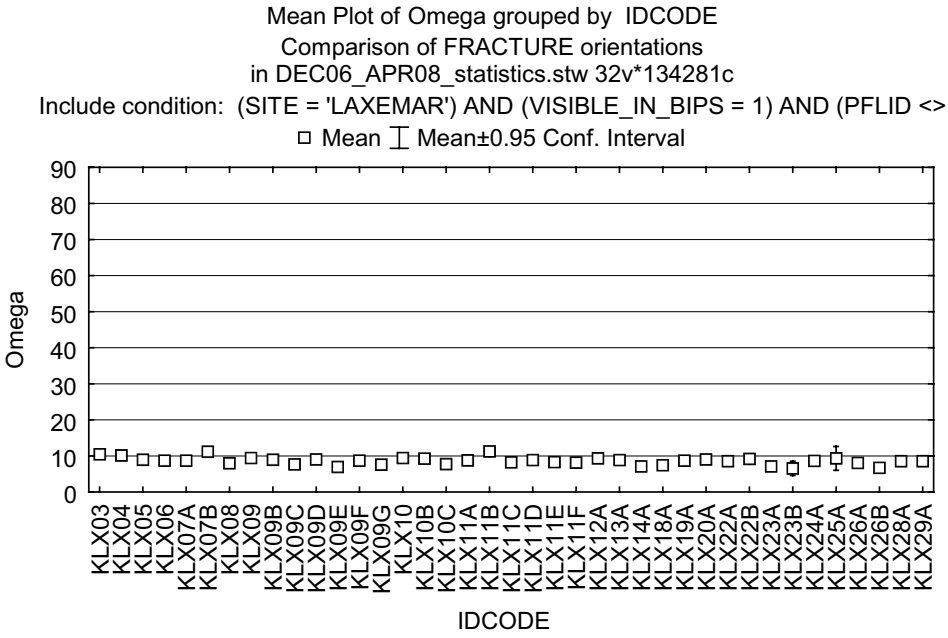

Figure 5-30. *Box-whisker plot of PFL orientation uncertainty, Ω.*

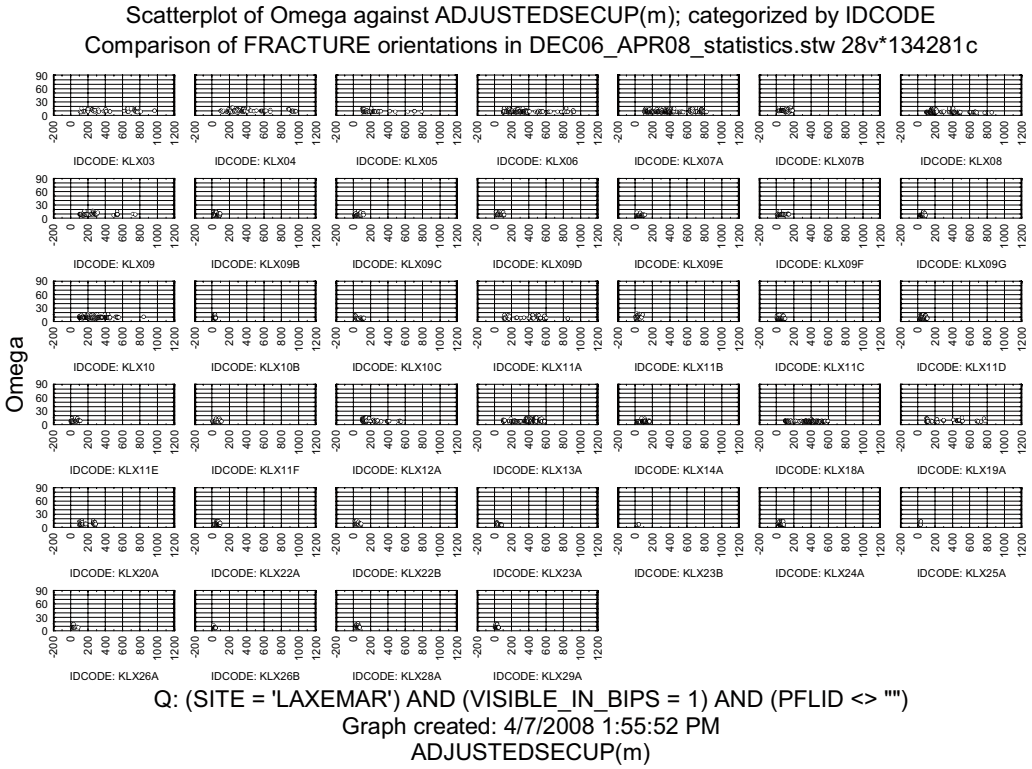

Figure 5-31. *Scatterplot of PFL orientation uncertainty, Ω, versus adjusted secup separated per borehole. See also Appendix 4 for a plot of Ω without categorisation.*

5.5 Conclusions of Chapter 5

Based on the performed analyses, visualisations of which are presented in this report, we conclude the following:

1. The difference between old and new orientation data is, on average, small. We therefore judge that previous DFN models are still adequate despite the changes to orientation data. However, the changes may locally be sufficiently large that a re-assessment might be justified. This ought to primarily affect deterministic modelling, e.g. of PFL-f features, local orientation of deformation zones or the position of rock contacts.
2. Fractures that are not visible in BIPS generally have very large uncertainties. When included in the analyses, *none* of the examined boreholes fulfilled the data acceptance criterion, regardless of whether percentiles or means were used. We therefore recommend *against* the use of *orientation data* for fractures not visible in BIPS. This is applicable to fractures only, as the "VISIBLE_IN_BIPS" parameter is not mapped for neither rock contacts (p_rock) nor structures (p_rock_struct_feat).
   Using a total of roughly 135 000 fracture orientations, we computed an average uncertainty (Ω) for both sites of about 20° (Table 5-27). The goal of obtaining uncertainties lower than 10° was, accordingly, not met for any of the sites. However, excluding fractures that were not visible in BIPS, the uncertainty decreases below 10° (Table 5-28).
3. We propose to use the average Ω to classify orientation data according to the following:

- $0° \leq \overline{\Omega} \leq 10°$, to accept a borehole entirely,
- $10° < \overline{\Omega} \leq 15°$, to eventually accept sections of a borehole,
- $15° < \overline{\Omega}$ to discriminate a borehole.

4. With the notable exception of KFM90B–F, all boreholes in Formark have sufficiently low uncertainties, to be confidently used for orientation analysis given that fracures not visible in BIPS are omitted and provided that the uncertainty here quantified is propagated into subsequent analyses.
5. Compared to Formark, boreholes in Laxemar have slightly larger average uncertainties if fractures not visible in BIPS are considered. However, if such fractures are omitted from analysis, Laxemar boreholes display slightly lower uncertainties compared to Forsmark. With the same disclaimer as for Forsmark, we conclude that all Laxemar boreholes can be safely used for analysis of fracture orientations.

Table 5-27. Summary of Ω for all boreholes, divided per site. All fractures included.

Breakdown Table of Descriptive Statistics (Comparison of FRACTURE orientations in DEC06_APR08_statistics.stw)
N=134281 (No missing data in dep. var. list)

SITE	Omega Means	Omega N	Omega Std.Dev.	Percentile 90.00000	Percentile 95.00000
FORSMARK	16.79450	57125	18.73304	53.23055	66.10200
LAXEMAR	21.90148	77156	21.93595	63.17034	70.12419
All Grps	19.72890	134281	20.78807	59.99169	69.05504

Table 5-28. Summary of Ω for all boreholes, divided per site. Only fractures visible in BIPS included.

Breakdown Table of Descriptive Statistics (Comparison of FRACTURE orientations in DEC06_APR08_statistics.stw)
N=101532 (No missing data in dep. var. list)
Include condition: (VISIBLE_IN_BIPS = 1)

SITE	Omega Means	Omega N	Omega Std.Dev.	Percentile 90.00000	Percentile 95.00000
FORSMARK	9.941219	48605	7.055085	14.80112	15.81504
LAXEMAR	8.857862	52927	2.541258	13.26755	14.66354
All Grps	9.376483	101532	5.242783	14.09676	15.30463

6 Recommendations

6.1 Recommendations for site investigations

Though the surface based site investigations and modelling efforts are heading towards their completion, there will be additional drilling and core mapping in the detailed investigations during construction of tunnels and shafts. Based on the experiences gained within the framework of this task force, we would recommend the following for future campaigns:

- If not absolutely necessary, we should aim at not drilling boreholes steeper than 80°, thereby minimising the problems associated to the levelling of the bubble. This also applies to measurements with compass, as the instrument is affected by inertia and unable to recuperate sufficiently rapidly after rotation of the probe.
- Several, non error marked, borehole deviation measurements, preferentially using different (independent) methods, should be conducted in the boreholes. This will enable us to *compute* a positional uncertainty rather than *assuming* a conservative estimate.
- When using the Magnetometer/accelerometer-based tools, we must make sure of having information on the solar magnetic eruptions. Such eruptions could, if intense, seriously affect the measurements and therefore necessitate new measurements.
- It is questionable, given the large uncertainties, if it is worth mapping *orientations* of fractures not visible in BIPS. We propose that this issue is discussed within the SDMs to provide input for a discussion within SKB on the matter.
- We need to address alternative means of orienting the core. It is important to have some additional information to use, albeit of lower resolution, should orientations be lost in the BIPS.
- The BIPS/Maxibor/Flexit array of instruments obviously needs to be developed to meet the high demands of SKB. This includes the size of the bubble level, the resolution of the BIPS, automation of orientation corrections, alarms for rapidly deviating orientations, full resolution and easy accessible backups, etc.
- We have not been able to evaluate uncertainties in boreholes with gentle (0°–45°) or negative plunges (pointing upwards from the starting point). As we anticipate a large amount of such holes during the construction of the repository, it would be wise to ensure that we will not encounter previously unknown problems associated to the deviation measurements. We therefore recommend that tests are performed on carefully selected boreholes at the Äspö laboratory, so that instruments may be fine-tuned, developed or replaced in due time.
- Some of the updated data tables in Sicada obtained their values computed in Boremap. We have not yet implemented all computations as described in this report within Sicada itself. We recommend that, once the algorithms have been implemented, sample checks are made to ensure that algorithms were correctly implemented.

6.2 Recommendations for Site Descriptive Modelling

We wish to share our reflection that DFN modelling to a very large extent uses averages of sizes, orientation, etc, as proxies for fracture patterns in fairly large volumes of rock. That is, from a DFN modelling perspective, the use of orientation data from selected portions of all boreholes but KFM02A and KLX09B, ought to be adequate and scientifically defendable provided, of course, that fractures tagged “VISIBLE_IN_BIPS = 0”are excluded from *orientation* analysis. However, in this process great care must be taken that other measures of importance,

such as the fracture intensity (P_{10}), are not inadvertently omitted from the modelling. Please note, that a safe omission of fractures not visible in BIPS from orientation analyses, presumes that this class of fractures is in every other sense, e.g. regarding mineralogy, surface roughness, etc, statistically identical to those that are visible in BIPS. It was beyond the scope of the study presented here to perform such analyses, but the issue was essentially addressed in /Fox et al. 2007/ using Forsmark data. The validity to Laxemar data is yet not addressed and we highly recommend that such analyses are conducted prior to elaborate DFN modelling.

The safety assessment SR-Can indicated that details of orientation statistics are of secondary importance. With regards to previous discussions on the type of distribution to be fit to fracture sets, i.e. /Bingham 1964/ versus /Fisher et al. 1987/, we believe that the outcome of the study presented here can still be used as support to assume a Fisher distribution for the *natural variability* of fracture orientations within defined sets, thereby sparing the modellers from the burden of less critical analyses. However, the instrumental and mapping uncertainties discussed in this report, ought to be propagated somehow to the orientation statistics for completeness, if nothing else.

Clearly, the orientation uncertainty is strongly asymmetrical around each individual datum and it is very tempting to evaluate the combination of natural variability and measurement uncertainties, that is, the overall propagated uncertainties in orientation, in terms of asymmetrical orientation distributions such as the bivariate Fisher or the Bingham distributions. However, this asymmetry is most probably smeared out when all data in a hole are analysed simultaneously. This is even more accentuated if several boreholes, and perhaps also outcrops, are analysed simultaneously.

Given the relatively small importance of fracture orientation statistics in SR Can, as compared to e.g. the size and intensity models, we are reluctant, at least for the moment, to *require* the full propagation of these uncertainties to all DFN models and all their variants. It would, though, in terms of good scientific practice, be unacceptable to neglect this aspect. We propose that the effect of the full propagation is evaluated for a limited data set, to be used as prerequisites for a discussion on the matter, within the SDMs or any of the "Net" groups (e.g. GeoNet).

Deterministic modelling and in particular modelling of hydraulically active fractures might be grossly affected by these orientation uncertainties. Data with very large uncertainties are, however, relatively scarce. It might therefore be practical to evaluate each individual datum with large uncertainty in the context of a potential impact upon the models.

7 References

Bingham C, 1964. Distributions on the sphere and on the projective plane, Yale University.

Döse C, Stråhle A, Rauséus G, Samuelsson E, Olsson, 2008. Revision of BIPS-orientations for geological objects in boreholes from Forsmark and Laxemar. SKB P-08-37, Svensk Kärnbränslehantering AB.

Fisher N I, Lewis T, Embleton B J, 1987. Statistical Analysis of Spherical Data, Cambridge University Press. Cambridge, U. K. ISBN: 0-521-45699-1.

Fox A, La Pointe P R, Hermanson J, Öhman J, 2007. Statistical geological discrete fracture network model. Forsmark modelling stage 2.2. SKB R-07-46, Svensk Kärnbränslehantering AB.

Glamheden R, Curtis P, 2006. Comparative evaluation of core mapping results for KFM06C and KLX07B. SKB R-06-55, Svensk Kärnbränslehantering AB. 1137247/R-06-55webb.pdf

INTERMAGNET, 2007. International Real-time Magnetic Observatory Network. www.intermagnet.org

Nilsson G, Nissen J, 2007. Revision of borehole deviation measurements in Forsmark. SKB P-07-28, Svensk Kärnbränslehantering AB. 1487208/P-07-28webb optimerad.pdf

Appendix 1

A1 Magnetic declination

In this appendix, we summarise magnetic measurements made during the period of borehole deviation measurements, to enable us to identify potential sources of measurement bias. The plots of magnetic declination stem from the International Real-time Magnetic Observatory Network /INTERMAGNET 2007/ within which the Swedish Geological Survey, SGU, is a participating organisation.

A1.1 Days with magnetic measurements at Forsmark

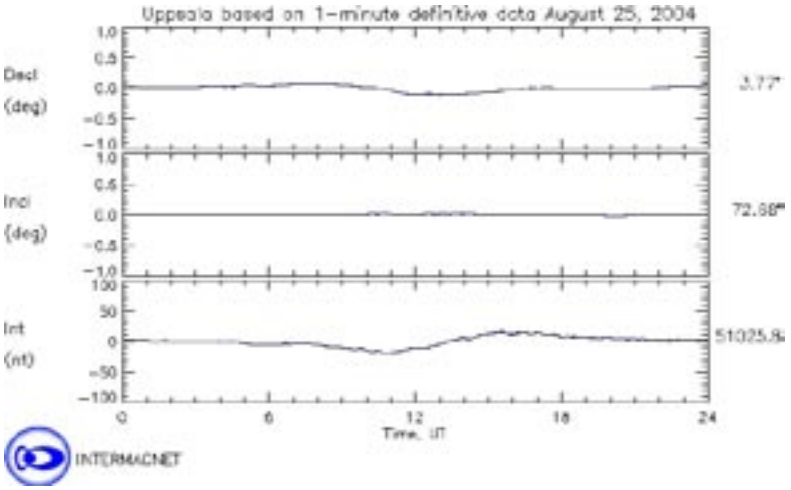

Measured borehole during August 25 2004: KFM05A

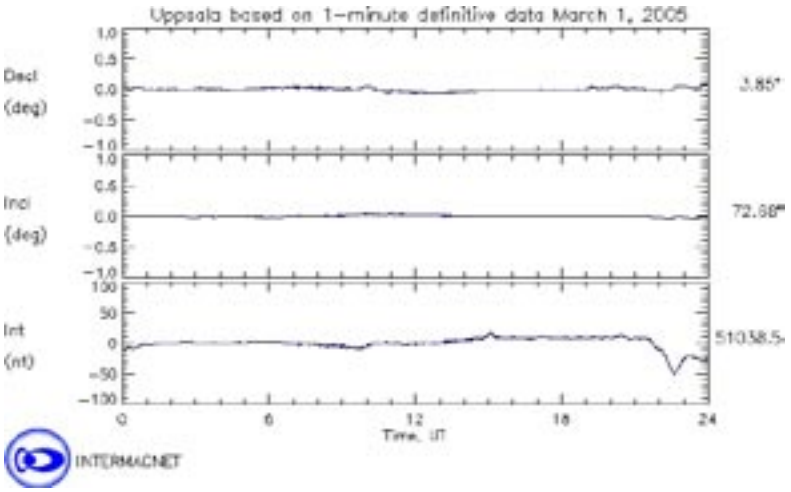

Measured borehole during March 1 2005: KFM08B

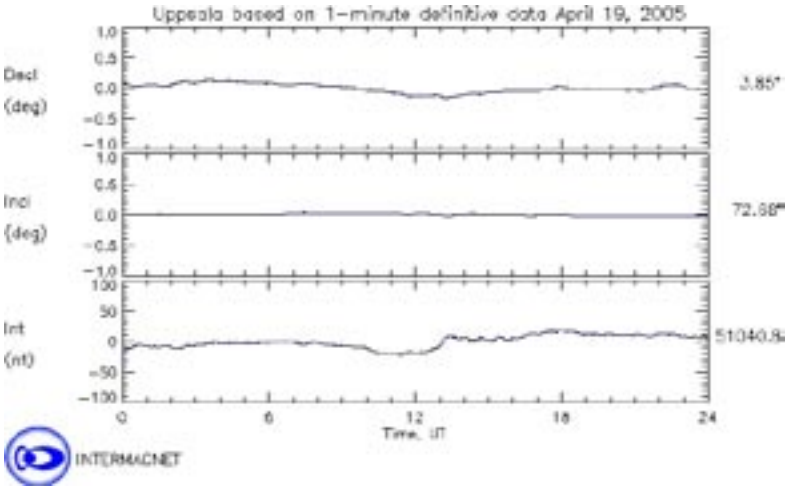

Measured borehole during April 19 2005: KFM08A

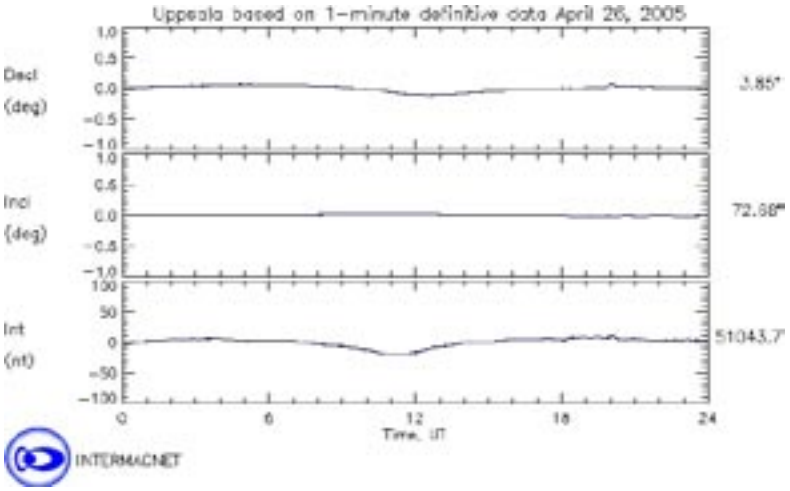

Measured borehole during April 26 2005: KFM02A

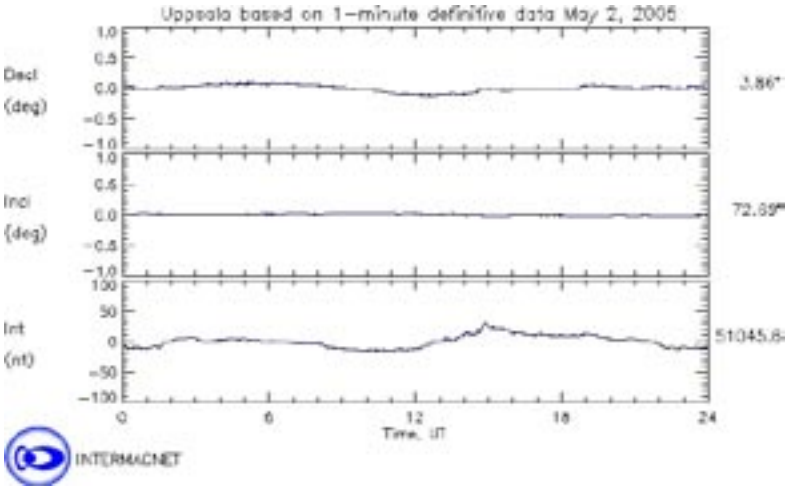

Measured borehole during May 2 2005: KFM07A

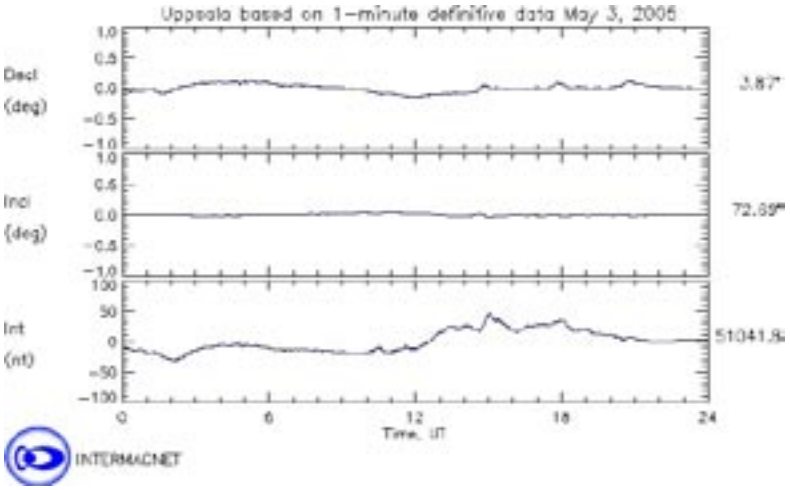

Measured boreholes during May 3 2005: KFM05A, KFM06A

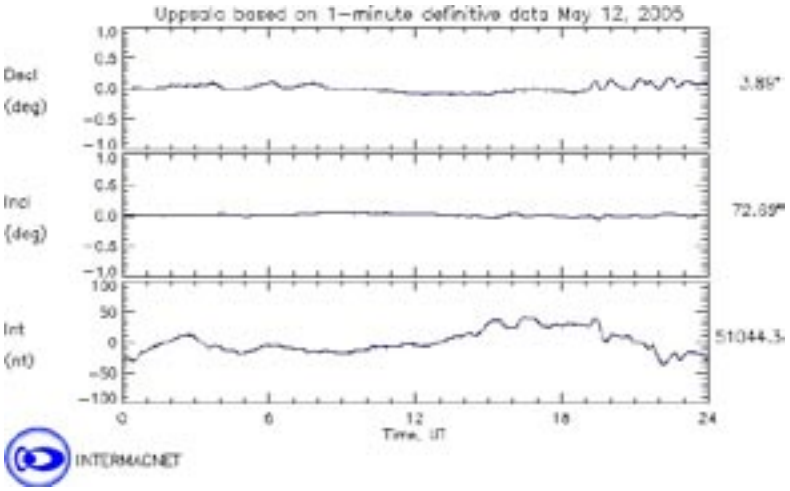

Measured borehole during May 12 2005: KFM08C

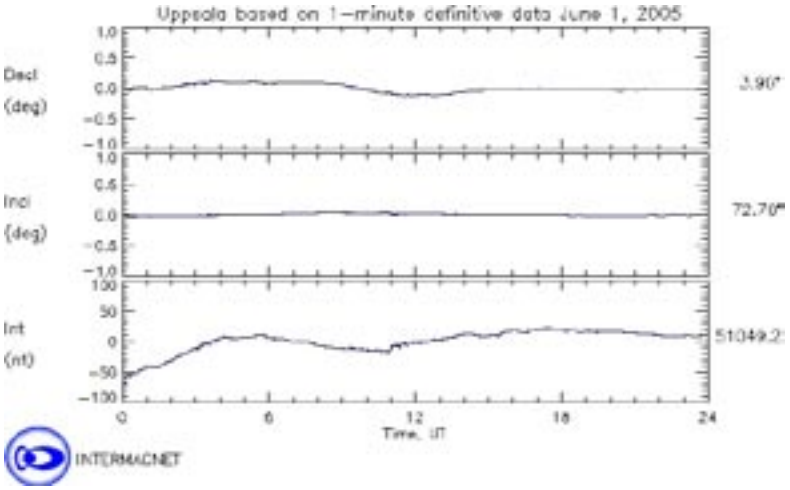

Measured borehole during June 1 2005: KFM04A

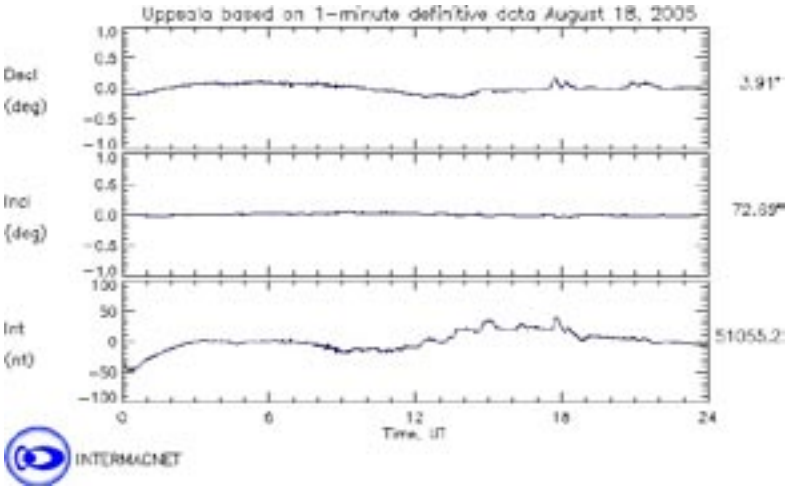

Measured borehole during August 18 2005: KFM06C

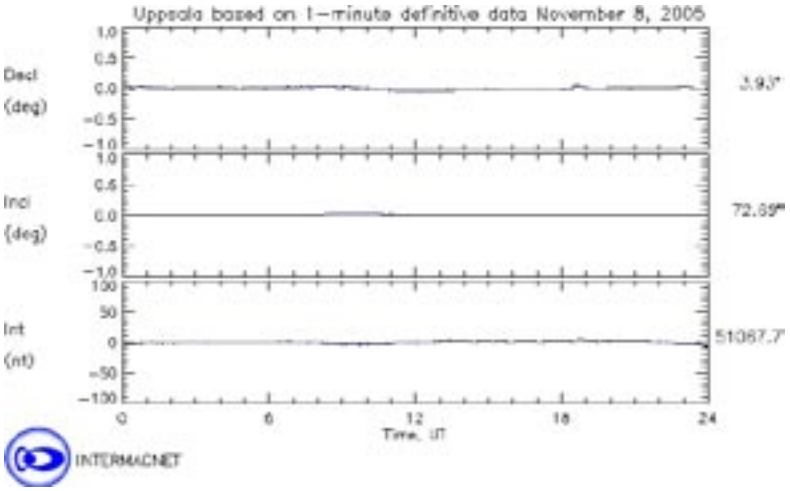

Measured borehole during November 8 2005: KFM09A

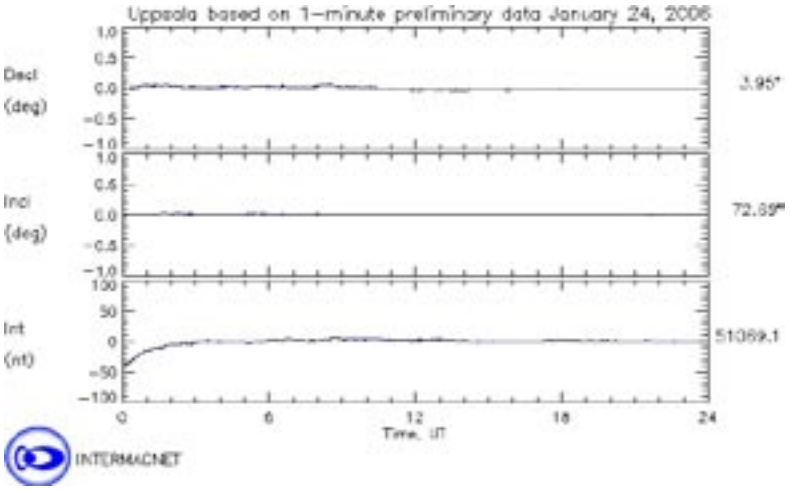

Measured borehole during January 24 2006: KFM01C

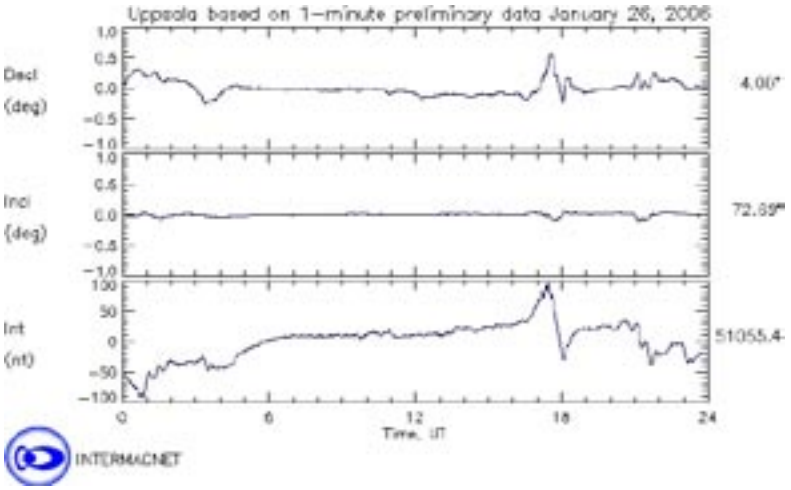

Measured borehole during January 26 2006: KFM09B

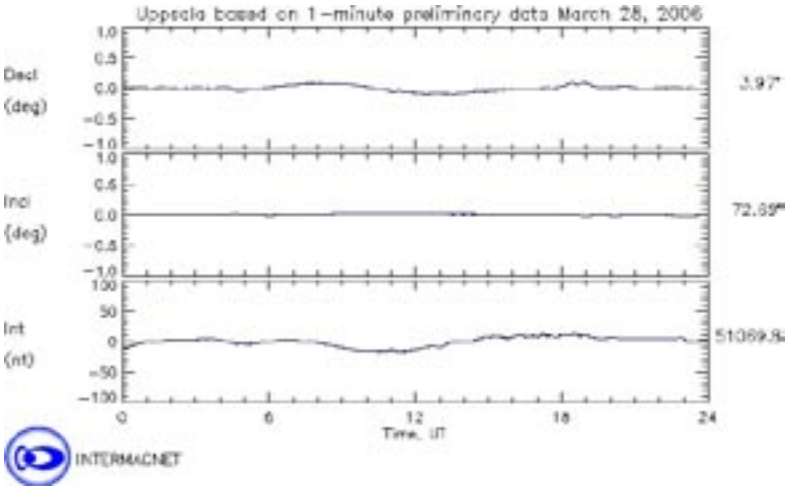

Measured borehole during March 28 2006: KFM01D

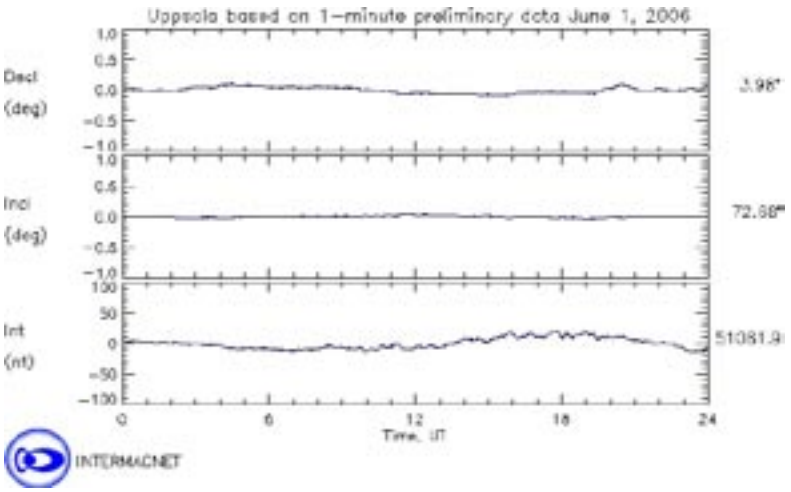

Measured borehole during June 1 2006: KFM08C

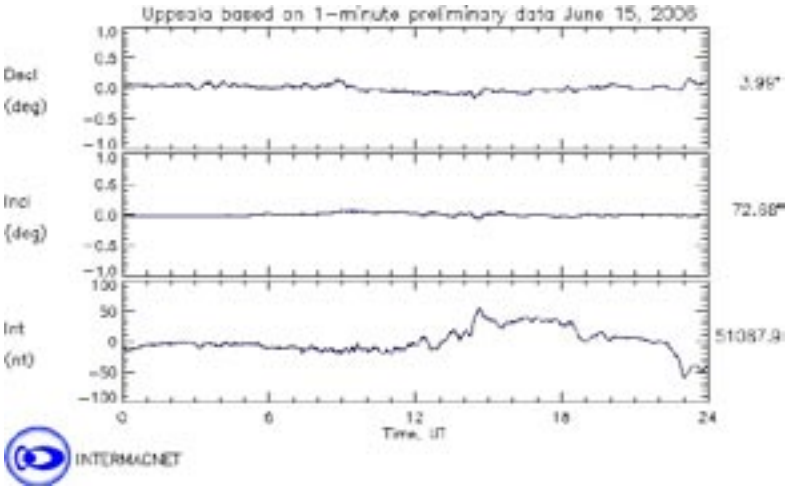

Measured borehole during June 15 2006: KFM10A

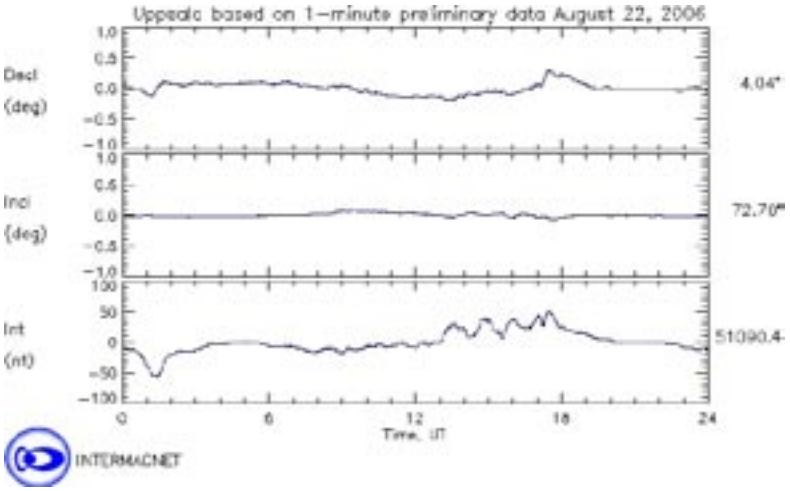

Measured borehole during August 22 2006: KFM07C

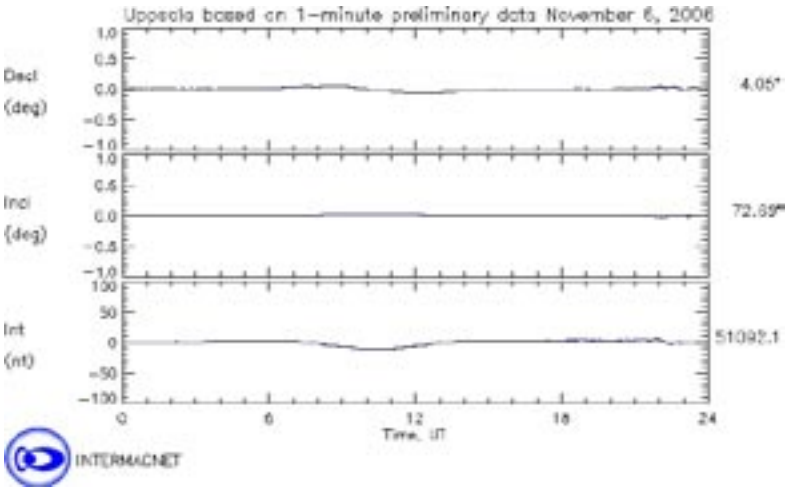

Measured borehole during November 6 2006: KFM07B

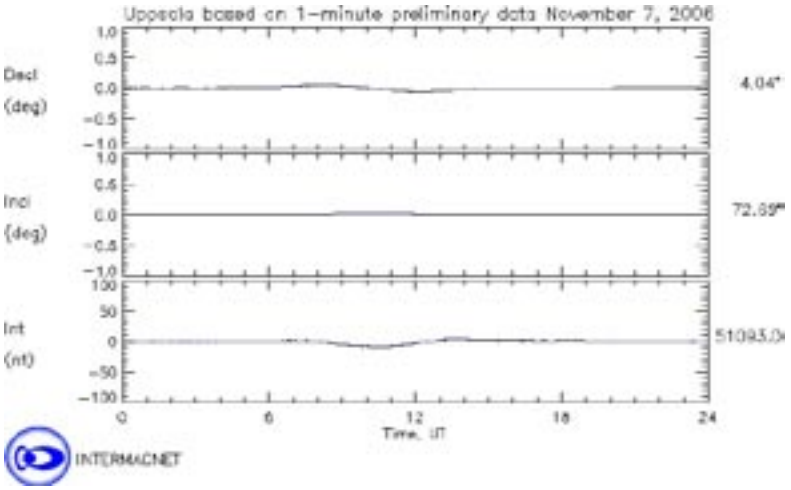

Measured borehole during November 7 2006: KFM07A

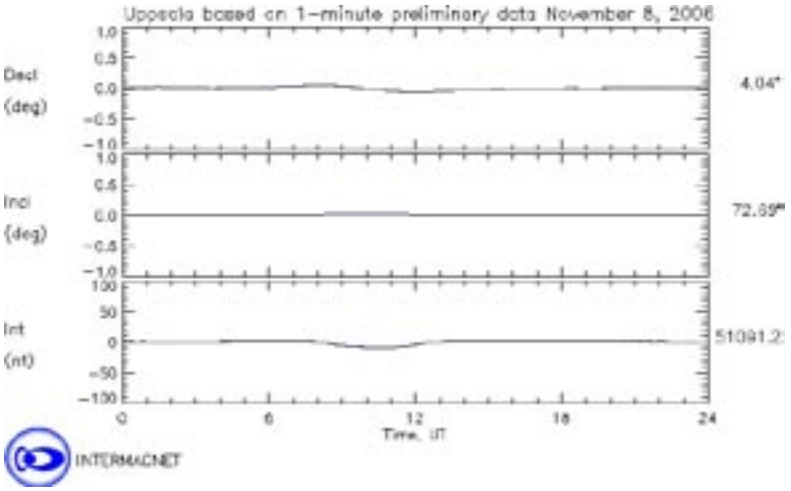

Measured boreholes during November 8 2006: KFM07C, KFM08C

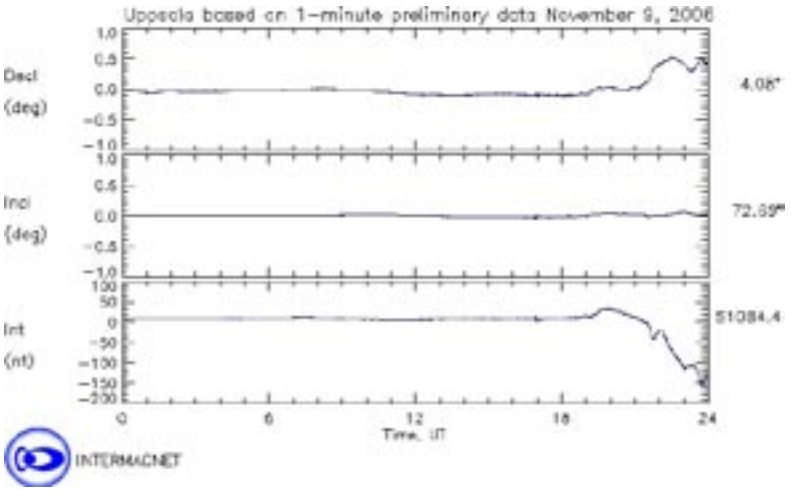

Measured borehole during November 9 2006: KFM08A

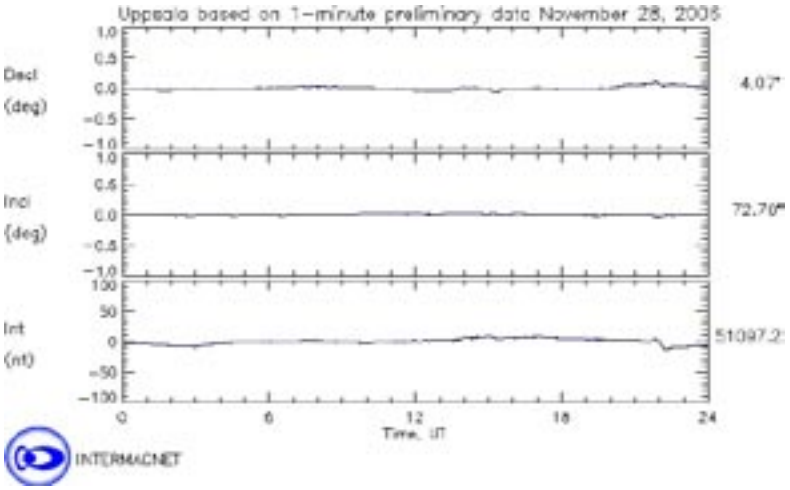

Measured borehole during November 28 2006: KFM11A

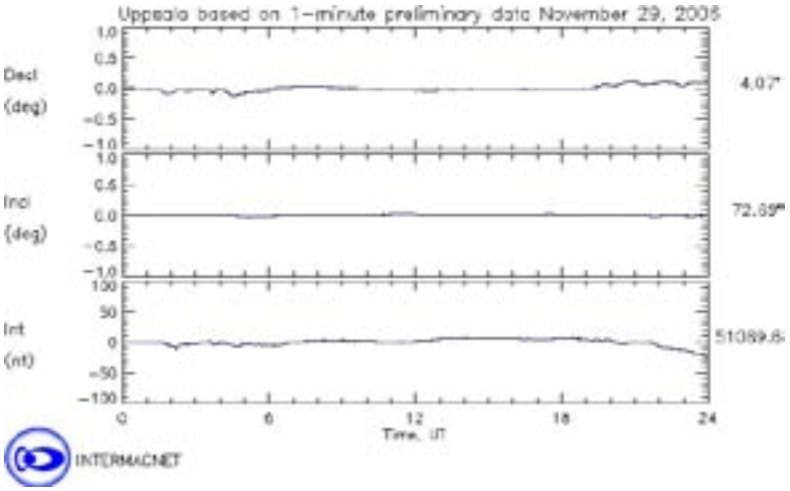

Measured borehole during November 29 2006: KFM01D

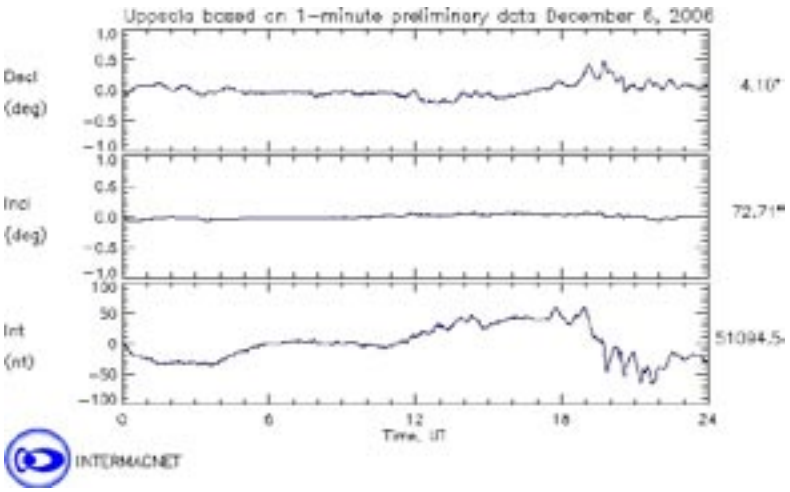

Measured borehole during December 6 2006: KFM10A

A1.2 Days with magnetic measurements at Laxemar

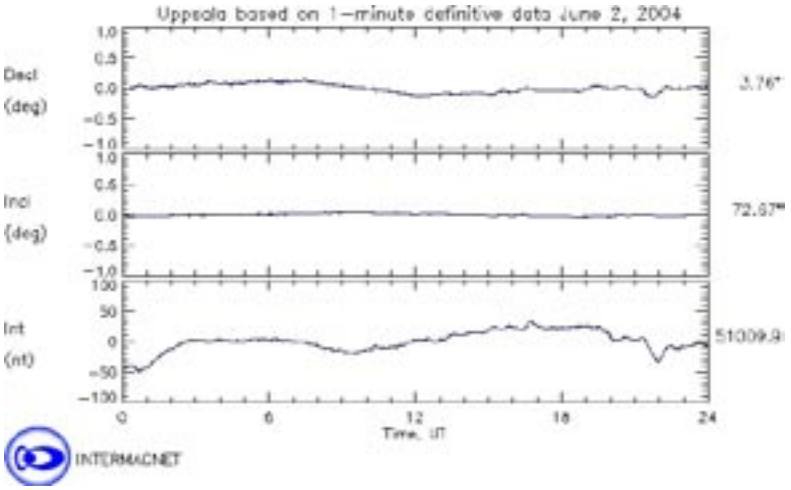

Measured borehole during June 2 2004: HLX15

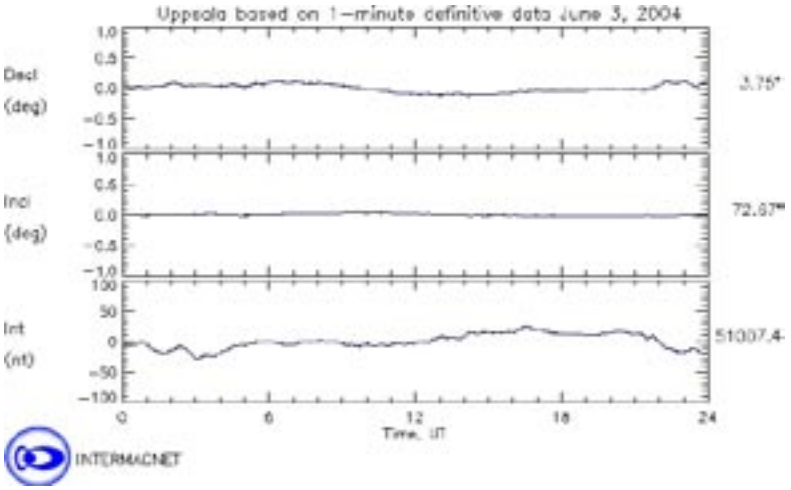

Measured borehole during June 3 2004: HLX13

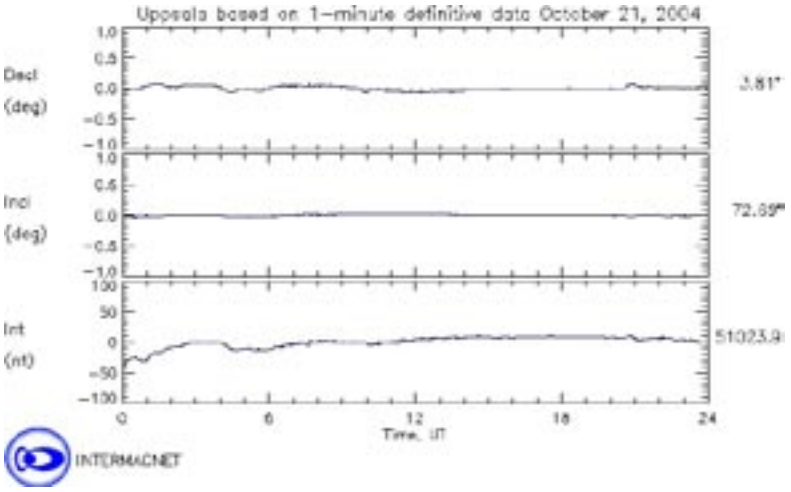

Measured borehole during October 21 2004: HLX27

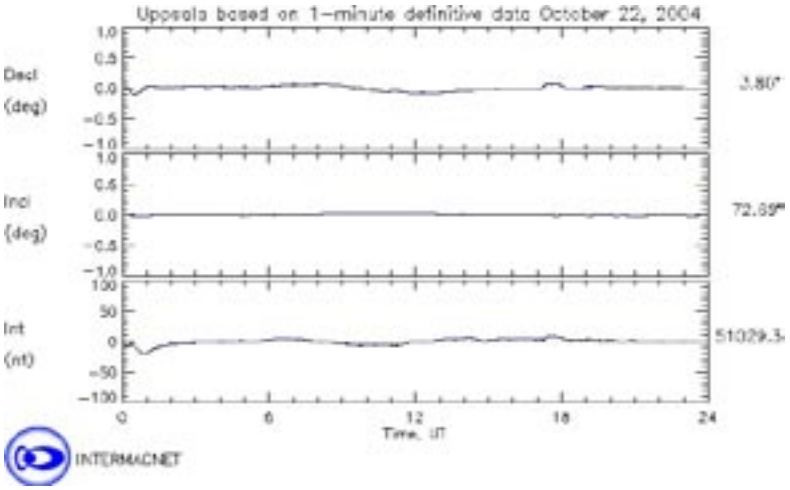

Measured borehole during October 22 2004: HLX26, HLX28

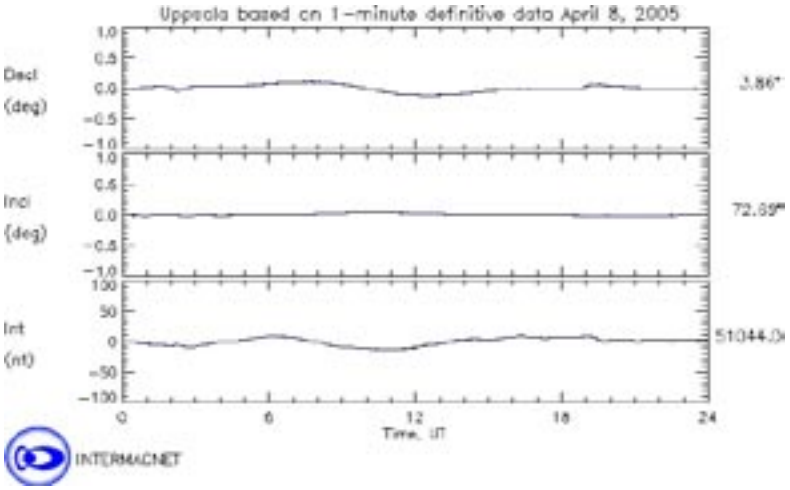

Measured borehole during April 8 2005: HLX32

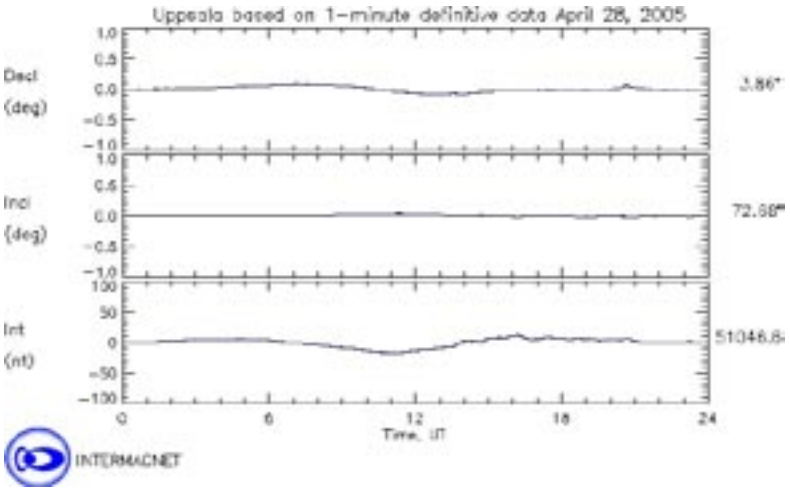

Measured borehole during April 28 2005: KLX03

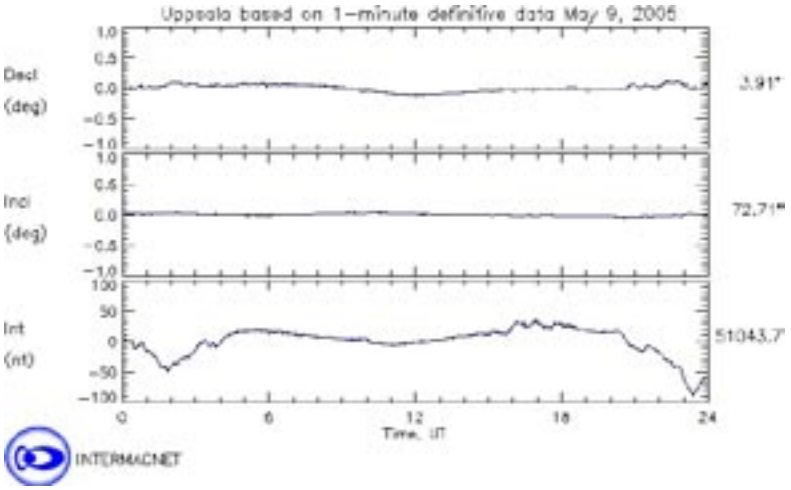

Measured borehole during May 9 2005: KLX07A

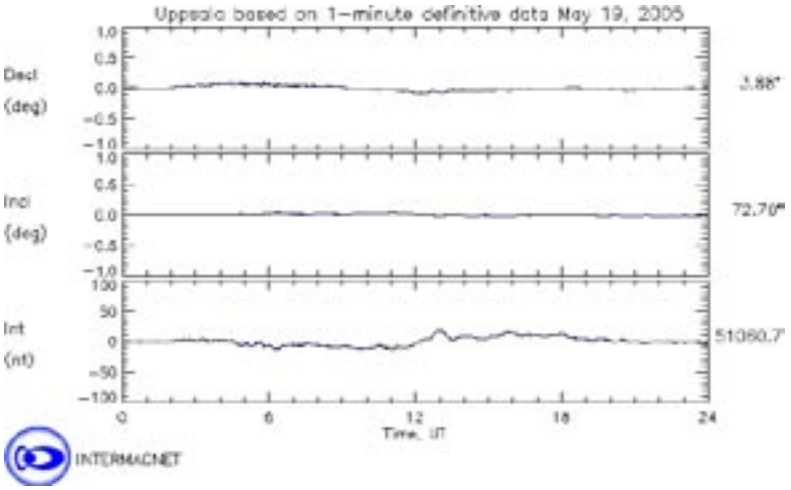

Measured borehole during May 19 2005: KLX05

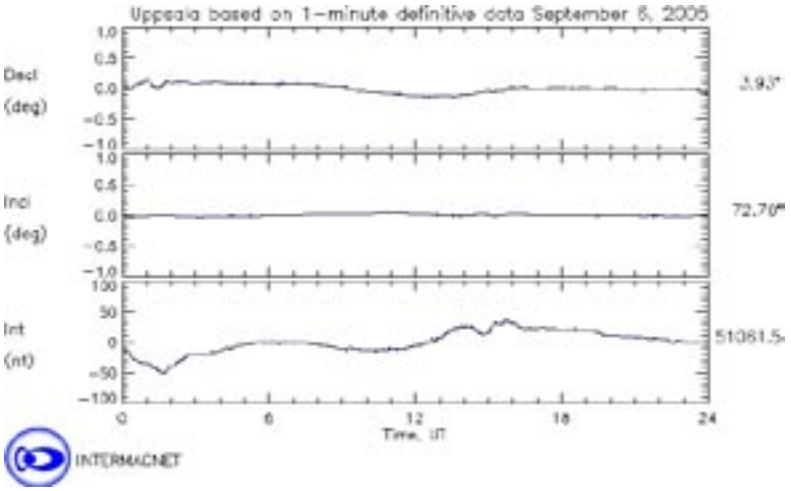

Measured borehole during September 6 2005: KLX08

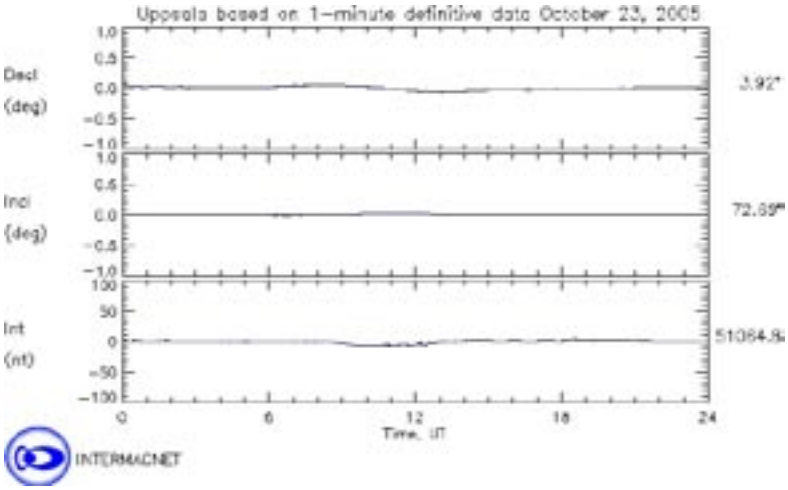

Measured borehole during October 23 2005: KLX10

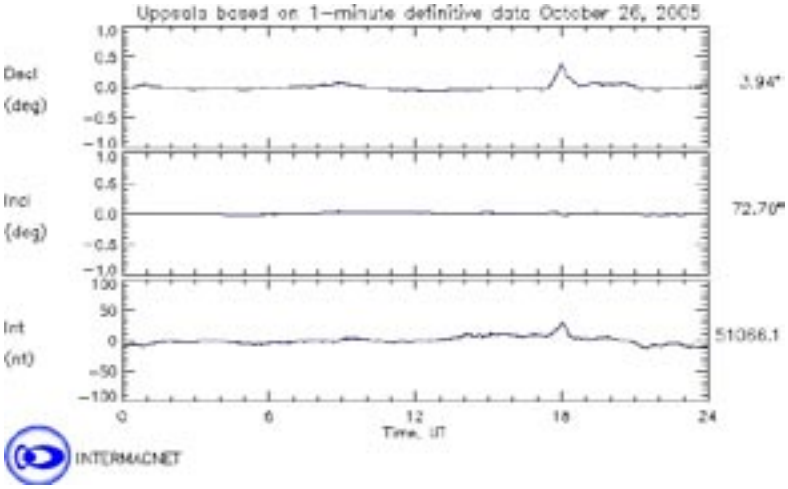

Measured borehole during October 26 2005: KLX09

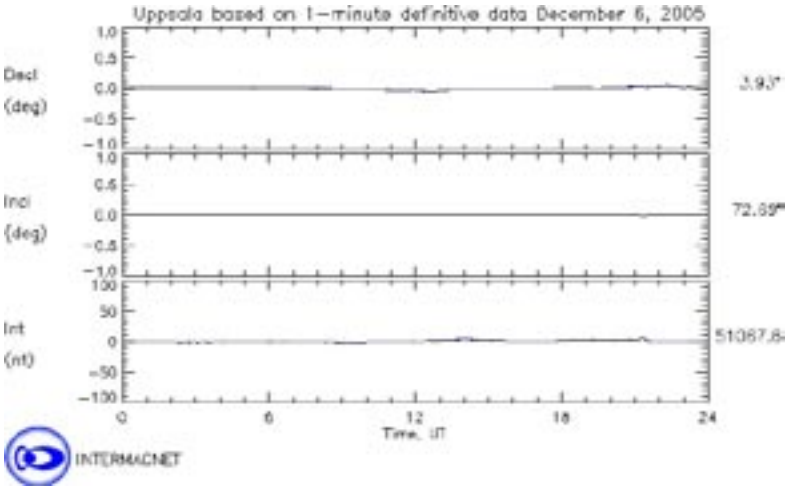

Measured borehole during December 6, 2005: HLX36

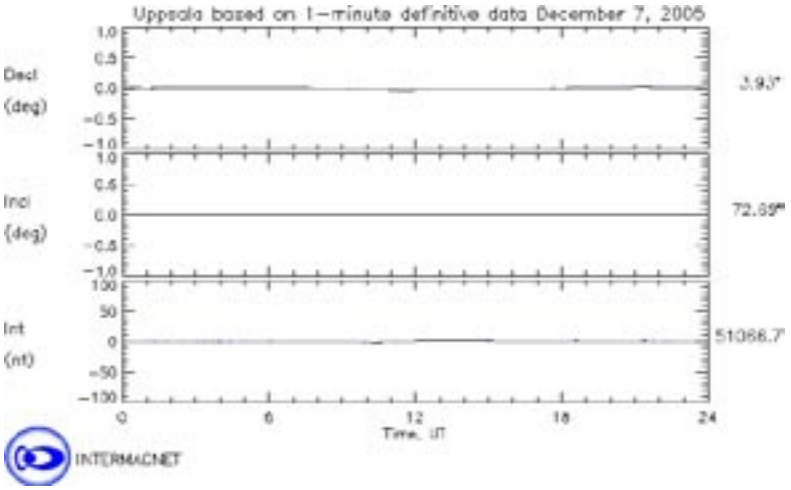

Measured borehole during December 7 2005: HLX37

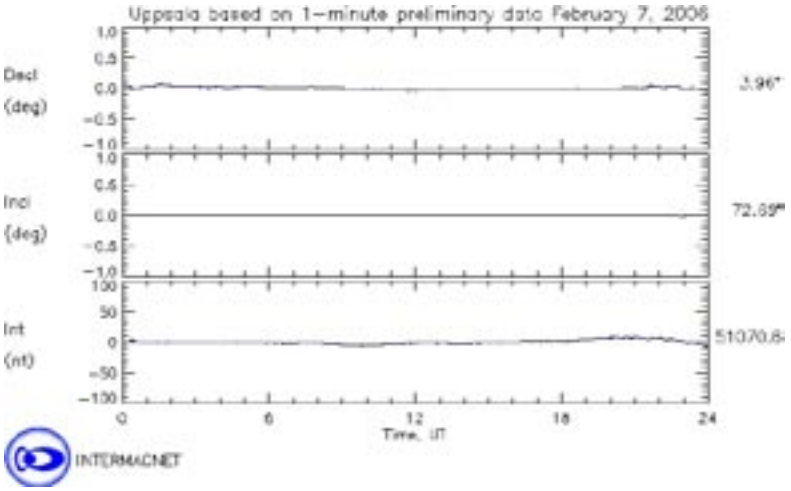

Measured borehole during February 7 2006: KLX09B, KLX09D, KLX09G

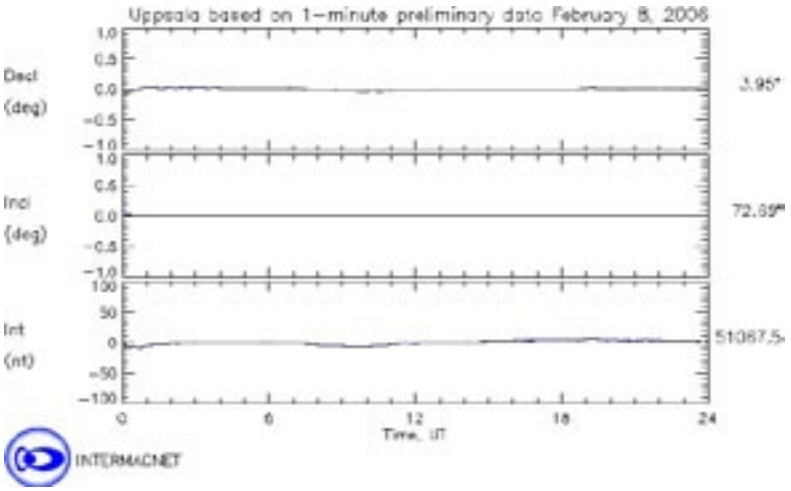

Measured borehole during February 8 2006: KLX09E

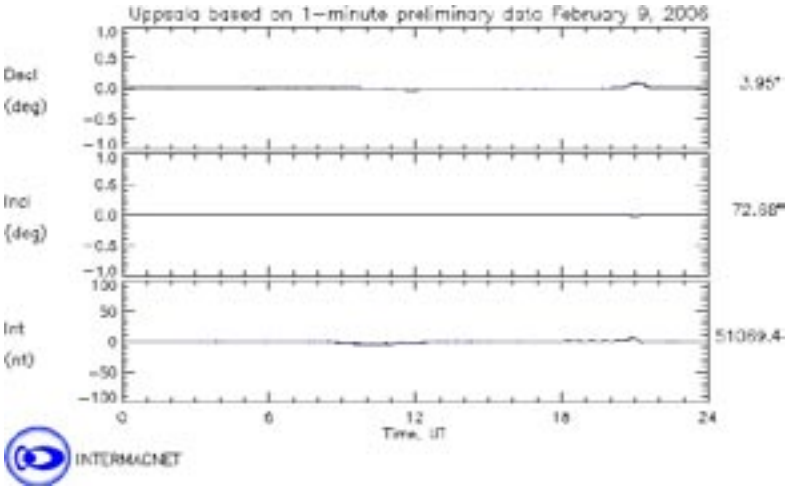

Measured borehole during February 9 2006: KLX09C, KLX09F

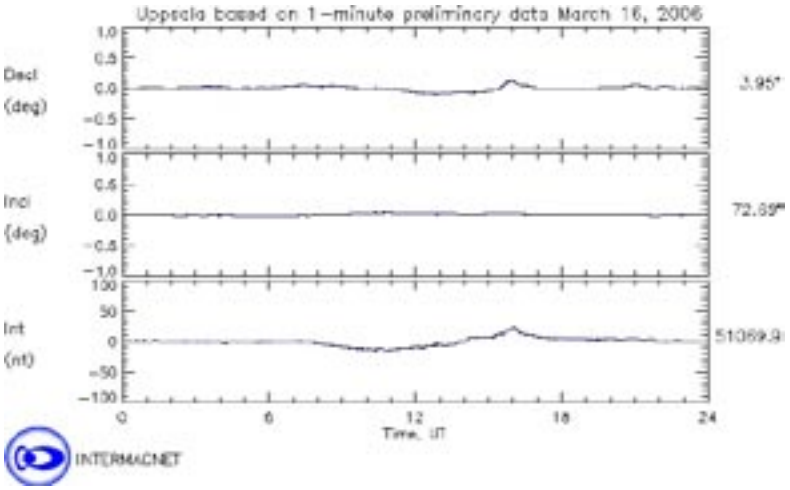

Measured borehole during March 16 2006: KLX11A

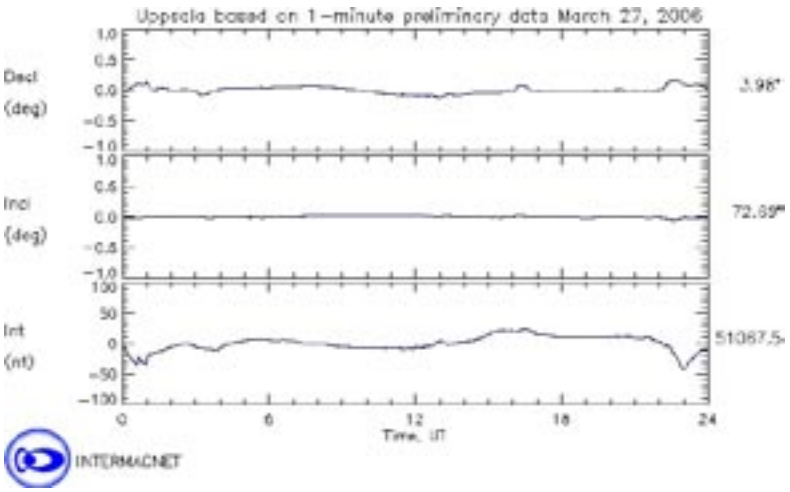

Measured borehole during March 27 2006: KLX10B, KLX10C, KLX12A

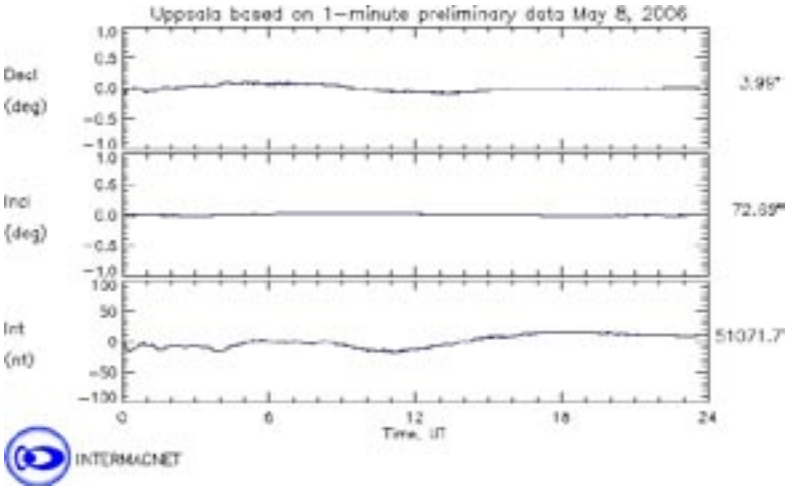

Measured borehole during May 8 2006: KLX11E, KLX11F, KLX20A

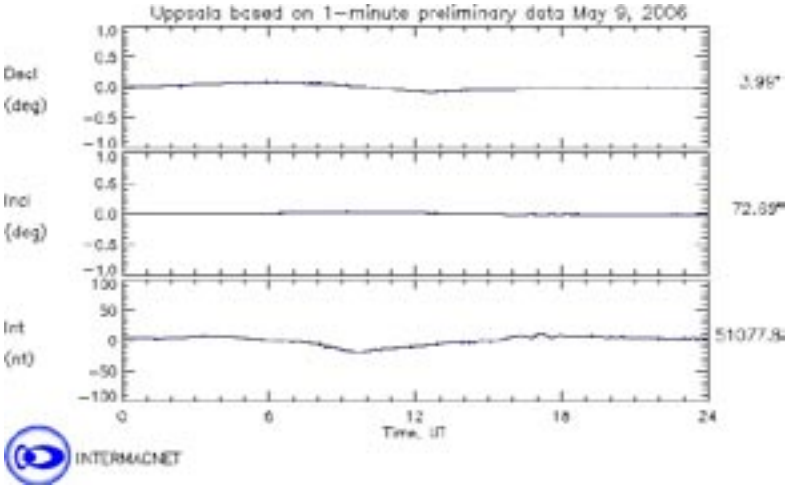

Measured borehole during May 9 2006: KLX11B, KLX11D

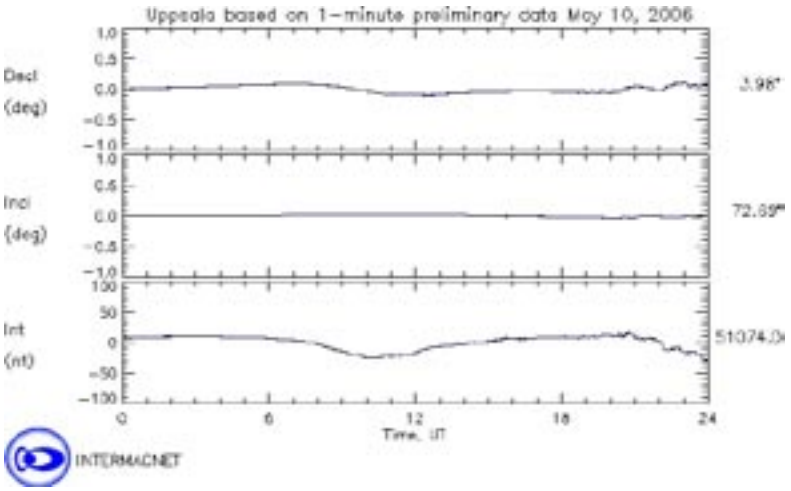

Measured borehole during May 10 2006: KLX11C

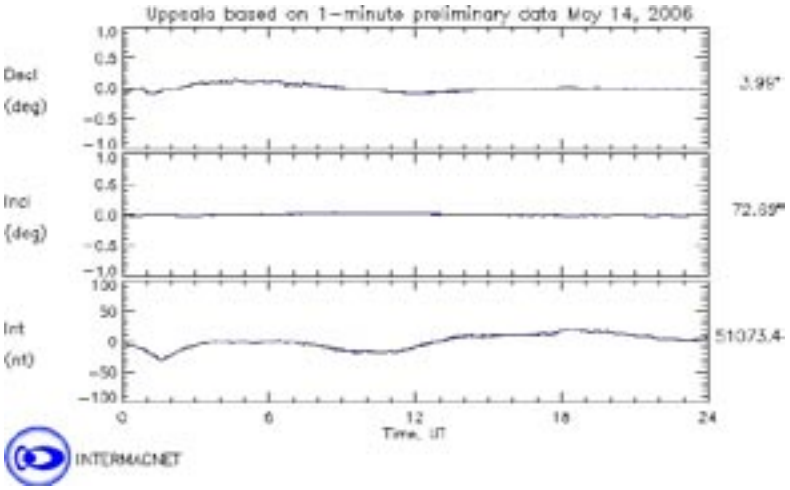

Measured borehole during May 14 2006: KLX19A, HLX38

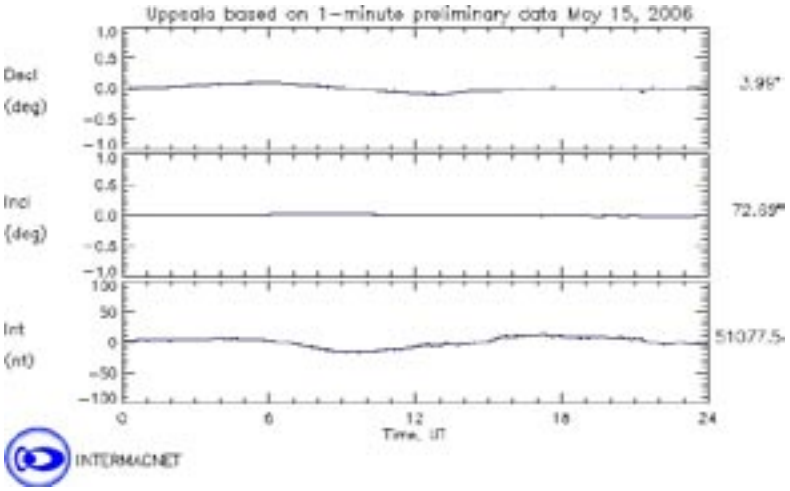

Measured borehole during May 15 2006: KLX18A

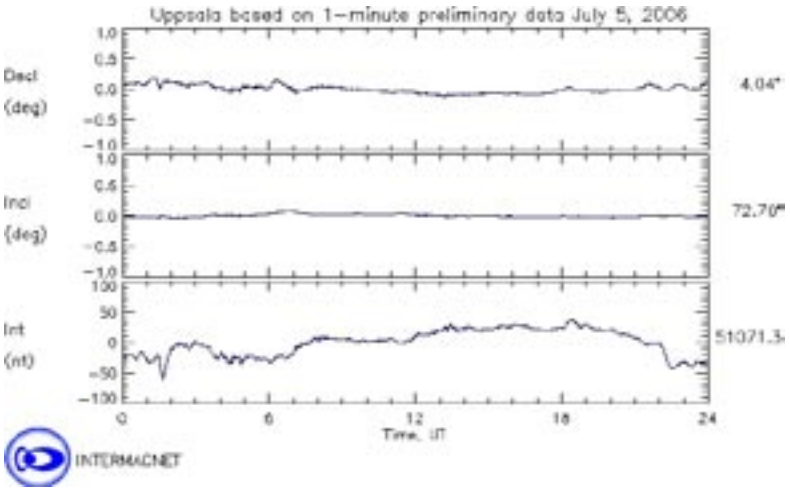

Measured borehole during July 5 2006: KLX22A, KLX22B, KLX23A, KLX23B

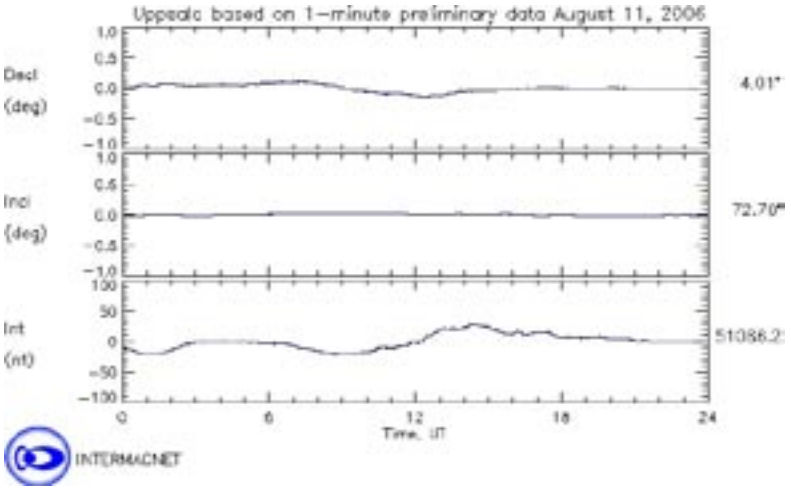

Measured borehole during August 11 2006: KLX24A

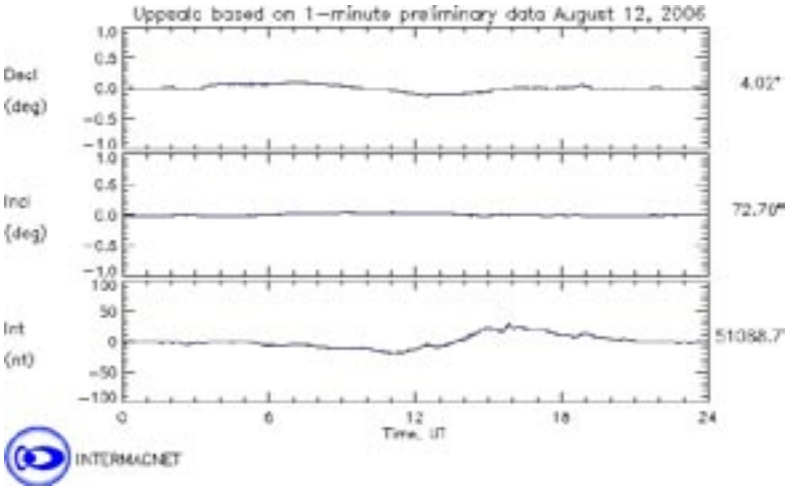

Measured borehole during August 12 2006: KLX25A

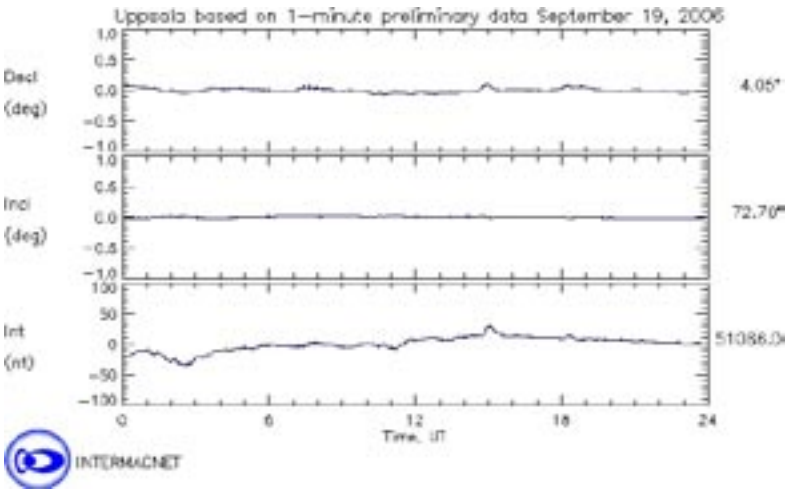

Measured borehole during September 19 2006: KLX13A

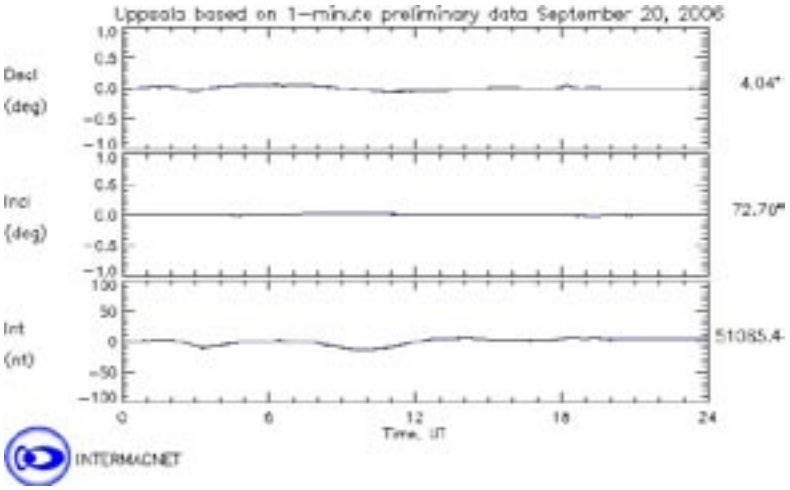

Measured borehole during September 20 2006: KLX13A, KLX14A, KLX26A,KLX26B

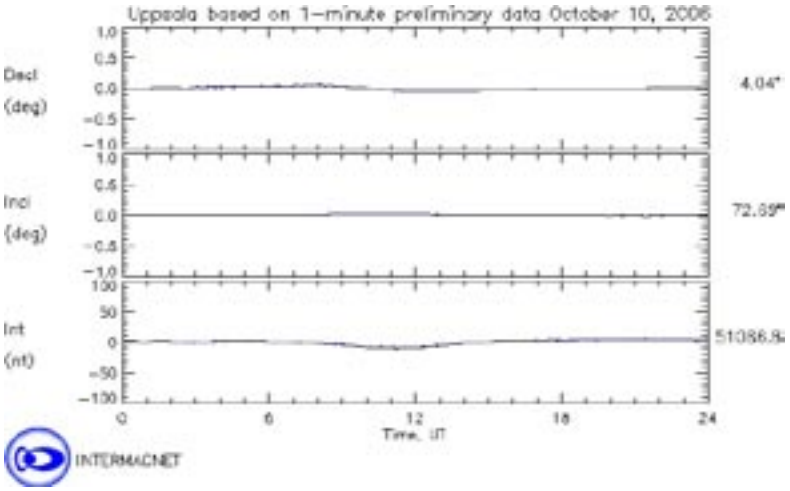

Measured borehole during October 10 2006: KLX19A

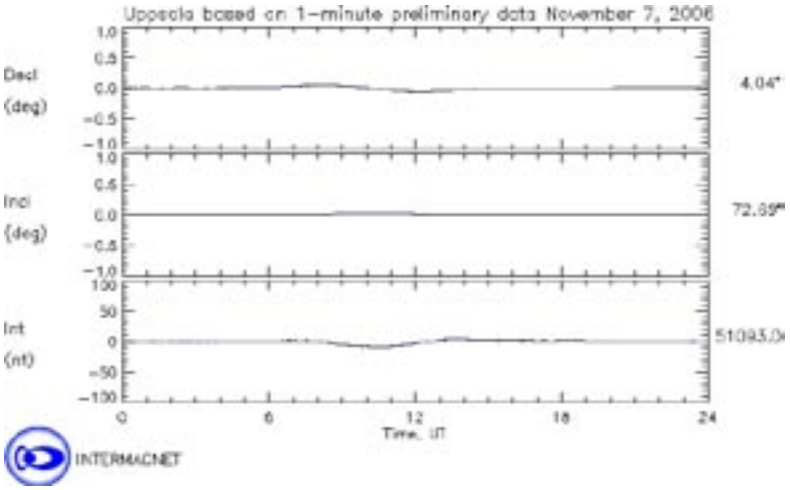

Measured borehole during November 7 2006: KLX29A

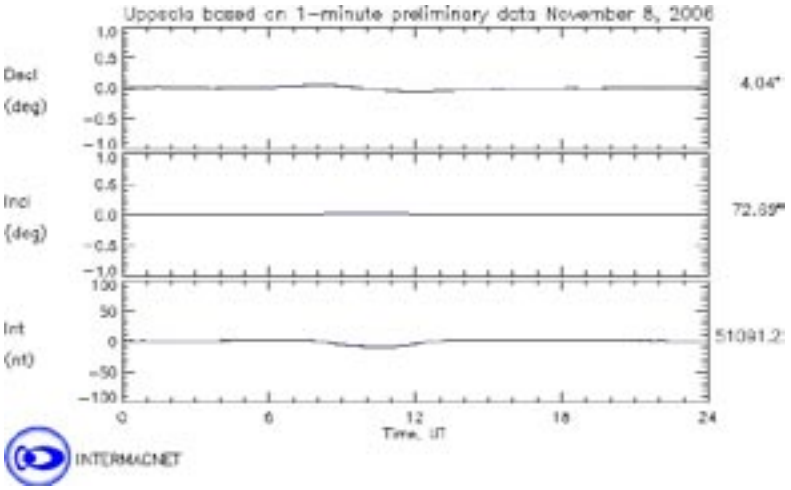

Measured borehole during November 8 2006: KLX28A

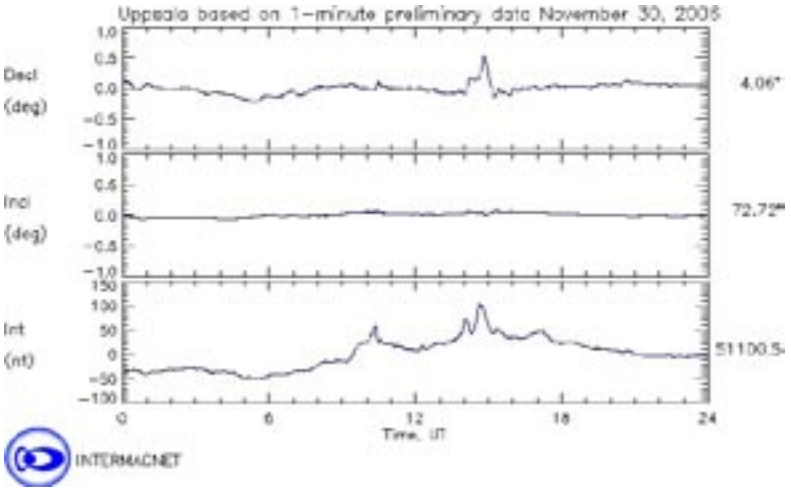

Measured borehole during November 30 2006: HLX43

A2 Algorithms and codes

A2.1 Dihedral angle

```
Function DihedralAngle(T1, P1, T2, P2 As Double) As Double
'Computes the dihedral angle between two lines. Input is trend (T) /plunge(P)
'Raymond Munier, January 2007
DihedralAngle = ArcCos(Abs(Cos((T1 - T2) * pi / 180) * Cos((P1) * pi / 180) * Cos((P2) *
pi / 180) + Sin((P1) * pi / 180) * Sin((P2) * pi / 180))) * 180 / pi
End Function
```

A2.2 Omega

```
'Computes the uncertainty in fracture orientations, using uncertainties in:
'alpha, beta, borehole bearing, borehole inclination.
'The result is the largest dihedral angle of all combinations, which provides a conser-
vative estimate.
'Raymond Munier, January 2007
'We assume all orientation are given as vectors, i.e. lines, all angles in degrees.
'The approach is the following:
'Step 1. Get the max of dihedral angles between alpha/beta and combinations of min and
max (alpha/beta)
'Step 2. Get the max range of dihedral angles between bearing/inclination and combina-
tions of min and max (bearing/inclination)
'Step 3. Add the maximum dihedral_borehole to max dihedral_fracture
Dim FractureOriArray(4, 2) As Double
Dim BoreHoleOriArray(4, 2) As Double
Dim dihedralArray(4, 2) As Double
Dim maxFractureDihedral, maxHoleDihedral, CurrentDihedral As Double
Dim i As Integer
'**********************
'Get the four extreme cases of fracture orientations, relative the core
'betaMax & alphaMax
FractureOriArray(1, 1) = beta + betaUncertainty 'betaMax
FractureOriArray(1, 2) = alpha + alphaUncertainty 'alphaMax
'betaMax & alphaMin
FractureOriArray(2, 1) = beta + betaUncertainty
FractureOriArray(2, 2) = alpha - alphaUncertainty
'betaMin & alphaMax
FractureOriArray(3, 1) = beta - betaUncertainty
FractureOriArray(3, 2) = alpha + alphaUncertainty
'betaMin & alphaMin
FractureOriArray(4, 1) = beta - betaUncertainty
FractureOriArray(4, 2) = alpha - alphaUncertainty
'**********************
'**********************
BoreHoleOriArray(1, 1) = Bearing + BearingUncertainty 'BearingMax
BoreHoleOriArray(1, 2) = Inclination
BoreHoleOriArray(2, 1) = Bearing - BearingUncertainty
BoreHoleOriArray(2, 2) = Inclination
BoreHoleOriArray(3, 1) = Bearing
BoreHoleOriArray(3, 2) = Inclination + InclinationUncertainty
BoreHoleOriArray(4, 1) = Bearing
BoreHoleOriArray(4, 2) = Inclination - InclinationUncertainty
'**********************
```

```
'Get the maximum dihedral angle between fracture and core by looping through the possi-
bilities
maxFractureDihedral = 0
CurrentDihedral = 0
For i = 1 To 4
    CurrentDihedral = Dihedral_Angle(beta, alpha, FractureOriArray(i, 1),
FractureOriArray(i, 2))
    If CurrentDihedral > maxFractureDihedral Then
        maxFractureDihedral = CurrentDihedral
    End If
Next i
'Get the maximum dihedral angle between the core and its uncertaities by looping through
the possibilities
maxHoleDihedral = 0
CurrentDihedral = 0
For i = 1 To 4
    CurrentDihedral = Dihedral_Angle(Bearing, Inclination, BoreHoleOriArray(i, 1),
BoreHoleOriArray(i, 2))
    If CurrentDihedral > maxHoleDihedral Then
        maxHoleDihedral = CurrentDihedral
    End If
Next i
ComputeUncertainty = maxFractureDihedral + maxHoleDihedral
End Function
```

A2.3 Check of implementations of algorithms

A2.3.1 Borehole orientation and uncertainty

```
'Microsoft(R) Excel 2002 VBA macro developped for checking the algorithms that
'are used to calculate the borehole deviation and uncertainty.

'Developped by Martin Stigsson January 2007

'The macro need 6 sheets named:
'EG_154_protocol
'Mag_acc_dev
'Maxibor
'mag_corr
'object_location
'orient_TOC

'The sheet EG_154_protocol need the following columns:
'D: IDCODE
'G: DEVIATION_ACTIVITY_ID
'H: DEVIATION_ANGLE_TYPE
'I: APPROVED_SECUP
'J: APPROVED_SECLOW
'It shall contain a header row and be sorted increasing on column D and H

'The sheet Mag_acc_dev need the following columns:
'A: ACTIVITY_ID
'C: ACTIVITY_TYPE
'D: ID_CODE
'I: BHLEN
```

```
'J: DIP
'K: MAGNETIC_BEARING
'It shall contain a header row and be sorted incraesing on column D, A and I

'The sheet Maxibor need the following columns:
'A: ACTIVITY_ID
'D: ID_CODE
'G: LENGTH
'L: INCLINATION
'M: BEARING
'It shall contain a header row and be sorted incraesing on column D, A and G

'The sheet mag_corr need the following columns:
'A: YEAR
'B: MAGNETIC_DECLINATION
'C: MEDIAN_CONVERGENCE
'It shall contain a header row and be sorted incraesing on column A

'The sheet object_location need the following columns:
'A: IDCODE
'E: NORTHING
'F: EASTING
'G: ELEVATION
'H: LENGTH
'O: INCLINATION
'P: BEARING
'Q: INCLINATION_UNCERT
'R: BEARING_UNCERT
'S: RADIUS_UNCERT
'It shall contain a header row and be sorted incraesing on column A, H

'The sheet orient_TOC need the following columns:
'C: IDCODE
'I: BEARING
'J: INCLINATION
'It shall contain a header row and be sorted incraesing on column C

Option Explicit
Sub Calc_dev_and_uncert()
Dim bhNameOld As String
Dim bhNameAct As String
Dim bhMatrix(1 To 100) As String  'vector containing the names of the boreholes in the
file
Dim televiewer As Boolean
Dim i As Integer
Dim j As Integer
Dim k As Integer
Dim nofBH As Integer  'number of boreholes in the files
Dim actId(0 To 10, 1 To 2) As Long 'Matrix containing the Activity_Id:s to be used for
```

```
calculating deviation
Dim bearSecUpLo(1 To 10, 1 To 2) As Double
Dim InclSecUpLo(1 To 10, 1 To 2) As Double
Sheets("EG_154_protocol").Select
Range("A1").Select
'Find the names of the boreholes and save them in bhMatrix, the number of Boreholes are
saved in nofBH
i = 1
j = 0
bhNameOld = ""
While ActiveCell.Offset(i, 3) <> ""
   bhNameAct = ActiveCell.Offset(i, 3).Text
   If bhNameAct <> bhNameOld Then
      j = j + 1
      bhMatrix(j) = bhNameAct
      bhNameOld = bhNameAct
   End If
   i = i + 1
Wend
nofBH = j
'Create the sheet for each borehole
For i = 1 To nofBH
   Call create_sheets(bhMatrix(i), i)
   Call write_bhLength(bhMatrix(i))
Next
Call create_sheets("Summary", nofBH + 1)
Call write_headers_in_Summary
For i = 1 To nofBH
'If bhMatrix(i) = "HLX13" Then
'i = i
'End If
   televiewer = False
   Call read_actId_and_secUpLo_4_dev(actId, bearSecUpLo, InclSecUpLo, bhMatrix(i))
   Call Check_if_telviewer(actId, bhMatrix(i), televiewer)
   If televiewer Then
      Call teleview_Bear_Incl_Calc(actId, bearSecUpLo, InclSecUpLo, bhMatrix(i))
   Else
      Call write_Bearing(actId, bearSecUpLo, bhMatrix(i))
      Call write_Inclination(actId, InclSecUpLo, bhMatrix(i))
      Call read_and_write_TOC_orientation(bhMatrix(i))
      Call calculate_new_deviation_file(bhMatrix(i))
   End If
   Call Copy_angle_data_from_object_location(bhMatrix(i))
   Call Fill_missing(bhMatrix(i))
   Call Calculate_angle_diff(bhMatrix(i))
   Call Calculate_spatial_diff(bhMatrix(i), i)
   Call Evaluation_of_diff(bhMatrix(i), i)
   Call calculate_90_percentile_MSt(bhMatrix(i), i)
   Call calculate_diff_90_percentile(bhMatrix(i), i)
   Call calculate_uncert_radius(bhMatrix(i), i)
Next
End Sub
'Create a new sheet at the end of the existing
Sub create_sheets(bhNameAct, bhNumber)
Sheets.Add After:=Sheets(bhNumber + 5)
Sheets(bhNumber + 6).Name = bhNameAct
End Sub
```

```
Sub write_bhLength(bhName)
Dim i As Integer
Sheets(bhName).Select
Range("A1").Select
ActiveCell.Offset(0, 0) = bhName
ActiveCell.Offset(1, 0) = "TOC"
For i = 0 To 336
   ActiveCell.Offset(i + 2, 0) = i * 3
Next
End Sub
Sub write_headers_in_Summary()
Sheets("Summary").Select
Range("A1").Select
ActiveCell.Offset(2, 2) = "Borehole"
ActiveCell.Offset(2, 3) = "Bearing (Max diff)"
ActiveCell.Offset(2, 4) = "Inklination (Max diff)"
ActiveCell.Offset(2, 5) = "90% bearing"
ActiveCell.Offset(2, 6) = "90% inclination"
ActiveCell.Offset(2, 7) = "90% bearing Sicada"
ActiveCell.Offset(2, 8) = "90% inclination Sicada"
ActiveCell.Offset(2, 9) = "Diff bearing 90%"
ActiveCell.Offset(2, 10) = "Diff inclination 90%"
ActiveCell.Offset(2, 11) = "Spatial (Max diff)"
ActiveCell.Offset(2, 12) = "Uncert radius (Max diff)"
End Sub
Sub read_actId_and_secUpLo_4_dev(actId, bearSecUpLo, InclSecUpLo, bhNameAct)
Dim i As Integer
Dim Bear As Integer
Dim Incl As Integer
Sheets("EG_154_protocol").Select
Range("A1").Select
i = 0
Bear = 0
Incl = 0
While ActiveCell.Offset(i, 3).Text <> ""
   If ActiveCell.Offset(i, 3).Text = bhNameAct Then
      If ActiveCell.Offset(i, 7).Text = "BEARING" Then
         Bear = Bear + 1
         actId(0, 1) = Bear
         actId(Bear, 1) = ActiveCell.Offset(i, 6)
         bearSecUpLo(Bear, 1) = ActiveCell.Offset(i, 8)
         bearSecUpLo(Bear, 2) = ActiveCell.Offset(i, 9)
      End If
      If ActiveCell.Offset(i, 7).Text = "INCLINATION" Then
         Incl = Incl + 1
         actId(0, 2) = Incl
         actId(Incl, 2) = ActiveCell.Offset(i, 6)
         InclSecUpLo(Incl, 1) = ActiveCell.Offset(i, 8)
         InclSecUpLo(Incl, 2) = ActiveCell.Offset(i, 9)
      End If
   End If
   i = i + 1
Wend
End Sub
Sub Check_if_telviewer(actId, bhNameAct, teleview_measure)
Dim i As Integer
```

```
Dim j As Integer
For i = 1 To actId(0, 1)
   'EG159 (televiwer measurement) is a magnetic measurement
   Sheets("Mag_acc_dev").Select
   Range("A1").Select
   j = 0
   While ActiveCell.Offset(j, 0) <> actId(i, 1) And ActiveCell.Offset(j, 0) <> ""
      j = j + 1
   Wend
   If ActiveCell.Offset(j, 2).Value = "EG159" Then teleview_measure = True
Next
End Sub
Sub teleview_Bear_Incl_Calc(actId, bearSecUpLo, InclSecUpLo, bhNameAct)
Dim i As Integer
Dim j As Integer
Dim k As Integer
Dim ki As Integer
Dim kb As Integer
'Dim cellOffset As Integer
Dim measureYear As Integer
Dim corrFact As Double
Dim topBearing As Double
Dim topInclination As Double
Dim tempdata(1 To 100) As Double
Dim actBHbear(1 To 3340, 1 To 2) As Double
Dim actBHincl(1 To 3340, 1 To 2) As Double
'The file is a magnetic measurement
Sheets("Mag_acc_dev").Select
Range("A1").Select
j = 0
While ActiveCell.Offset(j, 0) <> actId(1, 1) And ActiveCell.Offset(j, 0) <> ""
   j = j + 1
Wend
'calculate correction factor
If ActiveCell.Offset(j, 0) <> "" Then
   measureYear = Val(Left(ActiveCell.Offset(j, 6).Text, 4))
   Sheets("Mag_corr").Select
   Range("A1").Select
   corrFact = ActiveCell.Offset(1 + measureYear - ActiveCell.Offset(1, 0), 1).Value -
ActiveCell.Offset(1 + measureYear - ActiveCell.Offset(1, 0), 2).Value
   Sheets("Mag_acc_dev").Select
   Range("A1").Select
End If
ki = 0
kb = 0
While ActiveCell.Offset(j, 0) = actId(1, 1)
   If ActiveCell.Offset(j, 8) >= bearSecUpLo(1, 1) And ActiveCell.Offset(j, 8) <= bear-
SecUpLo(1, 2) Then
      kb = kb + 1
      actBHbear(kb, 1) = ActiveCell.Offset(j, 8)            'BH length
      actBHbear(kb, 2) = ActiveCell.Offset(j, 10) + corrFact 'bearing
   End If
   If ActiveCell.Offset(j, 8) >= InclSecUpLo(1, 1) And ActiveCell.Offset(j, 8) <= Incl-
SecUpLo(1, 2) Then
      ki = ki + 1
      actBHincl(ki, 1) = ActiveCell.Offset(j, 8)            'BH length
      actBHincl(ki, 2) = ActiveCell.Offset(j, 9)            'inclination
```

```
   End If
   j = j + 1
Wend
'Read TOC values
Call read_and_write_TOC_orientation(bhNameAct)
Sheets(bhNameAct).Select
Range("A1").Select
topBearing = ActiveCell.Offset(1, 1).Value
topInclination = ActiveCell.Offset(1, 11).Value
'Interpolate and write values
For i = 0 To 3 Step 3
   k = 1
   tempdata(k) = topBearing
   For j = 1 To 50
      If Abs(actBHbear(j, 1) - i) <= 4.5 Then
         k = k + 1
         tempdata(k) = actBHbear(j, 2)
      End If
   Next
   If k > 0 Then
      Call Bubble_Sort(tempdata, k)
      If k Mod 2 = 0 Then
         'there is an even number of data
         ActiveCell.Offset(i / 3 + 2, 21) = (tempdata(k / 2) + tempdata(k / 2 + 1)) / 2
      Else
         'There is an odd number of data
         ActiveCell.Offset(i / 3 + 2, 21) = tempdata((k + 1) / 2)
      End If
   End If
Next
For i = 0 To 3 Step 3
   k = 1
   tempdata(k) = topInclination
   For j = 1 To 50
      If Abs(actBHincl(j, 1) - i) <= 4.5 Then
         k = k + 1
         tempdata(k) = actBHincl(j, 2)
      End If
   Next
   If k > 0 Then
      Call Bubble_Sort(tempdata, k)
      If k Mod 2 = 0 Then
         'there is an even number of data
         ActiveCell.Offset(i / 3 + 2, 22) = (tempdata(k / 2) + tempdata(k / 2 + 1)) / 2
      Else
         'There is an odd number of data
         ActiveCell.Offset(i / 3 + 2, 22) = tempdata((k + 1) / 2)
      End If
   End If
Next
'Calculate and write the bearing
For i = 6 To 1002 Step 3
   k = 0
   For j = 1 To 3340
      If Abs(actBHbear(j, 1) - i) <= 4.5 Then
         k = k + 1
```

```
            tempdata(k) = actBHbear(j, 2)
         End If
      Next
      If k > 0 Then
         Call Bubble_Sort(tempdata, k)
         If k Mod 2 = 0 Then
            'there is an even number of data
            ActiveCell.Offset(i / 3 + 2, 21) = (tempdata(k / 2) + tempdata(k / 2 + 1)) / 2
         Else
            'There is an odd number of data
            ActiveCell.Offset(i / 3 + 2, 21) = tempdata((k + 1) / 2)
         End If
      End If
Next
'Calculate and write the Inclination
For i = 6 To 1002 Step 3
   k = 0
   For j = 1 To 3340
      If Abs(actBHincl(j, 1) - i) <= 4.5 Then
         k = k + 1
         tempdata(k) = actBHincl(j, 2)
      End If
   Next
   If k > 0 Then
      Call Bubble_Sort(tempdata, k)
      If k Mod 2 = 0 Then
         'there is an even number of data
         ActiveCell.Offset(i / 3 + 2, 22) = (tempdata(k / 2) + tempdata(k / 2 + 1)) / 2
      Else
         'There is an odd number of data
         ActiveCell.Offset(i / 3 + 2, 22) = tempdata((k + 1) / 2)
      End If
   End If
Next
'Interpolate when there are no calculated Bearing values
For i = 2 To 338
   If ActiveCell.Offset(i, 21) = "" Then
      j = 1
      While ActiveCell.Offset(i + j, 21) = "" And j + i < 338
         j = j + 1
      Wend
      If j + i < 338 Then
         If Abs(ActiveCell.Offset(i - 1, 21) - ActiveCell.Offset(i + j, 21)) < 180 Then
            ActiveCell.Offset(i, 21) = ActiveCell.Offset(i - 1, 21) * j / (j + 1) + Ac-
tiveCell.Offset(i + j, 21) * 1 / (j + 1)
         Else
            If ActiveCell.Offset(i - 1, 21) > 180 Then
               ActiveCell.Offset(i, 21) = (ActiveCell.Offset(i - 1, 21) - 360) * j / (j
+ 1) + ActiveCell.Offset(i + j, 21) * 1 / (j + 1)
               If ActiveCell.Offset(i, 21) < 0 Then ActiveCell.Offset(i, 21) = Active-
Cell.Offset(i, 21) + 360
            Else
               ActiveCell.Offset(i, 21) = (ActiveCell.Offset(i - 1, 21) + 360) * j / (j
+ 1) + ActiveCell.Offset(i + j, 21) * 1 / (j + 1)
               If ActiveCell.Offset(i, 21) > 360 Then ActiveCell.Offset(i, 21) = Active-
Cell.Offset(i, 21) - 360
            End If
         End If
```

```
      End If
   End If
Next
'Interpolate when there are no calculated Inclination values
For i = 2 To 338
   If ActiveCell.Offset(i, 22) = "" Then
      j = 1
      While ActiveCell.Offset(i + j, 22) = "" And j + i < 338
         j = j + 1
      Wend
      If j + i < 338 Then
         ActiveCell.Offset(i, 22) = ActiveCell.Offset(i - 1, 22) * j / (j + 1) + Active-
Cell.Offset(i + j, 22) * 1 / (j + 1)
      End If
   End If
Next
End Sub
Sub write_Bearing(actId, bearSecUpLo, bhNameAct)
Dim i As Integer
Dim j As Integer
Dim k As Integer
Dim cellOffset As Integer
Dim measureYear As Integer
Dim corrFact As Double
Dim actBH(1 To 3340, 1 To 2) As Double
For i = 1 To actId(0, 1)
   'If the file is a magnetic measurement
   Sheets("Mag_acc_dev").Select
   Range("A1").Select
   j = 0
   While ActiveCell.Offset(j, 0) <> actId(i, 1) And ActiveCell.Offset(j, 0) <> ""
      j = j + 1
   Wend
   'calculate correction factor
   If ActiveCell.Offset(j, 0) <> "" Then
      measureYear = Val(Left(ActiveCell.Offset(j, 6).Text, 4))
      Sheets("Mag_corr").Select
      Range("A1").Select
      corrFact = ActiveCell.Offset(1 + measureYear - ActiveCell.Offset(1, 0), 1).Value -
ActiveCell.Offset(1 + measureYear - ActiveCell.Offset(1, 0), 2).Value
      Sheets("Mag_acc_dev").Select
      Range("A1").Select
   End If
   k = 0
   While ActiveCell.Offset(j, 0) = actId(i, 1)
      k = k + 1
      actBH(k, 1) = ActiveCell.Offset(j, 8)             'BH length
      actBH(k, 2) = ActiveCell.Offset(j, 10) + corrFact 'bearing
      j = j + 1
   Wend
   Sheets(bhNameAct).Select
   Range("A1").Select
   For j = 1 To k
      If actBH(j, 1) >= bearSecUpLo(i, 1) And actBH(j, 1) <= bearSecUpLo(i, 2) Then
         cellOffset = Round(actBH(j, 1) / 3) + 2
         ActiveCell.Offset(cellOffset, i) = actBH(j, 2)
      End If
```

```
   Next
   'If the file is a Maxibor measurement
   Sheets("Maxibor").Select
   Range("A1").Select
   j = 0
   While ActiveCell.Offset(j, 0) <> actId(i, 1) And ActiveCell.Offset(j, 0) <> ""
      j = j + 1
   Wend
   k = 0
   While ActiveCell.Offset(j, 0) = actId(i, 1)
      k = k + 1
      actBH(k, 1) = ActiveCell.Offset(j, 6)
      actBH(k, 2) = ActiveCell.Offset(j, 12)
      j = j + 1
   Wend
   Sheets(bhNameAct).Select
   Range("A1").Select
   ActiveCell.Offset(0, i) = actId(i, 1)
   For j = 1 To k
      If actBH(j, 1) >= bearSecUpLo(i, 1) And actBH(j, 1) <= bearSecUpLo(i, 2) Then
         cellOffset = Round(actBH(j, 1) / 3) + 2
         ActiveCell.Offset(cellOffset, i) = actBH(j, 2)
      End If
   Next
Next
End Sub
Sub write_Inclination(actId, InclSecUpLo, bhNameAct)
Dim i As Integer
Dim j As Integer
Dim k As Integer
Dim cellOffset As Integer
Dim actBH(1 To 3340, 1 To 2) As Double
For i = 1 To actId(0, 2)
   'If the file is a magnetic measurement
   Sheets("Mag_acc_dev").Select
   Range("A1").Select
   j = 0
   While ActiveCell.Offset(j, 0) <> actId(i, 2) And ActiveCell.Offset(j, 0) <> ""
      j = j + 1
   Wend
   k = 0
   While ActiveCell.Offset(j, 0) = actId(i, 2)
      k = k + 1
      actBH(k, 1) = ActiveCell.Offset(j, 8)
      actBH(k, 2) = ActiveCell.Offset(j, 9)
      j = j + 1
   Wend
   Sheets(bhNameAct).Select
   Range("A1").Select
   ActiveCell.Offset(0, i) = actId(i, 2)
   For j = 1 To k
      If actBH(j, 1) >= InclSecUpLo(i, 1) And actBH(j, 1) <= InclSecUpLo(i, 2) Then
         cellOffset = Round(actBH(j, 1) / 3) + 2
         ActiveCell.Offset(cellOffset, i + 10) = actBH(j, 2)
      End If
   Next
```

```
   'If the file is a Maxibor measurement
   Sheets("Maxibor").Select
   Range("A1").Select
   j = 0
   While ActiveCell.Offset(j, 0) <> actId(i, 2) And ActiveCell.Offset(j, 0) <> ""
      j = j + 1
   Wend
   k = 0
   While ActiveCell.Offset(j, 0) = actId(i, 2)
      k = k + 1
      actBH(k, 1) = ActiveCell.Offset(j, 6)
      actBH(k, 2) = ActiveCell.Offset(j, 11)
      j = j + 1
   Wend
   'Chose right sheet
   Sheets(bhNameAct).Select
   Range("A1").Select
   ActiveCell.Offset(0, i + 10) = actId(i, 2)
   For j = 1 To k
      If actBH(j, 1) >= InclSecUpLo(i, 1) And actBH(j, 1) <= InclSecUpLo(i, 2) Then
         cellOffset = Round(actBH(j, 1) / 3) + 2
         ActiveCell.Offset(cellOffset, i + 10) = actBH(j, 2)
      End If
   Next
Next
End Sub
Sub read_and_write_TOC_orientation(bhNameAct)
Dim i As Integer
Dim Bearing As Double
Dim Inclination As Double
Sheets("orient_TOC").Select
Range("A1").Select
i = 0
While ActiveCell.Offset(i, 0) <> ""
   i = i + 1
   If ActiveCell.Offset(i, 2) = bhNameAct Then
      Bearing = ActiveCell.Offset(i, 8).Value
      Inclination = ActiveCell.Offset(i, 9).Value
   End If
Wend
Sheets(bhNameAct).Select
Range("A1").Select
ActiveCell.Offset(1, 1) = Bearing
ActiveCell.Offset(1, 11) = Inclination
End Sub
Sub calculate_new_deviation_file(bhNameAct)
Dim i As Integer
Dim j As Integer
Dim k As Integer
Dim m As Integer
Dim nofBearAngle As Integer
Dim nofInclAngle As Integer
Dim highest_bear As Integer
Dim highest_incl As Integer
Dim highest_measured As Integer
Dim secLo As Double
```

```
Dim Data(1 To 200) As Double
Sheets("EG_154_protocol").Select
Range("A1").Select
secLo = 0
i = 1
While ActiveCell.Offset(i, 0) <> ""
   If ActiveCell.Offset(i, 3) = bhNameAct Then
      If ActiveCell.Offset(i, 9) > secLo Then secLo = ActiveCell.Offset(i, 9)
   End If
   i = i + 1
Wend
highest_measured = Round(secLo / 3)
If bhNameAct = "KFM07A" Then
   bhNameAct = bhNameAct
End If
Sheets(bhNameAct).Select
Range("A1").Select
'Write headers
ActiveCell.Offset(0, 21) = "Calc"
ActiveCell.Offset(0, 22) = "Calc"
ActiveCell.Offset(1, 21) = "Median Bearing"
ActiveCell.Offset(1, 22) = "Median Inclination"
'CALCULATE MEDIAN VALUES
'bearing for first row
k = 0
For i = 1 To 3
   For j = 1 To 10
      If ActiveCell.Offset(i, j) <> "" Then
         k = k + 1
         Data(k) = ActiveCell.Offset(i, j)
      End If
   Next
Next
Call Bubble_Sort(Data, k)
'If the data is crossing North
If Data(1) - Data(k) > 180 Then
   For i = 1 To k
      If Data(i) > 180 Then
         Data(i) = Data(i) - 360
      End If
   Next
   Call Bubble_Sort(Data, k)
End If
If k Mod 2 = 0 Then
   'there is an even number of data
   ActiveCell.Offset(2, 21) = (Data(k / 2) + Data(k / 2 + 1)) / 2
Else
   'There is an odd number of data
   ActiveCell.Offset(2, 21) = Data((k + 1) / 2)
End If
If ActiveCell.Offset(2, 21) < 0 Then ActiveCell.Offset(2, 21) = ActiveCell.Offset(2, 21)
+ 360
If ActiveCell.Offset(2, 21) > 360 Then ActiveCell.Offset(2, 21) = ActiveCell.Offset(2,
21) - 360
'Inclination for first row
k = 0
For i = 1 To 3
```

```
   For j = 11 To 20
      If ActiveCell.Offset(i, j) <> "" Then
         k = k + 1
         Data(k) = ActiveCell.Offset(i, j)
      End If
   Next
Next
Call Bubble_Sort(Data, k)
If k Mod 2 = 0 Then
   'there is an even number of data
   ActiveCell.Offset(2, 22) = (Data(k / 2) + Data(k / 2 + 1)) / 2
Else
   'There is an odd number of data
   ActiveCell.Offset(2, 22) = Data((k + 1) / 2)
End If
'bearing for second row
k = 0
For i = 1 To 4
   For j = 1 To 10
      If ActiveCell.Offset(i, j) <> "" Then
         k = k + 1
         Data(k) = ActiveCell.Offset(i, j)
      End If
   Next
Next
Call Bubble_Sort(Data, k)
'If the data is crossing North
If Data(1) - Data(k) > 180 Then
   For i = 1 To k
      If Data(i) > 180 Then
         Data(i) = Data(i) - 360
      End If
   Next
   Call Bubble_Sort(Data, k)
End If
If k Mod 2 = 0 Then
   'there is an even number of data
   ActiveCell.Offset(3, 21) = (Data(k / 2) + Data(k / 2 + 1)) / 2
Else
   'There is an odd number of data
   ActiveCell.Offset(3, 21) = Data((k + 1) / 2)
End If
If ActiveCell.Offset(3, 21) < 0 Then ActiveCell.Offset(3, 21) = ActiveCell.Offset(3, 21)
+ 360
If ActiveCell.Offset(3, 21) > 360 Then ActiveCell.Offset(3, 21) = ActiveCell.Offset(3,
21) - 360
'Inclination for second row
k = 0
For i = 1 To 4
   For j = 11 To 20
      If ActiveCell.Offset(i, j) <> "" Then
         k = k + 1
         Data(k) = ActiveCell.Offset(i, j)
      End If
   Next
Next
Call Bubble_Sort(Data, k)
```

```
If k Mod 2 = 0 Then
   'there is an even number of data
   ActiveCell.Offset(3, 22) = (Data(k / 2) + Data(k / 2 + 1)) / 2
Else
   'There is an odd number of data
   ActiveCell.Offset(3, 22) = Data((k + 1) / 2)
End If
For m = 4 To highest_measured + 3
'For m = 4 To highest_measured + 2
   'Bearing median
   k = 0
   For i = -1 To 1
      For j = 1 To 10
         If ActiveCell.Offset(i + m, j) <> "" Then
            k = k + 1
            Data(k) = ActiveCell.Offset(i + m, j)
         End If
      Next
   Next
   If k > 0 Then
      Call Bubble_Sort(Data, k)
      'If the data is crossing North
      If Data(1) - Data(k) > 180 Then
         For i = 1 To k
            If Data(i) > 180 Then
               Data(i) = Data(i) - 360
            End If
         Next
         Call Bubble_Sort(Data, k)
      End If
      If k Mod 2 = 0 Then
         'there is an even number of data
         ActiveCell.Offset(m, 21) = (Data(k / 2) + Data(k / 2 + 1)) / 2
      Else
         'There is an odd number of data
         ActiveCell.Offset(m, 21) = Data((k + 1) / 2)
      End If
   End If
   If ActiveCell.Offset(m, 21) < 0 Then ActiveCell.Offset(m, 21) = ActiveCell.Offset(m,
21) + 360
   If ActiveCell.Offset(m, 21) > 360 Then ActiveCell.Offset(m, 21) = ActiveCell.
Offset(m, 21) - 360
   'Inclination median
   k = 0
   For i = -1 To 1
      For j = 11 To 20
         If ActiveCell.Offset(i + m, j) <> "" Then
            k = k + 1
            Data(k) = ActiveCell.Offset(i + m, j)
         End If
      Next
   Next
   If k > 0 Then
      Call Bubble_Sort(Data, k)
      If k Mod 2 = 0 Then
         'there is an even number of data
         ActiveCell.Offset(m, 22) = (Data(k / 2) + Data(k / 2 + 1)) / 2
```

```
      Else
         'There is an odd number of data
         ActiveCell.Offset(m, 22) = Data((k + 1) / 2)
      End If
   End If
Next
'Interpolate when there are no calculated Bearing values
For i = 2 To 338
   If ActiveCell.Offset(i, 21) = "" Then
      j = 1
      While ActiveCell.Offset(i + j, 21) = "" And j + i < 338
         j = j + 1
      Wend
      If j + i < 338 Then
         If Abs(ActiveCell.Offset(i - 1, 21) - ActiveCell.Offset(i + j, 21)) < 180 Then
            ActiveCell.Offset(i, 21) = ActiveCell.Offset(i - 1, 21) * j / (j + 1) + Ac-
tiveCell.Offset(i + j, 21) * 1 / (j + 1)
         Else
            If ActiveCell.Offset(i - 1, 21) > 180 Then
               ActiveCell.Offset(i, 21) = (ActiveCell.Offset(i - 1, 21) - 360) * j / (j
+ 1) + ActiveCell.Offset(i + j, 21) * 1 / (j + 1)
               If ActiveCell.Offset(i, 21) < 0 Then ActiveCell.Offset(i, 21) = Active-
Cell.Offset(i, 21) + 360
            Else
               ActiveCell.Offset(i, 21) = (ActiveCell.Offset(i - 1, 21) + 360) * j / (j
+ 1) + ActiveCell.Offset(i + j, 21) * 1 / (j + 1)
               If ActiveCell.Offset(i, 21) > 360 Then ActiveCell.Offset(i, 21) = Active-
Cell.Offset(i, 21) - 360
            End If
         End If
      End If
   End If
Next
'Interpolate when there are no calculated Inclination values
For i = 2 To 338
   If ActiveCell.Offset(i, 22) = "" Then
      j = 1
      While ActiveCell.Offset(i + j, 22) = "" And j + i < 338
         j = j + 1
      Wend
      If j + i < 338 Then
         ActiveCell.Offset(i, 22) = ActiveCell.Offset(i - 1, 22) * j / (j + 1) + Active-
Cell.Offset(i + j, 22) * 1 / (j + 1)
      End If
   End If
Next
End Sub
Sub Copy_angle_data_from_object_location(bhNameAct)
Dim i As Integer
Dim j As Integer
Dim cellOffset As Integer
Dim bhData(1 To 336, 1 To 3) As Double
Sheets("object_location").Select
Range("A1").Select
i = 0
While ActiveCell.Offset(i, 0) <> bhNameAct
   i = i + 1
Wend
```

```
j = 0
While ActiveCell.Offset(i, 0) = bhNameAct
   j = j + 1
   bhData(j, 1) = ActiveCell.Offset(i, 7)  'secup
   bhData(j, 2) = ActiveCell.Offset(i, 15) 'bearing
   bhData(j, 3) = ActiveCell.Offset(i, 14) 'inclination
   i = i + 1
Wend
Sheets(bhNameAct).Select
Range("A1").Select
ActiveCell.Offset(0, 23) = "Sicada"
ActiveCell.Offset(0, 24) = "Sicada"
ActiveCell.Offset(1, 23) = "bearing"
ActiveCell.Offset(2, 24) = "inclination"
For i = 1 To j
   cellOffset = bhData(i, 1) / 3 + 2
   ActiveCell.Offset(cellOffset, 23) = bhData(i, 2)
   ActiveCell.Offset(cellOffset, 24) = bhData(i, 3)
Next
End Sub
Sub Fill_missing(bhNameAct)
Dim i As Integer
Dim k As Integer
Dim maxI As Integer
Dim bh_length As Integer
Dim secLo As Double
Sheets("object_location").Select
Range("A1").Select
secLo = 0
i = 2
While ActiveCell.Offset(i, 0) <> ""
   If ActiveCell.Offset(i, 0) = bhNameAct Then
      If ActiveCell.Offset(i, 7) > secLo Then secLo = ActiveCell.Offset(i, 7)
   End If
   i = i + 1
Wend
bh_length = Round(secLo / 3)
Sheets(bhNameAct).Select
Range("A1").Select
'For i = 1 To 338
'   If ActiveCell.Offset(i, 23) <> "" Then
'      maxI = i
'   End If
'Next
'For i = 1 To maxI
For i = 1 To bh_length + 2
   If ActiveCell.Offset(i, 21) = "" Then
      ActiveCell.Offset(i, 21) = ActiveCell.Offset(i - 1, 21).Value
      ActiveCell.Offset(i, 22) = ActiveCell.Offset(i - 1, 22).Value
   End If
'   If ActiveCell.Offset(i, 23) = "" Then
'      ActiveCell.Offset(i, 23) = ActiveCell.Offset(i - 1, 23).Value
'      ActiveCell.Offset(i, 24) = ActiveCell.Offset(i - 1, 24).Value
'   End If
Next
'Delete the last row that by some reason sometimes gives erroneous values
```

```
For i = 2 To 338
   If ActiveCell.Offset(i, 23) <> "" Then k = i
Next
ActiveCell.Offset(k, 21) = ""
ActiveCell.Offset(k, 22) = ""
ActiveCell.Offset(k + 1, 21) = ""
ActiveCell.Offset(k + 1, 22) = ""
End Sub
Sub Calculate_angle_diff(bhNameAct)
Dim i As Integer
Sheets(bhNameAct).Select
Range("A1").Select
ActiveCell.Offset(0, 25) = "DIFF"
ActiveCell.Offset(0, 26) = "DIFF"
ActiveCell.Offset(1, 25) = "bearing"
ActiveCell.Offset(1, 26) = "inclination"
For i = 2 To 338
   If ActiveCell.Offset(i, 21) <> "" And ActiveCell.Offset(i, 23) <> "" Then
      ActiveCell.Offset(i, 25) = "=X" & i + 1 & "-V" & i + 1
   End If
   If ActiveCell.Offset(i, 22) <> "" And ActiveCell.Offset(i, 24) <> "" Then
      ActiveCell.Offset(i, 26) = "=Y" & i + 1 & "-W" & i + 1
   End If
Next
End Sub
Sub Calculate_spatial_diff(bhNameAct, holeNum)
Dim i As Integer
Dim pi_over_180 As Double
Dim x_MSt As Double
Dim y_MSt As Double
Dim z_MSt As Double
Dim x_CalC As Double
Dim y_CalC As Double
Dim z_CalC As Double
Dim x_old_MSt As Double
Dim y_old_MSt As Double
Dim z_old_MSt As Double
Dim x_old_CalC As Double
Dim y_old_CalC As Double
Dim z_old_CalC As Double
Dim diff As Double
Dim maxDiff As Double
pi_over_180 = Atn(1) / 45
Sheets(bhNameAct).Select
Range("A1").Select
ActiveCell.Offset(0, 27) = "DIFF"
ActiveCell.Offset(1, 27) = "Spatial"
x_old_MSt = 0
y_old_MSt = 0
z_old_MSt = 0
x_old_CalC = 0
y_old_CalC = 0
z_old_CalC = 0
maxDiff = 0
For i = 3 To 338
   If ActiveCell.Offset(i, 21) <> "" And ActiveCell.Offset(i, 23) <> "" Then
```

```
      x_MSt = Cos((ActiveCell.Offset(i, 21) + ActiveCell.Offset(i - 1, 21)) / 2 * pi_
over_180) * 3 * Cos((ActiveCell.Offset(i, 22) + ActiveCell.Offset(i - 1, 22)) / 2 * pi_
over_180) + x_old_MSt
      y_MSt = Sin((ActiveCell.Offset(i, 21) + ActiveCell.Offset(i - 1, 21)) / 2 * pi_
over_180) * 3 * Cos((ActiveCell.Offset(i, 22) + ActiveCell.Offset(i - 1, 22)) / 2 * pi_
over_180) + y_old_MSt
      z_MSt = Sin((ActiveCell.Offset(i, 22) + ActiveCell.Offset(i - 1, 22)) / 2 * pi_
over_180) * 3 + z_old_MSt
      x_CalC = Cos((ActiveCell.Offset(i, 23) + ActiveCell.Offset(i - 1, 23)) / 2 *
pi_over_180) * 3 * Cos((ActiveCell.Offset(i, 24) + ActiveCell.Offset(i - 1, 24)) / 2 *
pi_over_180) + x_old_CalC
      y_CalC = Sin((ActiveCell.Offset(i, 23) + ActiveCell.Offset(i - 1, 23)) / 2 *
pi_over_180) * 3 * Cos((ActiveCell.Offset(i, 24) + ActiveCell.Offset(i - 1, 24)) / 2 *
pi_over_180) + y_old_CalC
      z_CalC = Sin((ActiveCell.Offset(i, 24) + ActiveCell.Offset(i - 1, 24)) / 2 * pi_
over_180) * 3 + z_old_CalC
      diff = ((x_MSt - x_CalC) ^ 2 + (y_MSt - y_CalC) ^ 2 + (z_MSt - z_CalC) ^ 2) ^ 0.5
      ActiveCell.Offset(i, 27) = diff
      If diff > maxDiff Then maxDiff = diff
      x_old_MSt = x_MSt
      y_old_MSt = y_MSt
      z_old_MSt = z_MSt
      x_old_CalC = x_CalC
      y_old_CalC = y_CalC
      z_old_CalC = z_CalC
   End If
Next
Sheets("Summary").Select
Range("A1").Select
ActiveCell.Offset(holeNum + 2, 11) = maxDiff
End Sub
Sub Evaluation_of_diff(bhNameAct, holeNum)
Dim i As Integer
Dim MaxDiffBear As Double
Dim MaxDiffIncl As Double
Sheets(bhNameAct).Select
Range("A1").Select
MaxDiffBear = 0
MaxDiffIncl = 0
i = 2
While ActiveCell.Offset(i, 21) <> ""
   If ActiveCell.Offset(i, 25) <> "" Then
      If Abs(ActiveCell.Offset(i, 25).Value) > MaxDiffBear Then MaxDiffBear =
Abs(ActiveCell.Offset(i, 25).Value)
      If Abs(ActiveCell.Offset(i, 26).Value) > MaxDiffIncl Then MaxDiffIncl =
Abs(ActiveCell.Offset(i, 26).Value)
   End If
   i = i + 1
Wend
Sheets("Summary").Select
Range("A1").Select
ActiveCell.Offset(holeNum + 2, 2) = bhNameAct
ActiveCell.Offset(holeNum + 2, 3) = MaxDiffBear
ActiveCell.Offset(holeNum + 2, 4) = MaxDiffIncl
End Sub
Sub calculate_90_percentile(bhNameAct, holeNum)
Dim multipleMeasures As Boolean
Dim Bytt As Boolean
Dim i As Integer
```

```
Dim j As Integer
Dim k As Integer
Dim k_bear As Integer
Dim k_incl As Integer
Dim colSwitch As Integer
Dim measureYear As Integer
Dim bearDiffCounter As Integer
Dim inclDiffCounter As Integer
Dim activity As Long
Dim corrFact As Double
Dim sDummy As Double
Dim BearMatrix(0 To 336, 1 To 10) As Double
Dim InclMatrix(0 To 336, 1 To 10) As Double
Dim Sicada_bear(0 To 336) As Double
Dim Sicada_Incl(0 To 336) As Double
Dim bear_diff(0 To 3360) As Double
Dim incl_diff(0 To 3360) As Double
'Get magnetic Values
Sheets("Mag_acc_dev").Select
Range("A1").Select
i = 1
k = 0
While ActiveCell.Offset(i, 0) <> ""
   If ActiveCell.Offset(i, 3) = bhNameAct Then
      k = k + 1
      measureYear = Val(Left(ActiveCell.Offset(i, 6).Text, 4))
      Sheets("Mag_corr").Select
      Range("A1").Select
      corrFact = ActiveCell.Offset(1 + measureYear - ActiveCell.Offset(1, 0), 1).Value -
ActiveCell.Offset(1 + measureYear - ActiveCell.Offset(1, 0), 2).Value
      Sheets("Mag_acc_dev").Select
      Range("A1").Select
      activity = ActiveCell.Offset(i, 0)
      j = 0
      While ActiveCell.Offset(i + j, 3) = bhNameAct And activity = ActiveCell.Offset(i +
j, 0)
         BearMatrix(Round(ActiveCell.Offset(i + j, 8) / 3), k) = ActiveCell.Offset(i +
j, 10) + corrFact
         InclMatrix(Round(ActiveCell.Offset(i + j, 8) / 3), k) = ActiveCell.Offset(i +
j, 9)
         j = j + 1
      Wend
      i = i + j
   Else
      i = i + 1
   End If
Wend
'Get Maxibor Values
Sheets("Maxibor").Select
Range("A1").Select
i = 1
While ActiveCell.Offset(i, 0) <> ""
   If ActiveCell.Offset(i, 3) = bhNameAct Then
      k = k + 1
      activity = ActiveCell.Offset(i, 0)
      j = 0
      While ActiveCell.Offset(i + j, 3) = bhNameAct And activity = ActiveCell.Offset(i +
j, 0)
```

```
         BearMatrix(Round(ActiveCell.Offset(i + j, 6) / 3), k) = ActiveCell.Offset(i +
j, 12)
         InclMatrix(Round(ActiveCell.Offset(i + j, 6) / 3), k) = ActiveCell.Offset(i +
j, 11)
         j = j + 1
      Wend
      i = i + j
   Else
      i = i + 1
   End If
Wend
'check
'Open "d:\_slask\" & bhNameAct & "_bear.dat" For Output As #1
'Open "d:\_slask\" & bhNameAct & "_Incl.dat" For Output As #2
'For i = 0 To 336
'   Print #1, BearMatrix(i, 1) & ";" & BearMatrix(i, 2) & ";" & BearMatrix(i, 3) & ";" &
BearMatrix(i, 4) & ";" & BearMatrix(i, 5) & ";" & BearMatrix(i, 6) & ";" & BearMatrix(i,
7) & ";" & BearMatrix(i, 8) & ";" & BearMatrix(i, 9) & ";" & BearMatrix(i, 10)
'   Print #2, InclMatrix(i, 1) & ";" & InclMatrix(i, 2) & ";" & InclMatrix(i, 3) & ";" &
InclMatrix(i, 4) & ";" & InclMatrix(i, 5) & ";" & InclMatrix(i, 6) & ";" & InclMatrix(i,
7) & ";" & InclMatrix(i, 8) & ";" & InclMatrix(i, 9) & ";" & InclMatrix(i, 10)
'Next
'Close #1
'Close #2
Sheets(bhNameAct).Select
Range("A1").Select
For i = 0 To 336
   Sicada_bear(i) = ActiveCell.Offset(i + 2, 23).Value
   Sicada_Incl(i) = ActiveCell.Offset(i + 2, 24).Value
Next
bearDiffCounter = 0
inclDiffCounter = 0
multipleMeasures = False
For i = 0 To 336
   If BearMatrix(i, 2) <> 0 Then multipleMeasures = True
Next
If multipleMeasures Then
   For i = 0 To 336
      For j = 1 To 10
        If BearMatrix(i, j) <> 0 Then
           bear_diff(bearDiffCounter) = Abs(BearMatrix(i, j) - Sicada_bear(i))
           bearDiffCounter = bearDiffCounter + 1
         End If
      Next
      For j = 1 To 10
        If InclMatrix(i, j) <> 0 Then
           incl_diff(inclDiffCounter) = Abs(InclMatrix(i, j) - Sicada_Incl(i))
           inclDiffCounter = inclDiffCounter + 1
         End If
      Next
   Next
   bearDiffCounter = bearDiffCounter - 1
   inclDiffCounter = inclDiffCounter - 1
   'sort the bearing difference vector using Bubble sort
   Do
      Bytt = False
      For i = 0 To bearDiffCounter - 1
         If bear_diff(i) < bear_diff(i + 1) Then
```

```
            sDummy = bear_diff(i + 1)
            bear_diff(i + 1) = bear_diff(i)
            bear_diff(i) = sDummy
            Bytt = True
         End If
      Next
   Loop While Bytt
   Do
      Bytt = False
      For i = 0 To inclDiffCounter - 1
         If incl_diff(i) < incl_diff(i + 1) Then
            sDummy = incl_diff(i + 1)
            incl_diff(i + 1) = incl_diff(i)
            incl_diff(i) = sDummy
            Bytt = True
         End If
      Next
   Loop While Bytt
'check
Open "d:\_slask\" & bhNameAct & "_bear_diff.dat" For Output As #1
Open "d:\_slask\" & bhNameAct & "_Incl_diff.dat" For Output As #2
For i = 0 To bearDiffCounter
   Print #1, bear_diff(i)
Next
For i = 0 To inclDiffCounter
   Print #2, incl_diff(i)
Next
Close #1
Close #2
   Sheets("Summary").Select
   Range("A1").Select
   ActiveCell.Offset(holeNum + 2, 5) = bear_diff(Round(0.1 * bearDiffCounter))
   ActiveCell.Offset(holeNum + 2, 6) = incl_diff(Round(0.1 * inclDiffCounter))
'   ActiveCell.Offset(holeNum + 2, 5) = bear_diff(Round(0.1 * bearDiffCounter) + 1)
'   ActiveCell.Offset(holeNum + 2, 6) = incl_diff(Round(0.1 * inclDiffCounter) + 1)
End If
End Sub
Sub calculate_90_percentile_MSt(bhNameAct, holeNum)
Dim Bytt As Boolean
Dim i As Integer
Dim j As Integer
Dim k As Integer
Dim k_bear As Integer
Dim k_incl As Integer
Dim colSwitch As Integer
Dim measureYear As Integer
Dim bearDiffCounter As Integer
Dim inclDiffCounter As Integer
Dim activity As Long
Dim corrFact As Double
Dim sDummy As Double
Dim BearMatrix(0 To 336, 1 To 10) As Double
Dim InclMatrix(0 To 336, 1 To 10) As Double
Dim Sicada_bear(0 To 336) As Double
Dim Sicada_Incl(0 To 336) As Double
Dim bear_diff(0 To 3360) As Double
```

```
Dim incl_diff(0 To 3360) As Double
'Get magnetic Values
Sheets("Mag_acc_dev").Select
Range("A1").Select
i = 1
k = 0
While ActiveCell.Offset(i, 0) <> ""
   If ActiveCell.Offset(i, 3) = bhNameAct Then
      k = k + 1
      measureYear = Val(Left(ActiveCell.Offset(i, 6).Text, 4))
      Sheets("Mag_corr").Select
      Range("A1").Select
      corrFact = ActiveCell.Offset(1 + measureYear - ActiveCell.Offset(1, 0), 1).Value -
ActiveCell.Offset(1 + measureYear - ActiveCell.Offset(1, 0), 2).Value
      Sheets("Mag_acc_dev").Select
      Range("A1").Select
      activity = ActiveCell.Offset(i, 0)
      j = 0
      While ActiveCell.Offset(i + j, 3) = bhNameAct And activity = ActiveCell.Offset(i +
j, 0)
         BearMatrix(Round(ActiveCell.Offset(i + j, 8) / 3), k) = ActiveCell.Offset(i +
j, 10) + corrFact
         InclMatrix(Round(ActiveCell.Offset(i + j, 8) / 3), k) = ActiveCell.Offset(i +
j, 9)
         j = j + 1
      Wend
      i = i + j
   Else
      i = i + 1
   End If
Wend
'Get Maxibor Values
Sheets("Maxibor").Select
Range("A1").Select
i = 1
While ActiveCell.Offset(i, 0) <> ""
   If ActiveCell.Offset(i, 3) = bhNameAct Then
      k = k + 1
      activity = ActiveCell.Offset(i, 0)
      j = 0
      While ActiveCell.Offset(i + j, 3) = bhNameAct And activity = ActiveCell.Offset(i +
j, 0)
         BearMatrix(Round(ActiveCell.Offset(i + j, 6) / 3), k) = ActiveCell.Offset(i +
j, 12)
         InclMatrix(Round(ActiveCell.Offset(i + j, 6) / 3), k) = ActiveCell.Offset(i +
j, 11)
         j = j + 1
      Wend
      i = i + j
   Else
      i = i + 1
   End If
Wend
'check
'Open "d:\_slask\" & bhNameAct & "_bear.dat" For Output As #1
'Open "d:\_slask\" & bhNameAct & "_Incl.dat" For Output As #2
'For i = 0 To 336
'   Print #1, BearMatrix(i, 1) & ";" & BearMatrix(i, 2) & ";" & BearMatrix(i, 3) & ";" &
```

```
BearMatrix(i, 4) & ";" & BearMatrix(i, 5) & ";" & BearMatrix(i, 6) & ";" & BearMatrix(i,
7) & ";" & BearMatrix(i, 8) & ";" & BearMatrix(i, 9) & ";" & BearMatrix(i, 10)
'   Print #2, InclMatrix(i, 1) & ";" & InclMatrix(i, 2) & ";" & InclMatrix(i, 3) & ";" &
InclMatrix(i, 4) & ";" & InclMatrix(i, 5) & ";" & InclMatrix(i, 6) & ";" & InclMatrix(i,
7) & ";" & InclMatrix(i, 8) & ";" & InclMatrix(i, 9) & ";" & InclMatrix(i, 10)
'Next
'Close #1
'Close #2
Sheets(bhNameAct).Select
Range("A1").Select
For i = 0 To 336
   Sicada_bear(i) = ActiveCell.Offset(i + 2, 23).Value
   Sicada_Incl(i) = ActiveCell.Offset(i + 2, 24).Value
Next
bearDiffCounter = 0
inclDiffCounter = 0
For i = 0 To 336
   k_bear = 0
   k_incl = 0
   For j = 1 To 10
      If BearMatrix(i, j) <> 0 Then k_bear = k_bear + 1
      If InclMatrix(i, j) <> 0 Then k_incl = k_incl + 1
   Next
   If k_bear > 1 Then
      For j = 1 To 10
        If BearMatrix(i, j) <> 0 And Sicada_bear(i) <> 0 Then
           bear_diff(bearDiffCounter) = Abs(BearMatrix(i, j) - Sicada_bear(i))
           bearDiffCounter = bearDiffCounter + 1
         End If
      Next
   End If
   If k_incl > 1 Then
      For j = 1 To 10
        If InclMatrix(i, j) <> 0 And Sicada_Incl(i) <> 0 Then
           incl_diff(inclDiffCounter) = Abs(InclMatrix(i, j) - Sicada_Incl(i))
           inclDiffCounter = inclDiffCounter + 1
         End If
      Next
   End If
Next
'Add Top of Casing Value
Sheets("orient_TOC").Select
Range("A1").Select
i = 1
While ActiveCell.Offset(i, 2) <> bhNameAct
   i = i + 1
Wend
bear_diff(bearDiffCounter) = Abs(ActiveCell.Offset(i, 8) - Sicada_bear(0))
incl_diff(inclDiffCounter) = Abs(ActiveCell.Offset(i, 9) - Sicada_Incl(0))
bearDiffCounter = bearDiffCounter + 1
inclDiffCounter = inclDiffCounter + 1
'Check if differencies are erroneous due to passing the north
For i = 0 To bearDiffCounter - 1
   If bear_diff(i) > 180 Then bear_diff(i) = 360 - bear_diff(i)
Next
'sort the bearing difference vector using Bubble sort
Do
```

```
   Bytt = False
   For i = 0 To bearDiffCounter - 2
      If bear_diff(i) < bear_diff(i + 1) Then
         sDummy = bear_diff(i + 1)
         bear_diff(i + 1) = bear_diff(i)
         bear_diff(i) = sDummy
         Bytt = True
      End If
   Next
Loop While Bytt
Do
   Bytt = False
   For i = 0 To inclDiffCounter - 2
      If incl_diff(i) < incl_diff(i + 1) Then
         sDummy = incl_diff(i + 1)
         incl_diff(i + 1) = incl_diff(i)
         incl_diff(i) = sDummy
         Bytt = True
      End If
   Next
Loop While Bytt
'check
'If bhNameAct = "KLX09B" Then
'Open "D:\projects\0604_DeviationMeasurement\Work\Kontroll\Calc_of_deviation_and_uncer-
tainty\Laxemar\_slask\" & bhNameAct & "_bear_diff.dat" For Output As #1
'Open "D:\projects\0604_DeviationMeasurement\Work\Kontroll\Calc_of_deviation_and_uncer-
tainty\Laxemar\_slask\" & bhNameAct & "_Incl_diff.dat" For Output As #2
'For i = 0 To bearDiffCounter - 1
'   Print #1, bear_diff(i)
'Next
'For i = 0 To inclDiffCounter - 1
'   Print #2, incl_diff(i)
'Next
'Close #1
'Close #2
'End If
Sheets("Summary").Select
Range("A1").Select
'The number of data has to be lowered by 1 to fullfill the criteria that the highest va-
lue equals p=1 and lowest value equals p=0
bearDiffCounter = bearDiffCounter - 1
inclDiffCounter = inclDiffCounter - 1
If bearDiffCounter > 1 Then
   ActiveCell.Offset(holeNum + 2, 5) = (bear_diff(Int(0.1 * bearDiffCounter) + 1) -
bear_diff(Int(0.1 * bearDiffCounter))) * bearDiffCounter * (0.1 - Int(0.1 * bearDiff-
Counter) / bearDiffCounter) + bear_diff(Int(0.1 * bearDiffCounter))
'   sDummy = (bear_diff(Int(0.1 * bearDiffCounter) + 1) - bear_diff(Int(0.1 * bearDiff-
Counter))) * bearDiffCounter * (0.1 - Int(0.1 * bearDiffCounter) / bearDiffCounter) +
bear_diff(Int(0.1 * bearDiffCounter))
End If
If inclDiffCounter > 1 Then
   ActiveCell.Offset(holeNum + 2, 6) = (incl_diff(Int(0.1 * inclDiffCounter) + 1) -
incl_diff(Int(0.1 * inclDiffCounter))) * inclDiffCounter * (0.1 - Int(0.1 * inclDiff-
Counter) / inclDiffCounter) + incl_diff(Int(0.1 * inclDiffCounter))
'   sDummy = (incl_diff(Int(0.1 * inclDiffCounter) + 1) - incl_diff(Int(0.1 * inclDiff-
Counter))) * inclDiffCounter * (0.1 - Int(0.1 * inclDiffCounter) / inclDiffCounter) +
incl_diff(Int(0.1 * inclDiffCounter))
End If
End Sub
```

```
Sub calculate_diff_90_percentile(bhNameAct, holeNum)
Dim i As Integer
Dim Sicada_90_bear As Double
Dim Sicada_90_incl As Double
Sheets("object_location").Select
Range("A1").Select
i = 2
While ActiveCell.Offset(i, 0) <> bhNameAct
i = i + 1
Wend
Sicada_90_bear = ActiveCell.Offset(i, 17)
Sicada_90_incl = ActiveCell.Offset(i, 16)
Sheets("summary").Select
Range("A1").Select
ActiveCell.Offset(holeNum + 2, 7) = Sicada_90_bear
ActiveCell.Offset(holeNum + 2, 8) = Sicada_90_incl
If ActiveCell.Offset(holeNum + 2, 5) <> 0 Then ActiveCell.Offset(holeNum + 2, 9) =
Abs(ActiveCell.Offset(holeNum + 2, 5) - ActiveCell.Offset(holeNum + 2, 7))
If ActiveCell.Offset(holeNum + 2, 6) <> 0 Then ActiveCell.Offset(holeNum + 2, 10) =
Abs(ActiveCell.Offset(holeNum + 2, 6) - ActiveCell.Offset(holeNum + 2, 8))
End Sub
Sub calculate_uncert_radius(bhNameAct, holeNum)
Dim i As Integer
Dim j As Integer
Dim Sicada_90_bear As Double
Dim Sicada_90_incl As Double
Dim incl_r As Double
Dim bear_r As Double
Dim pi As Double
Dim maxDiff As Double
Dim data_matrix(1 To 338, 1 To 3) As Double
pi = 4 * Atn(1)
Sheets("object_location").Select
Range("A1").Select
i = 2
While ActiveCell.Offset(i, 0) <> bhNameAct
i = i + 1
Wend
Sicada_90_bear = (ActiveCell.Offset(i, 17) + ActiveCell.Offset(i + 1, 17)) / 2
Sicada_90_incl = (ActiveCell.Offset(i, 16) + ActiveCell.Offset(i + 1, 16)) / 2
'Sicada_90_bear = ActiveCell.Offset(i, 17)
'Sicada_90_incl = ActiveCell.Offset(i, 16)
data_matrix(1, 1) = ActiveCell.Offset(i, 18)
data_matrix(1, 2) = 0
data_matrix(1, 3) = 0
i = i + 1
j = 2
While ActiveCell.Offset(i, 0) = bhNameAct
   data_matrix(j, 1) = ActiveCell.Offset(i, 18)
'   incl_r = Tan(Sicada_90_incl * pi / 180) * 3
'   bear_r = Tan(Sicada_90_bear * pi / 180 * Cos(ActiveCell.Offset(i, 14) * pi / 180)) *
3
   incl_r = Sin(Sicada_90_incl * pi / 180) * 3
   bear_r = Sin(Sicada_90_bear * pi / 180) * Cos(ActiveCell.Offset(i, 14) * pi / 180) *
3
   If incl_r > bear_r Then
      data_matrix(j, 2) = incl_r + data_matrix(j - 1, 2)
```

```
   Else
      data_matrix(j, 2) = bear_r + data_matrix(j - 1, 2)
   End If
      data_matrix(j, 3) = data_matrix(j, 2) - data_matrix(j, 1)
   i = i + 1
   j = j + 1
Wend
Sheets(bhNameAct).Select
Range("A1").Select
ActiveCell.Offset(0, 28) = "uncert radius"
ActiveCell.Offset(0, 29) = "uncert radius"
ActiveCell.Offset(0, 30) = "uncert radius"
ActiveCell.Offset(0, 28) = "obj_loc"
ActiveCell.Offset(0, 29) = "calc"
ActiveCell.Offset(0, 30) = "diff"
maxDiff = 0
For i = 1 To j - 2
   ActiveCell.Offset(i + 1, 28) = data_matrix(i, 1)
   ActiveCell.Offset(i + 1, 29) = data_matrix(i, 2)
   ActiveCell.Offset(i + 1, 30) = data_matrix(i, 3)
   If data_matrix(i, 3) > maxDiff Then maxDiff = data_matrix(i, 3)
Next
Sheets("summary").Select
Range("A1").Select
ActiveCell.Offset(holeNum + 2, 12) = maxDiff
End Sub
Sub Bubble_Sort(Data, NofData)
Dim Bytt As Boolean
Dim i As Integer
Dim tempValue As Double
Do
   Bytt = False
   For i = 1 To NofData - 1
      If Data(i) < Data(i + 1) Then
         tempValue = Data(i + 1)
         Data(i + 1) = Data(i)
         Data(i) = tempValue
         Bytt = True
      End If
   Next
Loop While Bytt
End Sub
```

A2.3.2 Strike, dip + alpha and beta uncertainty

```
Option Explicit
Sub Calc_str_dip()
Dim dummy As Boolean
Call p_fract_core(dummy)
Call p_rock(dummy)
Call p_rock_struct_feat(dummy)
End Sub
'************************************************
'***                P_FRACT_CORE                ***
'************************************************
Sub p_fract_core(a)
Dim bhName As String
```

```
Dim i As Long
Dim alpha As Double
Dim beta As Double
Dim bear As Double
Dim incl As Double
Dim strike As Double
Dim dip As Double
Dim bh_len As Double
Dim secUp As Double
Dim angle_diff As Double
Dim offset As Double
Dim beta_roll_uncert As Double
Dim bh_Data(0 To 500, 1 To 6) As Double
Dim beta_Data(0 To 1000, 1 To 2) As Double
Sheets("p_fract_core").Select
Range("A1").Select
ActiveCell.offset(0, 63) = "Strike_Analysis"
ActiveCell.offset(0, 64) = "dip_Analysis"
ActiveCell.offset(0, 65) = "Strike_diff"
ActiveCell.offset(0, 66) = "dip_diff"
ActiveCell.offset(0, 67) = "dihedral_diff"
ActiveCell.offset(0, 68) = "Fracture_offset"
ActiveCell.offset(0, 69) = "a_uncert_analysis"
ActiveCell.offset(0, 70) = "a_unc_diff"
ActiveCell.offset(0, 71) = "b_uncert_analysis"
ActiveCell.offset(0, 72) = "b_unc_diff"
bhName = ""
i = 1
While ActiveCell.offset(i, 0) <> ""
   If ActiveCell.offset(i, 3) <> bhName Then
      bhName = ActiveCell.offset(i, 3)
      Call load_bh_data(bhName, bh_Data)
      Call load_beta_uncert(bhName, beta_Data)
      Sheets("p_fract_core").Select
      Range("A1").Select
   Else
      alpha = ActiveCell.offset(i, 31)
      beta = ActiveCell.offset(i, 33)
      bh_len = ActiveCell.offset(i, 5)
      secUp = ActiveCell.offset(i, 6)
      Call get_bh_orient(bh_len, bh_Data, bear, incl)
      Call calc_strike_dip(alpha, beta, bear, incl, strike, dip)
      Call calc_xyz_diff(bh_len, ActiveCell.offset(i, 60), ActiveCell.offset(i, 59), Ac-
tiveCell.offset(i, 61), bh_Data, angle_diff, offset)
      If ActiveCell.offset(i, 29) <> "" Then
         ActiveCell.offset(i, 63) = strike
         ActiveCell.offset(i, 64) = dip
         ActiveCell.offset(i, 65) = strike - ActiveCell.offset(i, 29)
         ActiveCell.offset(i, 66) = dip - ActiveCell.offset(i, 30)
         ActiveCell.offset(i, 67) = dihedral(ActiveCell.offset(i, 29), ActiveCell.
offset(i, 30), strike, dip)
         ActiveCell.offset(i, 68) = offset
      End If
      'Calculate alpha uncertainty and compare to stored value in p_fract_core
      If ActiveCell.offset(i, 31) <> "" Then
         If ActiveCell.offset(i, 10) = 0 Then
            ActiveCell.offset(i, 69) = 7.4
```

```
            ActiveCell.offset(i, 70) = 7.4 - ActiveCell.offset(i, 32)
         ElseIf ActiveCell.offset(i, 10) = 1 And ActiveCell.offset(i, 31) < 30 Then
'The alfa angle is less than 30
            ActiveCell.offset(i, 69) = 1.4
            ActiveCell.offset(i, 70) = 1.4 - ActiveCell.offset(i, 32)
         ElseIf ActiveCell.offset(i, 10) = 1 And ActiveCell.offset(i, 31) < 60 Then
'The alfa angle is less than 60
            ActiveCell.offset(i, 69) = 3
            ActiveCell.offset(i, 70) = 3 - ActiveCell.offset(i, 32)
         Else
'The alfa angle is larger than 60
            ActiveCell.offset(i, 69) = 3.6
            ActiveCell.offset(i, 70) = 3.6 - ActiveCell.offset(i, 32)
         End If
      End If
      'Calculate beta uncertainty and compare to stored value in p_fract_core
      Call get_beta_uncert(secUp, beta_Data, beta_roll_uncert)
      If ActiveCell.offset(i, 33) <> "" Then    'the beta has to be a number
         If ActiveCell.offset(i, 10) = 0 Then
            ActiveCell.offset(i, 71) = 70 + beta_roll_uncert
            ActiveCell.offset(i, 72) = 70 + beta_roll_uncert - ActiveCell.offset(i, 34)
         ElseIf ActiveCell.offset(i, 10) = 1 And ActiveCell.offset(i, 31) < 30 Then
            ActiveCell.offset(i, 71) = 4 + beta_roll_uncert
            ActiveCell.offset(i, 72) = 4 + beta_roll_uncert - ActiveCell.offset(i, 34)
         ElseIf ActiveCell.offset(i, 10) = 1 And ActiveCell.offset(i, 31) < 60 Then
            ActiveCell.offset(i, 71) = 5.6 + beta_roll_uncert
            ActiveCell.offset(i, 72) = 5.6 + beta_roll_uncert - ActiveCell.offset(i, 34)
         Else
            ActiveCell.offset(i, 71) = 25 + beta_roll_uncert
            ActiveCell.offset(i, 72) = 25 + beta_roll_uncert - ActiveCell.offset(i, 34)
         End If
      End If
      i = i + 1
   End If
Wend
End Sub
'*************************************************
'***                  P_ROCK                   ***
'*************************************************
Sub p_rock(a)
Dim bhName As String
Dim i As Long
Dim alpha As Double
Dim beta As Double
Dim bear As Double
Dim incl As Double
Dim strike As Double
Dim dip As Double
Dim bh_len As Double
Dim secUp As Double
Dim angle_diff As Double
Dim offset As Double
Dim beta_roll_uncert As Double
Dim bh_Data(0 To 500, 1 To 6) As Double
Dim beta_Data(0 To 1000, 1 To 2) As Double
Sheets("p_rock").Select
Range("A1").Select
```

```
ActiveCell.offset(0, 43) = "Strike_Analysis"
ActiveCell.offset(0, 44) = "dip_Analysis"
ActiveCell.offset(0, 45) = "Strike_diff"
ActiveCell.offset(0, 46) = "dip_diff"
ActiveCell.offset(0, 47) = "dihedral_diff"
ActiveCell.offset(0, 48) = "Fracture_offset"
ActiveCell.offset(0, 49) = "a_uncert_analysis"
ActiveCell.offset(0, 50) = "a_unc_diff"
ActiveCell.offset(0, 51) = "b_uncert_analysis"
ActiveCell.offset(0, 52) = "b_unc_diff"
bhName = ""
i = 1
While ActiveCell.offset(i, 0) <> ""
   If ActiveCell.offset(i, 3) <> bhName Then
      bhName = ActiveCell.offset(i, 3)
      Call load_bh_data(bhName, bh_Data)
      Call load_beta_uncert(bhName, beta_Data)
      Sheets("p_rock").Select
      Range("A1").Select
'If bhName = "KFM05A" Then
'i = i
'End If
   Else
      alpha = ActiveCell.offset(i, 23)
      beta = ActiveCell.offset(i, 25)
      bh_len = ActiveCell.offset(i, 4)
      secUp = ActiveCell.offset(i, 6)
      Call get_bh_orient(bh_len, bh_Data, bear, incl)
      Call calc_strike_dip(alpha, beta, bear, incl, strike, dip)
      Call calc_xyz_diff(bh_len, ActiveCell.offset(i, 39), ActiveCell.offset(i, 38), Ac-
tiveCell.offset(i, 40), bh_Data, angle_diff, offset)
      If ActiveCell.offset(i, 21) <> "" Then
         ActiveCell.offset(i, 43) = strike
         ActiveCell.offset(i, 44) = dip
         ActiveCell.offset(i, 45) = strike - ActiveCell.offset(i, 21)
         ActiveCell.offset(i, 46) = dip - ActiveCell.offset(i, 22)
         ActiveCell.offset(i, 47) = dihedral(ActiveCell.offset(i, 21), ActiveCell.
offset(i, 22), strike, dip)
         ActiveCell.offset(i, 48) = offset
      End If
      'Calculate alpha uncertainty and compare to stored value in p_rock
      If ActiveCell.offset(i, 23) <> "" Then
         If ActiveCell.offset(i, 23) < 30 Then      'The alfa angle is less than 30
            ActiveCell.offset(i, 49) = 1.4
            ActiveCell.offset(i, 50) = 1.4 - ActiveCell.offset(i, 24)
         ElseIf ActiveCell.offset(i, 23) < 60 Then  'The alfa angle is less than 60
            ActiveCell.offset(i, 49) = 3
            ActiveCell.offset(i, 50) = 3 - ActiveCell.offset(i, 24)
         Else                                       'The alfa angle is larger than 60
            ActiveCell.offset(i, 49) = 3.6
            ActiveCell.offset(i, 50) = 3.6 - ActiveCell.offset(i, 24)
         End If
      End If
      'Calculate beta uncertainty and compare to stored value in p_rock
      Call get_beta_uncert(secUp, beta_Data, beta_roll_uncert)
      If ActiveCell.offset(i, 25) <> "" Then    'the beta has to be a number
         If ActiveCell.offset(i, 23) < 30 Then
```

```
            ActiveCell.offset(i, 51) = 4 + beta_roll_uncert
            ActiveCell.offset(i, 52) = 4 + beta_roll_uncert - ActiveCell.offset(i, 26)
         ElseIf ActiveCell.offset(i, 23) < 60 Then
            ActiveCell.offset(i, 51) = 5.6 + beta_roll_uncert
            ActiveCell.offset(i, 52) = 5.6 + beta_roll_uncert - ActiveCell.offset(i, 26)
         Else
            ActiveCell.offset(i, 51) = 25 + beta_roll_uncert
            ActiveCell.offset(i, 52) = 25 + beta_roll_uncert - ActiveCell.offset(i, 26)
         End If
      End If
      i = i + 1
   End If
Wend
End Sub
'*************************************************
'***             P_ROCK_STRUCT_FEAT             ***
'*************************************************
Sub p_rock_struct_feat(a)
Dim bhName As String
Dim i As Long
Dim alpha As Double
Dim beta As Double
Dim bear As Double
Dim incl As Double
Dim strike As Double
Dim dip As Double
Dim bh_len As Double
Dim secUp As Double
Dim angle_diff As Double
Dim offset As Double
Dim beta_roll_uncert As Double
Dim bh_Data(0 To 500, 1 To 6) As Double
Dim beta_Data(0 To 1000, 1 To 2) As Double
Sheets("p_rock_struct_feat").Select
Range("A1").Select
ActiveCell.offset(0, 43) = "Strike_Analysis"
ActiveCell.offset(0, 44) = "dip_Analysis"
ActiveCell.offset(0, 45) = "Strike_diff"
ActiveCell.offset(0, 46) = "dip_diff"
ActiveCell.offset(0, 47) = "dihedral_diff"
ActiveCell.offset(0, 48) = "Fracture_offset"
ActiveCell.offset(0, 49) = "a_uncert_analysis"
ActiveCell.offset(0, 50) = "a_unc_diff"
ActiveCell.offset(0, 51) = "b_uncert_analysis"
ActiveCell.offset(0, 52) = "b_unc_diff"
bhName = ""
i = 1
While ActiveCell.offset(i, 0) <> ""
   If ActiveCell.offset(i, 3) <> bhName Then
      bhName = ActiveCell.offset(i, 3)
      Call load_bh_data(bhName, bh_Data)
      Call load_beta_uncert(bhName, beta_Data)
      Sheets("p_rock_struct_feat").Select
      Range("A1").Select
   Else
      alpha = ActiveCell.offset(i, 18)
```

```
      beta = ActiveCell.offset(i, 20)
      bh_len = ActiveCell.offset(i, 6)
      secUp = ActiveCell.offset(i, 8)
      Call get_bh_orient(bh_len, bh_Data, bear, incl)
      Call calc_strike_dip(alpha, beta, bear, incl, strike, dip)
      Call calc_xyz_diff(bh_len, ActiveCell.offset(i, 29), ActiveCell.offset(i, 28), Ac-
tiveCell.offset(i, 30), bh_Data, angle_diff, offset)
      If ActiveCell.offset(i, 14) <> "" Then
         ActiveCell.offset(i, 43) = strike
         ActiveCell.offset(i, 44) = dip
         ActiveCell.offset(i, 45) = strike - ActiveCell.offset(i, 14)
         ActiveCell.offset(i, 46) = dip - ActiveCell.offset(i, 15)
         ActiveCell.offset(i, 47) = dihedral(ActiveCell.offset(i, 14), ActiveCell.
offset(i, 15), strike, dip)
         ActiveCell.offset(i, 48) = offset
      ElseIf ActiveCell.offset(i, 16) <> "" Then ' Det som menas med Trend/plunge i p_
rock_struct_feat är dip direction/dip
         ActiveCell.offset(i, 43) = strike
         ActiveCell.offset(i, 44) = dip
         If ActiveCell.offset(i, 16) > 90 Then
            ActiveCell.offset(i, 45) = strike - (ActiveCell.offset(i, 16) - 90)
         Else
            ActiveCell.offset(i, 45) = strike - (ActiveCell.offset(i, 16) + 270)
         End If
         ActiveCell.offset(i, 46) = dip - ActiveCell.offset(i, 17)
         ActiveCell.offset(i, 47) = dihedral((ActiveCell.offset(i, 16) - 90), Active-
Cell.offset(i, 17), strike, dip)
         ActiveCell.offset(i, 48) = offset
      End If
      'Calculate alpha uncertainty and compare to stored value in p_rock
      If ActiveCell.offset(i, 18) <> "" Then
         If ActiveCell.offset(i, 18) < 30 Then      'The alfa angle is less than 30
            ActiveCell.offset(i, 49) = 1.4
            ActiveCell.offset(i, 50) = 1.4 - ActiveCell.offset(i, 19)
         ElseIf ActiveCell.offset(i, 18) < 60 Then  'The alfa angle is less than 60
            ActiveCell.offset(i, 49) = 3
            ActiveCell.offset(i, 50) = 3 - ActiveCell.offset(i, 19)
         Else                                       'The alfa angle is larger than 60
            ActiveCell.offset(i, 49) = 3.6
            ActiveCell.offset(i, 50) = 3.6 - ActiveCell.offset(i, 19)
         End If
      End If
      'Calculate beta uncertainty and compare to stored value in p_rock
      Call get_beta_uncert(secUp, beta_Data, beta_roll_uncert)
      If ActiveCell.offset(i, 20) <> "" Then    'the beta has to be a number
         If ActiveCell.offset(i, 18) < 30 Then
            ActiveCell.offset(i, 51) = 4 + beta_roll_uncert
            ActiveCell.offset(i, 52) = 4 + beta_roll_uncert - ActiveCell.offset(i, 21)
         ElseIf ActiveCell.offset(i, 18) < 60 Then
            ActiveCell.offset(i, 51) = 5.6 + beta_roll_uncert
            ActiveCell.offset(i, 52) = 5.6 + beta_roll_uncert - ActiveCell.offset(i, 21)
         Else
            ActiveCell.offset(i, 51) = 25 + beta_roll_uncert
            ActiveCell.offset(i, 52) = 25 + beta_roll_uncert - ActiveCell.offset(i, 21)
         End If
      End If
      i = i + 1
```

```
   End If
Wend
End Sub
Sub load_bh_data(nameOfBH, Data)
Dim i As Long
Dim k As Long
Sheets("object_location").Select
Range("A1").Select
i = 1
While ActiveCell.offset(i, 0) <> nameOfBH
   i = i + 1
Wend
k = 1
While ActiveCell.offset(i, 0) = nameOfBH
   Data(k, 1) = ActiveCell.offset(i, 7)  'length
   Data(k, 2) = ActiveCell.offset(i, 15)  'bearing
   Data(k, 3) = ActiveCell.offset(i, 14)  'inclination
   Data(k, 4) = ActiveCell.offset(i, 5)  'x
   Data(k, 5) = ActiveCell.offset(i, 4)  'y
   Data(k, 6) = ActiveCell.offset(i, 6)  'z
   k = k + 1
   i = i + 1
Wend
   Data(k, 1) = 3000
   Data(k, 2) = ActiveCell.offset(i - 1, 15) 'bearing
   Data(k, 3) = ActiveCell.offset(i - 1, 14) 'inclination
   Data(k, 4) = ActiveCell.offset(i - 1, 5) 'x
   Data(k, 5) = ActiveCell.offset(i - 1, 4) 'y
   Data(k, 6) = ActiveCell.offset(i - 1, 6) 'z
End Sub
Sub load_beta_uncert(nameOfBH, Data)
Dim i As Long
Dim k As Long
Sheets("BIPS_BETA_OFFSET").Select
Range("A1").Select
i = 1
While ActiveCell.offset(i, 0) <> nameOfBH And ActiveCell.offset(i, 0) <> ""
   i = i + 1
Wend
k = 1
If ActiveCell.offset(i, 0) = "" Then
   Data(k, 1) = 0
   Data(k, 2) = 180
   k = k + 1
Else
   While ActiveCell.offset(i, 0) = nameOfBH
      Data(k, 1) = ActiveCell.offset(i, 2)    'secUp
      If ActiveCell.offset(i, 6) <> "" Then
         Data(k, 2) = ActiveCell.offset(i, 6)  'betaUncertainty
      Else
         Data(k, 2) = 180                      'betaUncertainty if no value provided
      End If
      k = k + 1
      i = i + 1
   Wend
End If
```

```
   Data(k, 1) = 3000
   Data(k, 2) = 180
End Sub
Sub get_bh_orient(bh_len, bh_Data, bear, incl)
Dim i As Long
i = 1
While bh_len > bh_Data(i, 1)
   i = i + 1
Wend
bear = (bh_Data(i - 1, 2) + bh_Data(i, 2)) / 2
incl = (bh_Data(i - 1, 3) + bh_Data(i, 3)) / 2
'*****************************************************************
'bear = bh_Data(i - 1, 2)  'fel data endast för test av bugg 2263
'incl = bh_Data(i - 1, 3)  'fel data endast för test av bugg 2263
'*****************************************************************
End Sub
Sub calc_strike_dip(alpha180, beta180, bear180, incl180, strike180, dip180)
Dim pi As Double
Dim pi_over180 As Double
Dim alpha As Double
Dim beta As Double
Dim bear As Double
Dim incl As Double
Dim strike As Double
Dim dip As Double
Dim nx As Double
Dim ny As Double
Dim nz As Double
Dim xynx As Double
Dim xyny As Double
Dim cosAngle As Double
Dim sinAngle As Double
pi = 4 * Atn(1)
pi_over180 = Atn(1) / 45
alpha = alpha180 * pi_over180
beta = beta180 * pi_over180
bear = bear180 * pi_over180
incl = incl180 * pi_over180
nx = Cos(pi / 2 - bear) * Sin(-incl) * Cos(-beta) * Cos(alpha) - Sin(pi / 2 - bear) *
Sin(-beta) * Cos(alpha) - Cos(pi / 2 - bear) * Cos(-incl) * Sin(alpha)
ny = Sin(pi / 2 - bear) * Sin(-incl) * Cos(-beta) * Cos(alpha) + Cos(pi / 2 - bear) *
Sin(-beta) * Cos(alpha) - Sin(pi / 2 - bear) * Cos(-incl) * Sin(alpha)
nz = Cos(-incl) * Cos(-beta) * Cos(alpha) + Sin(-incl) * Sin(alpha)
strike180 = nx ^ 2 + ny ^ 2 + nz ^ 2
If nz > 0 Then
   nz = -nz
   xynx = -nx / (nx ^ 2 + ny ^ 2) ^ 0.5
   xyny = -ny / (nx ^ 2 + ny ^ 2) ^ 0.5
Else
   xynx = nx / (nx ^ 2 + ny ^ 2) ^ 0.5
   xyny = ny / (nx ^ 2 + ny ^ 2) ^ 0.5
End If
'Arcsin(x) = Atn(x / Sqr(-x * x + 1))
'Arccos(x) = Atn(-x / Sqr(-x * x + 1)) + 2 * Atn(1)
dip180 = 90 + Atn(nz / Sqr(-nz * nz + 1)) / pi_over180
cosAngle = (Atn(-xynx / Sqr(-xynx * xynx + 1)) + 2 * Atn(1)) / pi_over180
sinAngle = Atn(xyny / Sqr(-xyny * xyny + 1)) / pi_over180
```

```
If sinAngle >= 0 Then
   strike180 = 180 - cosAngle
Else
   strike180 = 180 + cosAngle
End If
End Sub
Sub calc_xyz_diff(bh_len, frac_x, frac_y, frac_z, bh_Data, angle_degrees, dist)
Dim i As Long
Dim x_up As Double
Dim y_up As Double
Dim z_up As Double
Dim x_down As Double
Dim y_down As Double
Dim z_down As Double
Dim v1x As Double
Dim v1y As Double
Dim v1z As Double
Dim v2x As Double
Dim v2y As Double
Dim v2z As Double
Dim a As Double
Dim angle_rad As Double
i = 1
While bh_len > bh_Data(i, 1)
   i = i + 1
Wend
'If bh_len > 901 Then
'i = i
'End If
'bear = (bh_Data(i - 1, 2) + bh_Data(i, 2)) / 2
'incl = (bh_Data(i - 1, 3) + bh_Data(i, 3)) / 2
x_up = bh_Data(i - 1, 4)
y_up = bh_Data(i - 1, 5)
z_up = bh_Data(i - 1, 6)
x_down = bh_Data(i, 4)
y_down = bh_Data(i, 5)
z_down = bh_Data(i, 6)
v1x = x_down - x_up
v1y = y_down - y_up
v1z = z_down - z_up
v2x = frac_x - x_up
v2y = frac_y - y_up
v2z = frac_z - z_up
If v2x <> 0 And v2y <> 0 And v2z <> 0 Then
   'Arccos(x) = Atn(-x / Sqr(-x * x + 1)) + 2 * Atn(1)
   a = (v1x * v2x + v1y * v2y + v1z * v2z) / ((v1x ^ 2 + v1y ^ 2 + v1z ^ 2) ^ 0.5 * (v2x
^ 2 + v2y ^ 2 + v2z ^ 2) ^ 0.5)
   If a < 1 Then
      angle_rad = Atn(-a / Sqr(-a * a + 1)) + 2 * Atn(1)
      angle_degrees = angle_rad * 4 * Atn(1)
      dist = Sin(angle_rad) * (v2x ^ 2 + v2y ^ 2 + v2z ^ 2) ^ 0.5
   Else
      angle_degrees = 0
      dist = 0
   End If
Else
   angle_degrees = 0
```

```
   dist = 0
End If
End Sub
Sub get_beta_uncert(secUp, Data, beta_roll_uncert)
Dim i As Long
i = 1
While secUp > Data(i, 1)
   i = i + 1
Wend
beta_roll_uncert = Data(i - 1, 2)
End Sub
Function dihedral(strike1, dip1, strike2, dip2)
Dim alfa1 As Double
Dim beta1 As Double
Dim gamma1 As Double
Dim alfa2 As Double
Dim beta2 As Double
Dim gamma2 As Double
Dim a As Double
alfa1 = Cos(-strike1 * Atn(1) / 45) * Sin(dip1 * Atn(1) / 45)
alfa2 = Cos(-strike2 * Atn(1) / 45) * Sin(dip2 * Atn(1) / 45)
beta1 = Sin(-strike1 * Atn(1) / 45) * Sin(dip1 * Atn(1) / 45)
beta2 = Sin(-strike2 * Atn(1) / 45) * Sin(dip2 * Atn(1) / 45)
gamma1 = Cos(dip1 * Atn(1) / 45)
gamma2 = Cos(dip2 * Atn(1) / 45)
a = Abs(alfa1 * alfa2 + beta1 * beta2 + gamma1 * gamma2)
'Arccos(x) = Atn(-x / Sqr(-x * x + 1)) + 2 * Atn(1)
If a < 1 Then
   dihedral = (Atn(-a / Sqr(-a * a + 1)) + 2 * Atn(1)) * 45 / Atn(1)
Else
   dihedral = 0
End If
End Function
```

Appendix 3

A3 Detailed analyses

A3.1 Borehole geometries

A3.1.1 Changes to ΔZ

Forsmark

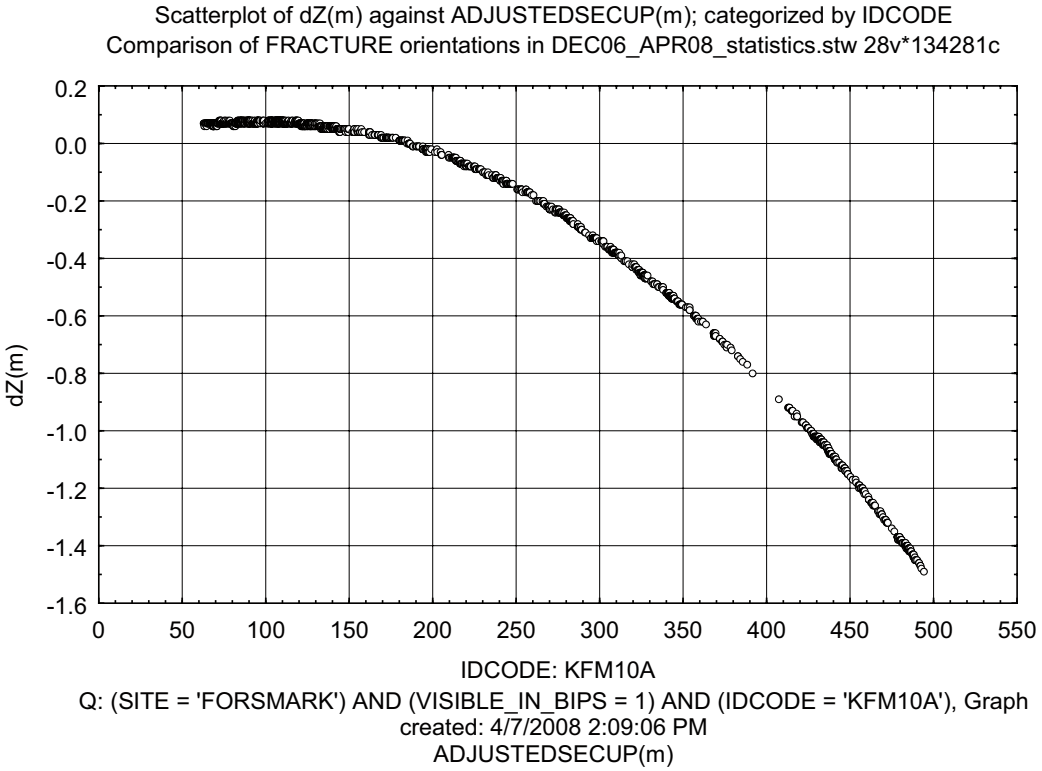

Scatterplot of dZ(m) against ADJUSTEDSECUP(m); categorized by IDCODE
Comparison of FRACTURE orientations in DEC06_APR08_statistics.stw 28v*134281c

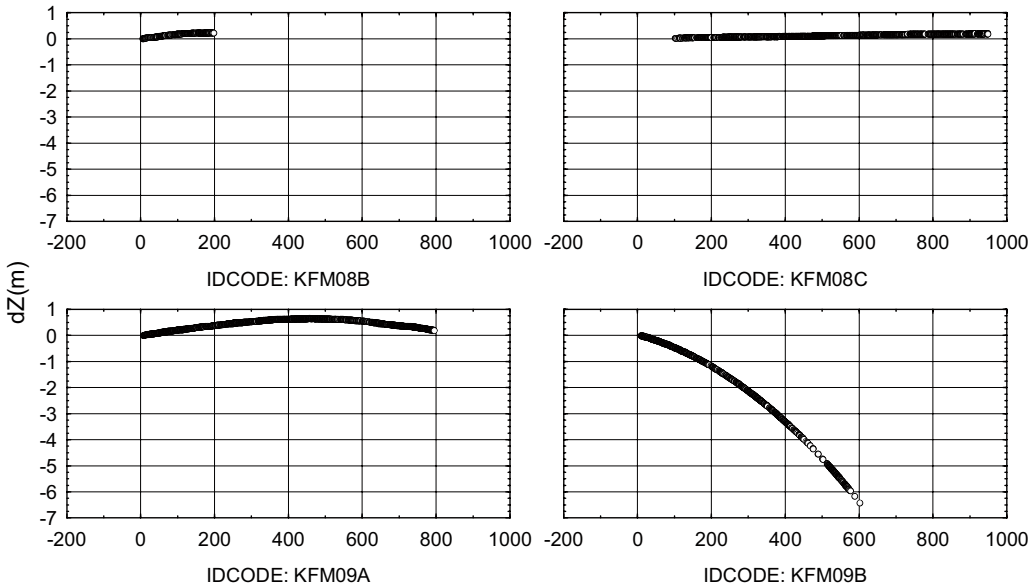

Q: (SITE = 'FORSMARK') AND (VISIBLE_IN_BIPS = 1) AND ((IDCODE = 'KFM08B') OR (IDCODE = 'KFM08C') OR (IDCODE = 'KFM09A') OR (IDCODE = 'KFM09B')), Graph created: 4/7/2008 2:08:32 PM
ADJUSTEDSECUP(m)

Scatterplot of dZ(m) against ADJUSTEDSECUP(m); categorized by IDCODE
Comparison of FRACTURE orientations in DEC06_APR08_statistics.stw 28v*134281c

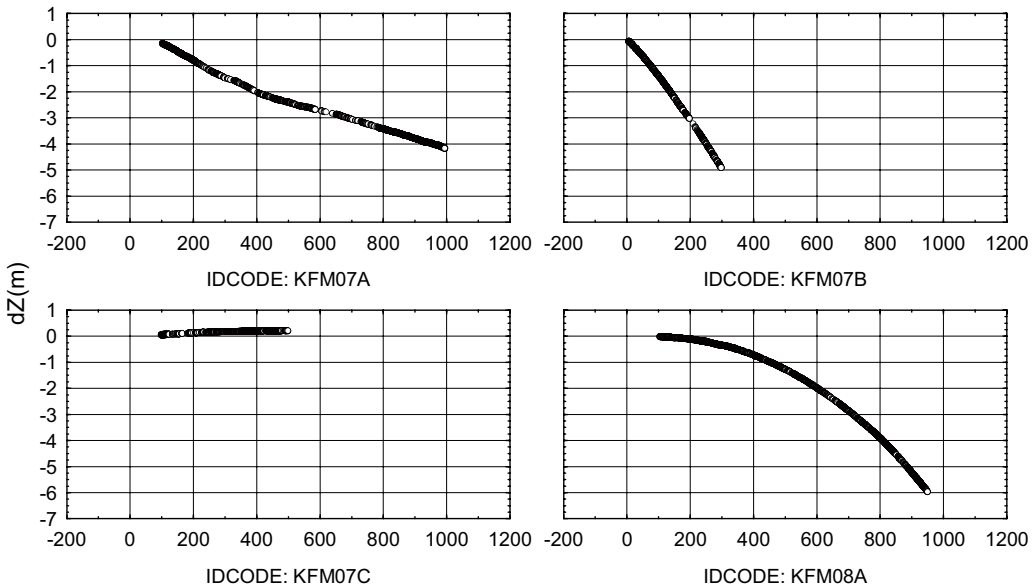

Q: (SITE = 'FORSMARK') AND (VISIBLE_IN_BIPS = 1) AND ((IDCODE = 'KFM07A') OR (IDCODE = 'KFM07B') OR (IDCODE = 'KFM07C') OR (IDCODE = 'KFM08A')), Graph created: 4/7/2008 2:07:59 PM
ADJUSTEDSECUP(m)

Scatterplot of dZ(m) against ADJUSTEDSECUP(m); categorized by IDCODE
Comparison of FRACTURE orientations in DEC06_APR08_statistics.stw 28v*134281c

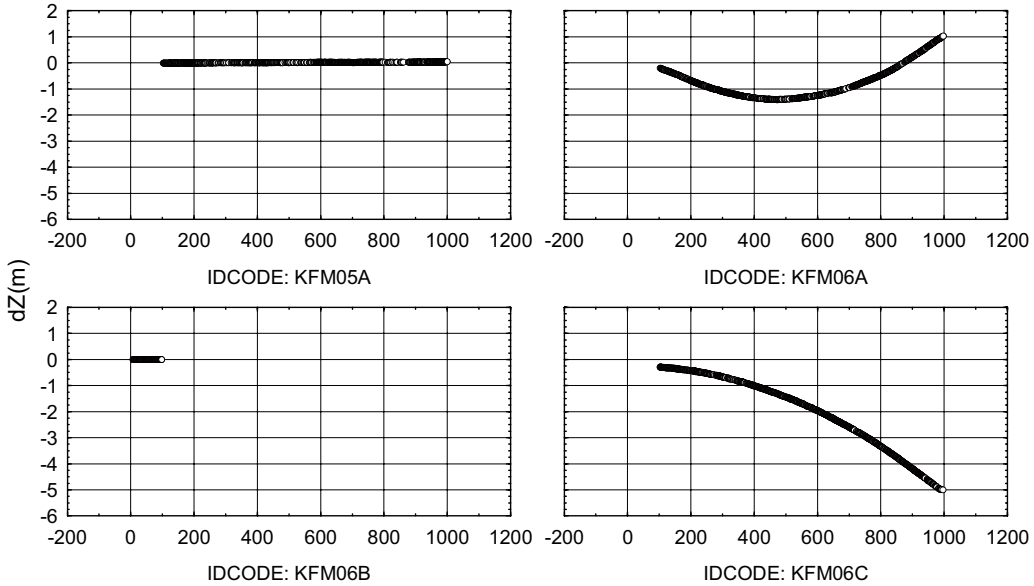

Q: (SITE = 'FORSMARK') AND (VISIBLE_IN_BIPS = 1) AND ((IDCODE = 'KFM05A') OR (IDCODE = 'KFM06A') OR (IDCODE = 'KFM06B') OR (IDCODE = 'KFM06C')), Graph created: 4/7/2008 2:07:27 PM
ADJUSTEDSECUP(m)

Scatterplot of dZ(m) against ADJUSTEDSECUP(m); categorized by IDCODE
Comparison of FRACTURE orientations in DEC06_APR08_statistics.stw 28v*134281c

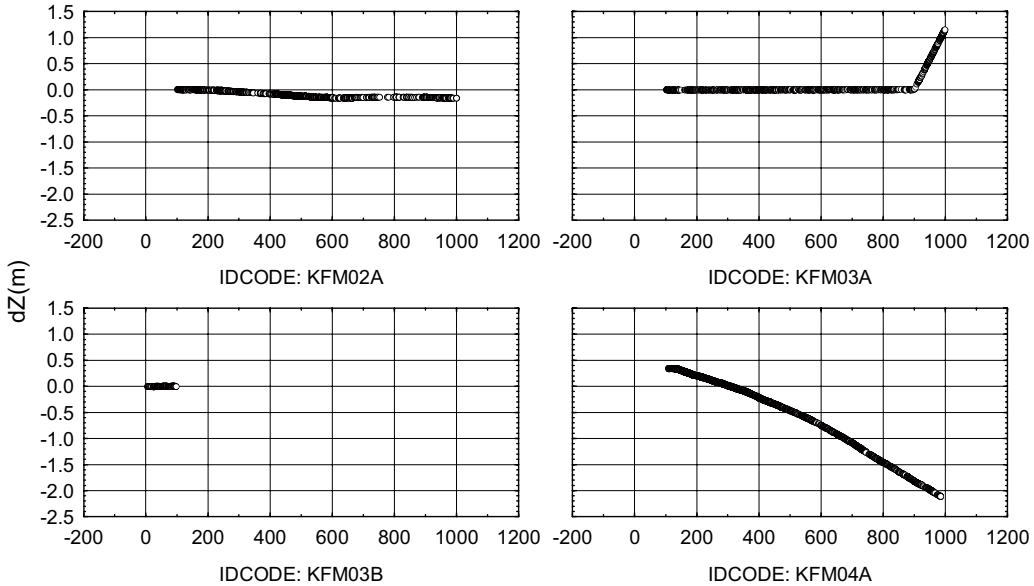

Q: (SITE = 'FORSMARK') AND (VISIBLE_IN_BIPS = 1) AND ((IDCODE = 'KFM02A') OR (IDCODE = 'KFM03A') OR (IDCODE = 'KFM03B') OR (IDCODE = 'KFM04A')), Graph created: 4/7/2008 2:06:54 PM
ADJUSTEDSECUP(m)

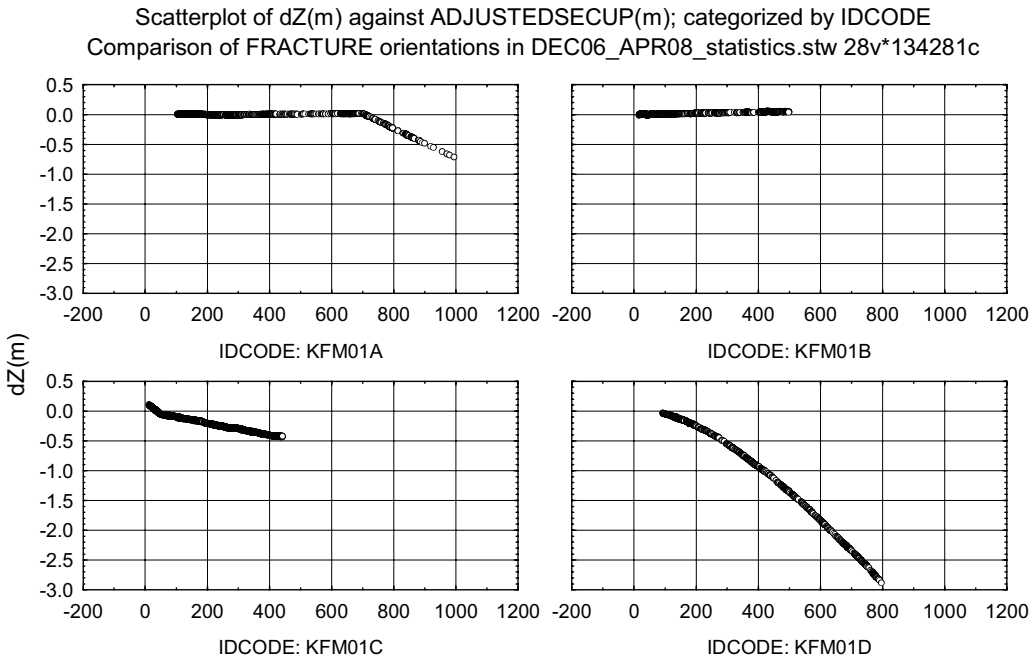
Scatterplot of dZ(m) against ADJUSTEDSECUP(m); categorized by IDCODE
Comparison of FRACTURE orientations in DEC06_APR08_statistics.stw 28v*134281c
dZ(m)
IDCODE: KFM01A
IDCODE: KFM01B
IDCODE: KFM01C
IDCODE: KFM01D
Q: (SITE = 'FORSMARK') AND (VISIBLE_IN_BIPS = 1) AND ((IDCODE = 'KFM01A') OR (IDCODE = 'KFM01B') OR (IDCODE = 'KFM01C') OR (IDCODE = 'KFM01D')), Graph created: 4/7/2008 2:06:20 PM
ADJUSTEDSECUP(m)

Laxemar

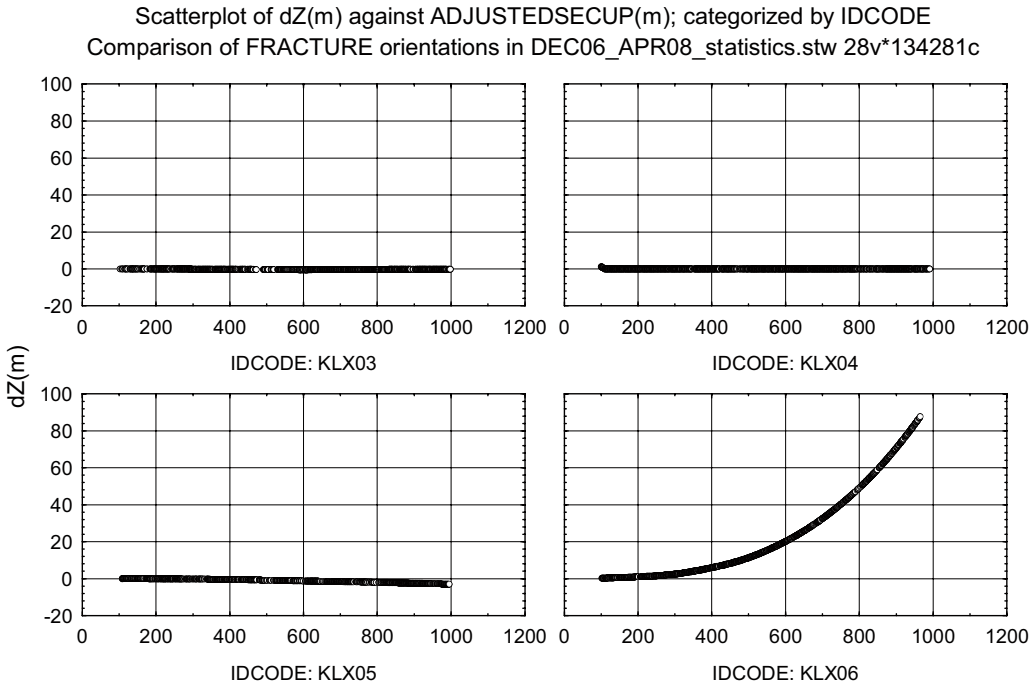
Scatterplot of dZ(m) against ADJUSTEDSECUP(m); categorized by IDCODE
Comparison of FRACTURE orientations in DEC06_APR08_statistics.stw 28v*134281c
dZ(m)
IDCODE: KLX03
IDCODE: KLX04
IDCODE: KLX05
IDCODE: KLX06
Q: (SITE = 'LAXEMAR') AND (VISIBLE_IN_BIPS = 1) AND ((IDCODE = 'KLX03') OR (IDCODE = 'KLX04') OR (IDCODE = 'KLX05') OR (IDCODE = 'KLX06')), Graph created: 4/7/2008 1:56:22 PM
ADJUSTEDSECUP(m)

Scatterplot of dZ(m) against ADJUSTEDSECUP(m); categorized by IDCODE
Comparison of FRACTURE orientations in DEC06_APR08_statistics.stw 28v*134281c

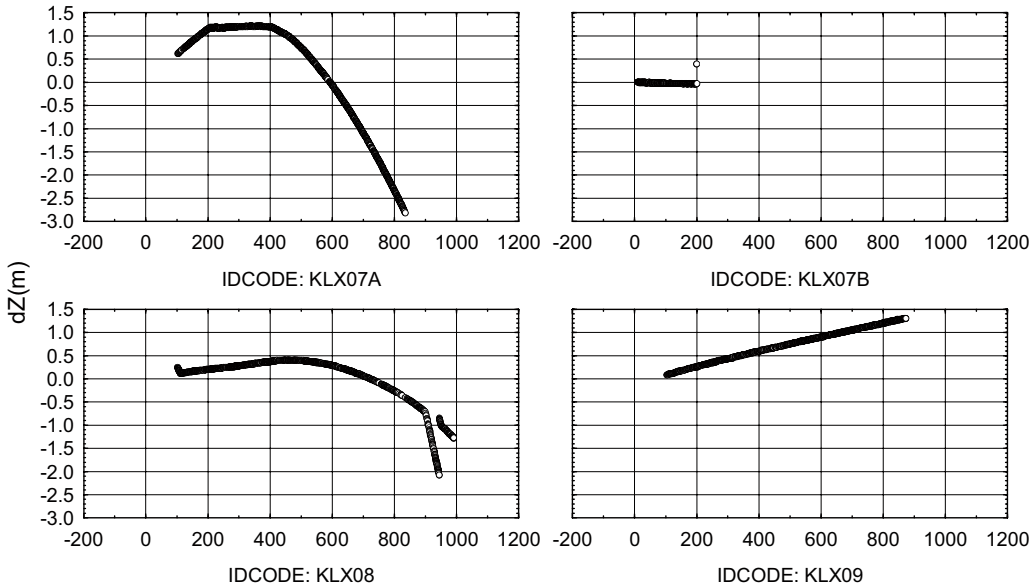

Q: (SITE = 'LAXEMAR') AND (VISIBLE_IN_BIPS = 1) AND ((IDCODE = 'KLX07A') OR (IDCODE = 'KLX07B') OR (IDCODE = 'KLX08') OR (IDCODE = 'KLX09')), Graph created: 4/7/2008 1:56:56 PM
ADJUSTEDSECUP(m)

Scatterplot of dZ(m) against ADJUSTEDSECUP(m); categorized by IDCODE
Comparison of FRACTURE orientations in DEC06_APR08_statistics.stw 28v*134281c

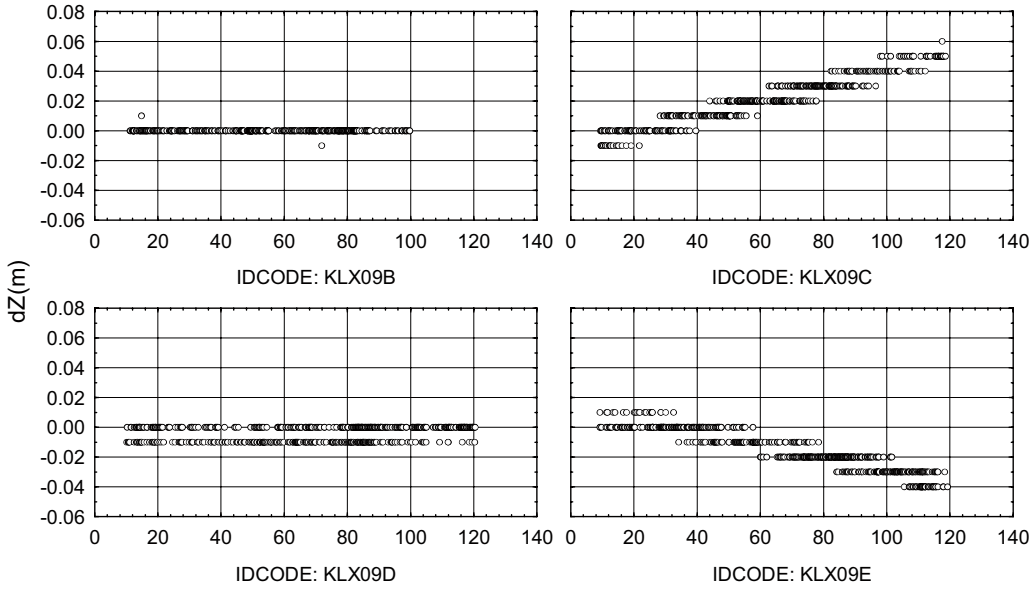

Q: (SITE = 'LAXEMAR') AND (VISIBLE_IN_BIPS = 1) AND ((IDCODE = 'KLX09B') OR (IDCODE = 'KLX09C') OR (IDCODE = 'KLX09D') OR (IDCODE = 'KLX09E')), Graph created: 4/7/2008 1:57:30 PM
ADJUSTEDSECUP(m)

Scatterplot of dZ(m) against ADJUSTEDSECUP(m); categorized by IDCODE
Comparison of FRACTURE orientations in DEC06_APR08_statistics.stw 28v*134281c

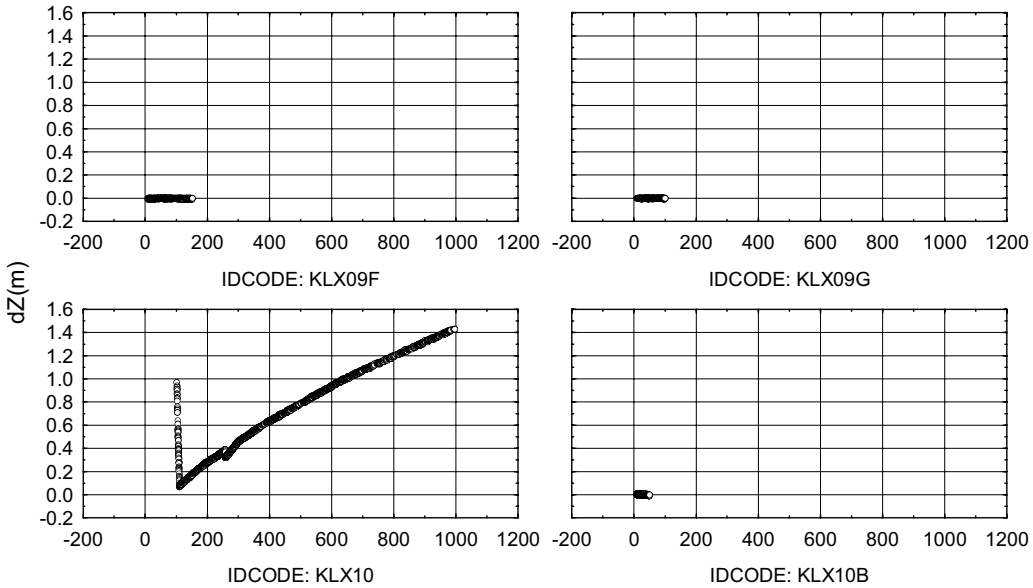

Q: (SITE = 'LAXEMAR') AND (VISIBLE_IN_BIPS = 1) AND ((IDCODE = 'KLX09F') OR (IDCODE = 'KLX09G') OR (IDCODE = 'KLX10') OR (IDCODE = 'KLX10B')), Graph created: 4/7/2008 1:58: 02 PM
ADJUSTEDSECUP(m)

Scatterplot of dZ(m) against ADJUSTEDSECUP(m); categorized by IDCODE
Comparison of FRACTURE orientations in DEC06_APR08_statistics.stw 28v*134281c

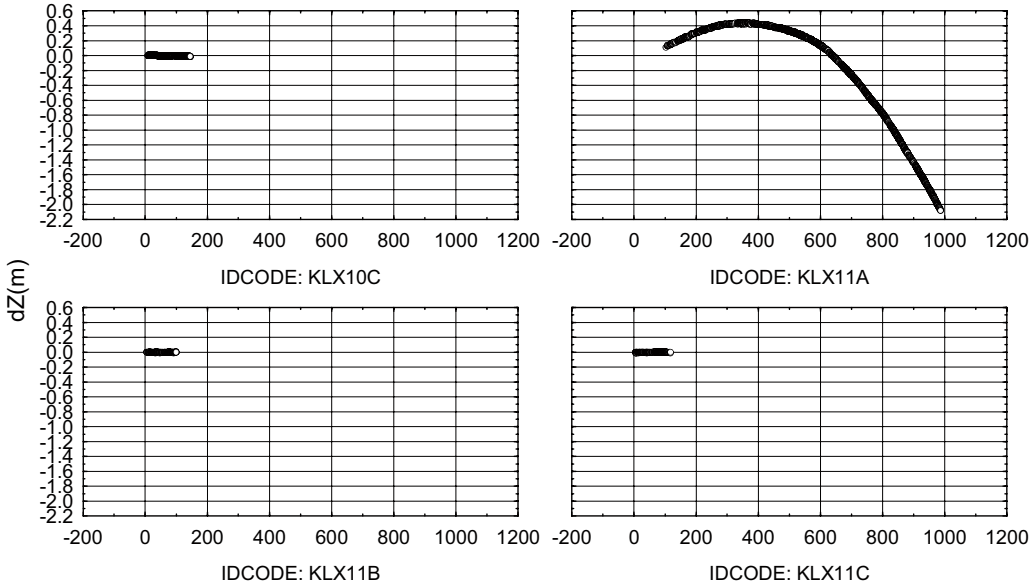

Q: (SITE = 'LAXEMAR') AND (VISIBLE_IN_BIPS = 1) AND ((IDCODE = 'KLX10C') OR (IDCODE = 'KLX11A') OR (IDCODE = 'KLX11B') OR (IDCODE = 'KLX11C')), Graph created: 4/7/2008 1:58: 36 PM
ADJUSTEDSECUP(m)

Scatterplot of dZ(m) against ADJUSTEDSECUP(m); categorized by IDCODE
Comparison of FRACTURE orientations in DEC06_APR08_statistics.stw 28v*134281c

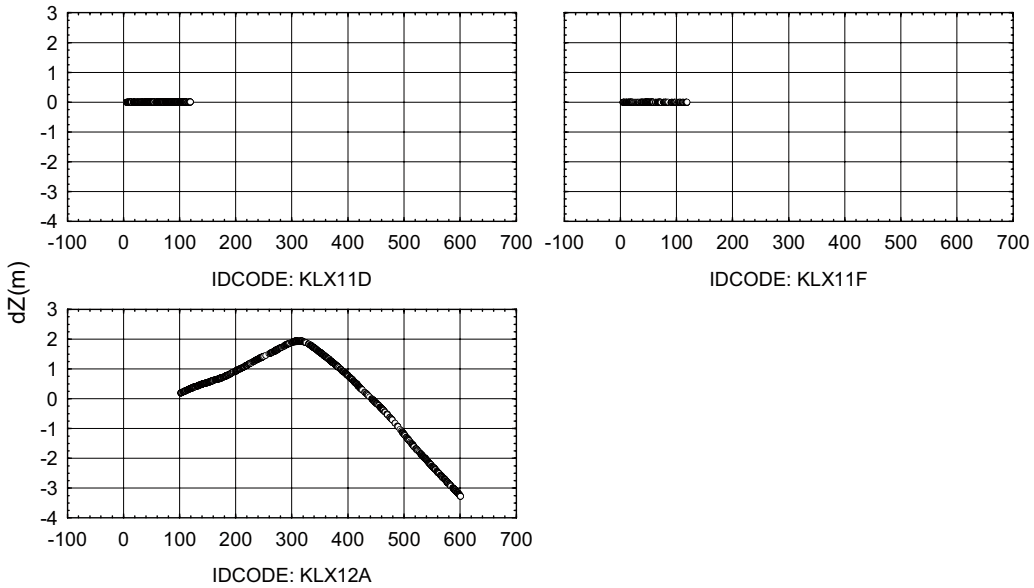

Q: (SITE = 'LAXEMAR') AND (VISIBLE_IN_BIPS = 1) AND ((IDCODE = 'KLX11D') OR (IDCODE = 'KLX101E') OR (IDCODE = 'KLX11F') OR (IDCODE = 'KLX12A')), Graph created: 4/7/2008 1:59:09 PM
ADJUSTEDSECUP(m)

Scatterplot of dZ(m) against ADJUSTEDSECUP(m); categorized by IDCODE
Comparison of FRACTURE orientations in DEC06_APR08_statistics.stw 28v*134281c

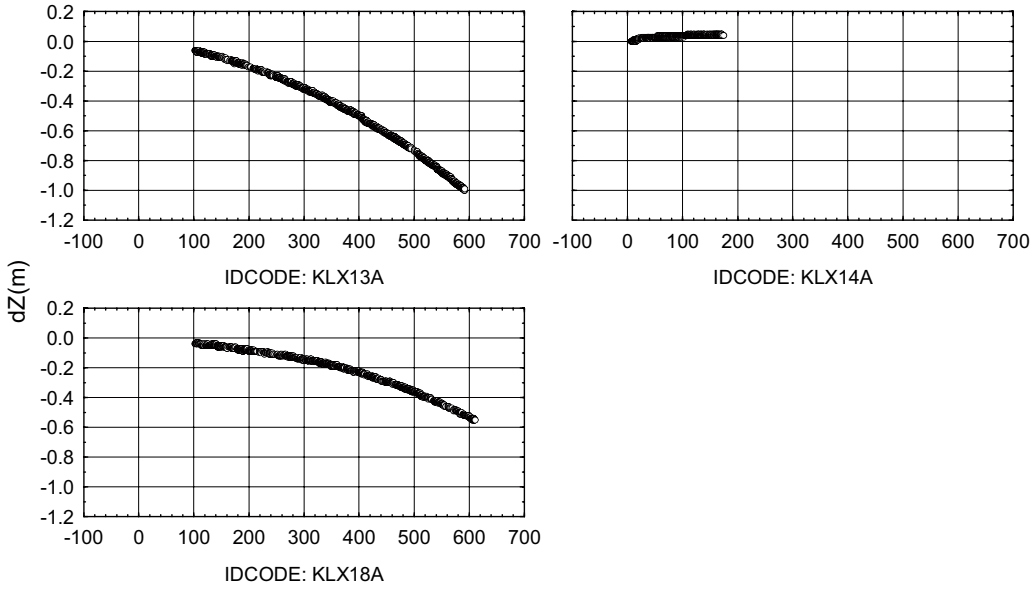

Q: (SITE = 'LAXEMAR') AND (VISIBLE_IN_BIPS = 1) AND ((IDCODE = 'KLX13A') OR (IDCODE = 'KLX14A') OR (IDCODE = 'KLX17A') OR (IDCODE = 'KLX18A')), Graph created: 4/7/2008 1:59:42 PM
ADJUSTEDSECUP(m)

Scatterplot of dZ(m) against ADJUSTEDSECUP(m); categorized by IDCODE
Comparison of FRACTURE orientations in DEC06_APR08_statistics.stw 28v*134281c

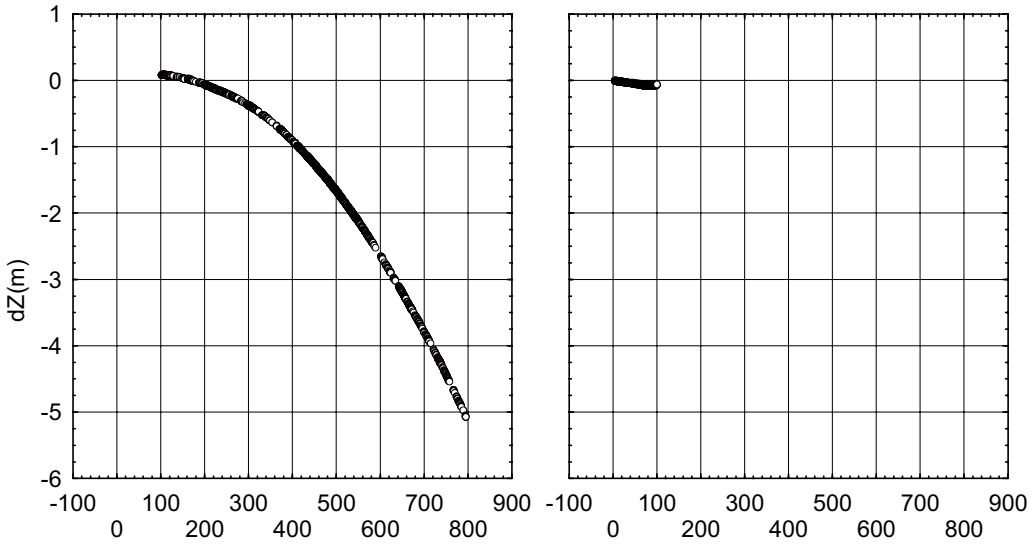

Q: (SITE = 'LAXEMAR') AND (VISIBLE_IN_BIPS = 1) AND ((IDCODE = 'KLX19A') OR (IDCODE = 'KLX20B') OR (IDCODE = 'KLX21B') OR (IDCODE = 'KLX22A')), Graph created: 4/7/2008 2:00: 16 PM
ADJUSTEDSECUP(m)

Scatterplot of dZ(m) against ADJUSTEDSECUP(m); categorized by IDCODE
Comparison of FRACTURE orientations in DEC06_APR08_statistics.stw 28v*134281c

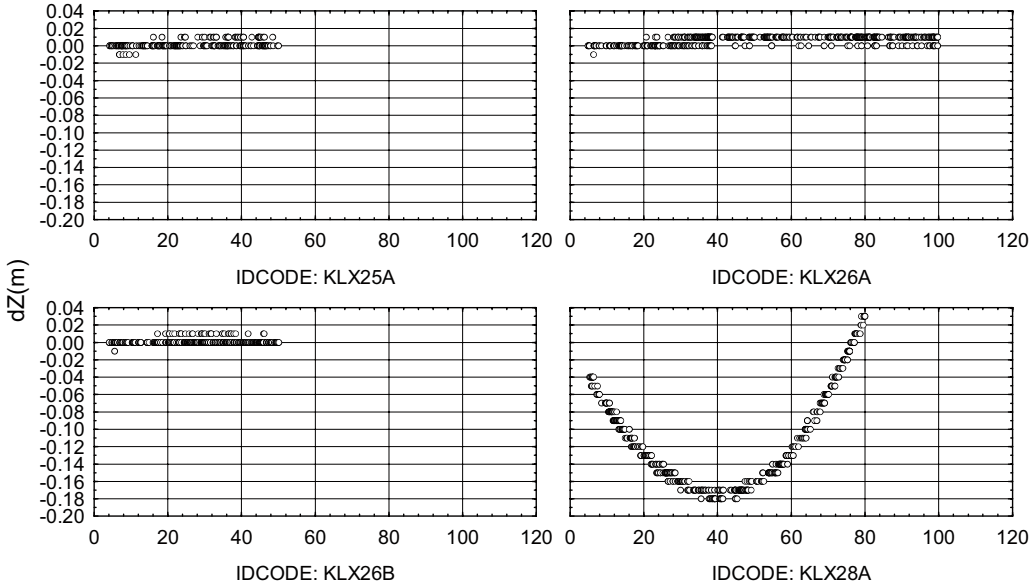

Q: (SITE = 'LAXEMAR') AND (VISIBLE_IN_BIPS = 1) AND ((IDCODE = 'KLX25A') OR (IDCODE = 'KLX26A') OR (IDCODE = 'KLX26B') OR (IDCODE = 'KLX28A')), Graph created: 4/7/2008 2:00: 48 PM
ADJUSTEDSECUP(m)

Scatterplot of dZ(m) against ADJUSTEDSECUP(m); categorized by IDCODE
Comparison of FRACTURE orientations in DEC06_APR08_statistics.stw 28v*134281c

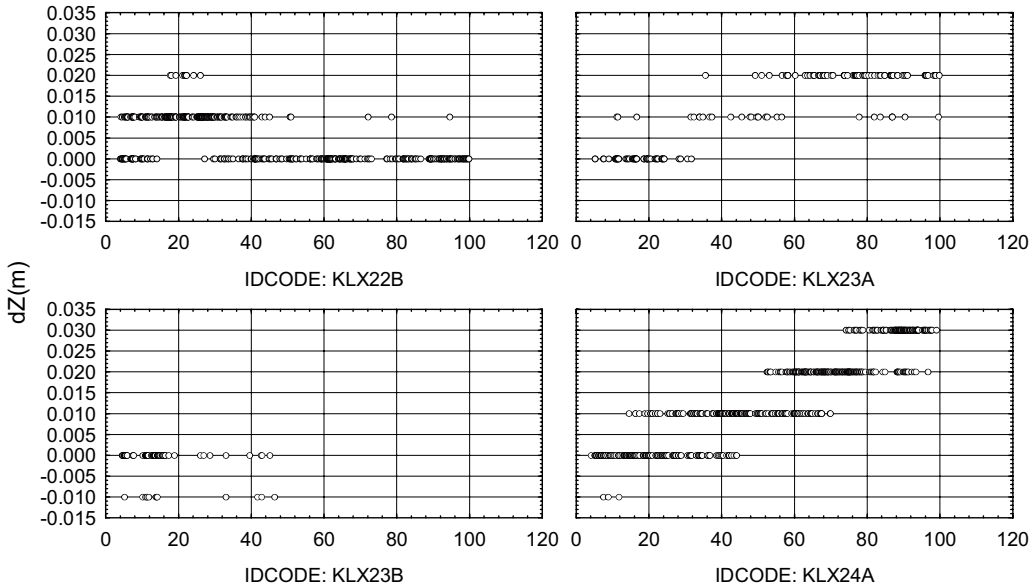

Q: (SITE = 'LAXEMAR') AND (VISIBLE_IN_BIPS = 1) AND ((IDCODE = 'KLX22B') OR (IDCODE = 'KLX23A') OR (IDCODE = 'KLX23B') OR (IDCODE = 'KLX24A')), Graph created: 4/7/2008 2:01: 21 PM
ADJUSTEDSECUP(m)

Scatterplot of dZ(m) against ADJUSTEDSECUP(m); categorized by IDCODE
Comparison of FRACTURE orientations in DEC06_APR08_statistics.stw 28v*134281c

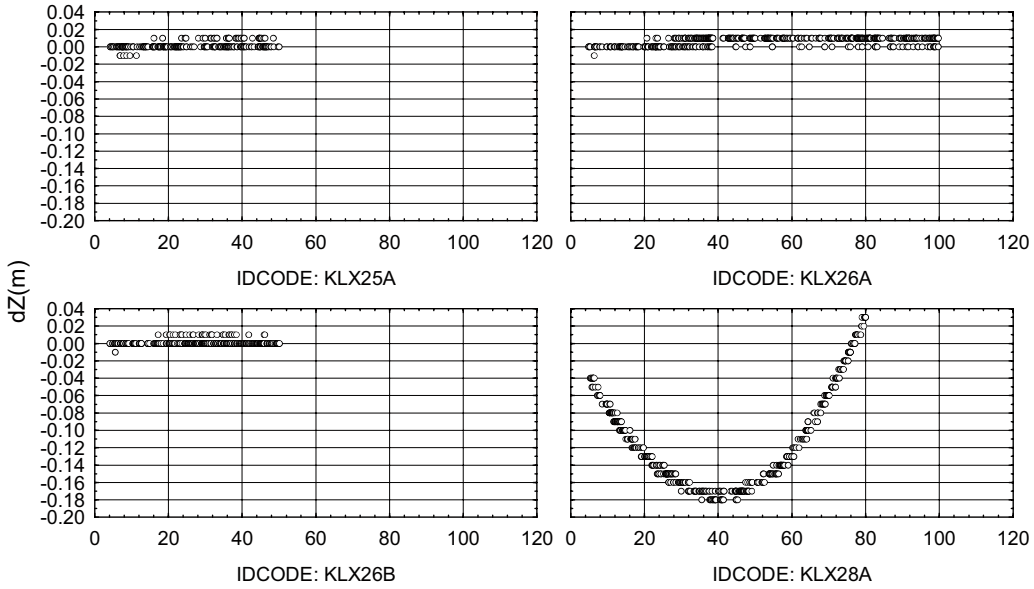

Q: (SITE = 'LAXEMAR') AND (VISIBLE_IN_BIPS = 1) AND ((IDCODE = 'KLX25A') OR (IDCODE = 'KLX26A') OR (IDCODE = 'KLX26B') OR (IDCODE = 'KLX28A')), Graph created: 4/7/2008 2:01: 54 PM
ADJUSTEDSECUP(m)

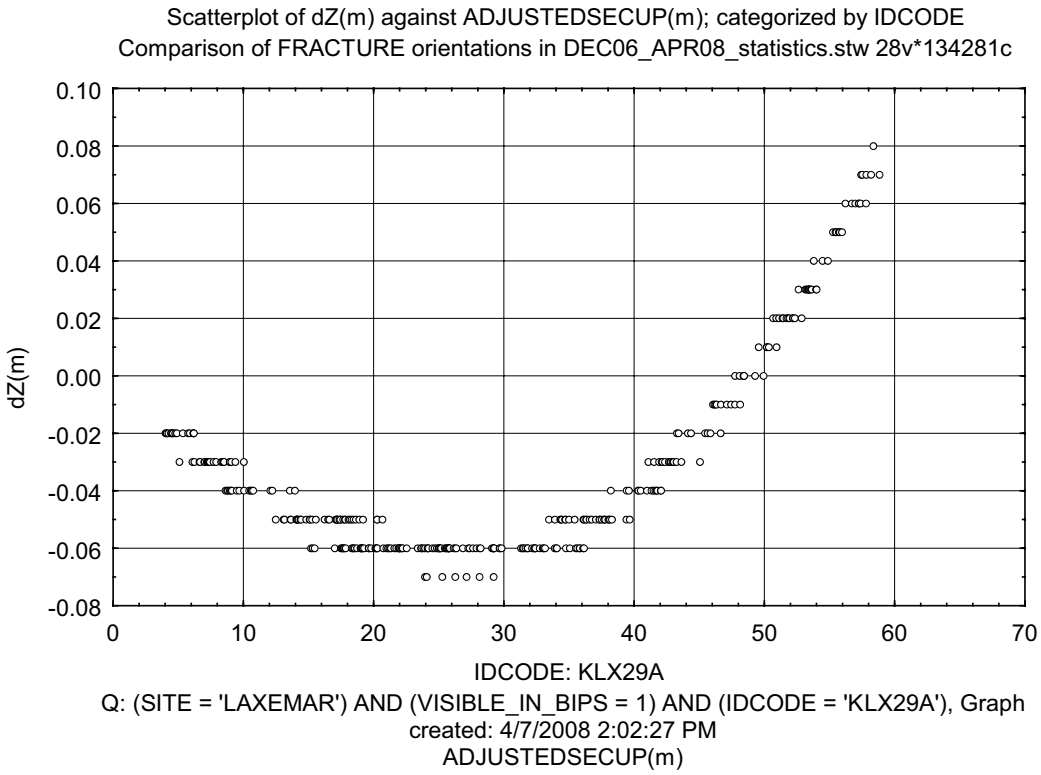

A3.1.2 Changes in absolute distance

Forsmark

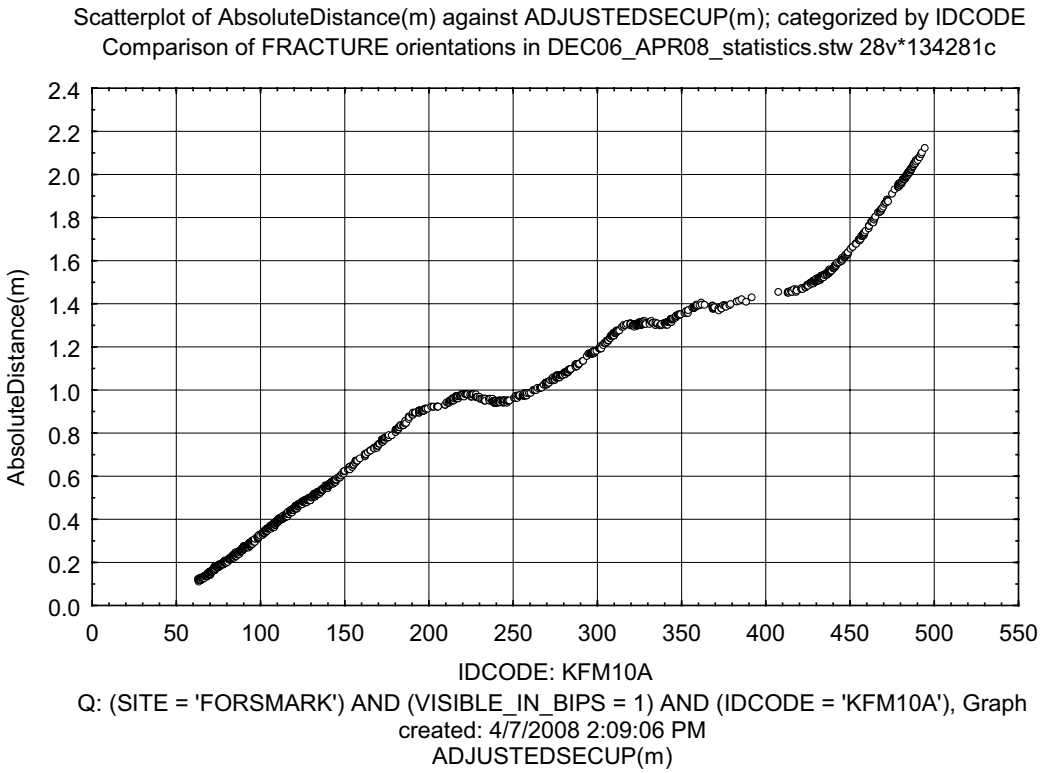

Scatterplot of AbsoluteDistance(m) against ADJUSTEDSECUP(m); categorized by IDCODE
Comparison of FRACTURE orientations in DEC06_APR08_statistics.stw 28v*134281c

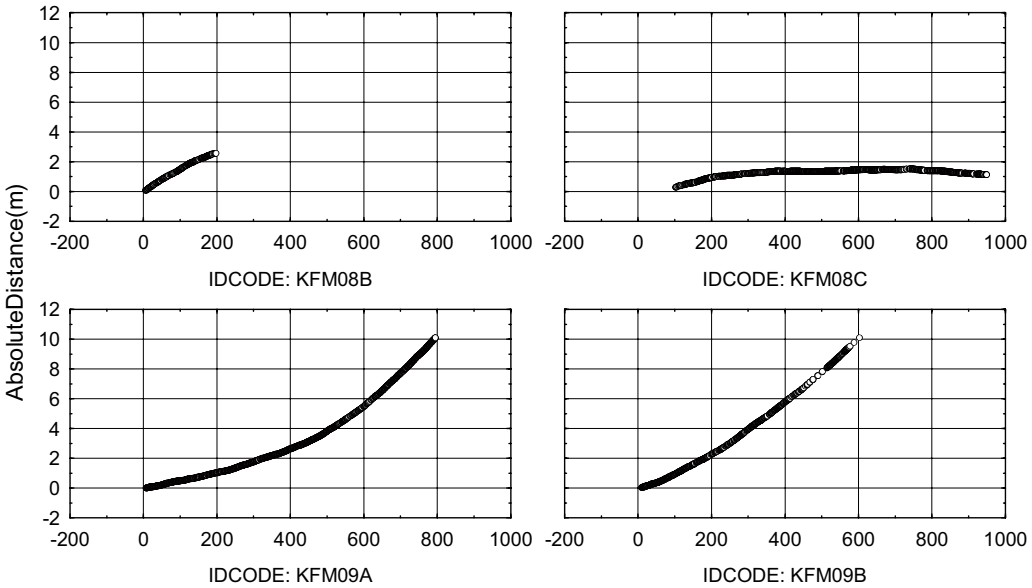

Q: (SITE = 'FORSMARK') AND (VISIBLE_IN_BIPS = 1) AND ((IDCODE = 'KFM08B') OR (IDCODE = 'KFM08C') OR (IDCODE = 'KFM09A') OR (IDCODE = 'KFM09B')), Graph created: 4/7/2008 2:08:32 PM
ADJUSTEDSECUP(m)

Scatterplot of AbsoluteDistance(m) against ADJUSTEDSECUP(m); categorized by IDCODE
Comparison of FRACTURE orientations in DEC06_APR08_statistics.stw 28v*134281c

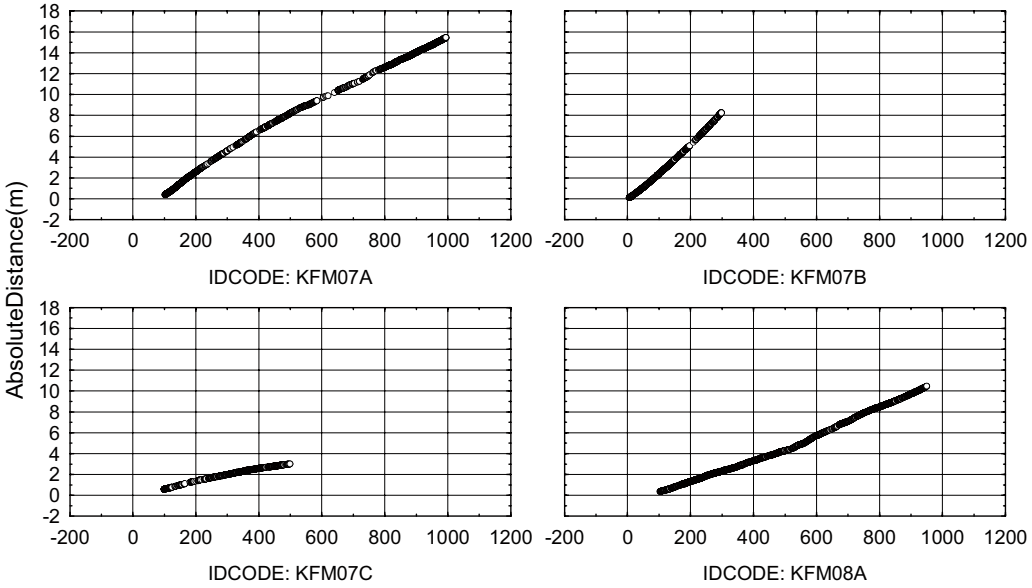

Q: (SITE = 'FORSMARK') AND (VISIBLE_IN_BIPS = 1) AND ((IDCODE = 'KFM07A') OR (IDCODE = 'KFM07B') OR (IDCODE = 'KFM07C') OR (IDCODE = 'KFM08A')), Graph created: 4/7/2008 2:07:59 PM
ADJUSTEDSECUP(m)

Scatterplot of AbsoluteDistance(m) against ADJUSTEDSECUP(m); categorized by IDCODE
Comparison of FRACTURE orientations in DEC06_APR08_statistics.stw 28v*134281c

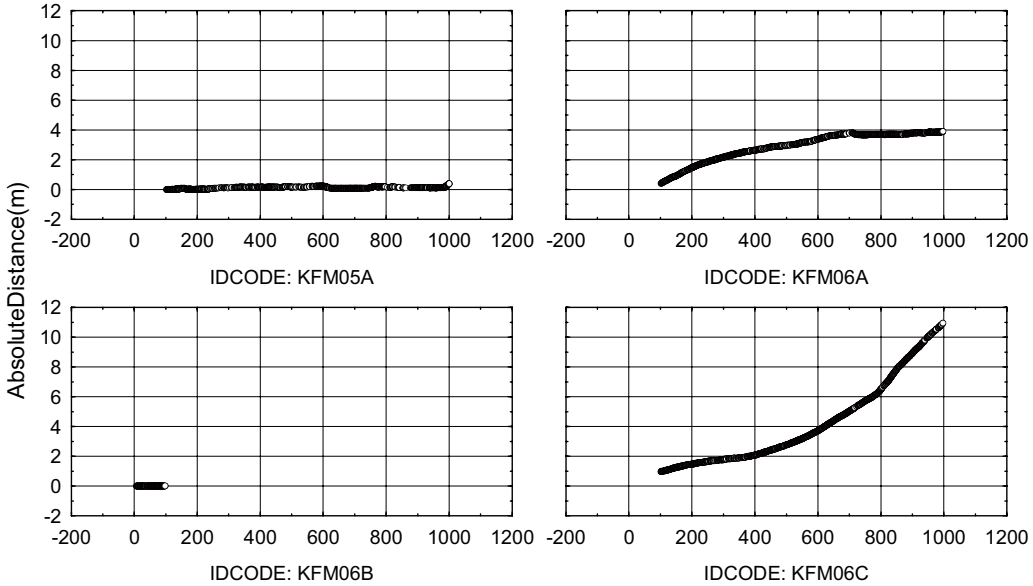

Q: (SITE = 'FORSMARK') AND (VISIBLE_IN_BIPS = 1) AND ((IDCODE = 'KFM05A') OR (IDCODE = 'KFM06A') OR (IDCODE = 'KFM06B') OR (IDCODE = 'KFM06C')), Graph created: 4/7/2008 2:07:27 PM
ADJUSTEDSECUP(m)

Scatterplot of AbsoluteDistance(m) against ADJUSTEDSECUP(m); categorized by IDCODE
Comparison of FRACTURE orientations in DEC06_APR08_statistics.stw 28v*134281c

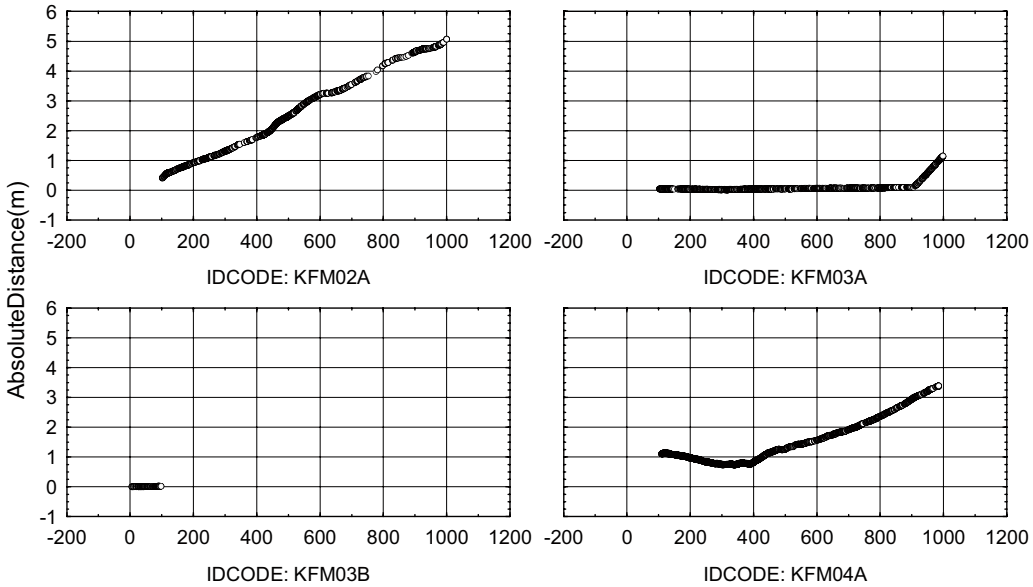

Q: (SITE = 'FORSMARK') AND (VISIBLE_IN_BIPS = 1) AND ((IDCODE = 'KFM02A') OR (IDCODE = 'KFM03A') OR (IDCODE = 'KFM03B') OR (IDCODE = 'KFM04A')), Graph created: 4/7/2008 2:06:54 PM
ADJUSTEDSECUP(m)

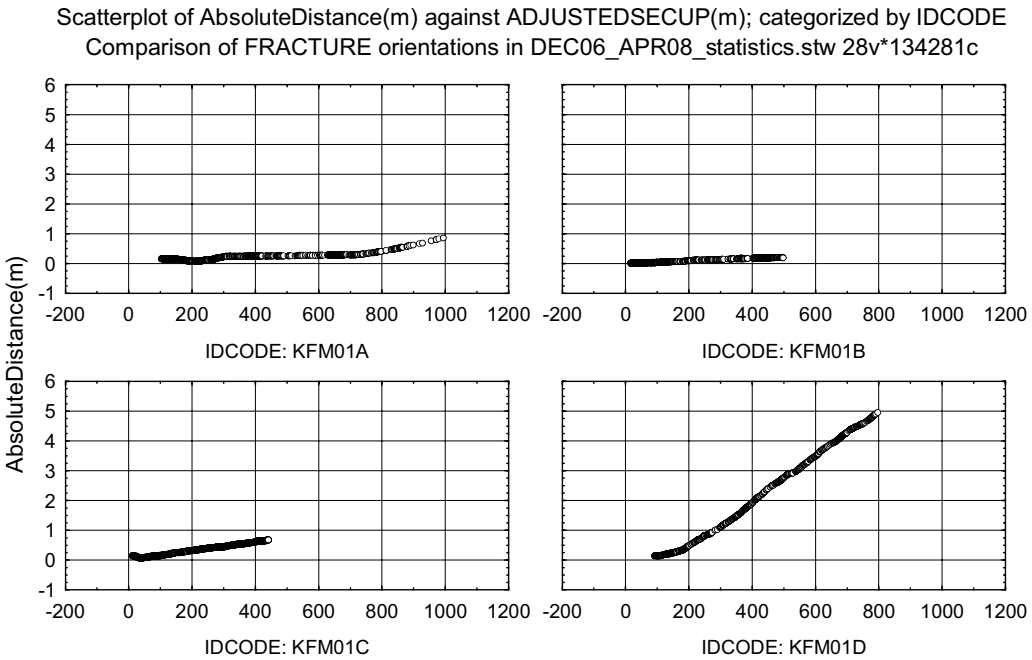
Scatterplot of AbsoluteDistance(m) against ADJUSTEDSECUP(m); categorized by IDCODE
Comparison of FRACTURE orientations in DEC06_APR08_statistics.stw 28v*134281c
AbsoluteDistance(m)
IDCODE: KFM01A
IDCODE: KFM01B
IDCODE: KFM01C
IDCODE: KFM01D
Q: (SITE = 'FORSMARK') AND (VISIBLE_IN_BIPS = 1) AND ((IDCODE = 'KFM01A') OR (IDCODE = 'KFM01B') OR (IDCODE = 'KFM01C') OR (IDCODE = 'KFM01D')), Graph created: 4/7/2008 2:06:20 PM
ADJUSTEDSECUP(m)

Laxemar

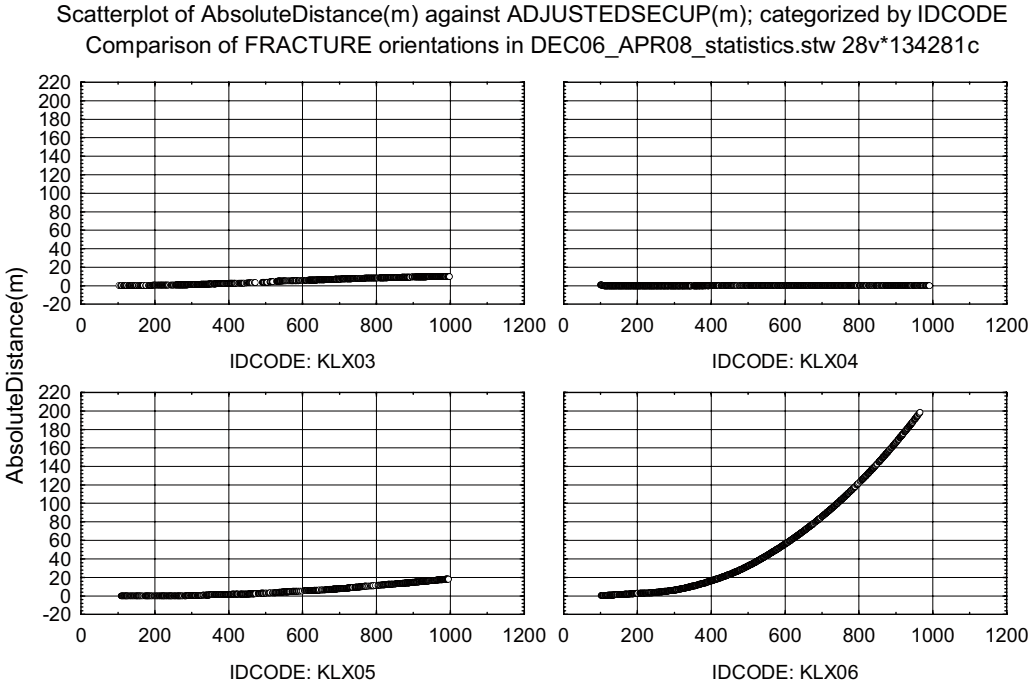
Scatterplot of AbsoluteDistance(m) against ADJUSTEDSECUP(m); categorized by IDCODE
Comparison of FRACTURE orientations in DEC06_APR08_statistics.stw 28v*134281c
AbsoluteDistance(m)
IDCODE: KLX03
IDCODE: KLX04
IDCODE: KLX05
IDCODE: KLX06
Q: (SITE = 'LAXEMAR') AND (VISIBLE_IN_BIPS = 1) AND ((IDCODE = 'KLX03') OR (IDCODE = 'KLX04') OR (IDCODE = 'KLX05') OR (IDCODE = 'KLX06')), Graph created: 4/7/2008 1:56:22 PM
ADJUSTEDSECUP(m)

Scatterplot of AbsoluteDistance(m) against ADJUSTEDSECUP(m); categorized by IDCODE
Comparison of FRACTURE orientations in DEC06_APR08_statistics.stw 28v*134281c

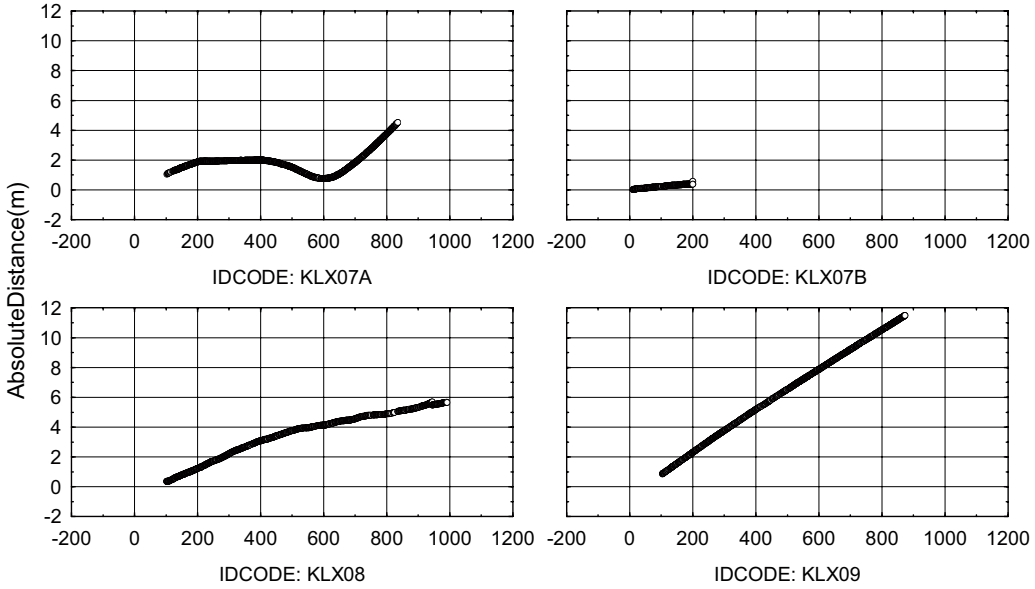

Q: (SITE = 'LAXEMAR') AND (VISIBLE_IN_BIPS = 1) AND ((IDCODE = 'KLX07A') OR (IDCODE = 'KLX07B') OR (IDCODE = 'KLX08') OR (IDCODE = 'KLX09')), Graph created: 4/7/2008 1:56:56 PM

ADJUSTEDSECUP(m)

Scatterplot of AbsoluteDistance(m) against ADJUSTEDSECUP(m); categorized by IDCODE
Comparison of FRACTURE orientations in DEC06_APR08_statistics.stw 28v*134281c

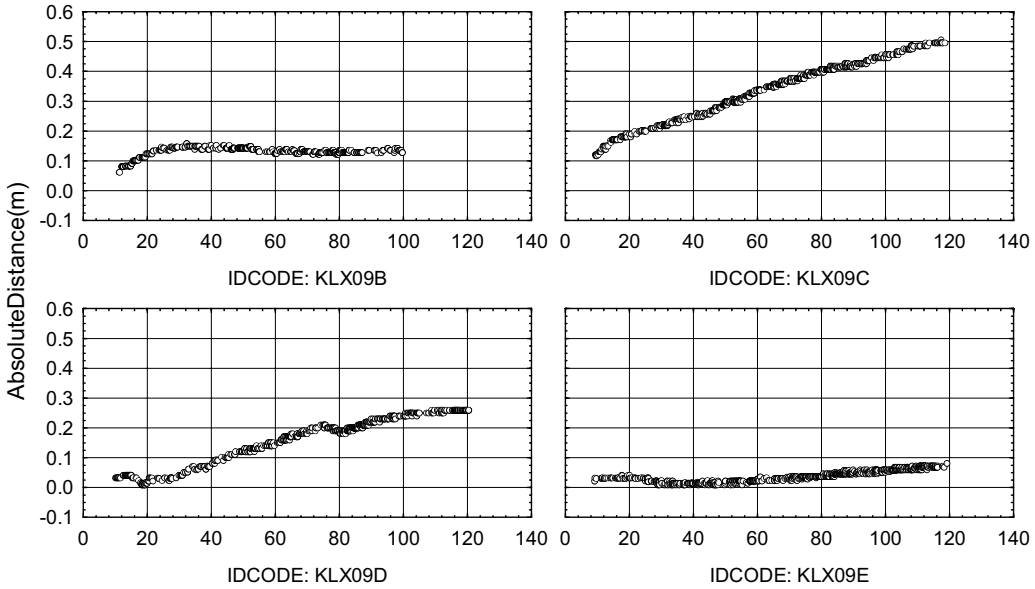

Q: (SITE = 'LAXEMAR') AND (VISIBLE_IN_BIPS = 1) AND ((IDCODE = 'KLX09B') OR (IDCODE = 'KLX09C') OR (IDCODE = 'KLX09D') OR (IDCODE = 'KLX09E')), Graph created: 4/7/2008 1:57:30 PM

ADJUSTEDSECUP(m)

Scatterplot of AbsoluteDistance(m) against ADJUSTEDSECUP(m); categorized by IDCODE
Comparison of FRACTURE orientations in DEC06_APR08_statistics.stw 28v*134281c

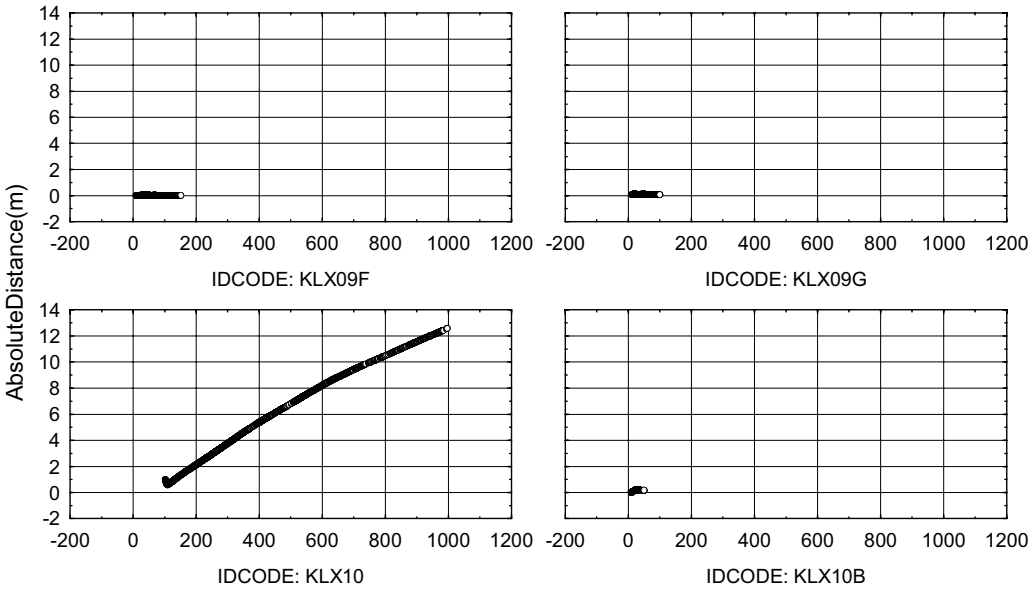

Q: (SITE = 'LAXEMAR') AND (VISIBLE_IN_BIPS = 1) AND ((IDCODE = 'KLX09F') OR (IDCODE = 'KLX09G') OR (IDCODE = 'KLX10') OR (IDCODE = 'KLX10B')), Graph created: 4/7/2008 1:58: 02 PM
ADJUSTEDSECUP(m)

Scatterplot of AbsoluteDistance(m) against ADJUSTEDSECUP(m); categorized by IDCODE
Comparison of FRACTURE orientations in DEC06_APR08_statistics.stw 28v*134281c

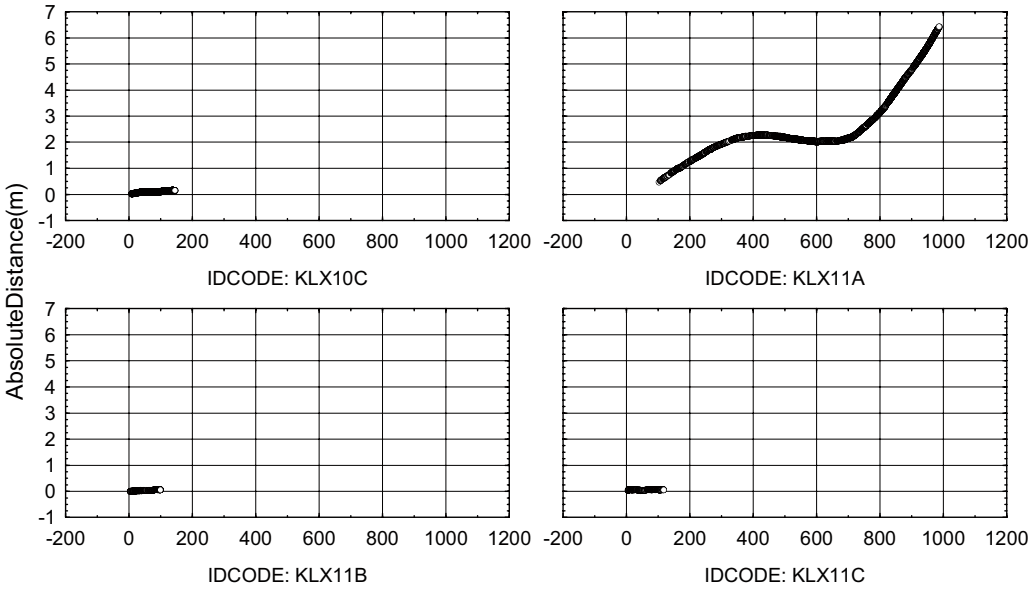

Q: (SITE = 'LAXEMAR') AND (VISIBLE_IN_BIPS = 1) AND ((IDCODE = 'KLX10C') OR (IDCODE = 'KLX11A') OR (IDCODE = 'KLX11B') OR (IDCODE = 'KLX11C')), Graph created: 4/7/2008 1:58: 36 PM
ADJUSTEDSECUP(m)

Scatterplot of AbsoluteDistance(m) against ADJUSTEDSECUP(m); categorized by IDCODE
Comparison of FRACTURE orientations in DEC06_APR08_statistics.stw 28v*134281c

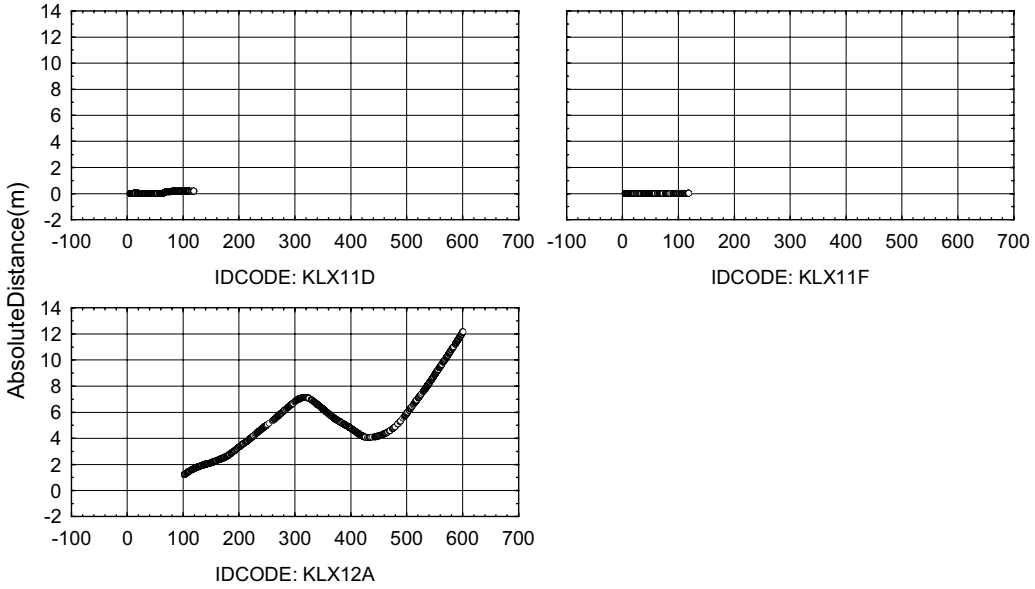

Q: (SITE = 'LAXEMAR') AND (VISIBLE_IN_BIPS = 1) AND ((IDCODE = 'KLX11D') OR (IDCODE = 'KLX101E') OR (IDCODE = 'KLX11F') OR (IDCODE = 'KLX12A')), Graph created: 4/7/2008 1:59:09 PM
ADJUSTEDSECUP(m)

Scatterplot of AbsoluteDistance(m) against ADJUSTEDSECUP(m); categorized by IDCODE
Comparison of FRACTURE orientations in DEC06_APR08_statistics.stw 28v*134281c

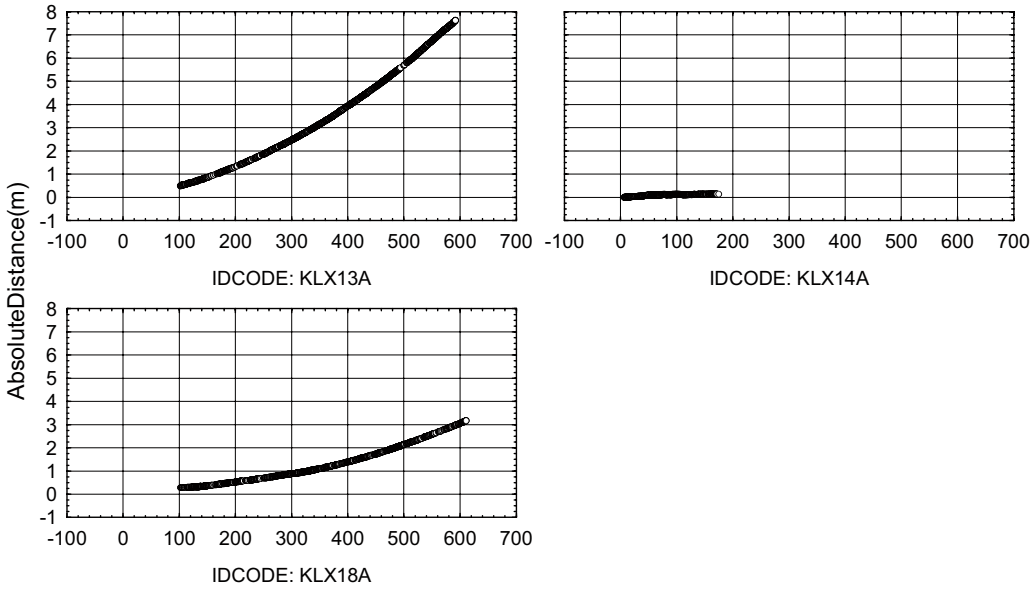

Q: (SITE = 'LAXEMAR') AND (VISIBLE_IN_BIPS = 1) AND ((IDCODE = 'KLX13A') OR (IDCODE = 'KLX14A') OR (IDCODE = 'KLX17A') OR (IDCODE = 'KLX18A')), Graph created: 4/7/2008 1:59:42 PM
ADJUSTEDSECUP(m)

Scatterplot of AbsoluteDistance(m) against ADJUSTEDSECUP(m); categorized by IDCODE
Comparison of FRACTURE orientations in DEC06_APR08_statistics.stw 28v*134281c

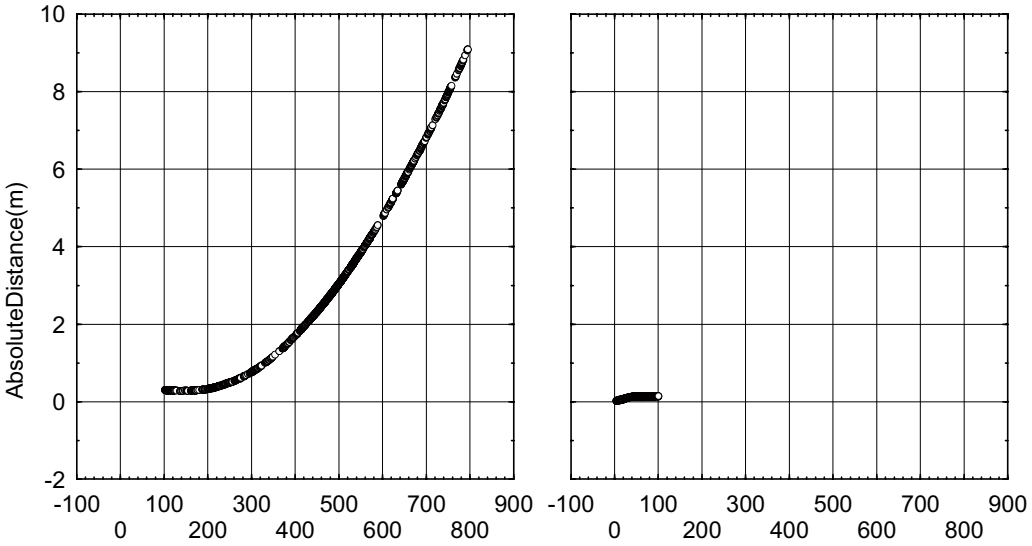

Q: (SITE = 'LAXEMAR') AND (VISIBLE_IN_BIPS = 1) AND ((IDCODE = 'KLX19A') OR (IDCODE = 'KLX20B') OR (IDCODE = 'KLX21B') OR (IDCODE = 'KLX22A')), Graph created: 4/7/2008 2:00: 16 PM

ADJUSTEDSECUP(m)

Scatterplot of AbsoluteDistance(m) against ADJUSTEDSECUP(m); categorized by IDCODE
Comparison of FRACTURE orientations in DEC06_APR08_statistics.stw 28v*134281c

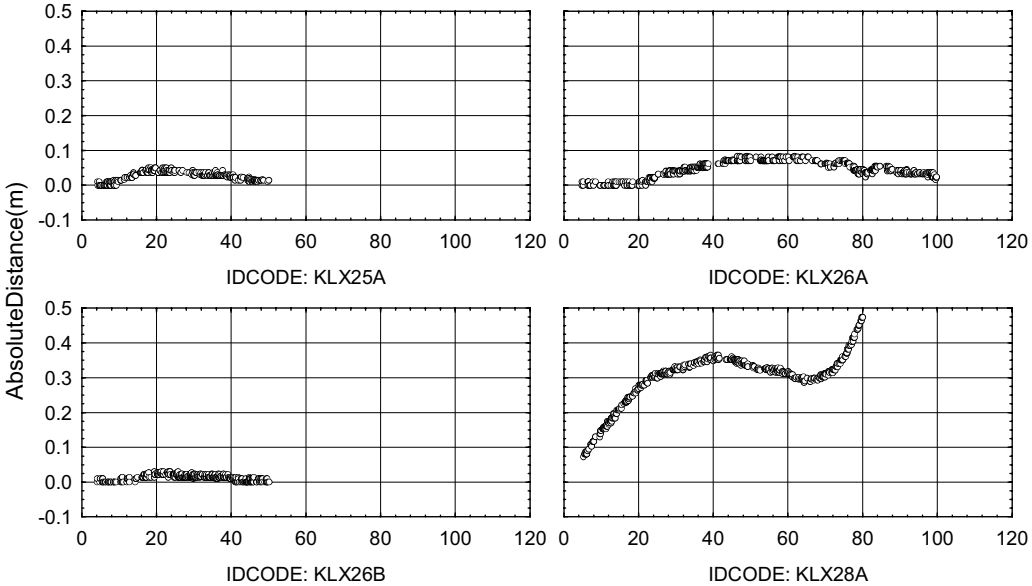

Q: (SITE = 'LAXEMAR') AND (VISIBLE_IN_BIPS = 1) AND ((IDCODE = 'KLX25A') OR (IDCODE = 'KLX26A') OR (IDCODE = 'KLX26B') OR (IDCODE = 'KLX28A')), Graph created: 4/7/2008 2:00: 48 PM

ADJUSTEDSECUP(m)

Scatterplot of AbsoluteDistance(m) against ADJUSTEDSECUP(m); categorized by IDCODE
Comparison of FRACTURE orientations in DEC06_APR08_statistics.stw 28v*134281c

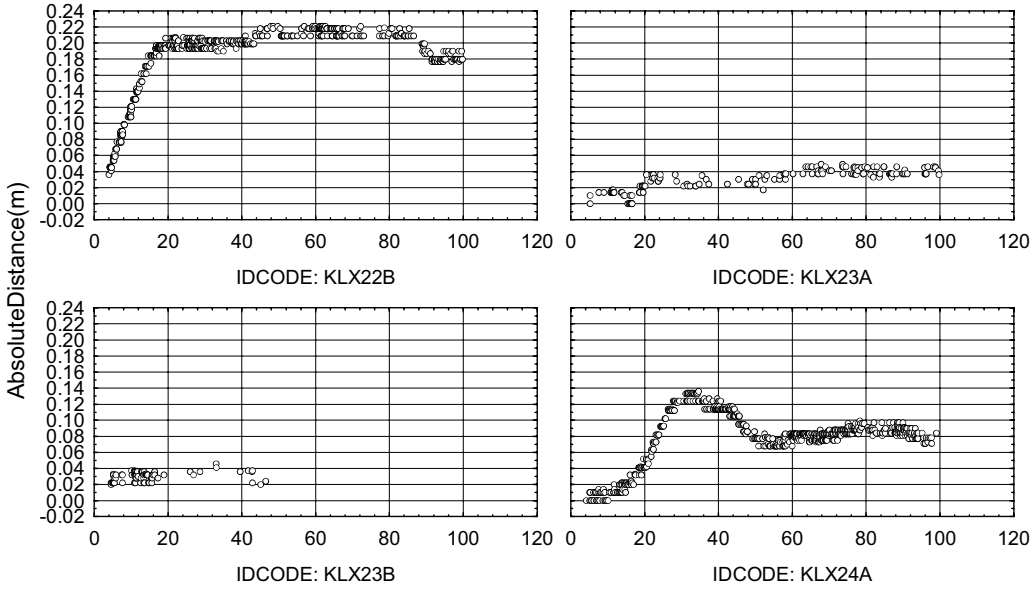

Q: (SITE = 'LAXEMAR') AND (VISIBLE_IN_BIPS = 1) AND ((IDCODE = 'KLX22B') OR (IDCODE = 'KLX23A') OR (IDCODE = 'KLX23B') OR (IDCODE = 'KLX24A')), Graph created: 4/7/2008 2:01: 21 PM
ADJUSTEDSECUP(m)

Scatterplot of AbsoluteDistance(m) against ADJUSTEDSECUP(m); categorized by IDCODE
Comparison of FRACTURE orientations in DEC06_APR08_statistics.stw 28v*134281c

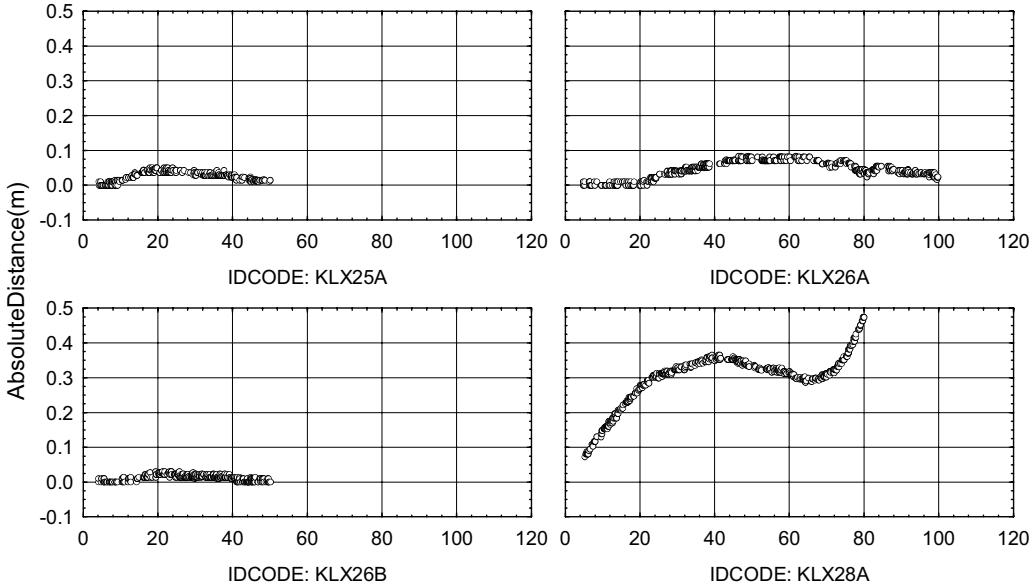

Q: (SITE = 'LAXEMAR') AND (VISIBLE_IN_BIPS = 1) AND ((IDCODE = 'KLX25A') OR (IDCODE = 'KLX26A') OR (IDCODE = 'KLX26B') OR (IDCODE = 'KLX28A')), Graph created: 4/7/2008 2:01: 54 PM
ADJUSTEDSECUP(m)

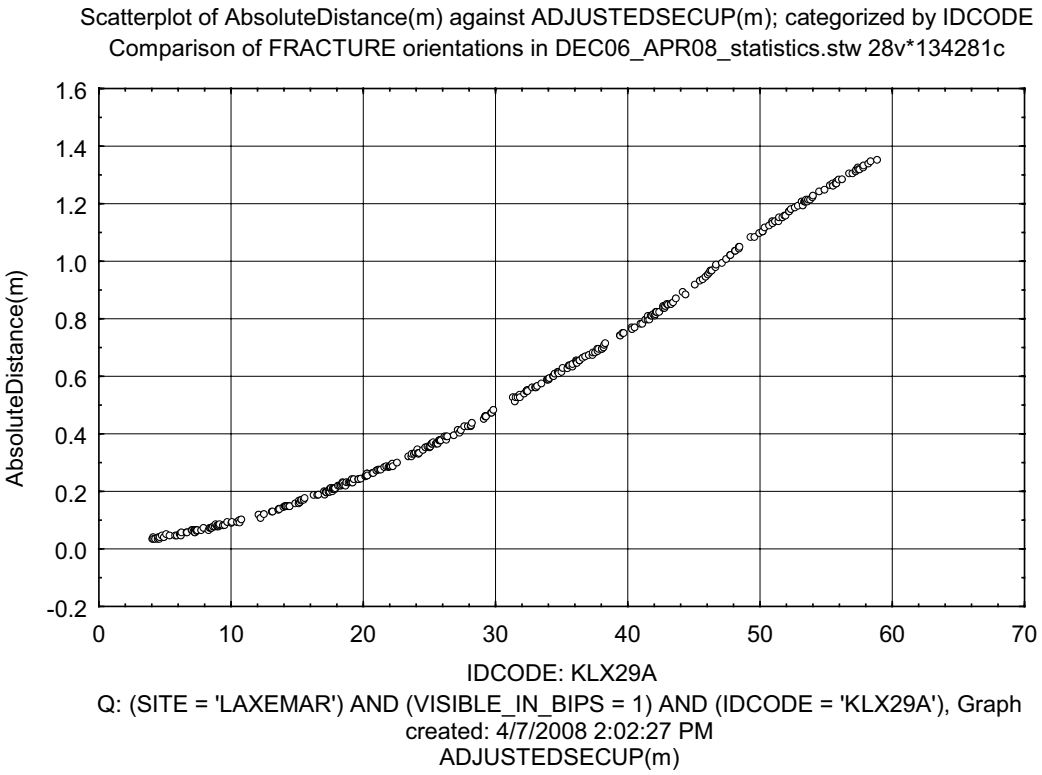

A3.2 Fracture orientations (only those visible in BIPS)

A3.2.1 Difference between old and new fracture datasets, θ

Forsmark

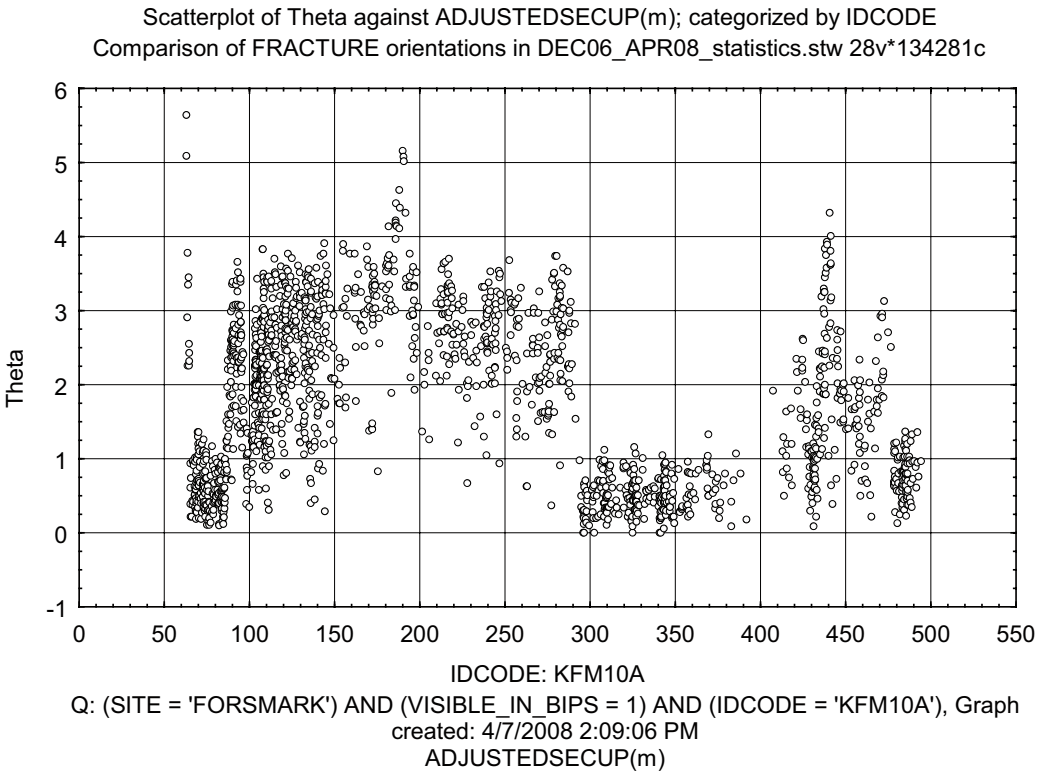

Scatterplot of Theta against ADJUSTEDSECUP(m); categorized by IDCODE
Comparison of FRACTURE orientations in DEC06_APR08_statistics.stw 28v*134281c

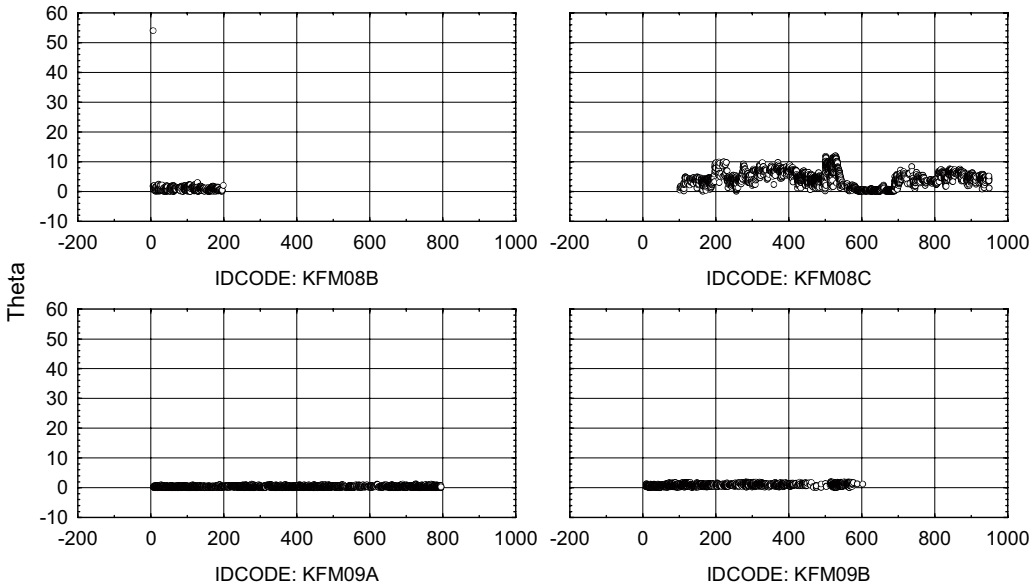

Q: (SITE = 'FORSMARK') AND (VISIBLE_IN_BIPS = 1) AND ((IDCODE = 'KFM08B') OR (IDCODE = 'KFM08C') OR (IDCODE = 'KFM09A') OR (IDCODE = 'KFM09B')), Graph created: 4/7/2008 2:08:32 PM
ADJUSTEDSECUP(m)

Scatterplot of Theta against ADJUSTEDSECUP(m); categorized by IDCODE
Comparison of FRACTURE orientations in DEC06_APR08_statistics.stw 28v*134281c

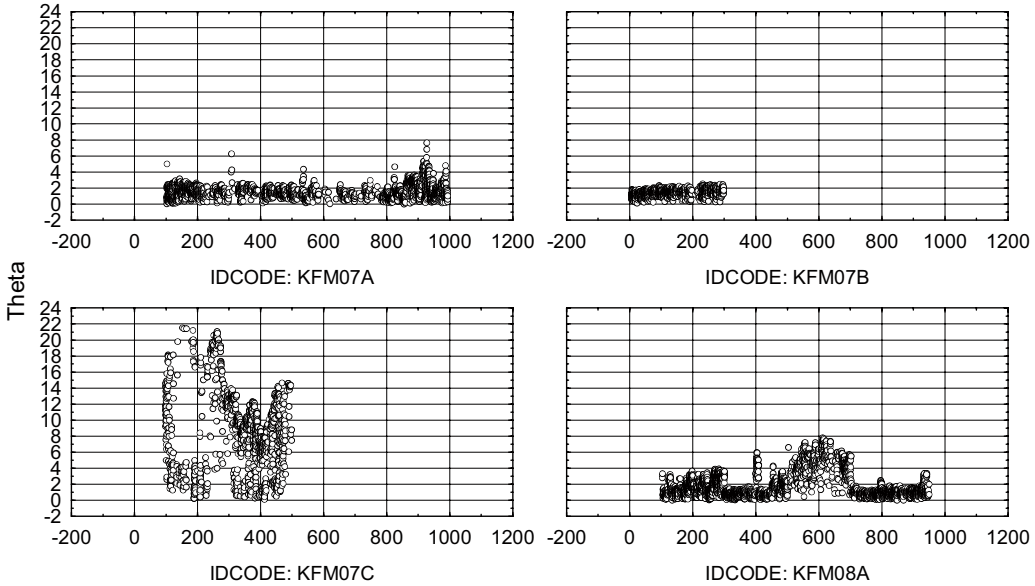

Q: (SITE = 'FORSMARK') AND (VISIBLE_IN_BIPS = 1) AND ((IDCODE = 'KFM07A') OR (IDCODE = 'KFM07B') OR (IDCODE = 'KFM07C') OR (IDCODE = 'KFM08A')), Graph created: 4/7/2008 2:07:59 PM
ADJUSTEDSECUP(m)

Scatterplot of Theta against ADJUSTEDSECUP(m); categorized by IDCODE
Comparison of FRACTURE orientations in DEC06_APR08_statistics.stw 28v*134281c

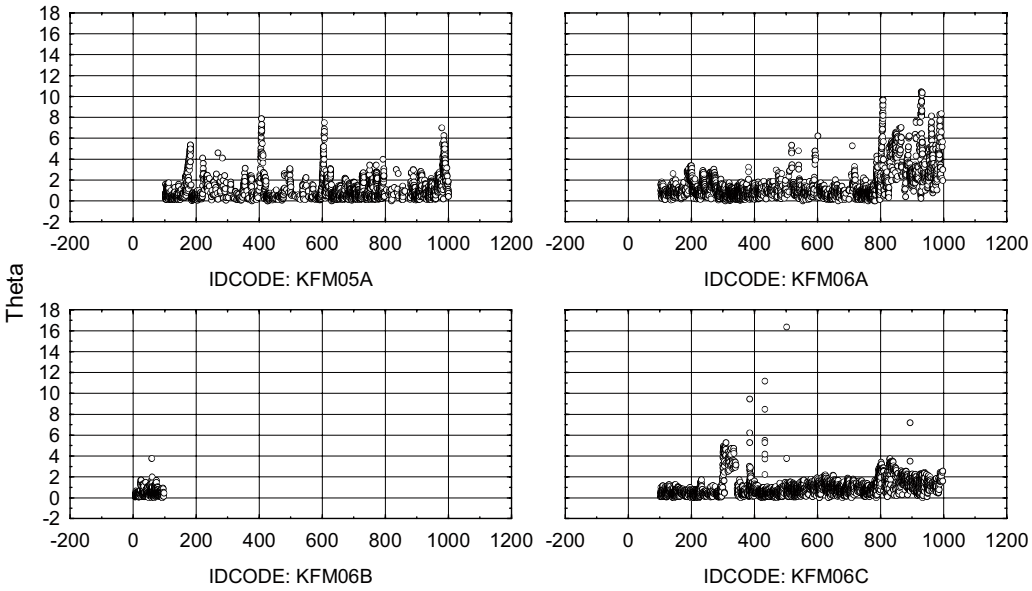

Q: (SITE = 'FORSMARK') AND (VISIBLE_IN_BIPS = 1) AND ((IDCODE = 'KFM05A') OR (IDCODE = 'KFM06A') OR (IDCODE = 'KFM06B') OR (IDCODE = 'KFM06C')), Graph created: 4/7/2008 2:07:27 PM
ADJUSTEDSECUP(m)

Scatterplot of Theta against ADJUSTEDSECUP(m); categorized by IDCODE
Comparison of FRACTURE orientations in DEC06_APR08_statistics.stw 28v*134281c

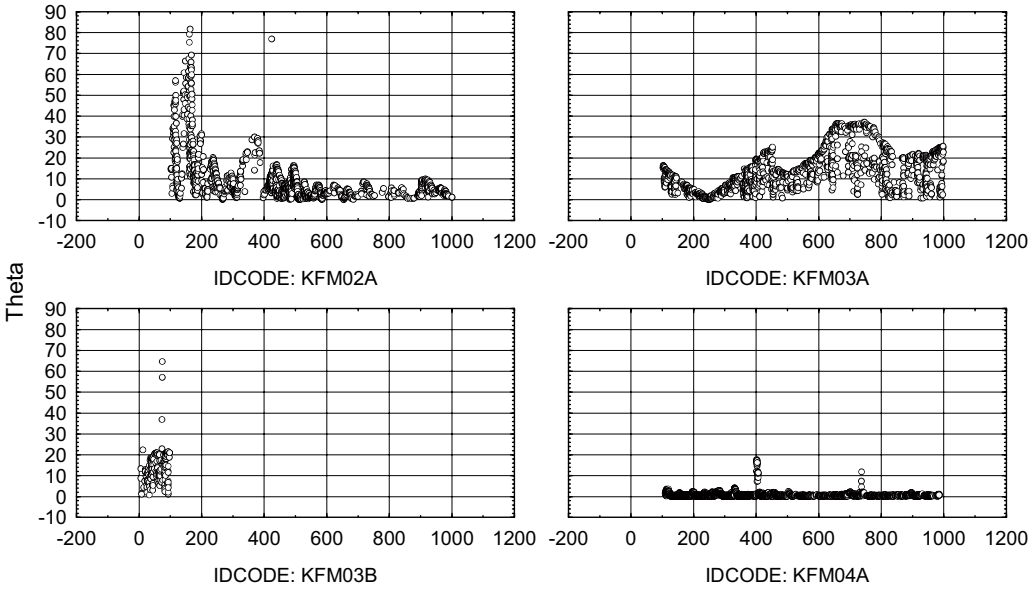

Q: (SITE = 'FORSMARK') AND (VISIBLE_IN_BIPS = 1) AND ((IDCODE = 'KFM02A') OR (IDCODE = 'KFM03A') OR (IDCODE = 'KFM03B') OR (IDCODE = 'KFM04A')), Graph created: 4/7/2008 2:06:54 PM
ADJUSTEDSECUP(m)

Scatterplot of Theta against ADJUSTEDSECUP(m); categorized by IDCODE
Comparison of FRACTURE orientations in DEC06_APR08_statistics.stw 28v*134281c

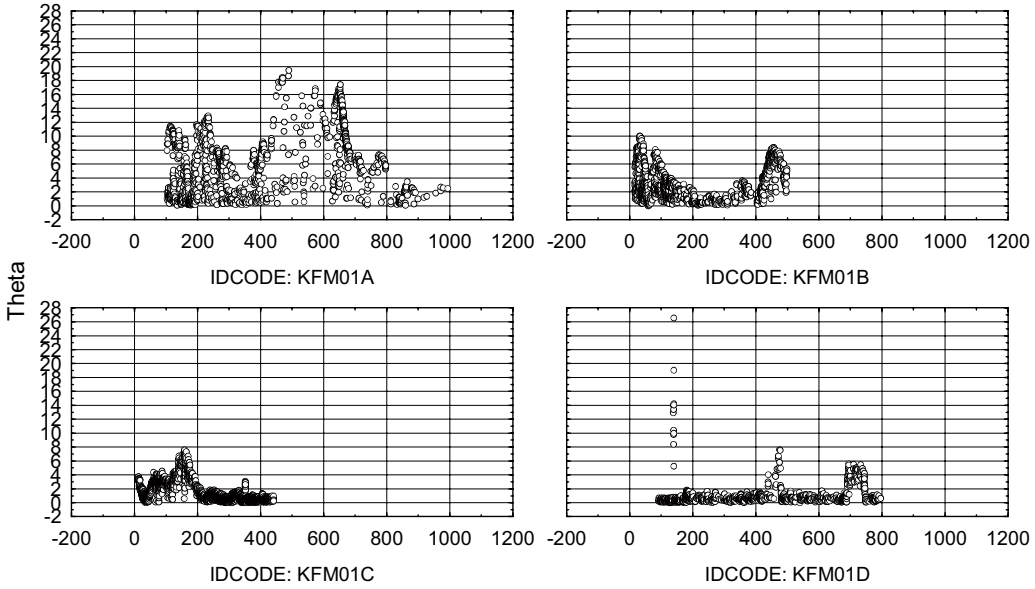

Q: (SITE = 'FORSMARK') AND (VISIBLE_IN_BIPS = 1) AND ((IDCODE = 'KFM01A') OR (IDCODE = 'KFM01B') OR (IDCODE = 'KFM01C') OR (IDCODE = 'KFM01D')), Graph created: 4/7/2008 2:06:20 PM
ADJUSTEDSECUP(m)

Laxemar

Scatterplot of Theta against ADJUSTEDSECUP(m); categorized by IDCODE
Comparison of FRACTURE orientations in DEC06_APR08_statistics.stw 28v*134281c

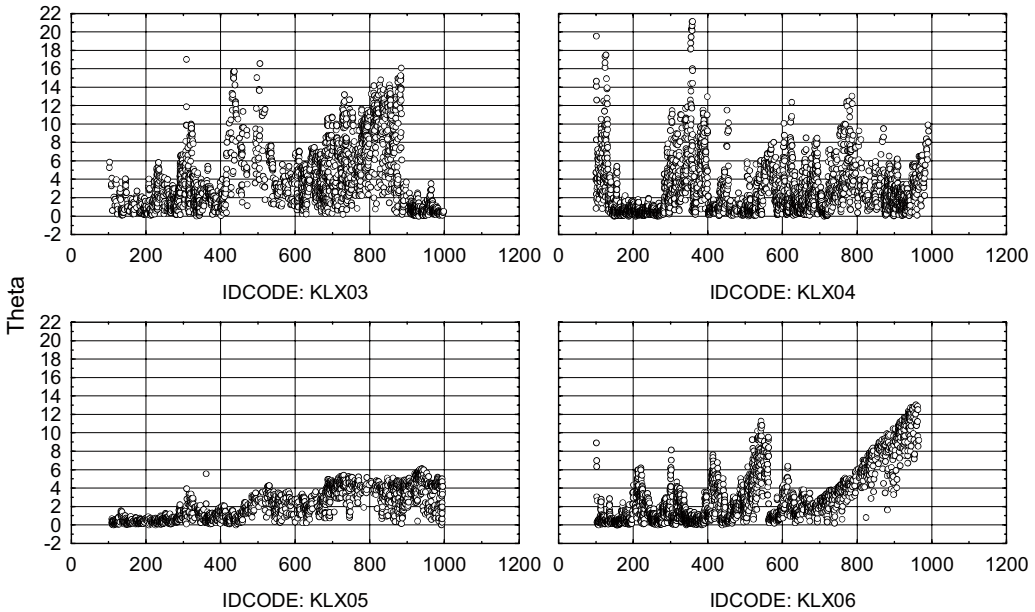

Q: (SITE = 'LAXEMAR') AND (VISIBLE_IN_BIPS = 1) AND ((IDCODE = 'KLX03') OR (IDCODE = 'KLX04') OR (IDCODE = 'KLX05') OR (IDCODE = 'KLX06')), Graph created: 4/7/2008 1:56:22 PM
ADJUSTEDSECUP(m)

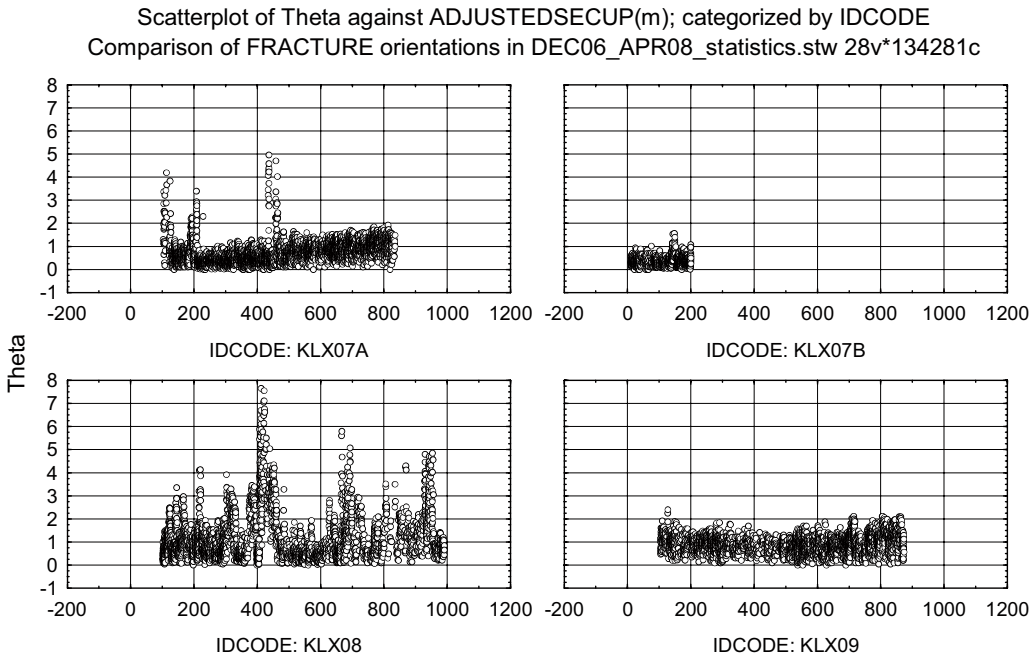
Scatterplot of Theta against ADJUSTEDSECUP(m); categorized by IDCODE
Comparison of FRACTURE orientations in DEC06_APR08_statistics.stw 28v*134281c
Theta
IDCODE: KLX07A
IDCODE: KLX07B
IDCODE: KLX08
IDCODE: KLX09
Q: (SITE = 'LAXEMAR') AND (VISIBLE_IN_BIPS = 1) AND ((IDCODE = 'KLX07A') OR (IDCODE = 'KLX07B') OR (IDCODE = 'KLX08') OR (IDCODE = 'KLX09')), Graph created: 4/7/2008 1:56:56 PM
ADJUSTEDSECUP(m)

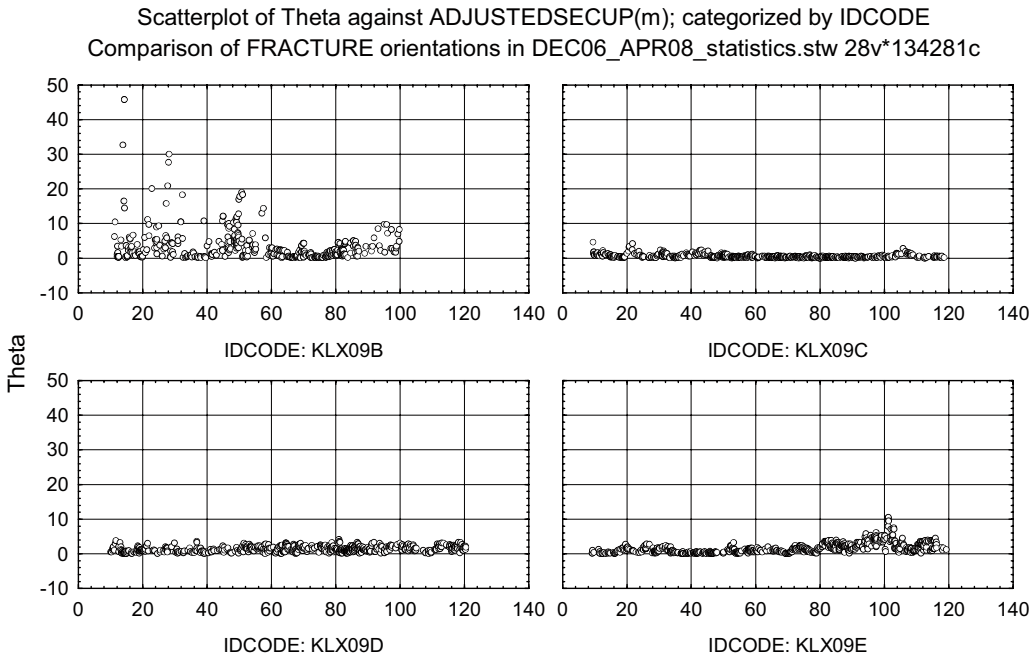
Scatterplot of Theta against ADJUSTEDSECUP(m); categorized by IDCODE
Comparison of FRACTURE orientations in DEC06_APR08_statistics.stw 28v*134281c
Theta
IDCODE: KLX09B
IDCODE: KLX09C
IDCODE: KLX09D
IDCODE: KLX09E
Q: (SITE = 'LAXEMAR') AND (VISIBLE_IN_BIPS = 1) AND ((IDCODE = 'KLX09B') OR (IDCODE = 'KLX09C') OR (IDCODE = 'KLX09D') OR (IDCODE = 'KLX09E')), Graph created: 4/7/2008 1:57:30 PM
ADJUSTEDSECUP(m)

Scatterplot of Theta against ADJUSTEDSECUP(m); categorized by IDCODE
Comparison of FRACTURE orientations in DEC06_APR08_statistics.stw 28v*134281c

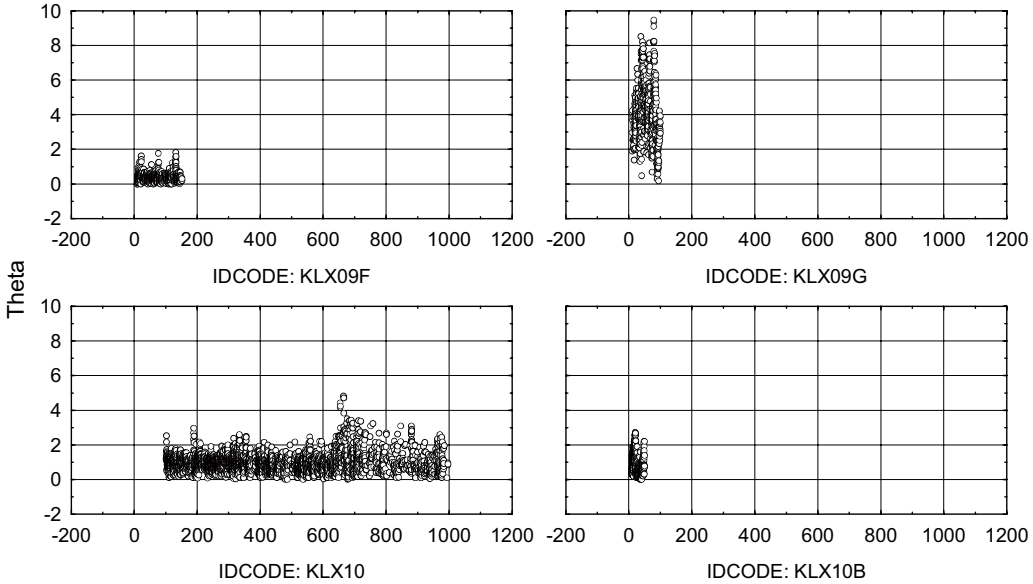

Q: (SITE = 'LAXEMAR') AND (VISIBLE_IN_BIPS = 1) AND ((IDCODE = 'KLX09F') OR (IDCODE = 'KLX09G') OR (IDCODE = 'KLX10') OR (IDCODE = 'KLX10B')), Graph created: 4/7/2008 1:58: 02 PM
ADJUSTEDSECUP(m)

Scatterplot of Theta against ADJUSTEDSECUP(m); categorized by IDCODE
Comparison of FRACTURE orientations in DEC06_APR08_statistics.stw 28v*134281c

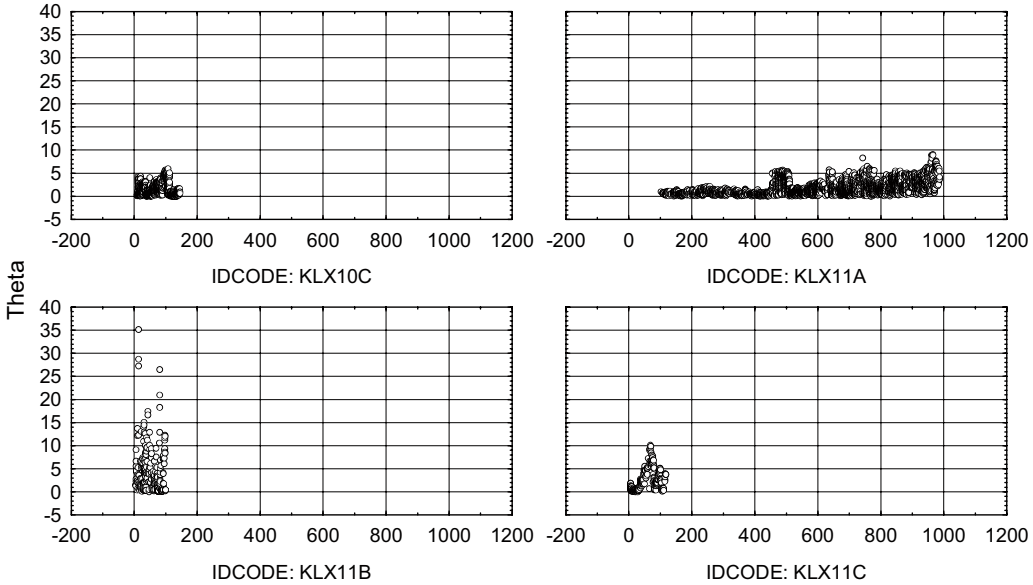

Q: (SITE = 'LAXEMAR') AND (VISIBLE_IN_BIPS = 1) AND ((IDCODE = 'KLX10C') OR (IDCODE = 'KLX11A') OR (IDCODE = 'KLX11B') OR (IDCODE = 'KLX11C')), Graph created: 4/7/2008 1:58: 36 PM
ADJUSTEDSECUP(m)

Scatterplot of Theta against ADJUSTEDSECUP(m); categorized by IDCODE
Comparison of FRACTURE orientations in DEC06_APR08_statistics.stw 28v*134281c

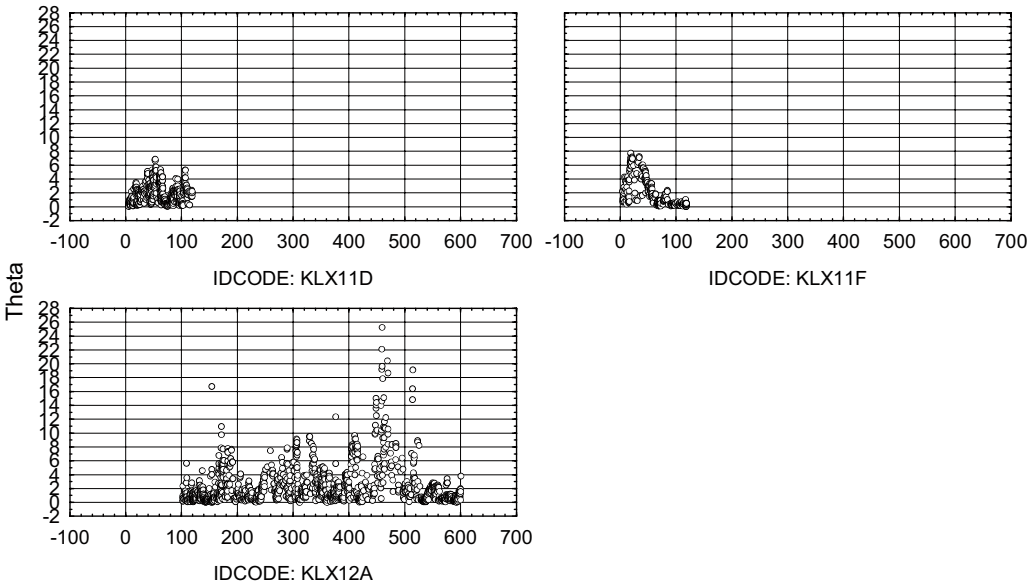

Q: (SITE = 'LAXEMAR') AND (VISIBLE_IN_BIPS = 1) AND ((IDCODE = 'KLX11D') OR (IDCODE = 'KLX101E') OR (IDCODE = 'KLX11F') OR (IDCODE = 'KLX12A')), Graph created: 4/7/2008 1:59:09 PM
ADJUSTEDSECUP(m)

Scatterplot of Theta against ADJUSTEDSECUP(m); categorized by IDCODE
Comparison of FRACTURE orientations in DEC06_APR08_statistics.stw 28v*134281c

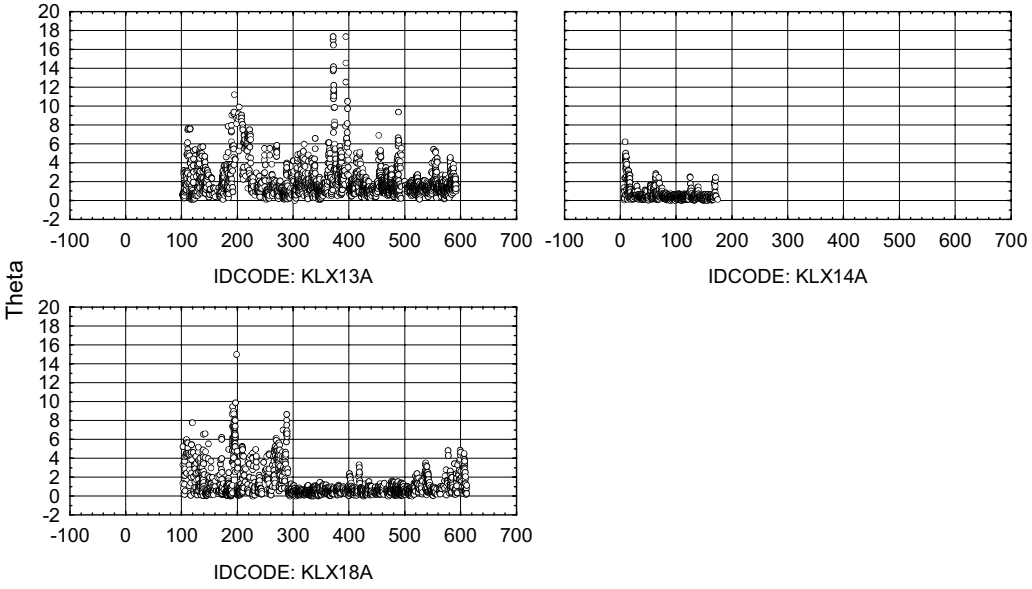

Q: (SITE = 'LAXEMAR') AND (VISIBLE_IN_BIPS = 1) AND ((IDCODE = 'KLX13A') OR (IDCODE = 'KLX14A') OR (IDCODE = 'KLX17A') OR (IDCODE = 'KLX18A')), Graph created: 4/7/2008 1:59:42 PM
ADJUSTEDSECUP(m)

Scatterplot of Theta against ADJUSTEDSECUP(m); categorized by IDCODE
Comparison of FRACTURE orientations in DEC06_APR08_statistics.stw 28v*134281c

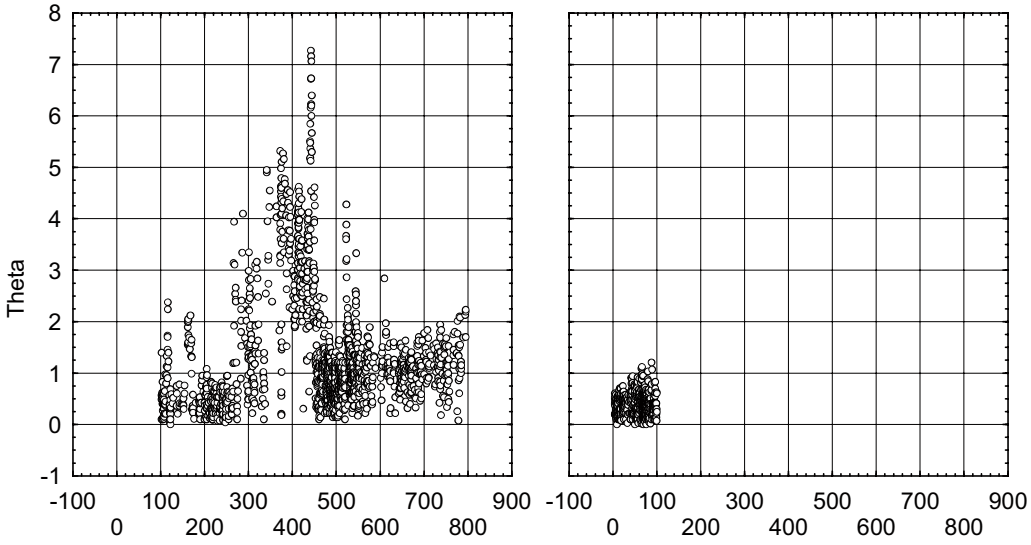

Q: (SITE = 'LAXEMAR') AND (VISIBLE_IN_BIPS = 1) AND ((IDCODE = 'KLX19A') OR (IDCODE = 'KLX20B') OR (IDCODE = 'KLX21B') OR (IDCODE = 'KLX22A')), Graph created: 4/7/2008 2:00: 16 PM
ADJUSTEDSECUP(m)

Scatterplot of Theta against ADJUSTEDSECUP(m); categorized by IDCODE
Comparison of FRACTURE orientations in DEC06_APR08_statistics.stw 28v*134281c

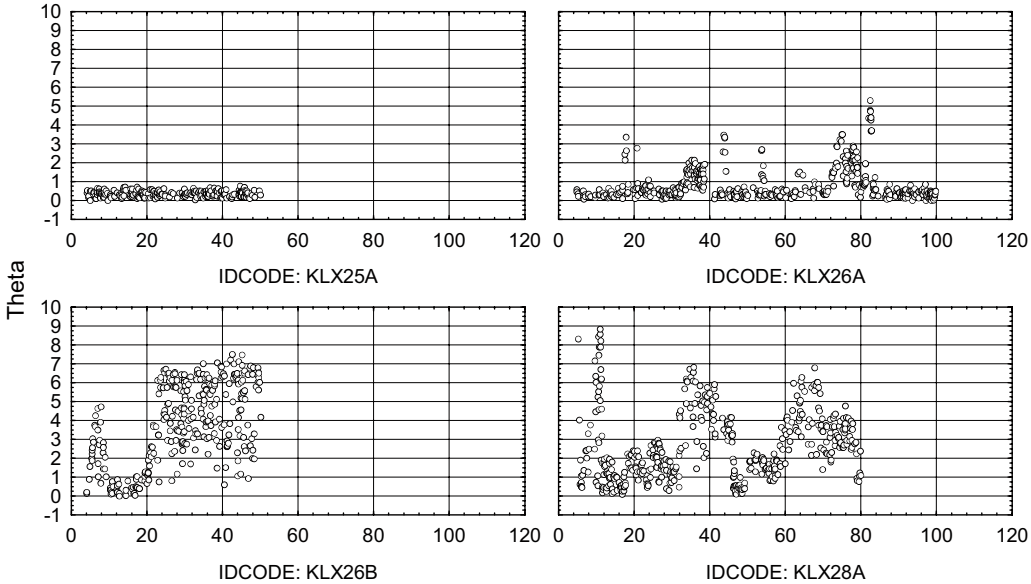

Q: (SITE = 'LAXEMAR') AND (VISIBLE_IN_BIPS = 1) AND ((IDCODE = 'KLX25A') OR (IDCODE = 'KLX26A') OR (IDCODE = 'KLX26B') OR (IDCODE = 'KLX28A')), Graph created: 4/7/2008 2:00: 48 PM
ADJUSTEDSECUP(m)

Scatterplot of Theta against ADJUSTEDSECUP(m); categorized by IDCODE
Comparison of FRACTURE orientations in DEC06_APR08_statistics.stw 28v*134281c

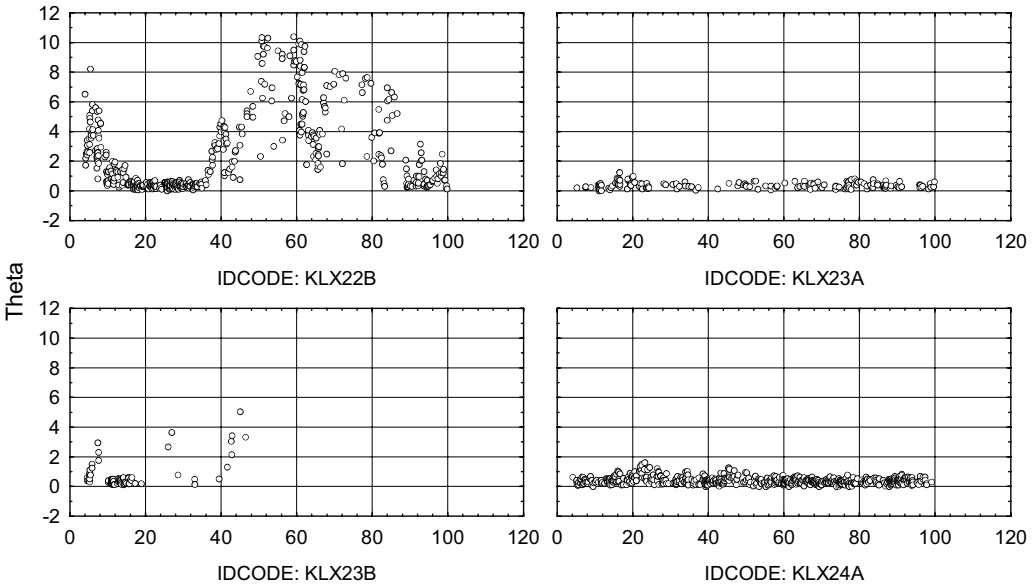

Q: (SITE = 'LAXEMAR') AND (VISIBLE_IN_BIPS = 1) AND ((IDCODE = 'KLX22B') OR (IDCODE = 'KLX23A') OR (IDCODE = 'KLX23B') OR (IDCODE = 'KLX24A')), Graph created: 4/7/2008 2:01: 21 PM
ADJUSTEDSECUP(m)

Scatterplot of Theta against ADJUSTEDSECUP(m); categorized by IDCODE
Comparison of FRACTURE orientations in DEC06_APR08_statistics.stw 28v*134281c

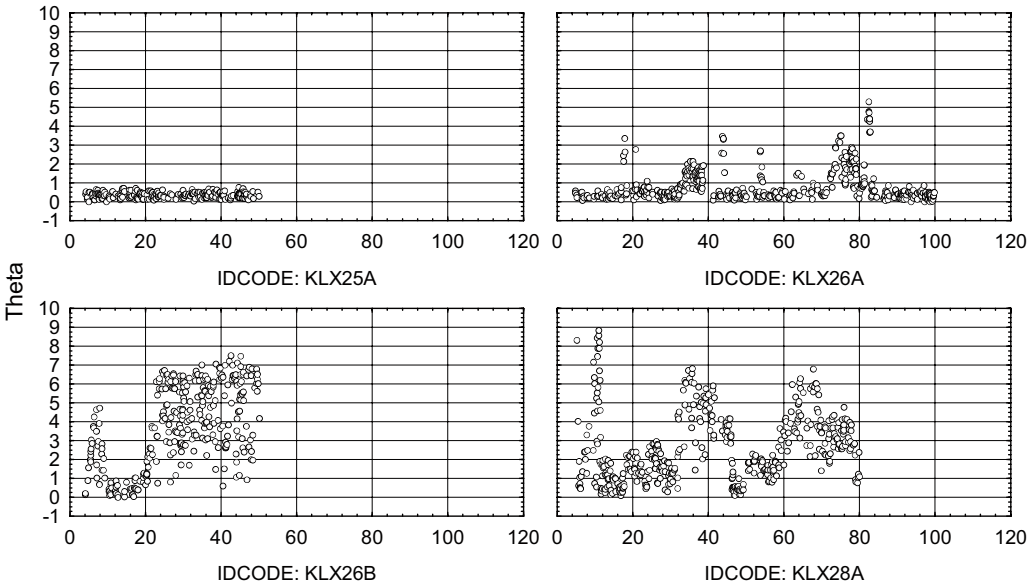

Q: (SITE = 'LAXEMAR') AND (VISIBLE_IN_BIPS = 1) AND ((IDCODE = 'KLX25A') OR (IDCODE = 'KLX26A') OR (IDCODE = 'KLX26B') OR (IDCODE = 'KLX28A')), Graph created: 4/7/2008 2:01: 54 PM
ADJUSTEDSECUP(m)

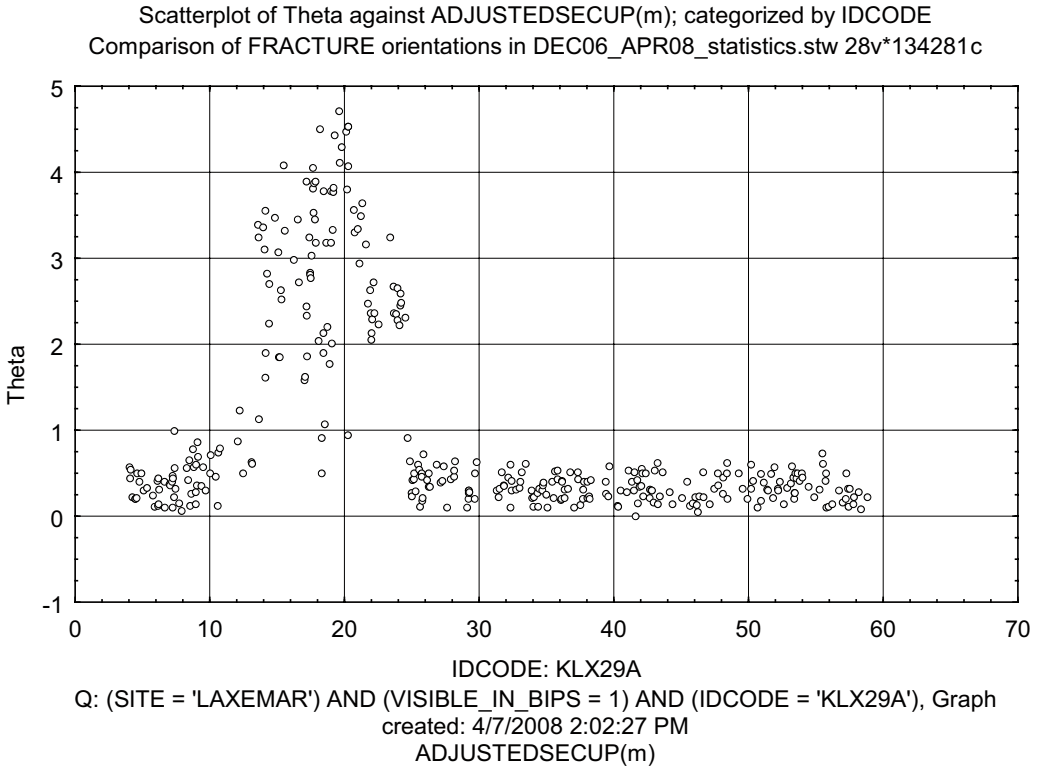

A3.2.2 Fracture orientation uncertainty, Ω

Forsmark

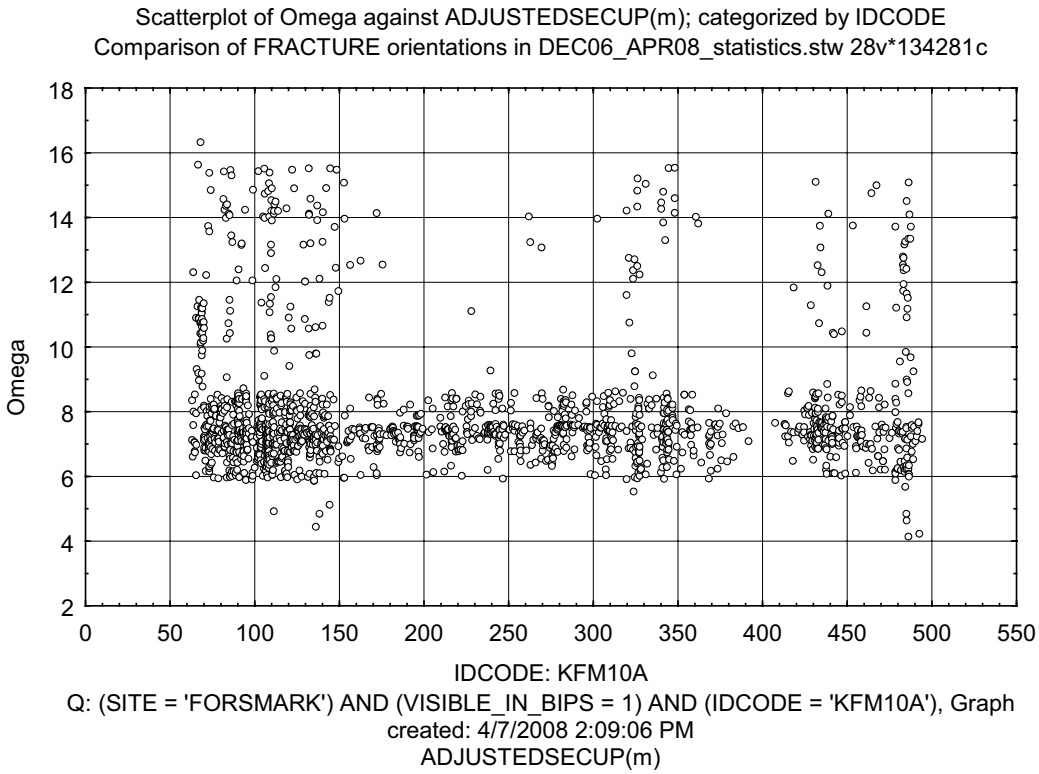

Scatterplot of Omega against ADJUSTEDSECUP(m); categorized by IDCODE
Comparison of FRACTURE orientations in DEC06_APR08_statistics.stw 28v*134281c

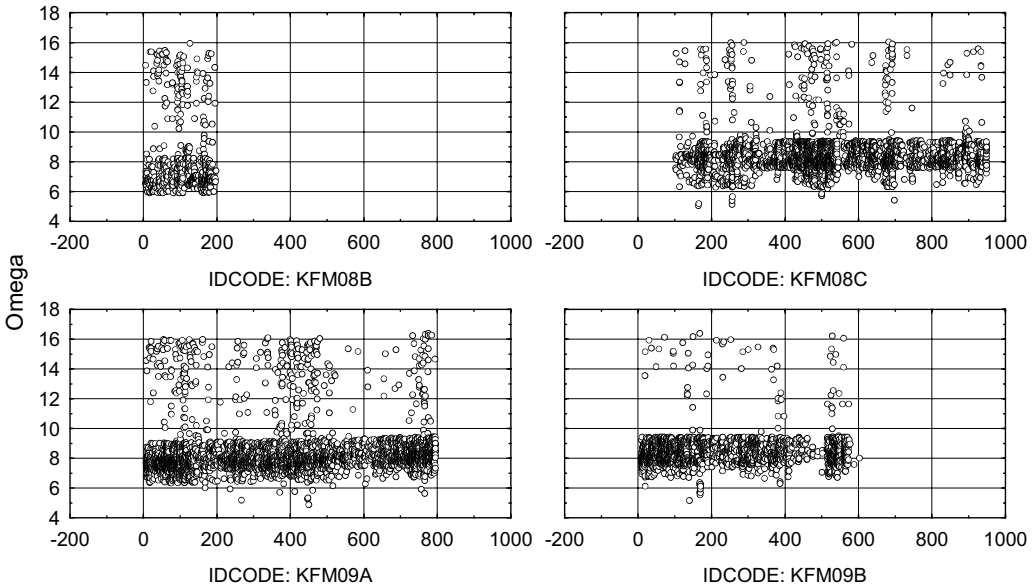

Q: (SITE = 'FORSMARK') AND (VISIBLE_IN_BIPS = 1) AND ((IDCODE = 'KFM08B') OR (IDCODE = 'KFM08C') OR (IDCODE = 'KFM09A') OR (IDCODE = 'KFM09B')), Graph created: 4/7/2008 2:08:32 PM
ADJUSTEDSECUP(m)

Scatterplot of Omega against ADJUSTEDSECUP(m); categorized by IDCODE
Comparison of FRACTURE orientations in DEC06_APR08_statistics.stw 28v*134281c

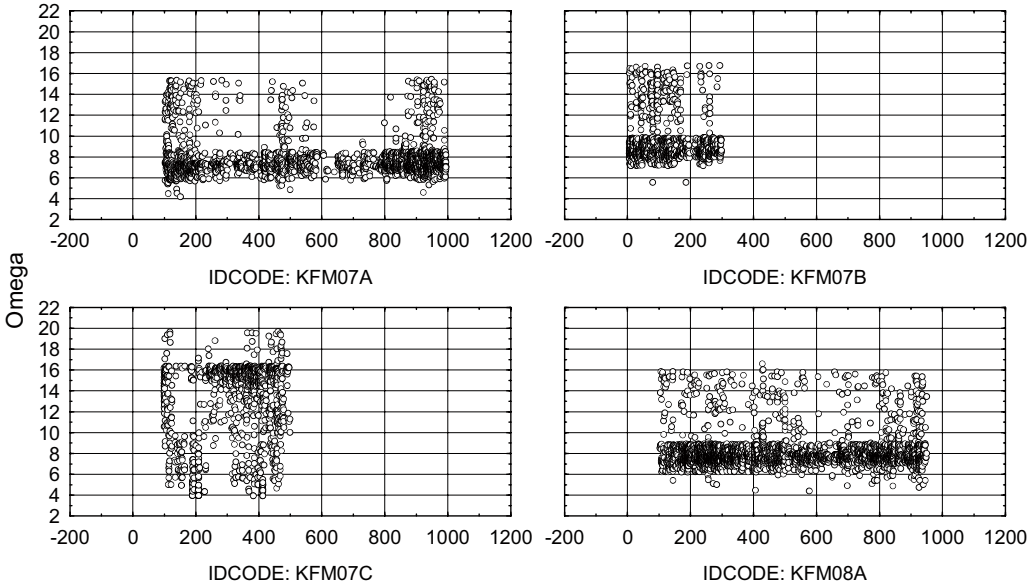

Q: (SITE = 'FORSMARK') AND (VISIBLE_IN_BIPS = 1) AND ((IDCODE = 'KFM07A') OR (IDCODE = 'KFM07B') OR (IDCODE = 'KFM07C') OR (IDCODE = 'KFM08A')), Graph created: 4/7/2008 2:07:59 PM
ADJUSTEDSECUP(m)

Scatterplot of Omega against ADJUSTEDSECUP(m); categorized by IDCODE
Comparison of FRACTURE orientations in DEC06_APR08_statistics.stw 28v*134281c

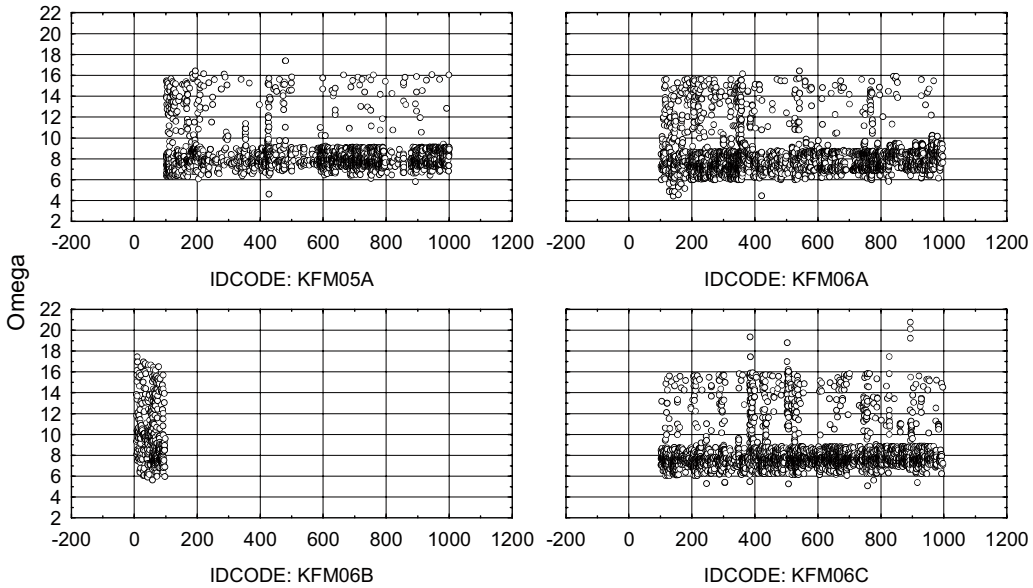

Q: (SITE = 'FORSMARK') AND (VISIBLE_IN_BIPS = 1) AND ((IDCODE = 'KFM05A') OR (IDCODE = 'KFM06A') OR (IDCODE = 'KFM06B') OR (IDCODE = 'KFM06C')), Graph created: 4/7/2008 2:07:27 PM
ADJUSTEDSECUP(m)

Scatterplot of Omega against ADJUSTEDSECUP(m); categorized by IDCODE
Comparison of FRACTURE orientations in DEC06_APR08_statistics.stw 28v*134281c

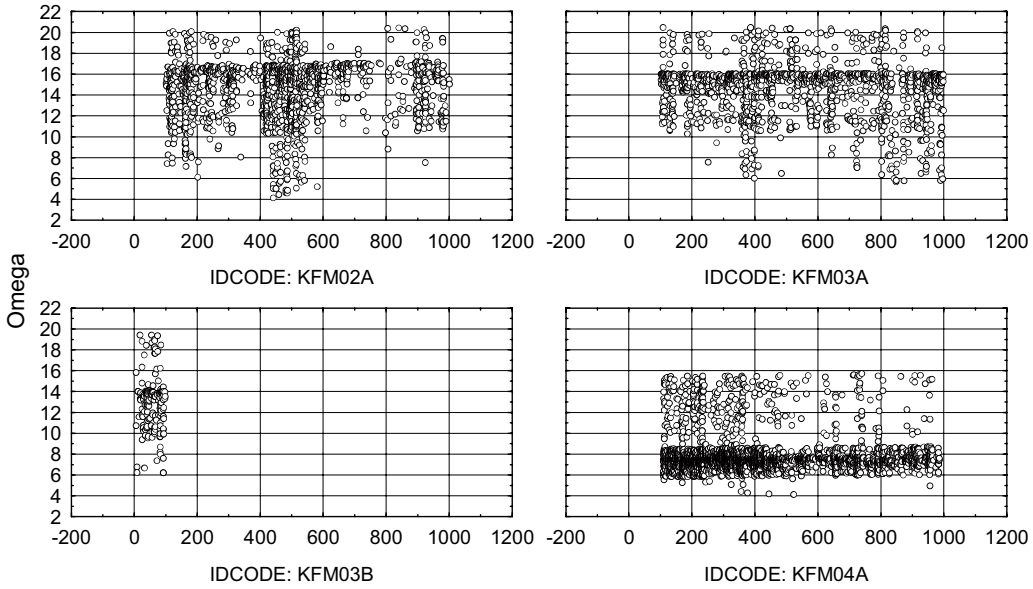

Q: (SITE = 'FORSMARK') AND (VISIBLE_IN_BIPS = 1) AND ((IDCODE = 'KFM02A') OR (IDCODE = 'KFM03A') OR (IDCODE = 'KFM03B') OR (IDCODE = 'KFM04A')), Graph created: 4/7/2008 2:06:54 PM
ADJUSTEDSECUP(m)

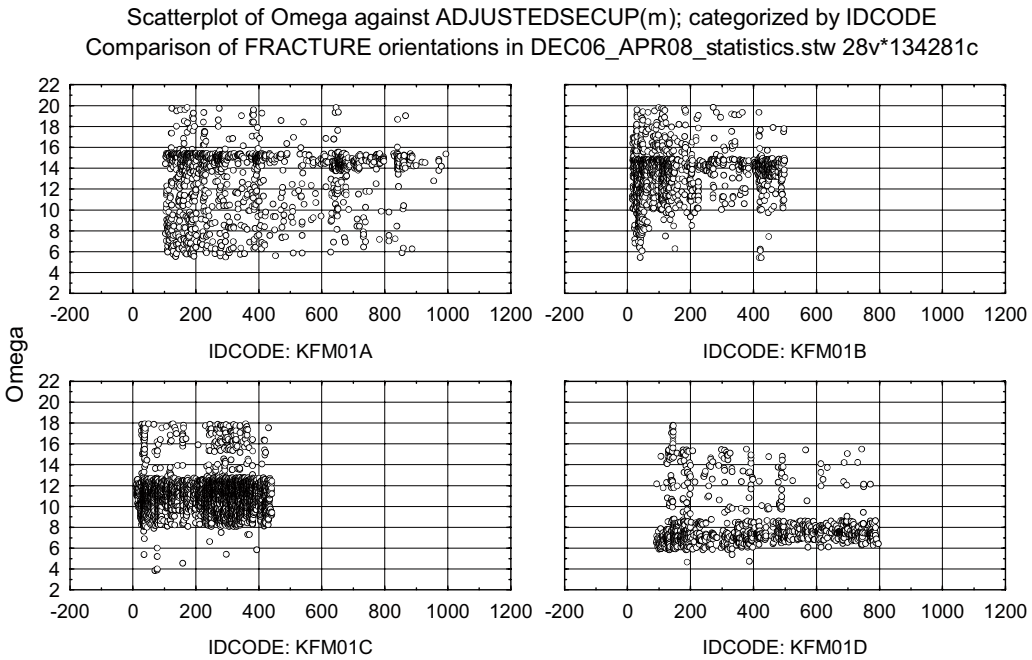
Scatterplot of Omega against ADJUSTEDSECUP(m); categorized by IDCODE
Comparison of FRACTURE orientations in DEC06_APR08_statistics.stw 28v*134281c
Omega
IDCODE: KFM01A
IDCODE: KFM01B
IDCODE: KFM01C
IDCODE: KFM01D
Q: (SITE = 'FORSMARK') AND (VISIBLE_IN_BIPS = 1) AND ((IDCODE = 'KFM01A') OR (IDCODE = 'KFM01B') OR (IDCODE = 'KFM01C') OR (IDCODE = 'KFM01D')), Graph created: 4/7/2008 2:06:20 PM
ADJUSTEDSECUP(m)

Laxemar

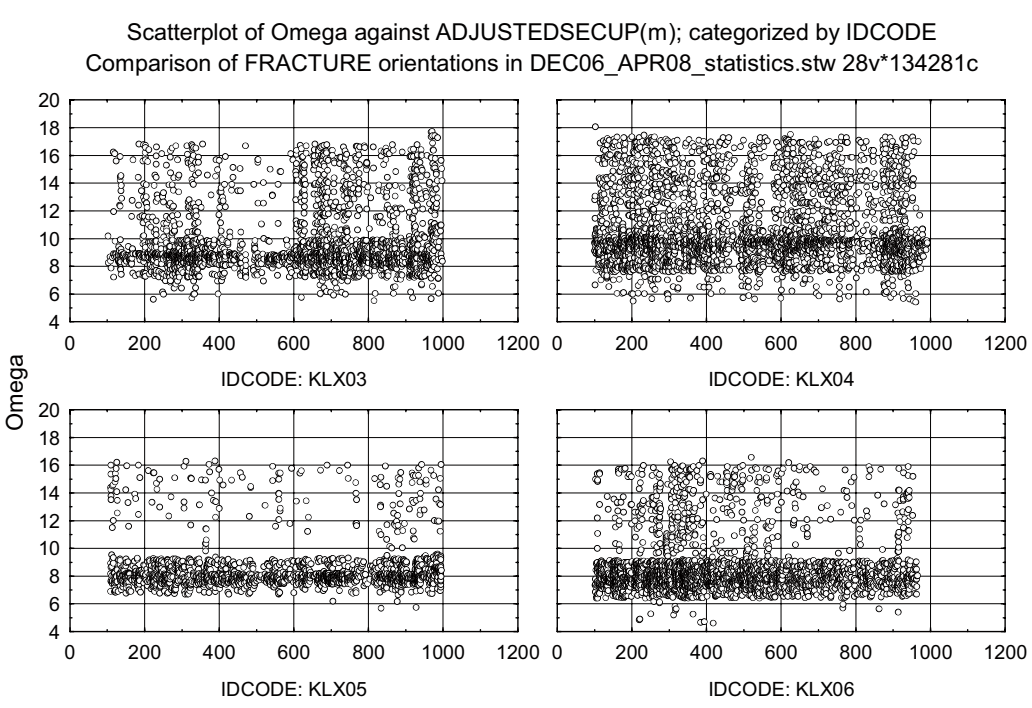
Scatterplot of Omega against ADJUSTEDSECUP(m); categorized by IDCODE
Comparison of FRACTURE orientations in DEC06_APR08_statistics.stw 28v*134281c
Omega
IDCODE: KLX03
IDCODE: KLX04
IDCODE: KLX05
IDCODE: KLX06
Q: (SITE = 'LAXEMAR') AND (VISIBLE_IN_BIPS = 1) AND ((IDCODE = 'KLX03') OR (IDCODE = 'KLX04') OR (IDCODE = 'KLX05') OR (IDCODE = 'KLX06')), Graph created: 4/7/2008 1:56:22 PM
ADJUSTEDSECUP(m)

Scatterplot of Omega against ADJUSTEDSECUP(m); categorized by IDCODE
Comparison of FRACTURE orientations in DEC06_APR08_statistics.stw 28v*134281c

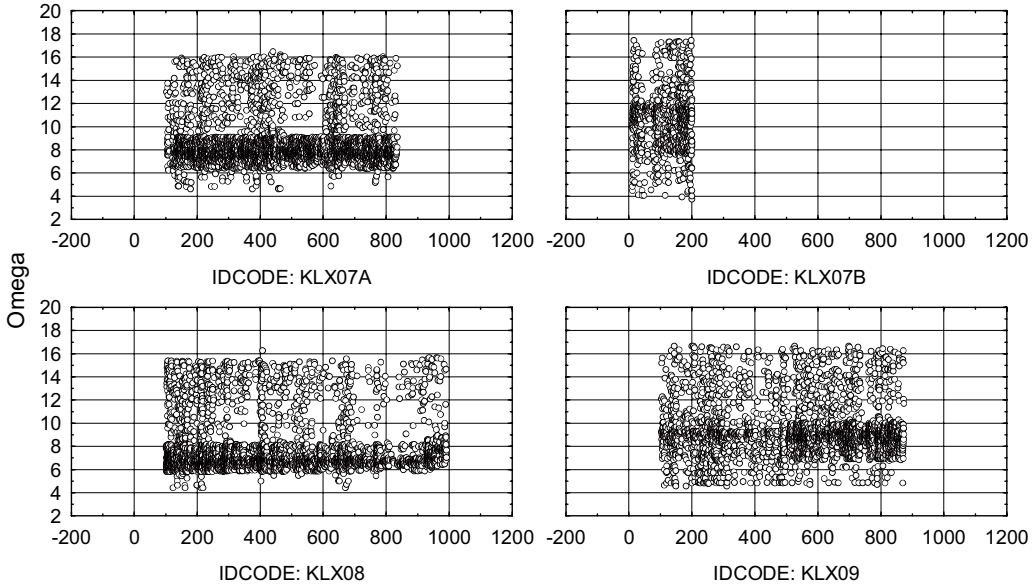

Q: (SITE = 'LAXEMAR') AND (VISIBLE_IN_BIPS = 1) AND ((IDCODE = 'KLX07A') OR (IDCODE = 'KLX07B') OR (IDCODE = 'KLX08') OR (IDCODE = 'KLX09')), Graph created: 4/7/2008 1:56:56 PM
ADJUSTEDSECUP(m)

Scatterplot of Omega against ADJUSTEDSECUP(m); categorized by IDCODE
Comparison of FRACTURE orientations in DEC06_APR08_statistics.stw 28v*134281c

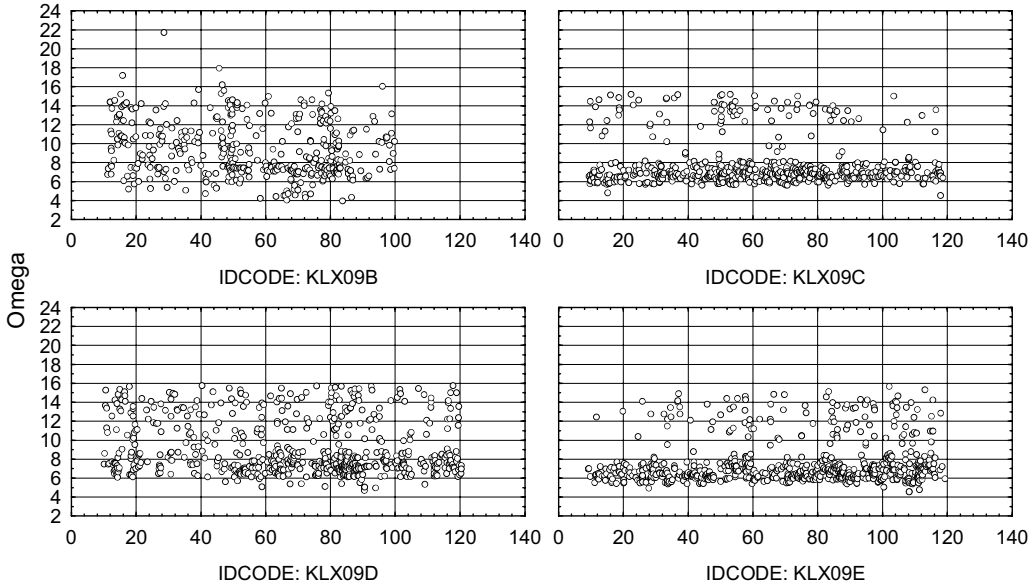

Q: (SITE = 'LAXEMAR') AND (VISIBLE_IN_BIPS = 1) AND ((IDCODE = 'KLX09B') OR (IDCODE = 'KLX09C') OR (IDCODE = 'KLX09D') OR (IDCODE = 'KLX09E')), Graph created: 4/7/2008 1:57:30 PM
ADJUSTEDSECUP(m)

Scatterplot of Omega against ADJUSTEDSECUP(m); categorized by IDCODE
Comparison of FRACTURE orientations in DEC06_APR08_statistics.stw 28v*134281c

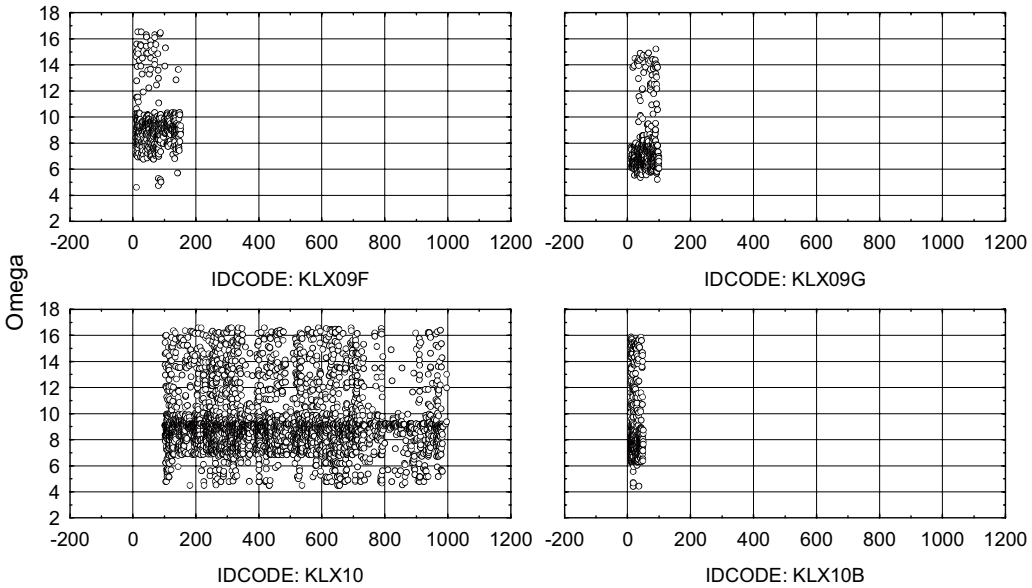

Q: (SITE = 'LAXEMAR') AND (VISIBLE_IN_BIPS = 1) AND ((IDCODE = 'KLX09F') OR (IDCODE = 'KLX09G') OR (IDCODE = 'KLX10') OR (IDCODE = 'KLX10B')), Graph created: 4/7/2008 1:58: 02 PM
ADJUSTEDSECUP(m)

Scatterplot of Omega against ADJUSTEDSECUP(m); categorized by IDCODE
Comparison of FRACTURE orientations in DEC06_APR08_statistics.stw 28v*134281c

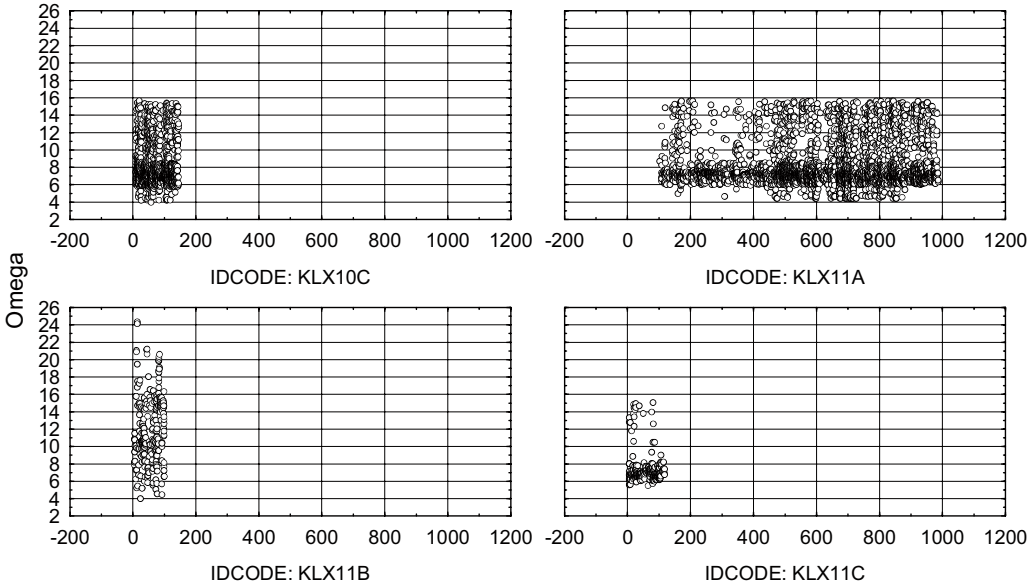

Q: (SITE = 'LAXEMAR') AND (VISIBLE_IN_BIPS = 1) AND ((IDCODE = 'KLX10C') OR (IDCODE = 'KLX11A') OR (IDCODE = 'KLX11B') OR (IDCODE = 'KLX11C')), Graph created: 4/7/2008 1:58: 36 PM
ADJUSTEDSECUP(m)

Scatterplot of Omega against ADJUSTEDSECUP(m); categorized by IDCODE
Comparison of FRACTURE orientations in DEC06_APR08_statistics.stw 28v*134281c

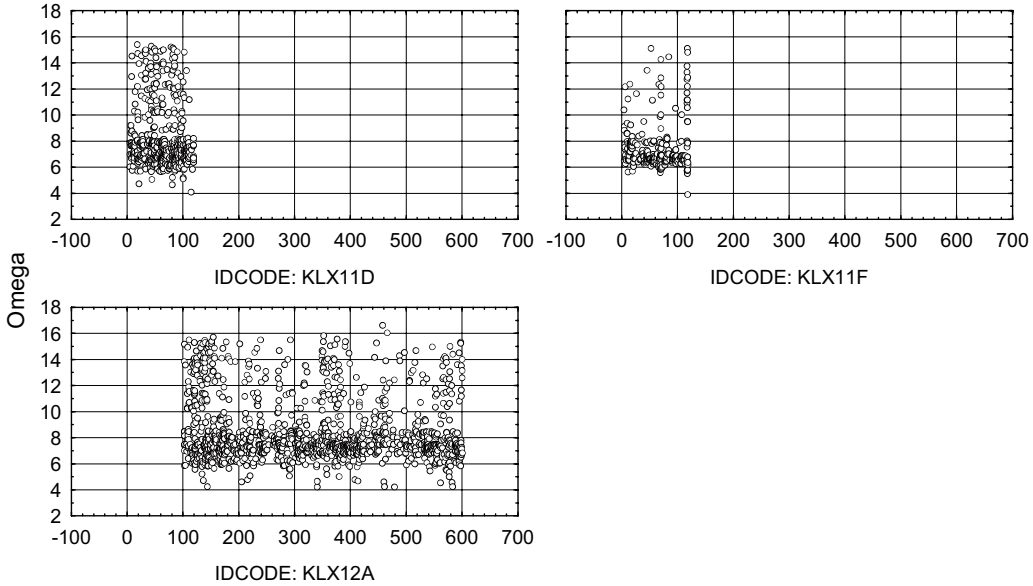

Q: (SITE = 'LAXEMAR') AND (VISIBLE_IN_BIPS = 1) AND ((IDCODE = 'KLX11D') OR (IDCODE = 'KLX101E') OR (IDCODE = 'KLX11F') OR (IDCODE = 'KLX12A')), Graph created: 4/7/2008 1:59:09 PM
ADJUSTEDSECUP(m)

Scatterplot of Omega against ADJUSTEDSECUP(m); categorized by IDCODE
Comparison of FRACTURE orientations in DEC06_APR08_statistics.stw 28v*134281c

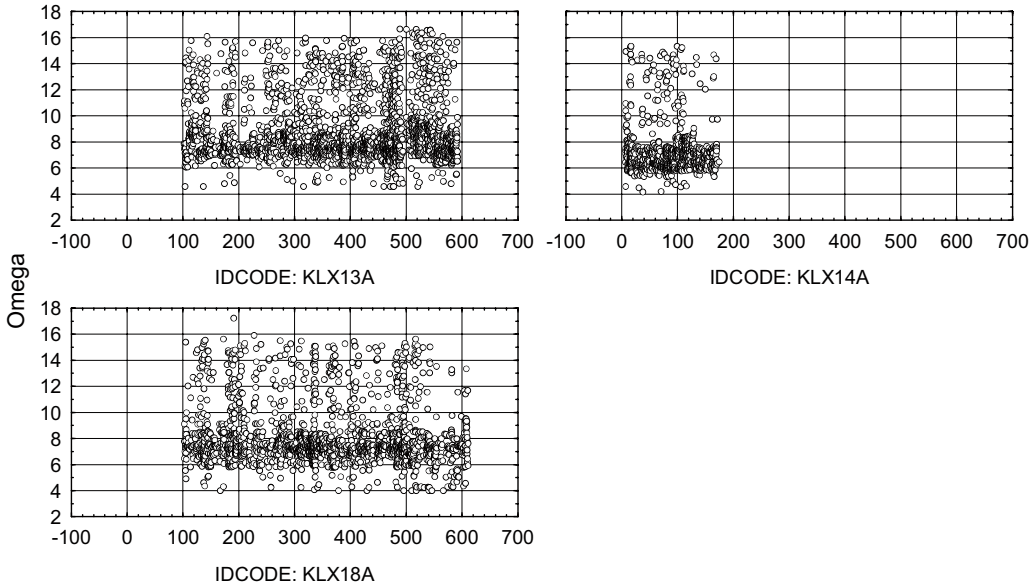

Q: (SITE = 'LAXEMAR') AND (VISIBLE_IN_BIPS = 1) AND ((IDCODE = 'KLX13A') OR (IDCODE = 'KLX14A') OR (IDCODE = 'KLX17A') OR (IDCODE = 'KLX18A')), Graph created: 4/7/2008 1:59:42 PM
ADJUSTEDSECUP(m)

Scatterplot of Omega against ADJUSTEDSECUP(m); categorized by IDCODE
Comparison of FRACTURE orientations in DEC06_APR08_statistics.stw 28v*134281c

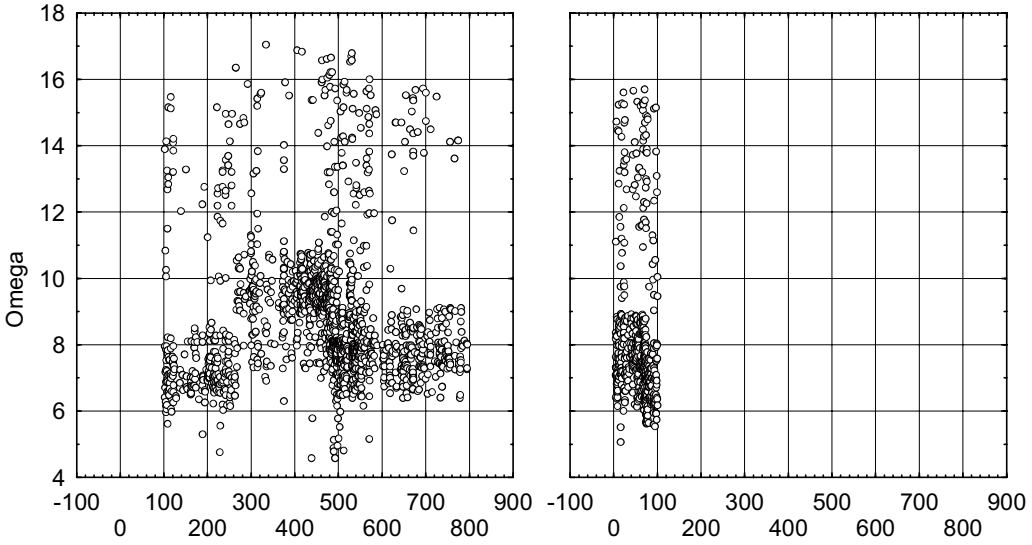

Q: (SITE = 'LAXEMAR') AND (VISIBLE_IN_BIPS = 1) AND ((IDCODE = 'KLX19A') OR (IDCODE = 'KLX20B') OR (IDCODE = 'KLX21B') OR (IDCODE = 'KLX22A')), Graph created: 4/7/2008 2:00:16 PM
ADJUSTEDSECUP(m)

Scatterplot of Omega against ADJUSTEDSECUP(m); categorized by IDCODE
Comparison of FRACTURE orientations in DEC06_APR08_statistics.stw 28v*134281c

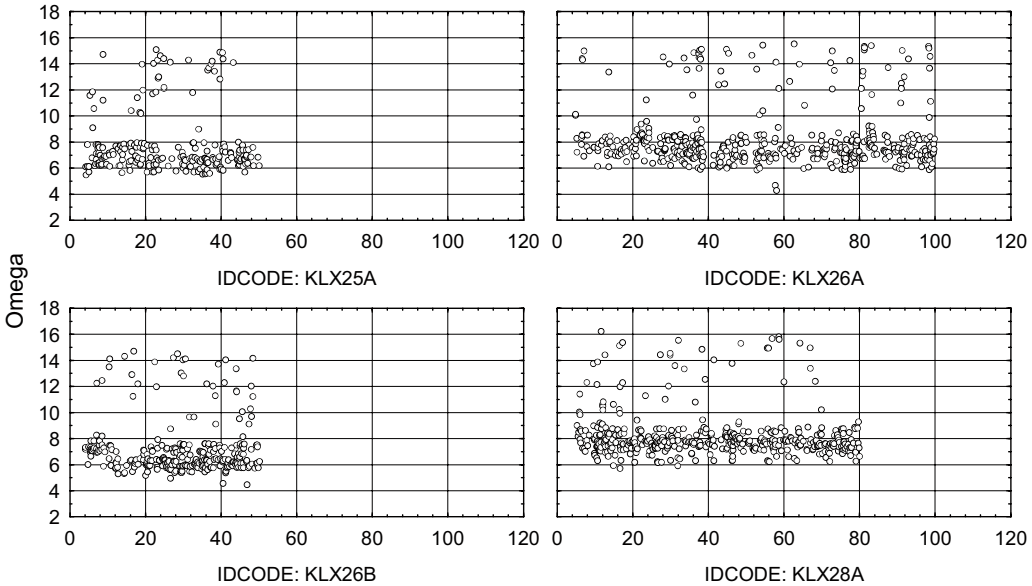

Q: (SITE = 'LAXEMAR') AND (VISIBLE_IN_BIPS = 1) AND ((IDCODE = 'KLX25A') OR (IDCODE = 'KLX26A') OR (IDCODE = 'KLX26B') OR (IDCODE = 'KLX28A')), Graph created: 4/7/2008 2:00:48 PM
ADJUSTEDSECUP(m)

Scatterplot of Omega against ADJUSTEDSECUP(m); categorized by IDCODE
Comparison of FRACTURE orientations in DEC06_APR08_statistics.stw 28v*134281c

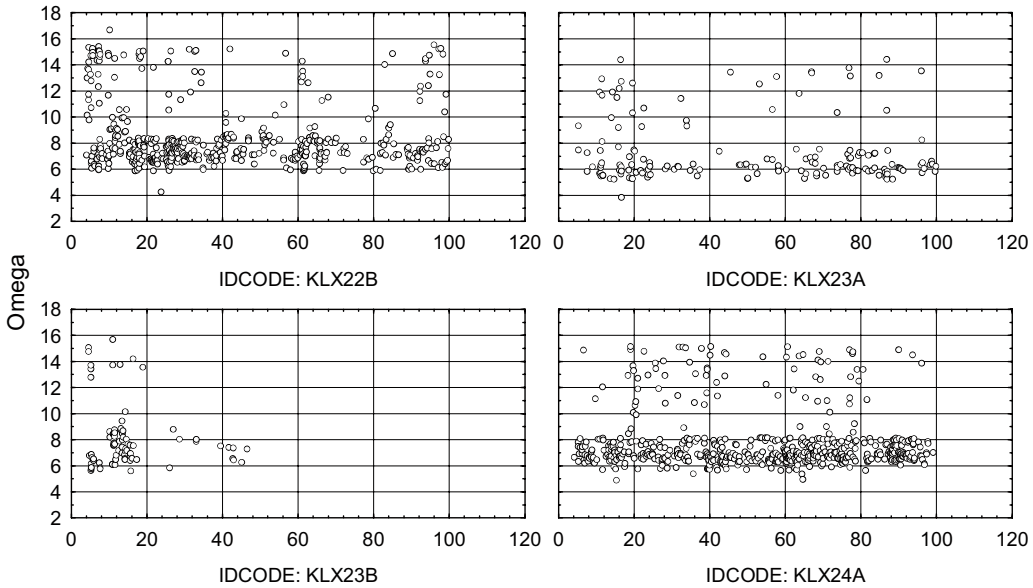

Q: (SITE = 'LAXEMAR') AND (VISIBLE_IN_BIPS = 1) AND ((IDCODE = 'KLX22B') OR (IDCODE = 'KLX23A') OR (IDCODE = 'KLX23B') OR (IDCODE = 'KLX24A')), Graph created: 4/7/2008 2:01: 21 PM
ADJUSTEDSECUP(m)

Scatterplot of Omega against ADJUSTEDSECUP(m); categorized by IDCODE
Comparison of FRACTURE orientations in DEC06_APR08_statistics.stw 28v*134281c

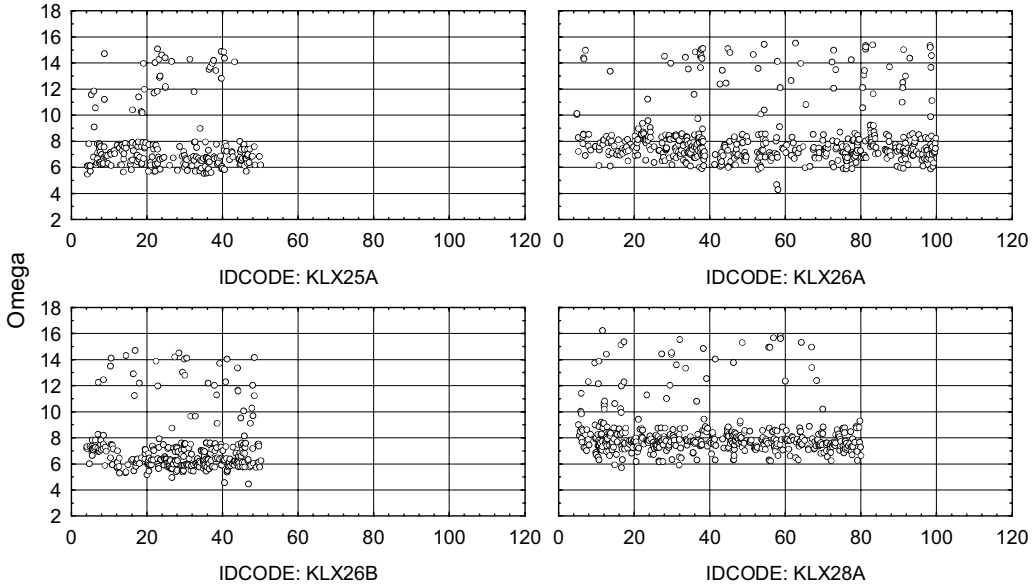

Q: (SITE = 'LAXEMAR') AND (VISIBLE_IN_BIPS = 1) AND ((IDCODE = 'KLX25A') OR (IDCODE = 'KLX26A') OR (IDCODE = 'KLX26B') OR (IDCODE = 'KLX28A')), Graph created: 4/7/2008 2:01: 54 PM
ADJUSTEDSECUP(m)

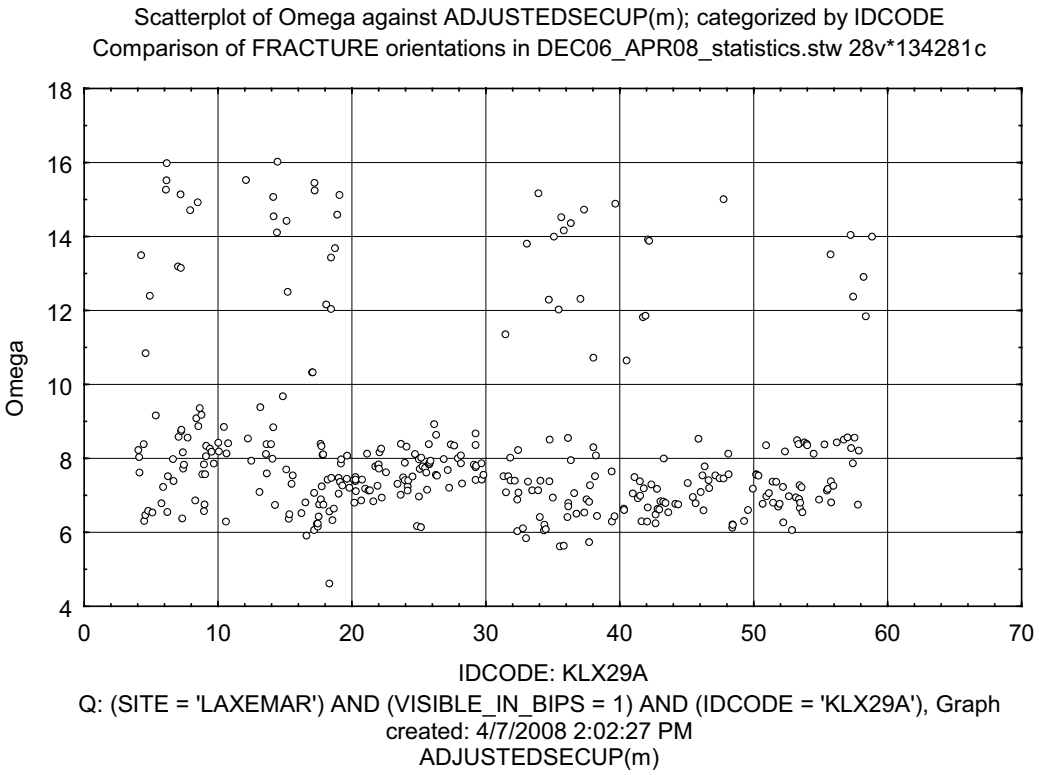
Scatterplot of Omega against ADJUSTEDSECUP(m); categorized by IDCODE
Comparison of FRACTURE orientations in DEC06_APR08_statistics.stw 28v*134281c
Omega
18
16
14
12
10
8
6
4
0
10
20
30
40
50
60
70
IDCODE: KLX29A
Q: (SITE = 'LAXEMAR') AND (VISIBLE_IN_BIPS = 1) AND (IDCODE = 'KLX29A'), Graph created: 4/7/2008 2:02:27 PM
ADJUSTEDSECUP(m)

A4 PFL-f features

A4.1 Forsmark

Breakdown Table of Descriptive Statistics (Comparison of FRACTURE orientations in DEC06_APR08_statistics.stw)
N=543 (No missing data in dep. var. list)
Include condition: (SITE = 'FORSMARK') AND (VISIBLE_IN_BIPS = 1) AND (PFLID <> "")

IDCODE	dZ(m) Means	AbsoluteDistance(m) Means	Theta Means	Omega Means
KFM01A	0.002727	0.163909	2.59273	12.83551
KFM01B				
KFM01C				
KFM01D	-0.334242	0.672606	0.37455	8.33274
KFM02A	-0.052903	1.524333	13.47742	14.32498
KFM03A	0.106800	0.141100	10.41920	14.09837
KFM03B				
KFM04A	0.167101	1.042855	0.70623	8.30363
KFM05A	0.000769	0.022154	0.68462	10.35485
KFM06A	-0.699468	1.512734	0.86457	9.06550
KFM06B				
KFM06C				
KFM07A	-0.680000	2.343700	1.02250	7.83658
KFM07B				
KFM07C	0.098000	0.986800	5.17933	10.13485
KFM08A	-0.359750	1.922075	1.24950	8.44551
KFM08B				
KFM08C	0.090526	1.174579	4.42158	8.44155
KFM09A				
KFM09B				
KFM10A	-0.237843	0.754706	1.49804	7.91164
All Grps	-0.187201	1.087512	4.28842	10.38763

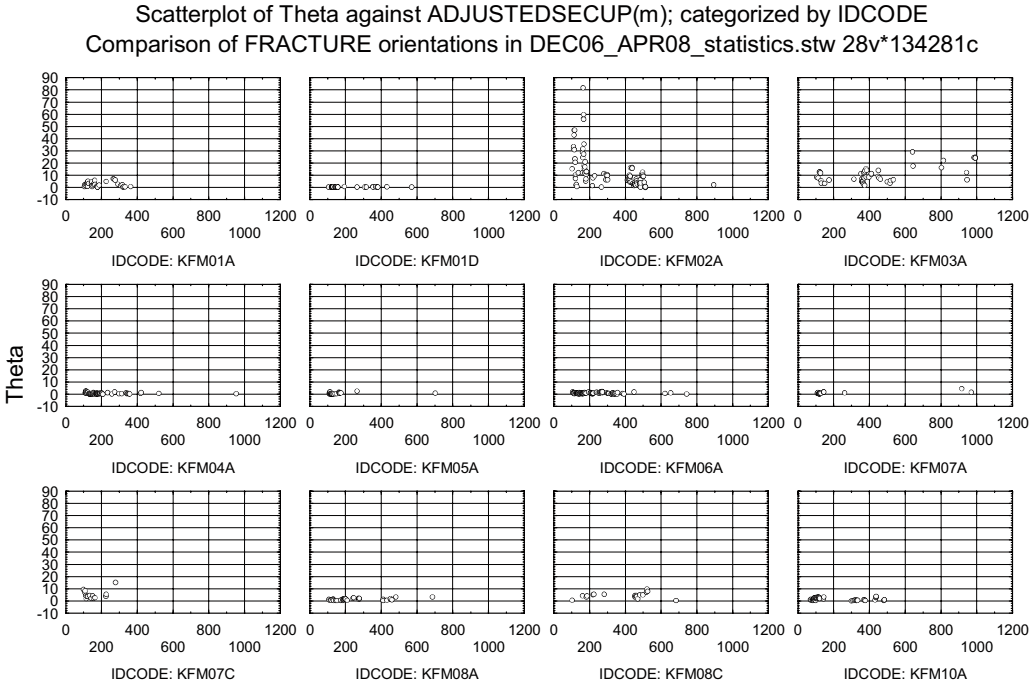

Scatterplot of dZ(m) against ADJUSTEDSECUP(m); categorized by IDCODE
Comparison of FRACTURE orientations in DEC06_APR08_statistics.stw 28v*134281c

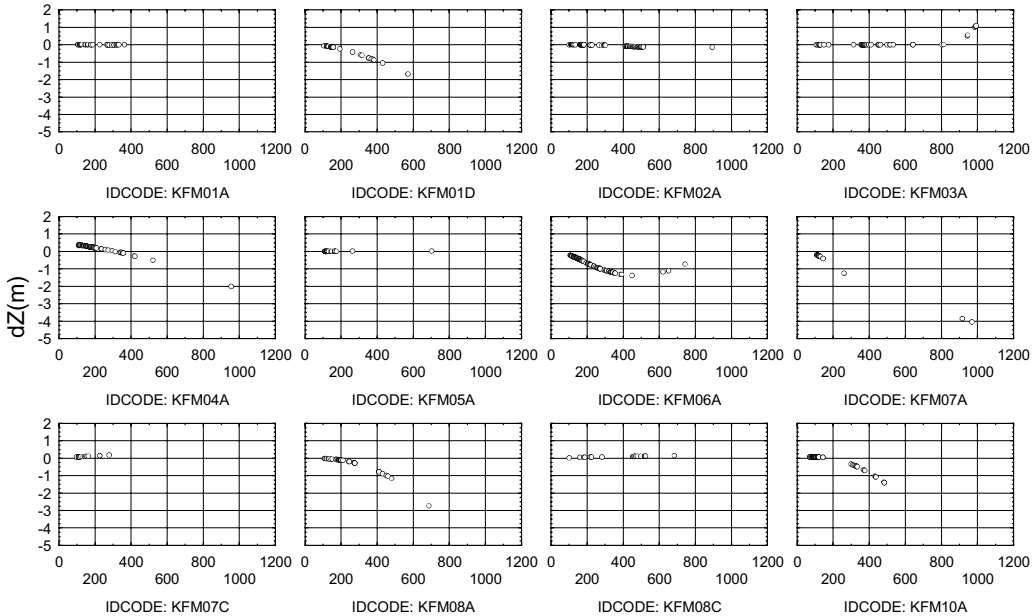

Q: (SITE = 'FORSMARK') AND (VISIBLE_IN_BIPS = 1) AND (PFLID <> ""), Graph created: 4/7 /2008 2:05:50 PM
ADJUSTEDSECUP(m)

Scatterplot of AbsoluteDistance(m) against ADJUSTEDSECUP(m); categorized by IDCODE
Comparison of FRACTURE orientations in DEC06_APR08_statistics.stw 28v*134281c

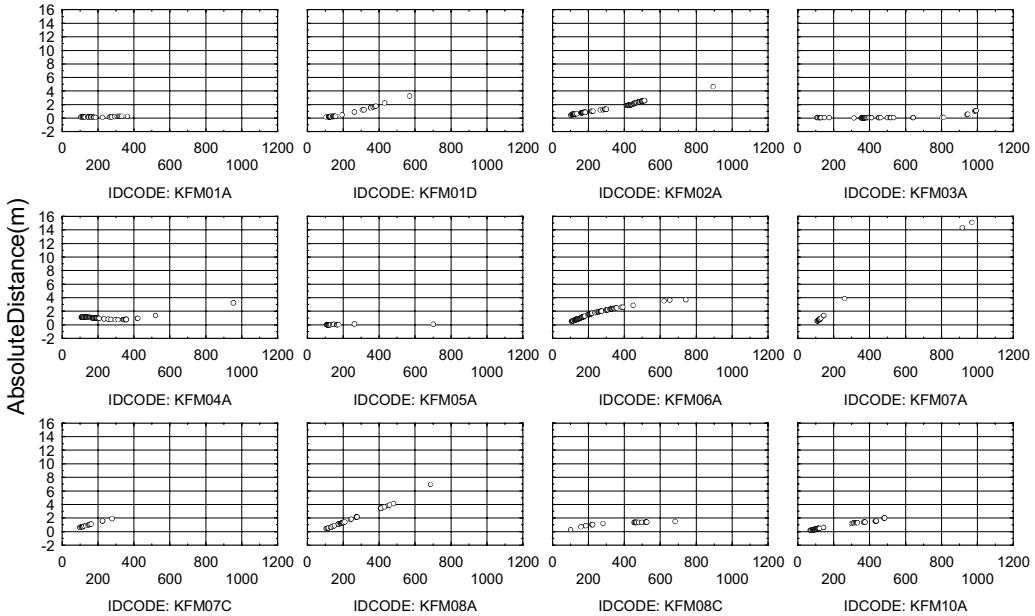

Q: (SITE = 'FORSMARK') AND (VISIBLE_IN_BIPS = 1) AND (PFLID <> ""), Graph created: 4/7 /2008 2:05:50 PM
ADJUSTEDSECUP(m)

Scatterplot of Omega against ADJUSTEDSECUP(m); categorized by IDCODE
Comparison of FRACTURE orientations in DEC06_APR08_statistics.stw 28v*134281c

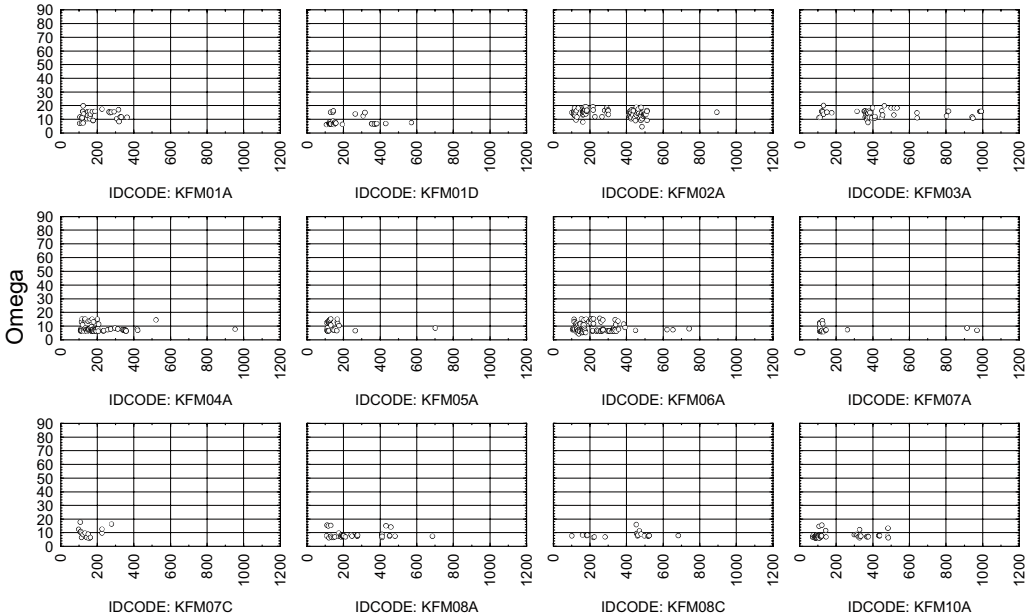

Q: (SITE = 'FORSMARK') AND (VISIBLE_IN_BIPS = 1) AND (PFLID <> "")
Graph created: 4/7/2008 2:05:50 PM
ADJUSTEDSECUP(m)

A4.2 Laxemar

Due to the much larger amount of boreholes, the plots representing Laxemar differ in layout from those representing Forsmark for clarity.

Breakdown Table of Descriptive Statistics (Comparison of FRACTURE orientations in DEC06_APR08_statistics.stw)
N=1956 (No missing data in dep. var. list)
Include condition: (SITE = 'LAXEMAR') AND (VISIBLE_IN_BIPS = 1) AND (PFLID <> "")

IDCODE	dZ(m) Means	AbsoluteDistance(m) Means	Theta Means	Omega Means
KLX03	-0.18843	3.941745	3.189804	10.45051
KLX04	0.02229	0.083896	3.289063	10.11812
KLX05	-0.11867	0.793200	0.779667	8.96425
KLX07A	0.55171	1.911905	0.758389	8.71783
KLX08	0.23549	2.138377	1.454344	8.01667
KLX09	0.39200	3.417550	0.980333	9.43403
KLX09B	0.00000	0.132976	3.624286	8.97630
KLX09C	0.01833	0.318167	0.671944	7.71337
KLX09D	-0.00400	0.148886	1.629429	9.05807
KLX09E	-0.01500	0.034844	1.766875	6.94667
KLX09F	-0.00150	0.029575	0.405000	8.73972
KLX09G	-0.00026	0.098842	4.718421	7.59898
KLX10	0.40377	3.218728	0.999877	9.43566
KLX10B	0.00000	0.177417	0.619583	9.24326
KLX10C	-0.00250	0.105625	1.586250	7.71951
KLX11A	0.22173	1.829115	1.013077	8.77629
KLX11B	0.00000	0.032793	3.485862	11.23922
KLX11C	-0.00029	0.055765	2.675294	8.19696
KLX11D	0.00565	0.091826	1.813913	8.88694
KLX11E	-0.01939	0.062333	2.363939	8.31775
KLX11F	-0.00050	0.009900	1.634000	8.14704
KLX12A	0.52603	3.263619	1.422381	9.33158
KLX13A	-0.47496	3.691976	2.463821	8.90640
KLX14A	0.03836	0.113463	0.411642	7.10857
KLX18A	-0.21672	1.300724	1.452836	7.47697
KLX19A	-1.11135	2.177769	0.993462	8.70238
KLX20A	-0.85857	1.331929	0.536429	8.98957
KLX22A	-0.05595	0.128619	0.435238	8.56372
KLX22B	0.00364	0.205455	2.433636	9.20974
KLX23A	0.01400	0.033400	0.280667	7.13282
KLX23B	-0.00333	0.031667	2.463333	6.56509
KLX24A	0.01475	0.088725	0.384000	8.63110
KLX25A	0.00143	0.035571	0.411429	9.33922
KLX26A	0.00773	0.048227	1.008182	8.06271
KLX26B	0.00250	0.019188	4.394375	6.71940
KLX28A	-0.12147	0.321029	2.362941	8.54486
KLX29A	-0.04000	0.567333	0.975926	8.57530
All Grps	0.04011	1.451797	1.559657	8.69079

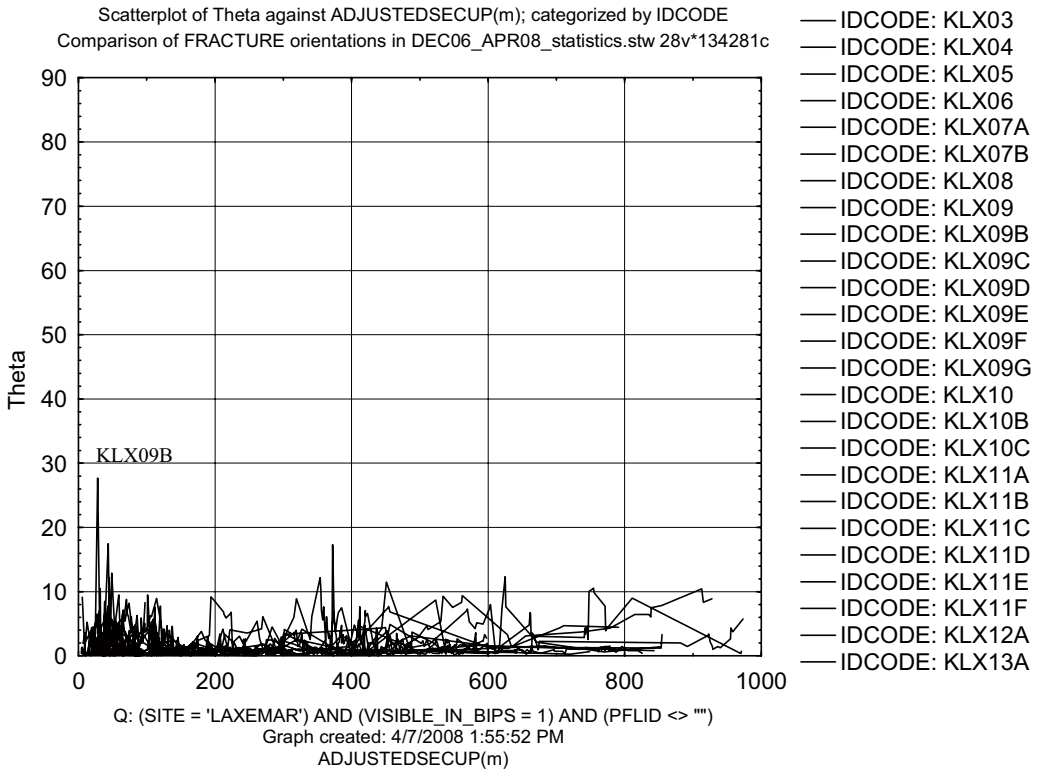
Scatterplot of Theta against ADJUSTEDSECUP(m); categorized by IDCODE
Comparison of FRACTURE orientations in DEC06_APR08_statistics.stw 28v*134281c
Theta
KLX09B
ADJUSTEDSECUP(m)
IDCODE: KLX03
IDCODE: KLX04
IDCODE: KLX05
IDCODE: KLX06
IDCODE: KLX07A
IDCODE: KLX07B
IDCODE: KLX08
IDCODE: KLX09
IDCODE: KLX09B
IDCODE: KLX09C
IDCODE: KLX09D
IDCODE: KLX09E
IDCODE: KLX09F
IDCODE: KLX09G
IDCODE: KLX10
IDCODE: KLX10B
IDCODE: KLX10C
IDCODE: KLX11A
IDCODE: KLX11B
IDCODE: KLX11C
IDCODE: KLX11D
IDCODE: KLX11E
IDCODE: KLX11F
IDCODE: KLX12A
IDCODE: KLX13A
Q: (SITE = 'LAXEMAR') AND (VISIBLE_IN_BIPS = 1) AND (PFLID <> "")
Graph created: 4/7/2008 1:55:52 PM

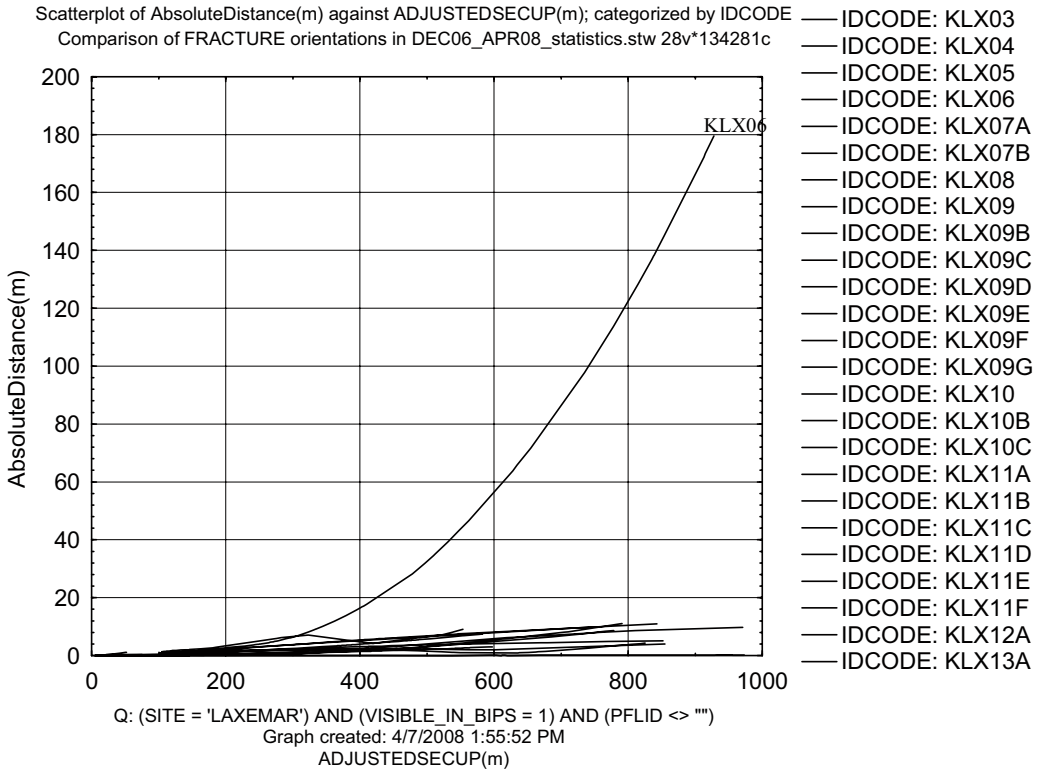
Scatterplot of AbsoluteDistance(m) against ADJUSTEDSECUP(m); categorized by IDCODE
Comparison of FRACTURE orientations in DEC06_APR08_statistics.stw 28v*134281c
AbsoluteDistance(m)
KLX06
ADJUSTEDSECUP(m)
IDCODE: KLX03
IDCODE: KLX04
IDCODE: KLX05
IDCODE: KLX06
IDCODE: KLX07A
IDCODE: KLX07B
IDCODE: KLX08
IDCODE: KLX09
IDCODE: KLX09B
IDCODE: KLX09C
IDCODE: KLX09D
IDCODE: KLX09E
IDCODE: KLX09F
IDCODE: KLX09G
IDCODE: KLX10
IDCODE: KLX10B
IDCODE: KLX10C
IDCODE: KLX11A
IDCODE: KLX11B
IDCODE: KLX11C
IDCODE: KLX11D
IDCODE: KLX11E
IDCODE: KLX11F
IDCODE: KLX12A
IDCODE: KLX13A
Q: (SITE = 'LAXEMAR') AND (VISIBLE_IN_BIPS = 1) AND (PFLID <> "")
Graph created: 4/7/2008 1:55:52 PM

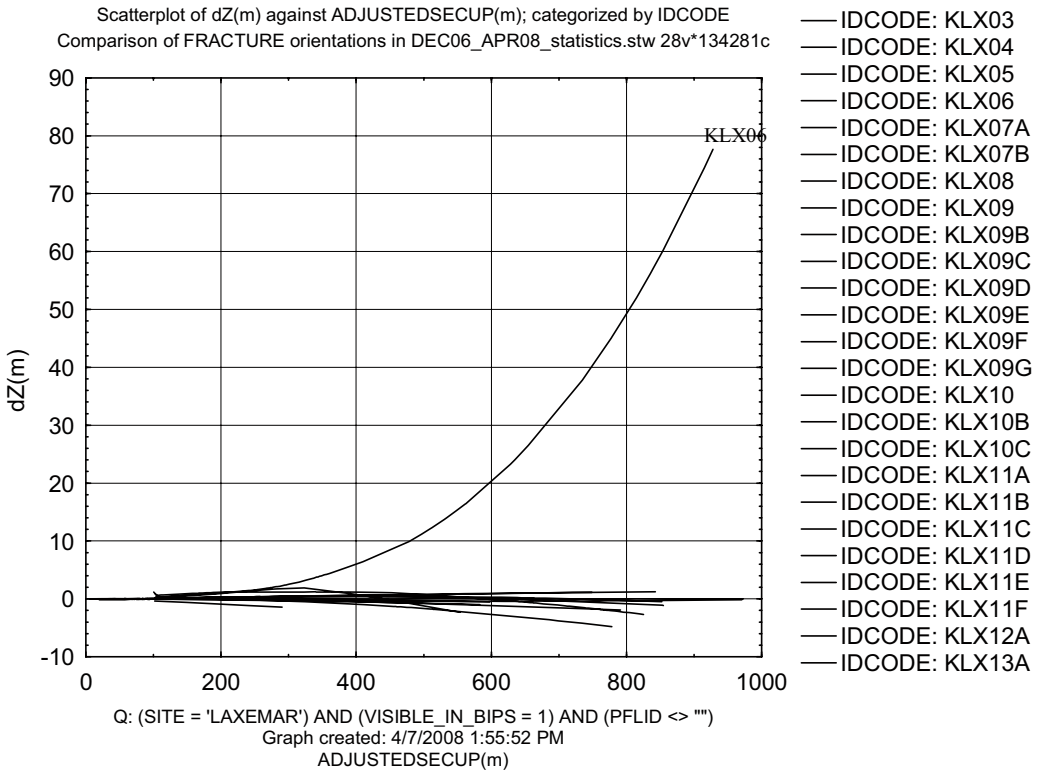
Scatterplot of dZ(m) against ADJUSTEDSECUP(m); categorized by IDCODE
Comparison of FRACTURE orientations in DEC06_APR08_statistics.stw 28v*134281c
dZ(m)
KLX06
90
80
70
60
50
40
30
20
10
0
-10
0
200
400
600
800
1000
Q: (SITE = 'LAXEMAR') AND (VISIBLE_IN_BIPS = 1) AND (PFLID <> "")
Graph created: 4/7/2008 1:55:52 PM
ADJUSTEDSECUP(m)
IDCODE: KLX03
IDCODE: KLX04
IDCODE: KLX05
IDCODE: KLX06
IDCODE: KLX07A
IDCODE: KLX07B
IDCODE: KLX08
IDCODE: KLX09
IDCODE: KLX09B
IDCODE: KLX09C
IDCODE: KLX09D
IDCODE: KLX09E
IDCODE: KLX09F
IDCODE: KLX09G
IDCODE: KLX10
IDCODE: KLX10B
IDCODE: KLX10C
IDCODE: KLX11A
IDCODE: KLX11B
IDCODE: KLX11C
IDCODE: KLX11D
IDCODE: KLX11E
IDCODE: KLX11F
IDCODE: KLX12A
IDCODE: KLX13A

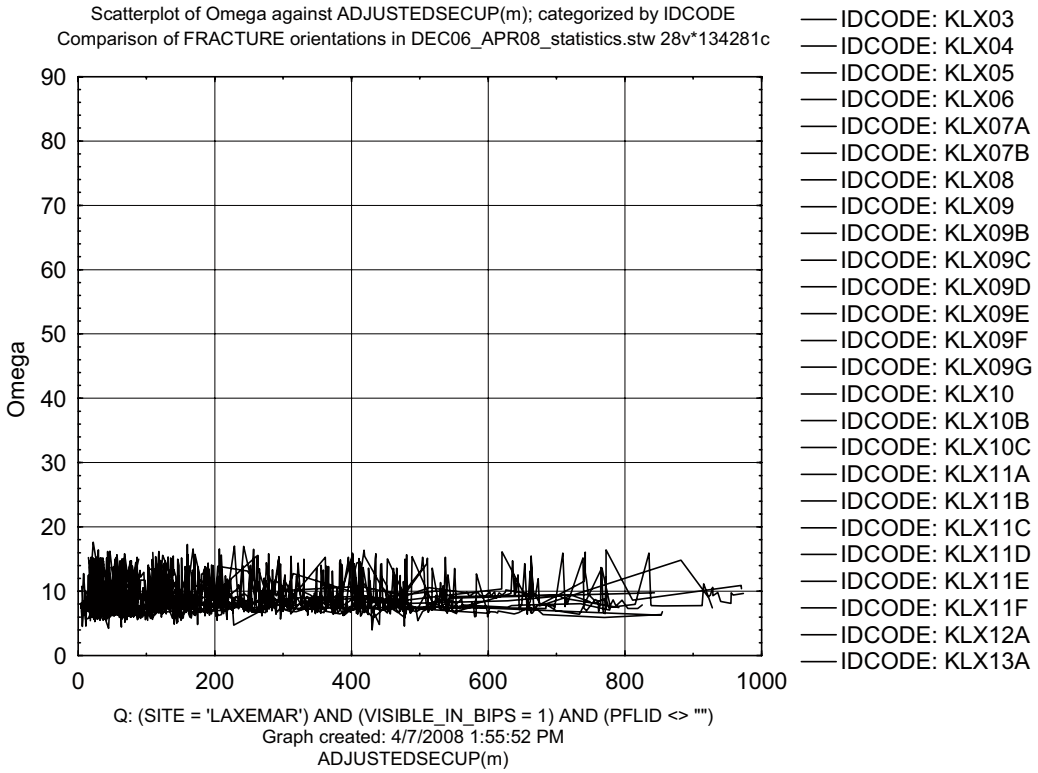
Scatterplot of Omega against ADJUSTEDSECUP(m); categorized by IDCODE
Comparison of FRACTURE orientations in DEC06_APR08_statistics.stw 28v*134281c
Omega
90
80
70
60
50
40
30
20
10
0
0
200
400
600
800
1000
Q: (SITE = 'LAXEMAR') AND (VISIBLE_IN_BIPS = 1) AND (PFLID <> "")
Graph created: 4/7/2008 1:55:52 PM
ADJUSTEDSECUP(m)
IDCODE: KLX03
IDCODE: KLX04
IDCODE: KLX05
IDCODE: KLX06
IDCODE: KLX07A
IDCODE: KLX07B
IDCODE: KLX08
IDCODE: KLX09
IDCODE: KLX09B
IDCODE: KLX09C
IDCODE: KLX09D
IDCODE: KLX09E
IDCODE: KLX09F
IDCODE: KLX09G
IDCODE: KLX10
IDCODE: KLX10B
IDCODE: KLX10C
IDCODE: KLX11A
IDCODE: KLX11B
IDCODE: KLX11C
IDCODE: KLX11D
IDCODE: KLX11E
IDCODE: KLX11F
IDCODE: KLX12A
IDCODE: KLX13A